Relationship Between Flavonoid Structure And Phase-II Metabolism

Rashim Singh

2010

Relationship Between Flavonoid Structure And Phase-II Metabolism

A

Dissertation

Presented to the Faculty of

The University of Houston
College of Pharmacy
Department of Pharmacological and Pharmaceutical Sciences

In Partial Fulfillment of
The Requirement for the Degree of
DOCTOR OF PHILOSOPHY

By
Rashim Singh

May, 2010

Dedicated to My Parents

Mr. S. P. Singh and Mrs. Munesh Singh

ABSTRACT

Objective: The overall objective is to develop structure-metabolism relationships (SMRs) between UGTs and flavonoids for predicting glucuronidation of flavonoids. The goals of this research project were to: 1) identify the major UGT isoform(s) contributing to the glucuronidation of flavonoids and predicting the major organ of metabolism; 2) establish the substrate-selectivity and regiospecificity of these major UGT isoform(s); 3) develop the *in silico* prediction models for UGT 1A8 and UGT1A9 using pharmacophore and 2-D/3-D QSAR modeling techniques; 4) study the effect of change in backbone on the disposition of flavonoids in Caco-2 cells; 5) study the rate-limiting role of efflux transporters in the disposition of flavonols in Caco-2 cells; and 6) study the regiospecific disposition of flavones in Caco-2 cells.

Method: For objectives 1 and 2, *in vitro* recombinant human UGT isoforms glucuronidation model was used. For objective 3, *in silico* pharmacophore and 2-D/3-D QSAR modeling was used along with *in vitro* glucuronidation intrinsic clearance values in recombinant human UGT isoforms. For objectives 4, 5 and 6, intact Caco-2 cell monolayers was used as the transport model, and Caco-2 cell lysate was used for measuring glucuronide formation rates.

Results: 1) To identify the major UGT isoform(s) contributing to the glucuronidation of flavonoids and predicting the major organ of metabolism, we found that flavonoids were

mainly glucuronidated by UGT1A1, 1A8 and 1A9 at the substrate concentration of 2.5, 10 and 35μM. 2) To establish the substrate-selectivity and regiospecificity of these major UGT isoform, we found that UGT1A1 showed no regiospecificity for glucuronidating any position, whereas, UGT1A8 and UGT1A9 showed either dominant, preferred or weak regiospecificity for 3-*O* or 7-*O* position, depending on the structure of the compound. In general, the addition of hydroxyl group at C-4' reduced, whereas the addition of hydroxyl group at C-5 and/or C-7 improved the rates of glucuronidation of flavonoids by UGT1A8 and 1A9. On the other hand, the rates of glucuronidation by UGT1A1 reduced as number of hydroxyl group in the structure increased. 3) To develop the *in silico* prediction models for UGT1A8 and UGT1A9 using pharmacophore and 2-D/3-D QSAR modeling techniques, we found that pharmacophore-based semi-quantitative SMR models for UGT1A9 with >75% predictive ability could be developed. But neither semi-quantitative SMR models for UGT1A8 nor the quantitative SMR models for UGT1A8 and UGT1A9 could be successfully developed. 4) To study the effect of change in backbone on the disposition of flavonoids in Caco-2 cells, we found that the change in backbone impacts the excretion of flavonoid sulfates more significantly than the excretion of their glucuronides except for genistein. 5) To study the rate-limiting role of efflux transporters in the disposition of flavonols in Caco-2 cells, we found that excretion of flavonol glucuronides in Caco-2 cells were not limited by efflux transporters and glucuronides of flavonols showed basolateral preference in their excretion. 6) To study the regiospecific conjugation of flavones in Caco-2 cells, we found that both

glucuronidation and sulfation of flavones mainly happened at hydroxyl group at C-7 position.

Conclusion: UGT1A9, UGT1A8 and UGT1A1 are the most important isoforms that can glucuronidate vast majority of tested flavonoids. Based on published UGT isoform expression pattern in human liver and intestine, they should serve as the major first-pass metabolism organs for flavonoids. UGT1A8 and UGT1A9 showed regiospecificity for 3-*O* or 7-*O* position, depending on the structure of the compound, whereas UGT1A1 showed no regiospecificity. Also, the addition of hydroxyl group at C-4' reduced, whereas the addition of hydroxyl group at C-5 and/or C-7 improved the rates of glucuronidation of flavonoids by UGT1A8 and 1A9, with rare exceptions. In contrast, the rates of glucuronidation by UGT1A1 reduced as number of hydroxyl group in the structure increased. Isoform-specific semi-quantitative Pharmacophore-based 3-D SMR prediction models could be developed for UGT1A9 with the predictive ability of more than 75%, but more efforts are needed to develop better quantitative models of prediction. We also probed the SMR experimentally using the Caco-2 model, and the results showed that the excretion of glucuronides was impacted more by the change in number and position of hydroxyl group in the flavonoid structure than changes in backbone. The excretion of glucuronides of flavones but not flavonols is rate-limited by efflux transporters. Future SMR research will incorporate more experimentally derived information to develop better models to predict glucuronidation of flavonoids in humans.

ACKNOWLEDGEMENT

I would like to express my sincere appreciation and gratitude to my advisor, Dr. Ming Hu, for his guidance, help, patience and wisdom. I feel truly fortunate to have had him as a mentor during the pursuit of my scientific interests. He is as good a human being as he is a scientist. His dedication and personality have been and will be an inspiration to me in my life.

I would also like to thank my co-advisor Dr. James M. Briggs for his valuable guidance in during the pursuit of this project. I would like to extend my sincere thanks to my committee members and teachers, Dr. Chow, Dr. Tam and Dr. Ghose for their support, guidance and cooperation during my Ph.D. I would also like to thanks all my teachers for being really nice and supportive to me as graduate student.

I would like to thank my family for being the driving force for pursing my Ph.D. The constant encouragement and support of my parents for which has given me the opportunities and freedom to pursue my interests in life even though some time it was not easy. My loving brother, Ankit Singh, though struggling with his own problems have always tried to be there for me in my difficult times. I do not have the right words to thank my husband and best friend Abhishek Verma for his unconditional love and support, which has provided me with the strength and motivation to finish this project even though it was really hard to live without him. I would also like to thank my father-in-law Dr. S. N. Verma for always being very loving, understanding and supporting.

I am thankful to all my labmates and friends, especially Lan and Baojian for helping me to finish my experiments. I am also thankful to Lucy, Steve, Haiyan, ZQ, KK, Tiby, Etta and Song for their help and teachings. I have an endlist of friends who have met me in different course of life and became my inspiration in one way or other, but some of them have truly played important roles, namely Garima, Atul, Shveta, Manvi, Harsh, Siva, Vicky, Dhara, Ila, Ananth, Sriram, Anand, Ashish, Shekar, and Vikram.

TABLE OF CONTENTS

LIST OF FIGURES

LIST OF TABLES

LIST OF APPENDICES

ABBREVIATIONS

SMR, structure-metabolism relationship; UGTs, Uridine diphospho glucuronosyltransferases; SULTs, sulfotransferases; 2-D, 2-dimensional; 3-D, 3-dimensional; SAR, structure-activity relationship; QSAR, quantitative structure-activity relationship; IC, inhibitory concentration; EC, effective concentration; PhIP, 2-Amino-1-methyl-6-phenylimidazol[4,5-β]pyridine; MRP, multidrug resistance protein; BCRP, breast cancer resistance protein; UDP, uridine diphospho; UDPGA, uridine diphosphoglucuronic acid; PAPS, 3'-phosphoadenosine-5'-phosphosulfate; NADPH, nicotinamide adenine dinucleotide phosphate; O-G, glucuronide; O-S, sulfate; V_{max}, maximum velocity; Km, michalelis-menton constant; Cl_{int}, intrinsic clearance; MM, michalelis-menton; OAT, organic anion transporter; PEPT; peptide transporter; P-gp, P-glycoprotein; mRNA, messenger ribonucleic acid; TR^-, transport deficient; $BCRP^-$, breast cancer resistance protein deficient; GST, glutathione-s-transferases; HepG2, hepatocellular carcinoma; Caco-2, colorectal adenocarcinoma; ATP, adenosine triphosphate; ATCC, American tissue culture collection; CYP, cytochrome; qRT-PCR, quantitative reverse transcription - polymerase chain reaction; QSMR, quantitative structure-metabolism relationship; $K_{i,app}$, apparent inhibitor constant; HBA, hydrogen-bond acceptor; HBD, hydrogen-bond donor; HBSS, Hank's buffered salt solution; KPI, potassium phosphate; rpm, rotation per minute; UPLC, ultra-performance liquid chromatography; PDA, photodiode array; LC, liquid chromatography; NH_4Ac, ammonium acetate; kV, kilo volts; psi, pound force per square inch; MS, mass

spectroscopy; UV, ultraviolet; MeOH, methanol; OH, hydroxyl; Gen, Genistein; Nar, naringenin; Phlor, phloretin; Api, apigenin; Kamp, kaempferol; HF, hydroxyflavone; DHF, dihydroxyflavone; THF, trihydroxyflavone; QHF, tetrahydroxyflavone; IS, internal standard; LLOQ, lower limit of quantification; min, minute; hr, hour; Avg, average; SD, standard deviation; HMF, hydroxy-methoxyflavone; DHMF, dihydroxy-methoxyflavone; DMHF, dimethoxy-hydroxyflavone; PLS, Partial Least Square; GFA, genetic function approximation; *Activ*, activity; *Uncert*, uncertainty of activity; HR, Hydrophobic region; AR; ring aromatic; RMS, root-mean-square; CoMFA, comparative molecular field analysis; EGCG, epigallocatechin gallate; AP, apical; BL, basolateral; and FDA, Food and Drug Administration.

LITERATURE REVIEW AND INTRODUCTION TO PROJECT

Flavonoids are the polyphenolic compounds which are shown to have various health benefits such as antioxidant, cancer chemoprevention, relief from post-menopausal systems, prevention against aging disorders and cardiovascular diseases.[1-5] Despite these beneficial properties, poor *in vivo* bioavailability (< 5%) of flavonoids poses a serious challenge in developing them as viable chemopreventive agents.[6-8]

Research done so far has proven that extensive *in vivo* metabolism by uridine-5'-diphospho-glucuronyltransferase enzymes (UGTs) in liver and intestine, is the main reason for the poor bioavailability of flavonoids.[9-11] Another but less important reason of flavonoids poor bioavailability is the sulfation pathway via sulfotransferase enzymes (SULTs). Studies done in our lab have shown that in and across different structural classes of flavonoids, compounds get metabolized by various UGT isoforms at different rates and extents.[9, 12, 13]

Our studies will first determine the main UGT isoforms responsible for metabolizing compounds from various sub-classes of flavonoids. We will then determine if the above compound-specific data can be utilized to predict which organ (liver or intestine) will play an important role in metabolizing a particular compound. Additionally, we will correlate the rates of glucuronidation of tested compounds by Caco-2 cell lysate to their respective rates of excretion of glucuronides in Caco-2 cell monolayers, highlighting the

role of efflux transporters such as MRP2 and BCRP in the excretion of glucuronides as the potential challenges in establishing this correlation.

Lastly, using the isoform-specific intrinsic clearance values, we will develop the isoform-specific semi-quantitative and quantitative structure-metabolism relationships (SMR) between the structures of flavonoids and metabolism by UGT 1A8 (mainly expressed in intestine) and UGT 1A9 (mainly expressed in liver). Various statistical and computational models such as logistic regression, pharmacophore, 2-D and 3-D quantitative structure-activity relationship (QSAR) modeling techniques will be used to establish the SMR of flavonoids metabolism by UGT1A8 and 1A9.

In this chapter (chapter 1), the first section (1.1) gives a detailed introduction of flavonoids related to their natural sources, chemical structures with classification, and problems with regards to their oral bioavailability. Section (1.2) introduces the main metabolic pathway for these compounds with focus on UGTs and SULTs, tissue-specific expression levels of UGT and SULT isoforms, and the structure-metabolism relationship between flavonoids and UGTs. Section (1.3) discusses the excretion/elimination of flavonoid glucuronides by efflux transporters. Section (1.4) introduces the role of UGT isoforms and Caco-2 cell culture model as the tools for studying drug metabolism and disposition respectively. Last section (1.5) describes various *in silico* techniques that can be used in developing metabolism prediction models.

1.1. Flavonoids

1.1.1. Introduction of flavonoids

Flavonoids are among the most ubiquitous groups of phytochemicals distributed in various plant substances such as fruits, vegetables, grains, barks, roots, stems, flowers, tea, and wine. These natural products were known for their beneficial effects on health long before flavonoids were isolated as the effective compounds.[14] However, during the past two decades, interest within the scientific community towards the research on flavonoids has increased many fold, mainly with the discovery of the French paradox, i.e., the low cardiovascular mortality rate observed in Mediterranean populations associated with red wine consumption and a high saturated fat intake. The flavonoids in red wine are responsible, at least in part, for this effect.[14, 15]

About 4000 natural flavonoid compounds of various structures are now known and more than 40 different types of biological activities have been attributed to these flavonoids including, anti-thrombogenic, anti-inflammatory, hepato-protective, cardio-protective, neuro-protective, antioxidant, sposmoiytic, anti-allergic, antiulcer, antimicrobial, antiviral, and anticancer.[14, 16-19]

1.1.2. Chemical structure of flavonoids

The basic structure of flavonoids contains a heterocyclic skeleton of flavan(2-phenylbenzopyrone). The structure is represented by a benzene ring (A), condensed with a heterocyclic six-member pyran or pyrane ring (C), which in 2nd or 3rd position carries a phenyl ring (B) as a substituent (Figure 1). Flavonoids are largely planar molecules due to the presence of double bond in the central aromatic ring and their structural variation comes in part from the pattern of substitution: hydroxylation, methoxylation, prenylation, or glycosylation. The constituent polyphenolic units are derived from the secondary plant metabolism of the shikimate pathway.[19, 20] Flavonoids are often hydroxylated at one or more of the following C- positions 3, 5, 7, 2', 3', 4', 5'.[19, 21]

Although they are sometimes found as their aglycones, flavonoids most commonly occur in plant kingdom as flavonoid-*O*-glycosides, in which one or more hydroxyl groups of the aglycones are bound to a sugar, forming an acid-labile glycosidic O-C bond.[22] There are certain hydroxyl groups in flavonoids that are usually glycosylated and the carbohydrate moiety can be L-rhamnose, D-glucose, gluco-rhamnose, galactose or arabinose.[19, 21] The glycosylated hydroxyl groups are the 7-hydroxyl group in flavones, flavanones, isoflavones and the 3- and 7-hydroxyl groups in flavonols and flavanols. 5-*O*-glycosides are rare for compounds with a carbonyl group at C-4, since the 5-hydroxyl group participates in hydrogen bonding with the adjacent carbonyl at C-4.[22]

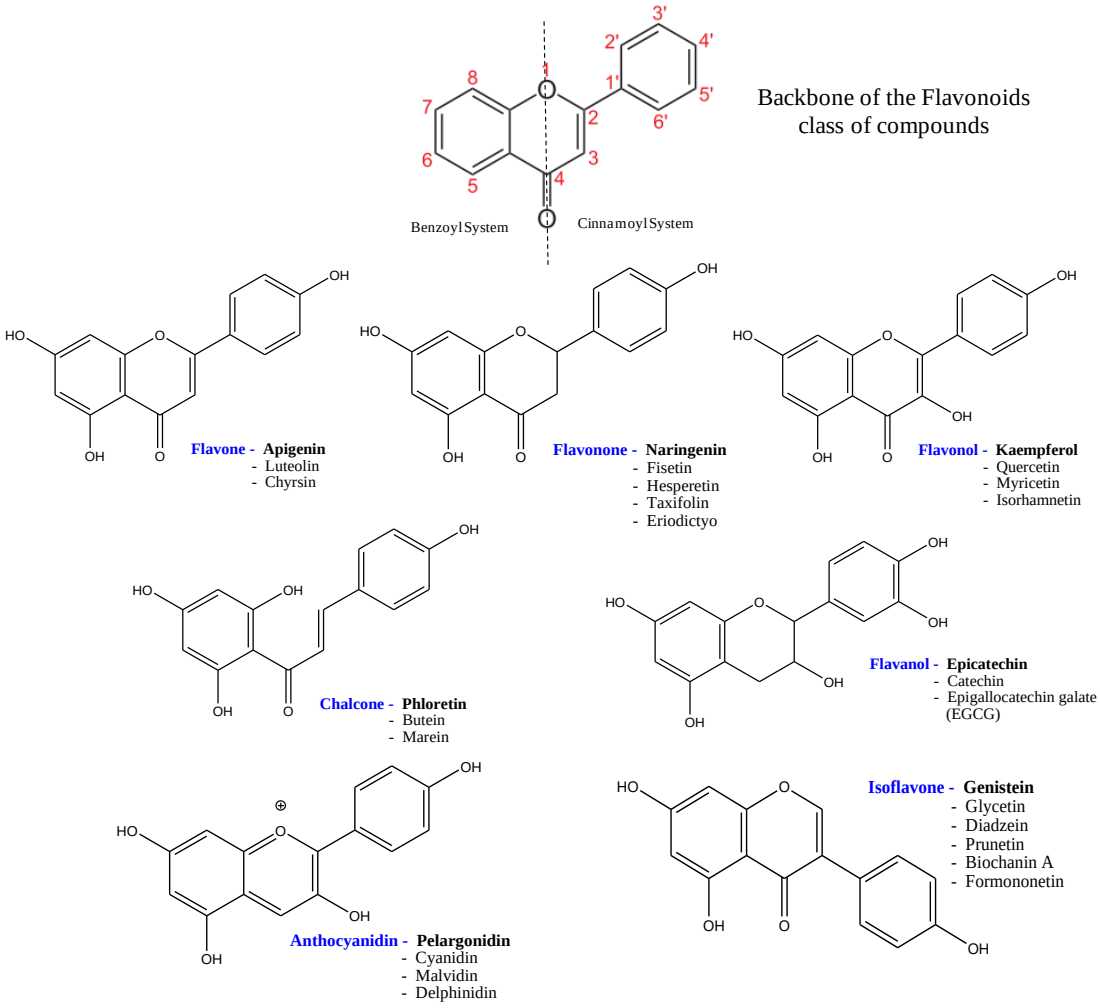

Figure 1. Chemical structure of various sub-classes of flavonoids.

Examples of compounds in each subclass are listed along with representative chemical structure and the name of the compound with representative structure is given in bold.

Flavonoid aglycones possess a common phenylbenzopyrone structure (C6-C3-C6), and they are categorized according to the saturation level and opening of the central pyran ring (Figure 1) into seven major sub-classes: flavone, flavonol, flavanone, flavanol, isoflavones, chalcone and antocyanidins. These sub-classes can easily be structurally differentiated based on the presence of a carbonyl carbon at C-4 (flavone), an OH group at C-3 (flavonol), a saturated single bond between C-2 and C-3 (flavonone), ring B attached to the C-3 position of ring C (isoflavone) and a combination of no carbonyl at C-4 and a saturated single bond between C-2 and C-3 with an OH group at C-3 (flavanol) (Figure 1).[14, 19, 22]

Chalcones are structurally different from other flavonoids because of opening of pyran ring at C-2. Anthocyanidines differ from other flavonoids as they have a positive charge in their structure (Figure 1). They are the salt derivatives of 2-phenylchromenylium cations, also known as flavylium cation. The counterion of the flavylium cation is mostly chloride.[14, 19, 22]

1.1.3. Sources of flavonoids

Flavonoids and other polyphenols are abundant in vegetables, fruits, chocolates, tea and wine. Vegetables such as spinach,[23] onion,[24] broccoli,[24] and fruits such as apples,[25, 26] pears,[27] grapes,[27] strawberries,[27] cherries,[28] and blueberries[28] have been shown to contain high amounts of flavonoids. Quercetin is most abundant in fruits and vegetables, such as

onions, apples, broccoli, and berries. Naringenin is mainly found in citrus fruits.[14, 22] Tea has also shown to contain high amounts of flavonoids with variations depending on types of tea leaves, the amount used, brewing time and temperature.[29] Red wine also contains large amounts of flavonoid whilst white wine has significantly smaller amounts of flavonoids.[30] Catechins are mainly found in green and black tea and in red wine, whereas anthocyanidins are found in strawberries and other berries, grapes, wine, and tea.[14, 22] More recently, new studies with regards to flavonoid contents in beverages and foods have shown that coffee also contain large amounts of polyphenols.[31, 32] Propolis (a resinous hive product collected by honey bees from different parts of plants) is another rich source of flavonoids.[22]

Isoflavones are selective with regards to their distribution as they are mainly found in the subfamily Papilionoideae of the Leguminosae. In comparison with flavonoids, natural sources of isoflavones are very restricted and are thus only found in certain dietary plants such as soybeans (which contain genistein and daidzein),[33] chickpeas (biochanin A),[34] alfalfa sprouts (formononetin),[35] red clover (daidzein and genistein, biochanin A and formononetin),[36] and groundnut (genistein)[37]. Highest total isoflavone concentration has been found in kudzu root with daidzein as the major isoflavone.[38]

1.2. Metabolism of Flavonoids

Despite reports of various beneficial biological activities *in vitro*, flavonoids have poor (less than 5%) and highly variable *in vivo* bioavailability in animals and humans.[1, 6-8, 39, 40] In plasma, flavonoids are present as conjugates (metabolites) with *in vivo* aglycone (drug molecule) concentrations ranging from 0.01 to 0.4 μM.[6, 40] These *in vivo* concentrations are significantly lower than the IC_{50} or EC_{50} values (5 to 50 μM) commonly reported for their anticancer effects *in vitro*.[1, 3, 41] Hence, use of flavonoids as anticancer agent is seriously limited by their poor bioavailability, which is mainly due to their high intestinal glucuronidation.[9-11]

Phase II metabolism, also known as conjugation reactions, is catalyzed by various transferases, such as UDP-glucuronosyltransferases (UGTs) and sulfotransferases (SULTs), leading to an increase in molecular weight of the parent molecule. It usually significantly increases the hydrophilicity of the drug so that it can be eliminated from the body, with the exception of methylation (e.g., methyldation of catechols), which either creates metabolite that are either less or equally polar. The main function of phase II metabolism is detoxifying in nature, so phase II metabolites usually are less bioactive (or toxic) than phase I metabolites, except in some cases such as glucuronides of morphine (more potent), ezitimibe (more potent), and PhIP (2-Amino-1-methyl-6-phenylimidazol[4,5-β]pyridine) (more toxic). Usually, *C*-glucuronides are more reactive and toxic than *O*-glucuronides.[42-45] Both enzyme systems (UGTs and SULTs) are

distributed widely in many tissues including liver and small intestine. UGTs are membrane-bound enzymes and are located in the endoplasmic reticulum in cells, while SULTs are present in the cytosol.[42, 46-48]

1.2.1. UDP-glucuronosyl transferases (UGTs)

UGTs utilize UDP-glucuronic acid as cofactor and transfer glucuronic acid to the substrates, forming hydrophilic conjugates called glucuronides (or β-D-glucopyranosiduronic acids, and these conjugates are usually β-glucuronidase sensitive). Substrates of UGTs includes endogenous compounds such as steroids, bile acids, bilirubin, hormones, dietary constituents like flavonoids, xenobiotics such as morphine and valproic acid, and environmental toxins and carcinogens such as PhIP.[43, 45, 49] UGT-catalyzed glucuronidation reactions are responsible for 35% of all drugs metabolized by phase II enzymes.[50]

For the glucuronidation reaction, the substrates typically possess hydroxyl group (alcoholic, phenolic), carboxyl, sulfuryl, carbonyl, or amino (primary, secondary, or tertiary) group in their structure. *O*-glucuronidations are more common than N- and C-glucuronidation. The normal function of the glucuronidation in mammals is to maintain the homeostasis of various endogenous substances such as bile acid, bilirubin and steroids, and to transport and detoxify xenobiotics.[43, 45, 49] Because the *UGT1A* locus is highly conserved and the individual UGT1 proteins are differentially expressed

throughout the gastrointestinal tract, it has been predicted that these proteins have evolved to facilitate the metabolism of digested matter, much of which exists as simple or complex phenols.[45]

Most of the substrates of UGTs are lipophilic in nature and therefore may be toxic to the cells. For these compounds to be eliminated through renal and biliary routes, they need to be converted to more hydrophilic metabolites such as glucuronides and hence glucuronidation by UGTs is considered as probably the most important detoxification pathway for a lot of xenobiotics and/or their phase-I metabolites. Hydrophilic phase II metabolites usually need a transporter to get excreted out of intestinal/liver cells. Various efflux transporters such as MRP2 and BCRPs are involved in efflux of phase II metabolites.[10, 51-54]

Nomenclature of UGTs: The UGT superfamily is comprised of 4 families (UGT1, UGT2, UGT3 and UGT8) and 5 subfamilies (UGT1A, UGT2A, UGT2B, UGT3A, and UGT8A).[55] Each family of UGTs must share at least 50% homology in their DNA sequences, whereas UGTs in each subfamily must share at least 60% homology in their DNA sequences. The nomenclature system uses Arabic numerals to represent the family (e.g., UGT1) whereas a letter designates the subfamily (e.g., UGT1A) and followed again by Arabic numeral denoting the individual gene (e.g., UGT1A1).[50, 56, 57]

In mammals, UGT1As expression results from a single gene locus *UGT1A*, located on chromosome 2q37, which is currently known to encode for the 9 functional proteins UGT1A1, 1A3, 1A4, 1A5, 1A6, 1A7, 1A8, 1A9 and 1A10. The mechanism by which the UGT1A mRNA transcript is spliced was attributed to the existence of 4 common downstream exons in conjunction with an upstream variable exon. Therefore, UGT1A nomenclature for example, is based on the *UGT1A* gene and the relative position of the first variable exon with respect to the 4 common exons on the un-spliced mRNA. From this organizational layout, the gene for UGT1A1 isoform is assumed to be the closest whilst gene for UGT1A12 is the most distant with respect to gene location between the variable and common exons. In addition, it is worthwhile to note that the gene sequences of the 4 common exons are conserved between all the mRNA transcripts within the UGT1A subfamily and is believed to make up the C-terminal portion of UGT1As and is responsible for co-factor binding. However, the variable exon is selected from a subset of 13 exon-1 sequences of the gene locus and transcripts for the N-terminal domain of the protein responsible for substrate binding.[50, 56]

With respect to the UGT2 family, multiple gene loci located on chromosome 4q13 comprise the following functional proteins: UGT2A1, UGT2B4, 2B7, 2B10, 2B11, 2B15, 2B17, and 2B28.[50, 56] In humans, *UGT2* genes have been characterized and shown to contain the same exon/intron branch points. Transcripts encoding UGT2A1, 2B4, 2B7, 2B10, 2B11, 2B15, and B17 have been characterized, and these genes have been mapped

to human chromosome 4q13 and 4q28.[45] The UGT2 family also shares common properties with UGT1A subfamily of enzymes in that they also have a conserved protein sequences at the C-terminal portion, whereas the N-terminal portion tends to be substrate-specific. However, the mRNA transcript in this family is spliced from 6 exons whereas only 5 exons are spliced in the UGT1A subfamily.[50, 56] A new *UGT2A3* gene (located on chromosome 4q13*)* has been found recently. cDNA clones of *UGT2A3* were isolated using pooled human liver RNA. UGT2A3 is a functional protein and UGT2A3 expressed by a baculovirus system shown to selectively glucuronidated bile acids, particularly hyodeoxycholic acid at the 6-hydroxy position.[58]

In contrast to the UGT1 and UGT2 families, which contain many members and which are primarily involved in xenobiotic metabolism, the UGT8 family contains only one identified member, UGT8A1, which has a biosynthetic role in the nervous system.[55] UGT8A1 is encoded by a gene of five exons on chromosome 4q26 and catalyzes the transfer of galactose from uridine diphospho (UDP) galactose to ceramide, an important step in the biosynthesis of the glycosphingolipids, cerebrosides, and sulfatides of the myelin sheath of nerve cells.[59]

UGT3 family contains two members, UGT3A1 and UGT3A2, which are encoded by genes of seven exons positioned adjacent to each other on human chromosome 5p13.2.[55] However, in contrast to the extensive studies on the function of the UGT1, UGT2, and UGT8 families, report on the function of UGT3 family is comparatively new and recently

published.[57] UGT3A1 enzyme catalyzes the transfer of *N*-acetylglucosamine from UDP *N*-acetylglucosamine to ursodeoxycholic acid (3α, 7β-dihydroxy-5β-cholanoic acid). This enzyme uses ursodeoxycholic acid and UDP *N*-acetylglucosamine in preference to other primary and secondary bile acids, and other UDP sugars such as UDP glucose, UDP glucuronic acid, UDP galactose, and UDP xylose. In addition to ursodeoxycholic acid, UGT3A1 has activity toward 17α-estradiol, 17β-estradiol, and the prototypic substrates of the UGT1 and UGT2 forms, 4-nitrophenol and 1-naphthol. UGT3A1 is found in the liver and kidney, and to a lesser, in the gastrointestinal tract.[57] There is no evidence that UGT1 and UGT2 forms use UDP galactose or UDP *N*-acetylglucosamine. In this study, we will focus on the *O*-glucuronidation of flavonoids with UGT1A and UGT2B subfamilies.

Localization and expression of UGTs: UGTs are mainly expressed in liver and various extrahepatic organs such as small intestine, bile ducts, stomach, colon, kidney, pancreas, brain and prostate. Some UGTs also are expressed (albeit not particularly abundantly) in lungs, esophagus, mammary and adrenal glands. There are 16 human UGT isoforms identified so far.[60] The most abundant isoform expressed in small intestine is UGT1A1, which is equally well-expressed in liver too. Quantitatively, UGT1A8 and 1A10 are major isoforms selectively expressed in small intestine while UGT1A9 is major isoform selectively expressed in liver and kidney.

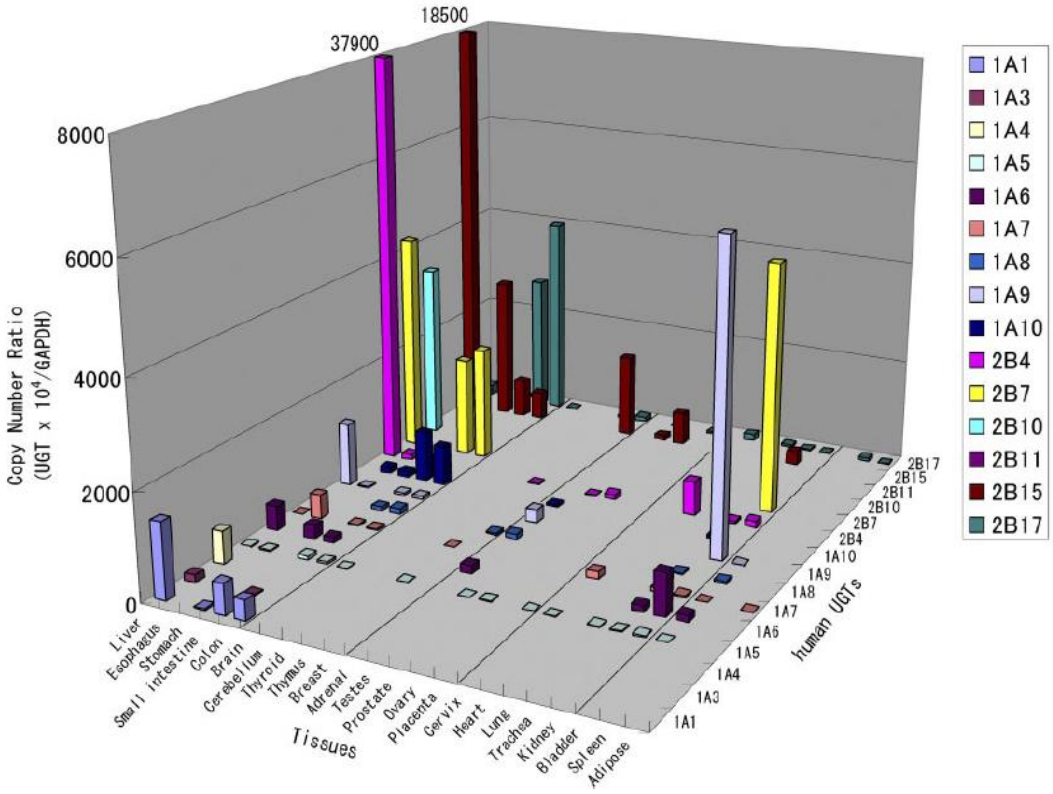

Figure 2. **Expression and localization of 15 human UGT isoforms in 23 human tissues.**

Twenty-three kinds of human cDNA were diluted 6 times with sterilized water, and 5 µl of each sample was subjected to real-time PCR using the respective specific primers under the condition as published.[61] The units of the *y*-axis represent the UGT copy number x 10^4 normalized to GAPDH, and the 37,900 and 18,500 values are included as off-scale data of UGT2B4 and UGT2B15, respectively. Each data point represents the mean value (n = 3–4), and error bars were omitted for clearer viewing. All of the data were reconfirmed by repeated examination. Figure is been reproduced here from Ohno and Nakajin (2009) with permission (Appendix H).[61]

Human small intestine UGTs also show greater inter-subject variability in their gene expression, protein abundance, and catalytic activity as compared to human liver UGTs. Human colon has shown markedly lower expression levels of UGTs as compared to small intestine, making it more susceptible to carcinogens.[44, 45, 48, 62, 63] Recently, Ohno and Nakajin (2009) published quantitative expression of mRNA levels of various UGT isoforms in several human tissues (Figure 2).[61]

1.2.2. Sulfotransferases (SULTs)

SULTs are the phase II enzymes which transfers a sulfonate group (SO_3^-) from the coenzyme 3'-phosphoadenosine-5'-phosphosulfate (PAPS) to a substrate. SULTs can either be cytosolic or membrane-bound which are located in Golgi apparatus. Membrane-bound SULTs sulfonate macromolecules such as peptides, proteins, lipids, and glycosaminoglycans and affect their structural and functional characteristics and even functions are not the focus of our discussion. Cytosolic SULTs, which are usually the ones involved in drug metabolism, are responsible for the sulfonation of xenobiotics and endogenous substrates such as hormones, steroids, bile acids and neurotransmitters.[64-68]

Usually the addition of a sulfonate moiety to a compound increases its water solubility and decreases its biological activity. Sulfation reaction in living cells is reversed by sulfatase, which hydrolyses the sulfonated conjugates. SULTs maintain and regulate the endocrine status of an individual by modulating the activity of steroid hormones and their

biosynthesis. Another important function of SULT is to inactivate xenobiotics. Although the primary goal of sulfoconjugation of xenobiotics is detoxification of the compound, it also results in the activation of certain chemical procarcinogens, such as turning certain dietary and environmental agents into more potent carcinogens.[64-70]

In humans, SULT superfamily consists of three families, SULT1, SULT2, and SULT4, with at least thirteen distinct members: SULT1 (1A1, 1A2, 1A3, 1A4, 1B1, 1C2, 1C4, 1E1); SULT2 (2A1 and 2B1_v1, 2B1_v2) and SULT4 (4A1_v1 and 4A1_v2). Semi-quantitatively, SULT1A1, 1A2, 1B1, 1E1 and 2A1 are exprerssed in human liver. Similarly, SULT1A1, 1A3, 1B1, 1E1, and 2A1 are expressed in human small intestine, whereas only SULT1A1, 1A3, and 1B1 can be detected in human colon.[69-72]

SULT1A1 is the major enzyme (>50% of total, range 420-4900 ng/mg cytosol protein) in the liver, followed by SULT2A1, SULT1B1 and SULT1E1, but no SULT1A3.[73, 74] Liver has also been shown to contain low levels of SULT1A2 expression.[73] SULT1E1 is present in the intestine and liver and is widely known as an "estrogen sulfotransferase".[75] In contrast, the small intestine contained the largest overall amount of SULT of any of the tissues, with SULT1B1 the major enzyme (36%), closely followed by SULT1A3 (31%), and SULT1A1, SULT1E1, and SULT2A1 more minor forms (19, 8, and 6% of total, respectively).[69, 76] SULT 1A1 and 1A3 in small intestine increases from jejunum to ileum.[69-72]

1.2.3. Structure-metabolism relationship (SMR) of flavonoids' and UGTs

Significance of SMR: Due to reported beneficial effects of flavonoids, various studies have been done with the focus on the structure–activity relationship (SAR) and quantitative SAR (QSAR) between flavonoids' structures and their various pharmacological activities such as antioxidative and radical scavenging activities, anti-inflammatory, cytotoxic effects, interactions with various receptors and estrogenic activities.[77] Interestingly, structure-metabolism relationship (SMR) between flavonoids' structures and UGTs have also been published, however the information is limited in nature as the crystal structure of any UGT has not been deduced yet. There can be two possible reasons why SMR of flavonoids and UGTs has attracted the attention of scientific community. One of them (as discussed above) is due to their poor bioavailability resulting from extensive *in vivo* metabolism by UGTs. Another reason is that glucuronides of flavonoids is shown to be equally or more active pharmacologically.[78, 79]

Currently, most of the focus is on quercetin glucuronides, and on isoflavone and catechin conjugates. For example, quercetin-7-G had stronger antioxidative property,[80] and was equally potent or even better inhibitor of human MRP1 and MRP2 than the quercetin aglycone.[81] Also, quercetin-3-G showed some cardiovascular protective effects in *in vitro* studies.[82] Similarly, epicatechin glucuronide was found to be able to inhibit NADPH oxidase that mediated oxidative stress in endothelial cells.[83]

Flavonoid glucuronides, including those of quercetin, kaempferol, daidzein and equol, are shown to be substrates for microsomal β-glucuronidase derived from various human organs/tissues including liver, intestine and neutrophils.[84] It has been suggested that glucuronides of flavonoids might pass through the vascular monolayers and then get converted back to (free) aglycones by the hydrolyzing enzymes. Therefore, the conjugated flavonoids in circulation may still play an important role in the treatment of various diseases. However, the exact mechanisms for the transport of flavonoid glucuronides into cells have not been clearly identified yet.[77] So, the debate is still on whether the focus should be on increasing the bioavailabilities of aglycones or their glucuronides. Irrespective, either focus will lead to better understanding of SMR between flavonoids and UGTs and further developing quantitative SMRs for the purposes of *in vivo* glucuronidation prediction that will aid better drug development designs.

Substrate Selectivity of UGT isoforms with respect to flavonoids: The UGT isoforms recognize and catalyze the glucuronidation of different functional groups (e.g., -OH, -COOH, -NH2, -SH and C-C). The isoforms demonstrate distinct, but often overlapping substrate selectivity. All of the UGT isoforms are capable of forming O-linked glucuronides with moieties such as acyl, phenolic, hydroxy, though with different efficiencies and turnover rates. The small molecules that form such phenolic-hydroxy glucuronides serve as substrates for most of the UGT proteins but are catalyzed most efficiently by the UGT1 proteins, with the exception of UGT1A4.[45]

The simple and complex phenols are also efficiently glucuronidated by the nasal mucosa-specific UGT2A1, but overall they are glucuronidated at reduced rates by UGT2B4, UGT2B7, and UGT2B15, about 10-20 folds lower than those of UGT1A proteins. There is considerable substrate-specific redundancy in phenolic glucuronidation between UGT1A1, UGT1A3, UGT1A7, UGT1A8, UGT1A9, and UGT1A10, as evident from the glucuronidation activities observed with small and bulky phenols as well as the hydroxy-glucuronide forming polynuclear hydrocarbons, anthraquinones, flavones, and coumarins.[45] The slightly larger bulky phenols and those that include the naturally occurring anthraquinones and flavanoids, although excellent substrates for most of the UGT1 proteins, are not readily glucuronidated by UGT1A6.[45]

In general, flavone and flavonol sub-classes are better substrates of many UGTs than their isoflavone counterparts. UGTs 1A1, 1A3, 1A6 and 2B7 were capable of metabolizing apigenin faster than the isoflavone genistein.[53] Similarly, UGTs 1A7, 1A8 and 1A9 were able to glucuronidate other flavonoid subclasses faster than isoflavones.[85] However, UGT1A10 was able to glucuronidate isoflavones as fast as flavones, flavonols, flavanones and chalcones.[85, 86] Recently, Tang *et al.* (2009) showed that for six isoflavones genistein, daidzein, glycitein, formononetin, biochanin A and prunetin, 1A1, 1A8, 1A9 and 1A10 were the most important isoforms, although the top isoform kept changing depending on the compounds and/or substrate concentrations.[87] Substrate

selectivities of different UGT isoforms have been published in a recent review article by Wong *et al*. (2009).[77]

Regiospecific glucuronidation of flavonoids by UGT isoforms: Flavonoids are polyphenolic compounds with several OH groups. Therefore, conjugations of glucuronic acid mainly occur at different OH and *O*-glucuronides are formed.[45] These products can demonstrate different pharmacological activities in humans. For example, quercetin-7-*O*-G had stronger antioxidative property than quercetin-3-*O*-G.[80] Hence, studying the regiospecificity of various UGT isoforms becomes important.

Day *et al.* (2000) published that the *K*m obtained at different OH positions in quercetin was in the order of 4′- < 3′- << 7- < 3, although the V_{max} at the 7-position was the greatest [88]. It was also found that the 5-position did not seem to be a site for glucuronidation. Boersma *et al*. (2002) showed that that the major metabolites of quercetin formed were isoform-dependent, and 7-*O*-G and 3′-*O*-G were the major glucuronides.[89] In the same study, luteolin which is flavone counterpart of quercetin and lacks OH at C-3 position was glucuronidated by UGT1A9 in human liver and UGTs 1A1 and 1A8 in human intestine, similar to quercetin. The percentages of metabolites formed from luteolin and quercetin followed the same trend: human liver microsome 7 >> 3′ > 3 (quercetin only) > 4′; human intestine microsome 3′ > 4′ > 3 (quercetin only) >> 7. Unlike quercetin, 7-*O*-G was the major metabolite of luteolin in most of the studied UGT isoforms expect for UGT1A1.[89]

In case of isoflavones, the C7-OH group was suggested to be the major site of glucuronidation, because the only compound with a blocked C7-OH group (i.e., prunetin, with C7-OCH3) was very poorly glucuronidated in Caco-2 cell model.[90] In the glucuronidation of genistein and diadzein, UGT1A isoforms were shown to more selective towards C7-OH than C4′-OH, with formation of 7-*O*-G higher than 4′-*O*-G by an order of magnitude.[91] Joseph *et al.* (2008) showed that different UGT isoform show regiospecificity in the glucuronidation of prunetin, 5-*O*-G by liver isoforms and 4'-*O*-G by intestinal isoforms.[51]

Both of the examples shown above suggest the glucuronidation of a particular OH group in flavonoid, depending upon the regiospecificity of UGT isoform. Furthermore, based on the UGT isoform expression pattern of a specific metabolic organ, e.g. liver with 1A1 and 1A9 and intestine with 1A1, 1A8 and 1A10, the main glucuronide formed upon i.v. or oral administration should be significantly different.

Investigations of SMR, including substrate selectivity and regiospecificity of particular UGT isoform can provide valuable information. The knowledge of UGT substrate and inhibitor selectivities, and binding affinities can aid in the identification of compounds whose elimination may be impaired in subjects with variant genotypes (such as Gilbert syndrome for UGT1A1 substrates). It can also help in the prediction of either drug-drug or inhibitory interactions with other xenobiotics and endogenous compounds metabolized by a particular isoform.[92]

The proposed mechanism of action of glucuronidation by UGTs was SN_2 nucleophilic attack by the ~OH group of the flavonoids on the C-1 of pyranose acid ring of UDP-glucuronic acid.[93] Therefore, the position of the ~OH groups of flavonoids coupled with the nucleophilicity and steric characteristics may affect its overall glucuronidation efficacy.[77] Some of the flavonoids' structural features that have shown to affect the SMR between flavonoids and UGTs are, presence of phenolic group in the structure of flavonoids;[94] position and number of OH groups and nucleophilicity;[95, 96] low activity of C-5 position;[86] planar conformation;[77, 86] effect of sugar moieties;[86] and effect of methoxylation.[77]

1.3. Role of Efflux Transporters in Disposition of Flavonoids

The efflux transporters for conjugates of flavonoids play an important role in deciding the actual intracellular disposition of flavonoids in intestine. The role of efflux transporters is particularly seen in cases of flavonoids where the phase II conjugation reactions results in a highly hydrophilic metabolites (glucuronides or sulfates) which are incapable of passively diffusing across the cellular membrane. Hence, the excretion of conjugated metabolites from cells is dependent upon their transport by efflux transporter on apical and/or basolateral membrane. Also, it is more complex to sort out the mechanism of drug-drug interactions due to drugs and flavonoids being a substrate of enzyme(s) and drugs and flavonoid conjugates being a substrate of transporter(s).[54, 97-100]

1.3.1. Expression of efflux transporter in intestine

Intestinal epithelial cells express a variety of uptake transporters (such as PEPT1 and OATPs) and efflux transporters (P-gp, MRPs, BCRP) on the apical and basolateral membrane, for the influx and efflux of the endogenous and xenobiotic substrates, respectively. The efflux transporters have a critical role in limiting influx and facilitating efflux to prevent the intracellular accumulation of the flavonoids and its phase II metabolites. In tumor cells, such functions confer multidrug resistance for various anticancer agents.[101-105]

The enterocytes show localized expression of the efflux transporters on apical and basolateral membrane. Apical membrane expresses known transporters such as P-gp, MRP2, MPR4 and BCRP, while basolateral membrane expresses MRP1, MRP3 and MRP5. The small intestine shows a high expression of MRP2, MRP3, P-gp and BCRP and lower expression of MRP1, whereas colon expresses P-gp highly but shows a lower expression of MRP1, MRP2 and MRP3 but no BCRP.[101-107]

The expression of efflux transporter also varies between different segments of small intestine. In human intestine, the mRNA levels of the efflux transporters were ranked in the various segments of intestine, which was MRP3>>P-gp>MRP2>MRP5>MRP4>MRP1 in the duodenum; BCRP_MRP2>P-gp_MRP3~ MRP6~MRP5_MRP1>MRP4>MDR3 in the jejunum; P-gp>MRP3>>MRP1~MRP5~

MRP4>MRP2 in the terminal ileum; and MRP3>>P-gp>MRP4~MRP5>MRP1>> MRP2 in the colon. Interestingly, basolateral transporters, MRP1, MRP3, and MRP5 show reduction in transporter expression from ascending to sigmoid colon, whereas, the expression levels of apical transporters P-gP, MRP2 and MRP4 remain constant throughout the entire colon.[103, 105]

The P-gp, MRPs and BCRP also show substrate overlapping in the transport of parent drugs and their metabolites, which can result in possible drug-drug interaction in the liver and intestine. It also explain the possible compensation process in the efflux of the drug and conjugated metabolites in TR^- rats (MRP2 deficient rats) or $BCRP^-$ mice, where in absence of one efflux transporter, expression of other efflux transporters on apical and/or basolateral membrane of liver and intestine tends to increase to compensate for the deficiency.[97, 99, 108, 109] In case of flavonoids, MRP2, MRP3 and BCRP are shown to be the most important efflux transporters involved in excretion of flavonoid conjugates.[13, 110-114]

1.3.2. Coupling of metabolizing enzymes and efflux transporters

Coupling of enzymes and transporters are found in the biological systems to maximize the absorption of nutrients such as proteins and carbohydrates. It also often plays an important role in the cellular excretion of hydrophilic phase II conjugated metabolites and thus has a profound impact on bioavailability, drug metabolism and drug-drug and drug-herb interactions. Coupling process in drug disposition can be defined as a phenomenon

where process of drug metabolism and excretion/elimination of drug and its metabolites can influence each other and change the dynamics substantially.[53, 115]

The process of coupling of efflux transporters and phase II enzyme in the intestinal disposition of flavonoids can be explained by the "revolving door" theory. According to the "revolving door" theory, the hydrophilic conjugate metabolites (glucuronides and/or sulfates) of flavonoids cannot freely move out of the cells by passive diffusion. Rather, they depend on action of the efflux transporters for their excretion. Hence, the disposition fate of flavonoids is decided by the fact one of these two processes may act as the rate-limiting step. In other words, either formation of flavonoid metabolites by enzymes or the excretion of the metabolites by efflux transporters can be the rate-limiting step. The consequences of the coupling according to this theory can be an imbalance between formation and excretion of hydrophilic conjugates of flavonoids.[10, 13, 53, 116, 117]

If the excretion of metabolites (glucuronides and/or sulfates) of flavonoids by efflux transporters is the rate-limiting step, then the rate of metabolite excretion will be lesser than the maximal rate of metabolite formation. It can increase the accumulation of metabolite inside cell which might have one of two consequences or both. First, the reverse-enzymatic reaction can cause the conjugated metabolite to be converted back to the parent drug compound. This can decrease the net forward rate of metabolite formation. Or, the metabolite can cause inhibition of forward enzyme reaction (negative

feedback mechanism via classical product inhibition) which in turn can decrease the net rate of metabolite formation.[10, 13, 53, 116, 117]

On the other hand, if formation rate of metabolites (glucuronides and/or sulfates) of flavonoids is the rate limiting step, then the efflux transporter can readily remove the formed metabolites which could have inhibitory effects via product inhibition. Therefore, the action of efflux transporters can favor the forward enzymatic reaction of conversion of parent drug into metabolite. This can result in higher than expected excretion rates of metabolites based on cellular enzyme activities measured using sub-cellular fractions.[10, 13, 53, 116, 117]

The process of coupling can be simple, involving one enzyme isoform and one specific transporter. However, it is often more complex in nature as it may involve more than one individual process that somehow affects and influences the other processes. The factors or individual processes that may contribute to overall coupling phenomenon in flavonoid disposition are: (a) efflux of flavonoids at apical or basolateral side or both; (b) sequestration of metabolites in cytosol by some of efflux transporters and then pumping them out once metabolite-transporter complex merged into cell membrane; (c) involvement of multiple transporters in the efflux of flavonoid metabolites; (d) involvement of multiple enzyme systems and isoforms in metabolizing the flavonoids; (e) formation of multiple metabolites each using similar yet different sets of efflux transporters; and (f) effect of activity of one enzyme or transporter system on the

performance of others. For example, glutathione is used as a co-substrate by the efflux transporters, such as MRPs. It is also a co-factor of enzyme glutathione-s-transferases (GST). The overall activity of GST can diminish glutathione pool in cells and hence in turn can reduce efflux of conjugate metabolites and therefore decrease the overall metabolism and bioavailability of flavonoids.[13, 53, 117]

The scientific community has been facing a lot of challenges in sorting out this complex process. The major reason has been the lack of specific inhibitors for enzymes or transporters involved in drug disposition. To overcome this, various approaches such as gene-silencing and transfection, has been used in various cell lines in order to under- or over-express certain enzyme and/or transporters respectively. But, it is difficult to extrapolate the *in vitro* data obtained by using these approaches to *in vivo* conditions.[99, 115, 117-120]

The compensation process is seen in animals that are deficient in one transport or enzyme as a result of knock-out or transgenic manipulation or natural breeding, which is another major problem. It is known that enzyme and/or transporters of same family and/or subfamily shows higher expression, but the mechanism of compensation is not known when gene(s) of interest is silenced or induced for prolonged period of time.[99, 115, 117-121]

Besides increasing the drug metabolism, coupling process also increases the potential of drug-drug and drug-herbal interactions. However, the coupling makes it difficult to sort

out the mechanisms of drug interactions as it is much more difficult to sort out complex network of barriers as discussed above. It is possible that more than one agent and/or multiple mechanisms of modulation of action (inhibition or induction) might affect the output from the network i.e. clinically significant drug interaction. Even if the mechanism of drug interaction is somehow established, it is difficult to develop the drugs that will not modulate the enzyme and/or the efflux transporter involved in the interaction. The drugs which interact with enzyme and/or transporters can cause modulation of cellular excretion process, resulting in more severe drug interactions.

1.4. In-vitro Models of Studying Drug Metabolism and Disposition

In order to study glucuronidation of flavonoids, we need models which can provide UGT isoform specific data and can mimic in-vivo condition of enzyme-transporter interplay. The two most important method of studying metabolism and disposition of drugs via glucuronidation respectively have been UGT isoforms model and Caco-2 cells monolayer model.

1.4.1. UGT isoform model

Recombinant human UGT isoforms are commercially available as Supersomes™. Supersomes™ developed by BD biosciences are the UGT isoforms derived from baculovirus infected insect cells expression system. The baculoviruses used to infect the insect cells have been engineered to express specific UGT isoform cDNA. So far, only 12

UGT isoforms (Supersomes™) are commercially available UGT1A1, 1A3, 1A4, 1A6, 1A7, 1A8, 1A9, 1A10, 2B4, 2B7, 2B15 and 2B17. Recombinant human UGT isoforms are usually used in the reaction phenotyping studies.[122, 123]

The goals of the reaction phenotyping is to determine the relative contribution of UGT metabolism to overall clearance of the compound, followed by identification of the metabolic profile and systematic characterization of the specific UGT isoforms involved in formation of each major metabolite. To achieve these goals, two approaches can be employed. One, the individual recombinant human UGT isoforms can be used to evaluate the intrinsic ability of each individual isoform to metabolize a drug candidate.[51, 87, 124, 125] However, if the drug is metabolized by more than two recombinant human UGT isoforms, measurements of enzymatic activity alone do not provide sufficient information to estimate the relative contributions of each UGT isoform to the total glucuronidation of the drug. Further studies with highly selective chemical inhibitors and/or antibodies should be conducted in pooled human hepatic or intestinal microsomes to address the relative contribution of each isoform.[122, 123]

It should be noted that sometimes a recombinant human UGT isoforms, which is shown to be active in glucuronidation in the absence of other isoforms, may play little or no role in microsomal or cellular glucuronidation in the presence of other UGT isoforms due to the competition for substrate. The other approach is to determine the K_m and V_{max} values of the drug with each active recombinant human UGT isoform to calculate intrinsic

clearance ($Cl_{int} = V_{max}/K_m$) values for each UGT isoform. Based on the intrinsic clearance and the relative abundance of each UGT isoform in human liver or intestinal cells, the relative importance of different UGT isoforms in the glucuronidation of the compound of interest can be evaluated.[122]

Usually, both these approaches have worked successfully in case of P-450 isoforms,[122, 123] but there are some major limitations in use of these approaches to accurately predict the *in vivo* metabolic fate of drug via glucuronidation by UGTs. The various isoforms involved in drug glucuronidation are not expressed at the same level in normal drug-metabolizing cells such as hepatocytes, enterocytes, HepG2 and Caco-2 cells. As a result, rates of glucuronidation in recombinant human UGT isoforms must be normalized for their cell expression levels. The extrapolation of glucuronidation rates to predict the relative contributions of the various UGTs to overall glucuronidation is challenging due to limited information regarding the relative expression and activities of the various UGT isoforms in above-mentioned cells.[122] In addition, there appears to be significant inter-individual variability in UGT enzyme activities.[62]

Also, there are no known selective chemical inhibitors and/or antibodies available for UGT isoforms to run inhibition studies.[122] Therefore, reaction phenotyping studies for glucuronidation are generally used as an alert for compounds that may be metabolized by UGT1A1 and thus present a risk for potential competition with bilirubin glucuronidation, or to provide an overall alert for compounds that may be metabolized by only one

isoform and, thus, present a higher risk for drug–drug interactions than a compound that may have more balanced elimination by multiple pathways.[122]

The other limitations of reaction phenotyping for predicting glucuronidation are: (1) many UGT isoforms follow atypical or mixed kinetics instead of Michaelis menten kinetics, so determining accurate K_m and Cl_{int} are difficult;[87] (2) UGT isoforms have over-lapping substrate selectiveities to an extent that sometime about 5-10 isoforms might be involved in overall contribution of drug glucuronidation in *in vitro* studies.[87] However, it is difficult to say, if all these isoforms are involved and contribution in the overall *in vivo* glucuronidation also; (3) the glucuronides produced from *in vitro* incubations cannot be removed from the reaction mixture and can potentially inhibit glucuronidation by product inhibition, whereas efflux transporters are removing the glucuronides from the intact cell *in vivo*;[50] (4) saccharolactone is added as β-glucuronidase inhibitor whereas no such inhibition is happening *in vivo;* (5) no enteric or enterohepatic recycling which can increase the overall glucuronidation of drug does not happen *in vitro*; and finally is the issue of "latency".[50] Generally, detergents or pore forming molecules such as alamethicin is incorporated into *in vitro* reaction mixtures to overcome this latency effect. Alamethicin is the preferred activating agent because it is non-denaturing to UGT isoforms at excess concentrations.

1.4.2. Caco-2 cell culture model

The Caco-2 cell model has proven to be the most popular *in vitro* model used in pharmaceutical industries and academia (a) to rapidly assess the cellular permeability of potential drug candidates, (b) to elucidate pathways of drug transport (e.g., passive versus carrier mediated), (c) to assess formulation strategies designed to enhance membrane permeability, (d) to determine the optimal physicochemical characteristics for passive diffusion of drugs, and (e) to assess potential toxic effects of drug candidates or formulation components on this biological barrier.[126, 127] The Caco-2 cells are human colon adeno-carcinoma cells that differentiate into polarized epithelial monolayer upon reaching confluence and are shown to express several morphological and biochemical characteristics of small intestinal enterocytes (e.g., formation of microvilli, tight junctions and desmosomes, hydrolases, nutrient transporters, and expression of brush-border enzymes such as sucrase-isomaltase).[128]

Since, differentiated Caco-2 cells express various phase I enzymes such as cytochrome P-450 isoforms and phase II enzymes such as UDP-glucuronosyltransferases, sulfotransferases and glutathione-S-transferases, as well as transport proteins of the ATP-binding cassette family, such as P-gp, MRPs and BCRP, this model can also allow the study of presystemic drug metabolism.[127, 129, 130] Published reports have shown interplay between drug-metabolizing enzymes and efflux transporters.[131, 132] Hence, studying drug

metabolism in Caco-2 cells not only can be a tool to estimate clearance rate but also can be used for better understanding of the enzyme-transporter interplay.[133, 134]

Caco-2 Cell variant (TC-7): The initial parental Caco-2 cell line was obtained from American Tissue Culture Collection (ATCC). Caco-2 cell culture, even in stationary phase of growth showed heterogeneity in subpopulations with different morphologies. Therefore, to improve the homogeneity and the stability of the cell population, clonal cell lines were isolated and characterized. The Caco-2 subclone TC-7 was generated by passaging Caco-2 cells 198 times, thereby selecting faster growing cells from the inhomogeneous Caco-2 population. TC-7 cells differ from the parental Caco-2 cells in many characteristics, such as their shorter population doubling time; higher cell density; higher glucose consumption; elevated expression level of CYP3A4, UGTs and SULTs.[129] Due to higher UDP-glucuronosyltransferase (UGT) expression in TC-7 cells as compared to the parental Caco-2 cells, TC-7 cells have been widely used as a tool to investigate the metabolism and transport of conjugates of xenobiotics with glucuronic acid.[130, 135]

Enzyme Expression in Caco-2 cells: Enzyme expressions in Caco-2 cell lines suggest a closer resemblance of these cells to fetal rather than to adult ileal enterocytes.[136] In case of different CYP isoforms, Caco-2 TC-7 cells have shown equivalent or many folds higher expression levels of CYP1A1, 1A2, 2C8-19, 2D6, 2E1 and 3A5 as compared to human liver.[137]

Table 1 Expression levels of different UGT isoforms in fully differentiated Caco-2 cells, grown on filter for at-least 21 days, at several passage levels determined by qRT-PCR

UGT Isoforms	mRNA expression levels at Caco-2 cell passage number			
	P31	P37	P43	P49
1A1	+	+	++	+
1A4	+	+	+	±
1A5	+	+	++	+
1A6	++++	++++	++++	+++
1A7	++	+	++	+
1A8	++	++	+++	++
1A9	+	+	++	+
1A10	+	+	++	+
2B4	±	±	±	+
2B7	++	+	++	+
2B10	±	±	±	±
2B11	++	+	++	++
2B15	+	±	±	±
2B17	++	++	+++	+++
2B28	+	±	±	±

Expression levels relative to β-actin: + means >0.0005; ++ means >0.0015; +++ means > 0.005; ++++ means > 0.01. Table Adopted from Siissalo *et al.* (2008).[134]

The major cytochrome P-450 isoforms CYP3A4 present in the liver and intestine is shown to have a very low expression level in the Caco-2 cells.[137] Studies have shown that UGT isoforms 1A1, 1A3, 1A4, 1A5, 1A6, 1A7, 1A8, 1A9, 1A10, 2B7, 2B11 and 2B17 are detected in Caco-2 cells lines.[130, 134, 138]

However, the expression level of UGT 1A subfamily in Caco-2 cells[130, 134] and its variant TC-7[138] varied significantly in the published reports, with UGT1A6 being the most expressed isoform. In Caco-2/TC-7 cell lines, UGT1A1, 1A3, 1A4, 1A6 have high expression levels whereas levels of UGT1A8, UGT1A9 are poorly expressed. UGT1A7, 1A10 are almost undetectable.[138] Unfortunately, the UGT2B4, 2B7, 2B15 and 2B17 isoform expression levels in Caco-2 cell lines were not published in this study. Siissalo *et al.* (2008) recently published relative expression level of all UGT isoforms except UGT1A3, determined by qRT-PCR, in fully differentiated 21 days old Caco-2 cells samples grown on filters (Table 1).[134]

In case of sulfotransferases, SULT1A1, 1A2, 1A3, 1B1, 1C1, 1C2, and 2A1 were expressed in both parental Caco-2 and TC-7 cell lines. SULT2B1a, SULT2B1b, and SULT4A1 were absent. SULT1E1 protein was found in TC-7 but not in Caco-2 cells. However, expression of several SULT forms started earlier in Caco-2 cells than in TC-7 cells and SULT1B1 and SULT2A1 levels were much lower in Caco-2 cells than in TC-7 cells. Overall, differentiated Caco-2 and TC-7 cells show higher levels of SULTs as is human intestinal mucosa.[129]

Table 2 SULT expression levels in Caco-2 and TC-7 cells compared with colonic and ileal mucosa

SULT Isoform	mRNA[b]	ng SULT Protein/mg Cytosolic Protein[a]			
		Caco-2[c]	TC-7[c]	Colon[d]	Ileum[d]
1A1	++	70	70	180	1200
1A2	n.t.[b]	40	65	<25[d]	<75[d]
1A3	+++	1100	2200	320	1500
1B1	-	11	77	120	420
1C1	+	10	25	<3-D	<3-D
1C2	+++	60	95	n.t.	n.t.
1E1	+	<10	70	<6	50
2A1	+++	80	430	<10	150
2B1a	-	<100	<100	n.t.	n.t.
2B1b	-	<100	<100	n.t.	n.t.
4A1	n.t.	<400	<400	n.t.	n.t.

a Determined by immunoblotting. For negative results, the limit of detection is given (which can vary depending on the antiserum used, the amount of protein loaded on the polyacrylamide gel, and the presence of other SULT forms).

b n.t., not tested or tested with an insufficient limit of detection.

c Determined at 19 and 14 days after reaching confluence for Caco-2 and TC-7 cells, respectively.

d Individual samples showed faint immunoreactivity near the limit of detection.

Table adopted from Meinl *et al.* (2008)[129]

The SULT pattern is most similar to that found in small intestine, although levels of SULT1A1 and SULT1B1 are lower, and those of SULT1C1 are higher in Caco-2 and TC-7 cells than previously found in intestinal samples (Table 2).[129]

Efflux Transporters Expression in Caco-2 cells: Taipulensuu *et al.* (2001) showed that transcript levels of 9 ABC transporters were correlated well between jejunum and Caco-2 cells (r^2 = 0.90). However, *BCRP* exhibited a 100-fold lower transcript level in Caco-2 cells compared with jejunum.[103] In Caco-2 cells grown for 21 days on filter inserts, the rank order of efflux transporter was MRP2 > Pgp ≈ MRP3 > BCRP. Table 3 shows the transporter expression in Caco-2 cells relative to the expression in different regions of the human intestine.[106] The MDR1, MDR3, MRP2, and BCRP proteins are all located at the apical part of the plasma membrane of polarized cells such as epithelia, whereas the MRP1, MRP3, MRP5, and MRP6 proteins seem to be basolaterally localized.[103]

Studies have shown that the passage number (the number of times the cells in the culture have been detached, diluted, and grown again to near confluence) of Caco-2 cells also affects many of their properties, such as cell viability, growth in culture and expression levels of various enzymes and transporters. UGTs expression and glucuronidation activity of Caco-2 cells has been shown to change with the passage number.[133, 134] Our lab has also established that due to morphological and functional changes in the cell monolayer, results of Caco-2 cell transport studies should not be compared beyond 10 passages.

Table 3 The transporter mRNA expression in Caco-2 cells relative to the expression in different regions of the human intestine presented as the 18S-normalized mRNA expression levels in Caco-2 cells (21 days old) (triplicates) relative to the expression in human duodenum (n=14), ileum (n=13) and colon (n=14).

Transporters	**Relative mRNA expression level in Caco-2 cells with respect to**		
	Duodenum	**Ileum**	**Colon**
P-gP	3.1	0.4	1.9
BCRP	0.1	0.05	0.1
MRP2	7.3	8.4	1080
MRP3	3.4	4.2	1.5

Table adopted from Englund *et al.* (2006)[106]

1.5. *In silico* Techniques for Developing Metabolism Prediction Models

Use of *in silico* techniques in the of metabolism prediction models had increasingly gained attention in past two decades.[139-141] In order to exploit the beneficial effects, flavonoids with low UGT metabolism need to be screened from naturally occurring flavonoids and/or their synthetic analogues and be developed into chemopreventive agents. In order to screen for the better compounds in terms of desired metabolic outcome and lower drug-drug interactions UGT "fingerprinting" can be used. UGT "fingerprinting" is required to be done in the initial phase of drug development to understand the metabolic fate of a new chemical entity via glucuronidation pathways and possible drug-drug interaction it can cause with the marketed drugs. Therefore, there is a need to study the metabolism of flavonoids by specific UGT isoforms.

Also, comparing the rate of excretion of metabolites in the Caco-2 cell culture model with the rate of metabolism by various recombinant human UGT isoform(s) reported in Caco-2 cell lines, can provide insights about how the structure of flavonoids are correlated to their disposition in the Caco-2 cell culture models and help in developing semi-quantitative structure-disposition relationships of flavonoids in intestinal cells. It is difficult to perform *in vitro* UGT "fingerprinting" of all the naturally available (~4000 compounds) and synthetically designed flavonoids. Therefore, there is a need to use more

economic and time saving screening tools, such as *in silico* quantitative SMR (QSMR) prediction models.[139-141]

Based on direct analysis of the experimental data from UGT isoforms or human liver or intestinal microsomes, it is somewhat difficult to develop good QSMR models, so better computational (*in silico*) tools are required to develop QSMR models with good predictive ability. These prediction models however then has to be correlated with more complex data from *in vitro* models such as cell cultures and *in vivo* models such as whole animal. Because of the involvement of efflux transporters in the complex models mentioned above, such *in silico- in vitro* and *in silico-in vivo* correlation will be a greater challenge to develop.

Homology and pharmacophore modeling and two/ three dimensional quantitative structure activity relationships (2-D/ 3-D QSAR) are the *in silico* approaches that can be used to establish QSMR.[139-145] Homology modeling uses the 3-D structure of a homologous enzyme (with ≥ 50% sequence identity) to develop a 3-D structure for the target enzyme (UGT in this case), whose structure is not known. The developed structure of enzyme is then used to establish a 3-D QSMR between the enzyme and substrate using 3-D QSAR modeling. However, until now, it's been impossible to use homology model for predicting glucuronidation because of the poorly understood structure-function relationship of UGT and lack of availability of a 3-D X-ray crystal structure of an enzyme homologous to UGT.[142, 146, 147]

In silico modeling for glucuronidation has focused on Pharmacophore-based 2-D and 3-D QSAR modeling to develop a QSMR. A pharmacophore is a defined 3-D geometrical arrangement of those interactive functional groups in the structure of a molecule, which is recognized at the receptor (i.e. enzyme interaction) site and is responsible for the biological activity (i.e. glucuronidation) of that molecule. Pharmacophore modeling uses pharmacophore(s) of substrate and non-substrates of the target protein to develop a QSMR[141, 147]. Many studies have been published in the literature regarding 3-D QSAR models for CYP (Cytochrome P-450) enzyme isoforms,[146, 148-150] but development of such models for UGT isoforms[141, 151, 152] have been started recently and very few studies have been published. Ekins *et al.* (2005),[146] developed quantitative pharmacophore models for inhibitors of CYP isoforms (3A4, 3A5 and 3A7) using Catalyst® software (version 4.6, Accelrys, San Diego, CA, USA), with a high correlation (>0.9) between observed and predicted values.

Sorich *et al*. (2002) presented the first generalized 2-D and 3-D QSAR and pharmacophore models developed for UGT.[92] Different methodologies were used to develop models which predicted the substrate selectivity and binding affinity toward UGT1A1. The substrate affinity (as reflected by low apparent inhibitor constant ($K_{i,app}$) was in the order: quercetin ~ naringenin >> 3-HF; this was consistent with the substrate selectivity study on UGT1A1 mentioned above.[153] Another study on UGT1A9 indicated

that the substrate affinity is in the order: quercetin ~ 3-HF >> naringenin,[154] which is different from that observed for UGT1A1.

However, it is important to note that these models are for predicting substrate selectivity and binding affinity, rather than the glucuronidation efficiencies. It is very much possible that a bulky flavonoid substrate might fit in the active site, but might not be glucuronidated, or only weakly glucuronidated. A QSAR study for UGTs 1A6 and 1A9 on simple phenols was done to study the effects of 4-substutients (i.e., para position) on phenol glucuronidation. The authors found that in UGTs 1A6 and 1A9, V_{max} decreased as substrates' molecular volume increased, which means that bulky flavonoids might act as UGTs inhibitors instead of substrates.[155]

These models have shown reasonably good predictive ability (in range of 60-80%). But, so far no UGT QSMR model has been developed which focuses on predicting the level of metabolism of substrates, which is of great interest to us in the case of flavonoids. In order to generate computational model for flavonoid glucuronidation, various kinetics parameters such as K_m, V_{max} and intrinsic clearance values ($Cl_{int} = V_{max}/K_m$) can be used as metabolism activity. At substrate concentration lower than K_m, Cl_{int} values can be approximated as ratio of rate of metabolism and substrate concentration (~V/S), which can be generated with lesser time and resources than V_{max} and K_m. Hence in our study, approximate Cl_{int} values of flavonoids with specific UGT isoform will be used as metabolism activity to develop SMR models.

The discriminative feature pharmacophore-based models predicted the biological property ($K_{i,app}$ in this case) on the chemical structural features of the substrate such as hydrogen bond donors, hydrogen bond acceptor and hydrophobic or aromatic regions in 3-D. It was found that the UGTs 1A1 and 1A4 pharmacophores share a high similarity in their core features, such as, the site of glucuronidation is invariably adjacent to a hydrophobic region, with another hydrophobic domain located 6 – 8 Å from the site of conjugation. The core features in the structure of substrates for UGT1A9 were similar to that of UGT1A1/1A4 substrates but there was an extra hydrogen-bond acceptor (HBA) region near the outermost hydrophobic region.[154] However, UGT1A10 pharmacophore generated with two hydrophobic regions and a HBA[86] was very similar to that of UGT1A9.[154]

As discussed above there are various factors which could affect the cellular disposition of flavonoids via glucuronidation. We think that during the development of isoform-specific SMR between UGT and flavonoids, we will face challenges due to several factors such as, substrate overlapping between various UGT isoforms; production of multiple regiospecific glucuronides in different ratios based on substrate structure and UGT isoforms; unavailability of sufficient information on active site conformation and crystal structure of UGT; rate-limitation of excretion of glucuronides by efflux transporters in intact cells (e.g. Caco-2 cells, hepatocytes); and atypical kinetics of glucuronidation.

Additionally, we are not yet sure which is the best kinetic parameter (K_m, V_{max}, Cl_{int}) to develop the SMR prediction models.

In present study, for generating *in silico* models for glucuronidation of flavonoid by UGTs, we will be using 2-D QSAR and Pharmacophore-based 3-D QSAR modeling using approximate Cl_{int} as metabolic activity. Pharmacophore modeling will use pharmacophore(s) of substrates and non-substrates of the UGT isoform 1A8 (major isoform in intestinal cells) and 1A9 (major isoform in liver cells) to develop the QSMR. The 2-D QSAR model for compounds will be based on the 2-D descriptors such as, mean topological charge, log of the octanol/water partition coefficient and number of aromatic rings of the flavonoid chemical structure. Validation and hypothesis testing will be done for all the developed prediction models.

Due to closely related structure of compounds in and among different classes of flavonoids, we believe that the development of a 3-D QSMR model will be straight forward. On the other hand, it may prove to be difficult to develop a good 3-D QSMR model because of selected data set not being able to cover the whole chemical space due to closely related structure of the limited number of selected flavonoids. The current selection of modeling approach is based on already published literature on *in silico* modeling of CYP isoforms modeling approach is based on already published literature on *in silico* modeling of CYP isoforms[146, 148-150] and some of the UGT isoforms.[86, 92, 151, 156]

OBJECTIVES AND HYPOTHESIS

Despite reports of various beneficial biological activities *in vitro*, flavonoids have poor (less than 5%) and highly variable *in vivo* bioavailability in animals and humans.[1, 6-8, 39, 40] In plasma, flavonoids are present as conjugates (metabolites) with *in vivo* aglycone (drug molecule) concentrations ranging from 0.01 to 0.4 μM.[6, 40] These *in vivo* concentrations are significantly lower than the IC_{50} or EC_{50} values (5 to 50 μM) commonly reported for their anticancer effects *in vitro*.[1, 3, 41] Hence, use of flavonoids as anticancer agent is seriously limited by their poor bioavailability, which is mainly due to their high intestinal metabolism by phase II enzymes, mainly UGTs followed by SULTs.[9-11] These conjugates comprise over 95% of the total AUC found in the body upon oral administration and might or might not have pharmacological activity.[80-83] Moreover, these conjugates after conjugation are classified as hydrophilic organic anions and need to be actively excreted out of the cell by efflux transporters.

There are more than 4000 flavonoids identified so far and there is a need to classify them based on their *in vivo* metabolic stability, in order to promote the research of flavonoids as cancer preventive agents. Since laboratories experiments using recombinant human UGT isoforms and transport vesicles are time and resource consuming, we need better *in silico* structure-metabolism relationship (SMR) based prediction models to estimate the *in vivo* metabolic fate based on *in vitro* data. However, it is very challenging to develop

such models due to the co-involvement of multiple enzymes and efflux transporters with overlapping substrate selectivities in the intestinal and liver disposition of flavonoids.

2.1. Objectives

The overall objective is to develop structure-metabolism relationship between UGTs and flavonoids for predicting intestinal metabolism of flavonoids. The goals of this research project were to: 1) identify the major UGT isoform(s) contributing to the glucuronidation of flavonoids and predicting the major organ of metabolism; 2) establish the substrate selectivity and regiospecificity of these major UGT isoform(s); 3) develop the *in silico* prediction models for major UGT isoform(s) using pharmacophore and 2-D/3-D QSAR modeling techniques; 4) study the effect of change in backbone on the disposition of flavonoids in Caco-2 cells; 5) study the rate-limiting role of efflux transporters in the disposition of flavonols in Caco-2 cells; and 6) study the rate-limiting role of efflux transporters in the excretion of regiospecific glucuronides of flavones in Caco-2 cells. In attempt to achieve the overall goal of this research, certain data have already been published demonstrating the use of UGT isoform 'fingerprinting" in predicting the metabolism of isoflavones[87] and mono- and di-hydroxyflavone[157] in human liver and intestine.

2.2. Hypothesis

Structure-metabolism relationship between UGT and glucuronidation is affected by the substrate-selectivity, regiospecificity and organ/tissue expression levels of various UGT isoforms, as well as the rate-limiting role of efflux transporters in the excretion of glucuronides. The hypothesis(s) for this thesis are as follows:

H1(a). Change in structure of flavonoids across and within sub-classes largely affects the major UGT isoform(s) contributing to the metabolism of flavonoids.

H1(o). Irrespective of change in structure of flavonoids across and within sub-classes, there is only couple of major UGT isoform(s) that contributes to the metabolism of flavonoids.

H2(a). Major UGT isoform(s) differs in their substrate-selectivity and regiospecificity of glucuronidation of flavones and flavonols.

H2(o). There is not much difference in the substrate-selectivity and regiospecificity of the major UGT isoform(s) in glucuronidating flavones and flavonols.

H3(a) Isoform-specific *in silico* SMR prediction models for the glucuronidation of flavonoids by major UGT isoforms can be developed with a predictive ability of $\geq$ 75%.

H3(o) It is not possible to develop isoform-specific *in silico* SMR prediction models for the glucuronidation of flavonoids by major UGT isoforms, with a predictive ability of $\geq$ 75%.

H4(a). Glucuronidation of flavonoids in Caco-2 cells is significantly affected by the difference in backbone across different sub-classes.

H4(o). Glucuronidation of flavonoids in Caco-2 cells is not significantly affected by the difference in backbone across different sub-classes.

H5(a). Rates of excretion of flavonols glucuronides are dependent on the formation rate of glucuronides and not rate-limited by the efflux transporters in Caco-2 cells.

H5(o). Rates of excretion of flavonols glucuronides are rate-limited by the efflux transporters and not by the formation rate of glucuronides in Caco-2 cells.

H6(a). Rates of excretion of regiospecific glucuronides of flavonols are rate-limited by the efflux transporters and not by the formation rate of glucuronides in Caco-2 cells.

H6(o). Rates of excretion of regiospecific glucuronides of flavonols are dependent on the formation rate of glucuronides and not rate-limited by the efflux transporters in Caco-2 cells.

GENERAL METHODOLOGY

3.1 Solubility and Stability of the Flavonoids

Flavonoids showed a wide range of solubility depending upon the hydroxyl and/or methoxyl substitution in their structure. It is important to determine if the compound is soluble at the concentration in interest for various experiments; Caco-2 cell transport study (10µM), determination of intrinsic clearance (at 2.5µM substrate concentration), and glucuronidation reaction with various UGT isoforms and Caco-2 cell lysate (at 2.5, 10 and 35 µM substrate concentration).

Certain flavonoids are very susceptible to oxidative degradation, hence it was important to determine that the selected flavonoids were stable for during the time of experimentation in the glucuronidation reaction media (UGT isoforms (~0.53 mg/ml), magnesium chloride (0.88mM), saccharolactone (4.4mM), alamethicin (0.022mg/ml) in 50mM potassium phosphate buffer (pH 7.4)) and Caco-2 cell transport study media (HBSS buffer (pH 7.4). The unstable compounds were stabilized using 0.1% vitamin C as an antioxidant and pH was adjusted to pH 7.4. Saccharolactone was added as the inhibitor of the reverse enzymatic reaction by β-glucuronidase, which converts glucuronides to aglycone. Alamethicin was surfactant used to form pores in the supersomes membrane such that the substrate reaches the enzyme located on the inner membrane of supersomes.

3.1.1. Solubility and stability of the flavonoids in HBSS (pH 7.4)

For the flavonoids used in Caco-2 cell transport study, it was determined if the compound is soluble at 10µM in HBSS buffer (pH 7.4) at room temperature. 2µl of 2, 1, 0.5 and 0.25 mM of stock solution of compounds in 100% methanol were diluted 100 times using HBSS buffer to obtain 20, 10, 5and 2.5 µM, respectively. The samples were centrifuged at 15000 rpm for 15 mins and analyzed immediately after collection in UPLC. The linearity of the concentration versus peak area was used to determine if the compound was soluble at 10µM in HBSS buffer (pH 7.4).

For the flavonoids used in Caco-2 cell transport study, it was determined if the 10µM compound solution in HBSS buffer (pH 7.4) is stable for 4 hours (time span of experimentation) at 37ºC. Samples were collected at 0, 1, 2, 3 and 4 hr(s). The samples were centrifuged at 15000 rpm for 15 mins and analyzed immediately after collection in UPLC. For the compounds which were not found to be stable for 4 hours at 37ºC, 0.1% vitamin C was added; pH adjusted to 7.4, and stability was tested again. Using 3,4'-dihydroxyflavone as model compound, which was stable at the experimental condition, we validated that 0.1% vitamin C does not interfere with the transport or metabolism of the tested compound.

3.1.2. Solubility and stability of the flavonoids in glucuronidation reaction mixture

For the flavonoids used for the glucuronidation reactions, it was determined if the compound is soluble at 2.5, 10 and 35µM in glucuronidation reaction media. 2µl of 4, 2, 1, 0.5, 0.25 and 0.125 mM of stock solution of compounds in 100% methanol were diluted 100 times using HBSS buffer to obtain 40, 20, 10, 5, 2.5 and 1.25 µM, respectively. For the flavonoids which were used only for determining intrinsic clearance, it was determined if the compound was soluble at 2.5µM in glucuronidation reaction media. 2µl of 0.5, 0.25, 0.125 and 0.625 mM of stock solution of compounds in 100% methanol were diluted 100 times using HBSS buffer to obtain 5, 2.5, 1.25 and 0.625 µM, respectively. The samples were centrifuged at 15000 rpm for 15 minutes and analyzed immediately after collection in UPLC. The linearity of the concentration versus peak area was used to determine if the compound was soluble at 2.5, 10, 35µM in glucuronidation reaction media.

For the flavonoids used in glucuronidation reactions, it was determined if the 2.5, 10µM and 35 compound solution in glucuronidation reaction mixture is stable for 120 minutes. Samples were collected at 0, 30, 60 and 120 minutes. In case of very unstable compounds (such as 3-hydroxyflavone), stability samples were taken at 15, 30 and 60 minutes. The samples were centrifuged at 15000 rpm for 15 mins and analyzed immediately after collection in UPLC. Compounds which were not found to be stable for 2 hours at 37ºC, 0.1% vitamin C was added, pH adjusted to 7.4, and stability was tested again. Using 3,4'-

dihydroxyflavone, which was stable at the experimental condition, we validated that 0.1% vitamin C does not interfere with the glucuronidation of the tested compound.

3.2. Glucuronidation Experiment

For measuring UDP-glucuronosyltransferase (UGT) activities in an *in vitro* glucuronidation reactions using specific recombinant human UGT isoforms is performed as using the following procedures. (1) Thaw solution A and solution B (both stored at -20 ºC) in a water bath maintained at 37 ºC and store in bucket filled with ice during experiment. Solution A contains 25mM uridine diphosphoglucuronic acid (UDPGA) and solution B contains 5mM magnesium chloride, 25mM saccharolactone and 0.125 mg/ml alamethicin. (2) Thaw UGT isoforms (5mg of protein/ml) (aliquoted into 50µl and stored at -80 ºC) in a water bath maintained at 37 ºC and store in bucket filled with ice during experiment. UGT isoforms are diluted with 50mM KPI to reach the optimum concentration to be used in step 5. However, freshly prepared Caco-2 cell lysate was used for the glucuronidation reaction. (3) Add 120 µl of solution B to ice-cold 421.2µl of 50 mM potassium phosphate buffer (pH 7.4) (with or without 0.1% vitamin C) in an ice-cold 1.5ml micro-centrifuge tube. (4) Add 36 µl of supersomes of 0.25, 0.5 or 1 mg of protein/ml so as to reach the optimum final concentration, such that the pipette tip and the contents did not touch the micro-centrifuge tube. (5) Add 6.8 µl of 0.25, 1, or 3.5 mM concentrations of substrates was added to the reaction mixture to obtain a final compound concentration of 2.5, 10 or 35 µM respectively. (6) Add 96 µl of solution A to obtain a

final volume of 680 µl such that the pipette tip and the contents did not touch the micro-centrifuge tube. (7) Mix the reaction mixture well by turning the micro-centrifuge tube upside down multiple times. (8) Transfer 200µl of reaction mixture to each of the three ice-cold 1.5 ml micro-centrifuge tubes and incubate at 37°C for optimum time (15-120 mins). (9) Stop the reaction by adding 50µl of 94% acetonitrile/6% glacial acetic acid containing 100µM of appropriate internal standard to each tube containing a reaction mixture of 200 µl.

3.3. Analysis of Flavonoids and Their Glucuronides Using UPLC.

The Waters Acquity UPLC (Ultra performance liquid chromatography) system equipped with photodiode array detector (PDA), Sample manager, Binary solvent manager, EmPower^{TM} software, and BEH C_{18} column (7 µm, 2.1 × 50 mm) was used to analyze the flavonoids and their respective glucuronides(s) in the sample. The general LC method parameters used were: mobile phase B, 100% acetonitrile; mobile phase A, 100% aqueous buffer (2.5mM NH_4Ac, pH 4.5); flow rate 0.45 mL/min; gradient: 0 to 2min, 10-20% B, 2 to 3 min, 20–70%B, 3 to 3.5 min, 70%B, 3.5 to 4.0 min, 70-90% B, 4.0 to 4.5 min, 90-10% B, and 4.5 to 5.0 min, 10% B and injection volume, 10 µL. However, for some compounds different mobile phase A, mobile phase A and/or gradient method were adopted, which will be described in the relevant sections ahead.

3.4. Confirmation of Flavonoids Conjugate(s) and Their Degree of Substitution Using UPLC-MS/MS

Glucuronide(s) and sulfate(s) of flavonoids with more than one hydroxyl group in their structure were confirmed for the degree of glucuronic acid or sulfate substitution (i.e. mono- or di-glucuronides/sulfates) using UPLC/MS/MS method. Similar UPLC conditions as explained above were used to separate the flavonoids and their respective conjugate(s). The effluent from Waters Acquity UPLC system was introduced into an API 3200 Qtrap triple-quadrupole mass spectrometer (Applied Biosystem/MDS SCIEX, Foster City, CA) mounted with a TurboIonSpray^{TM} source. The working parameters for the mass spectrometers and compound-specific MS conditions were optimized. The mass of each individual peak of separated glucuronides and sulfates was measured using QSMS mode. Precursor scan or MS2 scan mode was used to confirm the identity of each peak as glucuronide/sulfate by fragmenting the parent ion into glucuronic acid/sulfate and aglycone daughter ions.[158, 159]

The main working parameters for the mass spectrometers are set as follows: ion-spray voltage, -4.5 kV; ion source temperature, 600°C; nebulizer gas (gas1), nitrogen, 40 psi; turbo gas (gas2), nitrogen, 40 psi; curtain gas, nitrogen, 20 psi; collision cell energy; 30 volts, collision cell exit potential, 3 volts and minor adjustments were then made for each flavonoids. The mass spectrometer was operated in negative or positive ion mode to

perform the analysis of flavonoids and their conjugates. Compound-specific MS conditions are listed in future chapters.

3.5. Quantification of Glucuronides of Flavonoids

Since, the reference standards of glucuronides are not available commercially; using the standard curves of parent compounds is the only available method to quantify the respective glucuronides. Many labs had used calibration curves of the aglycones to quantify glucuronides and showed reasonable recovery.[87, 95, 160] Beer's Law states that molar absorptivity is a constant and the absorbance is proportional to concentration for a given substance dissolved in a given solute and measured at a given wavelength. For this reason, molar absorptivities are called molar absorption coefficients or molar extinction coefficients ($M^{-1}cm^{-1}$). The standard curve of the parent compound could be used without any correction to quantify glucuronide within acceptable error limits, only if the extinction coefficient of the glucuronide is close to aglycone, such that the ratio of the extinction coefficients of the glucuronide and the aglycone ranges between 0.9-1.1.

But it was observed that that the ratio of the extinction coefficients of the glucuronides of flavonoids might vary a lot among different compounds and different glucuronides of same compound (also called as glucuronide-isomers), which was a wavelength-dependent phenomenon. This made it very important that the ratio of extinction coefficients of each

glucuronide must be calculated at a particular wavelength so that it could be used as correction factor while quantifying the glucuronides using the standard curve of the parent compound at a specific wavelength.

The method of calculating correction factors (K) of single and multiple glucuronides of flavonoids are shown as flow chart in Figure 3. The flavonoids were glucuronidated (at three different concentration 2.5, 10 and 25μM) using selected UGT isoforms to generate the mixture of mono-glucuronide(s) of the flavonoids in different concentrations and ratios. Glucuronides produced by UGTs incubation were further purified using solid phase if the amount of glucuronide(s) formed were less than 60% of the parent compound concentration used in the reaction. Samples were loaded on C_{18} columns after 2 mL MeOH and 1 mL water wash, 1 mL water was then used to clear up the salts and saccharolactone, successive 2 mL MeOH elution of glucuronides were collected finally. This was followed by 2 hours' air dying and reconstitution with potassium phosphate butter (pH 7.4). A 500μl portion of the metabolite solution (purified or without purification) was taken and 415 unit/ml of β-D-glucuronidase enzyme was added to hydrolyze the metabolites (into aglycone) at 37°C for 5 mins. The control reaction was run using equivalent volume of purified water in place of enzyme solution. The samples were analyzed using UPLC.

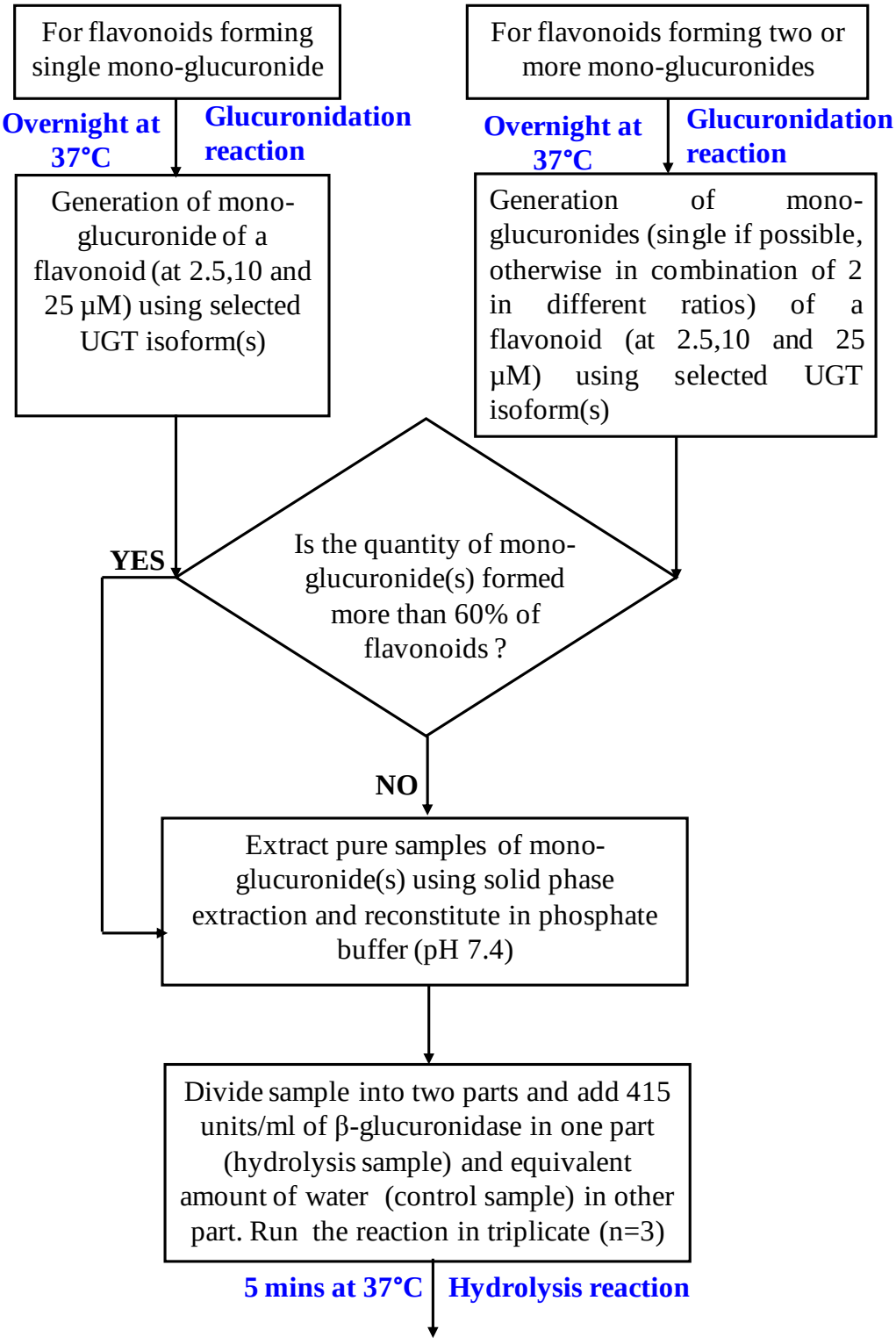
For flavonoids forming single mono-glucuronide
For flavonoids forming two or more mono-glucuronides
Overnight at 37°C
Glucuronidation reaction
Overnight at 37°C
Glucuronidation reaction
Generation of mono-glucuronide of a flavonoid (at 2.5,10 and 25 µM) using selected UGT isoform(s)
Generation of mono-glucuronides (single if possible, otherwise in combination of 2 in different ratios) of a flavonoid (at 2.5,10 and 25 µM) using selected UGT isoform(s)
Is the quantity of mono-glucuronide(s) formed more than 60% of flavonoids ?
YES
NO
Extract pure samples of mono-glucuronide(s) using solid phase extraction and reconstitute in phosphate buffer (pH 7.4)
Divide sample into two parts and add 415 units/ml of β-glucuronidase in one part (hydrolysis sample) and equivalent amount of water (control sample) in other part. Run the reaction in triplicate (n=3)
5 mins at 37°C
Hydrolysis reaction

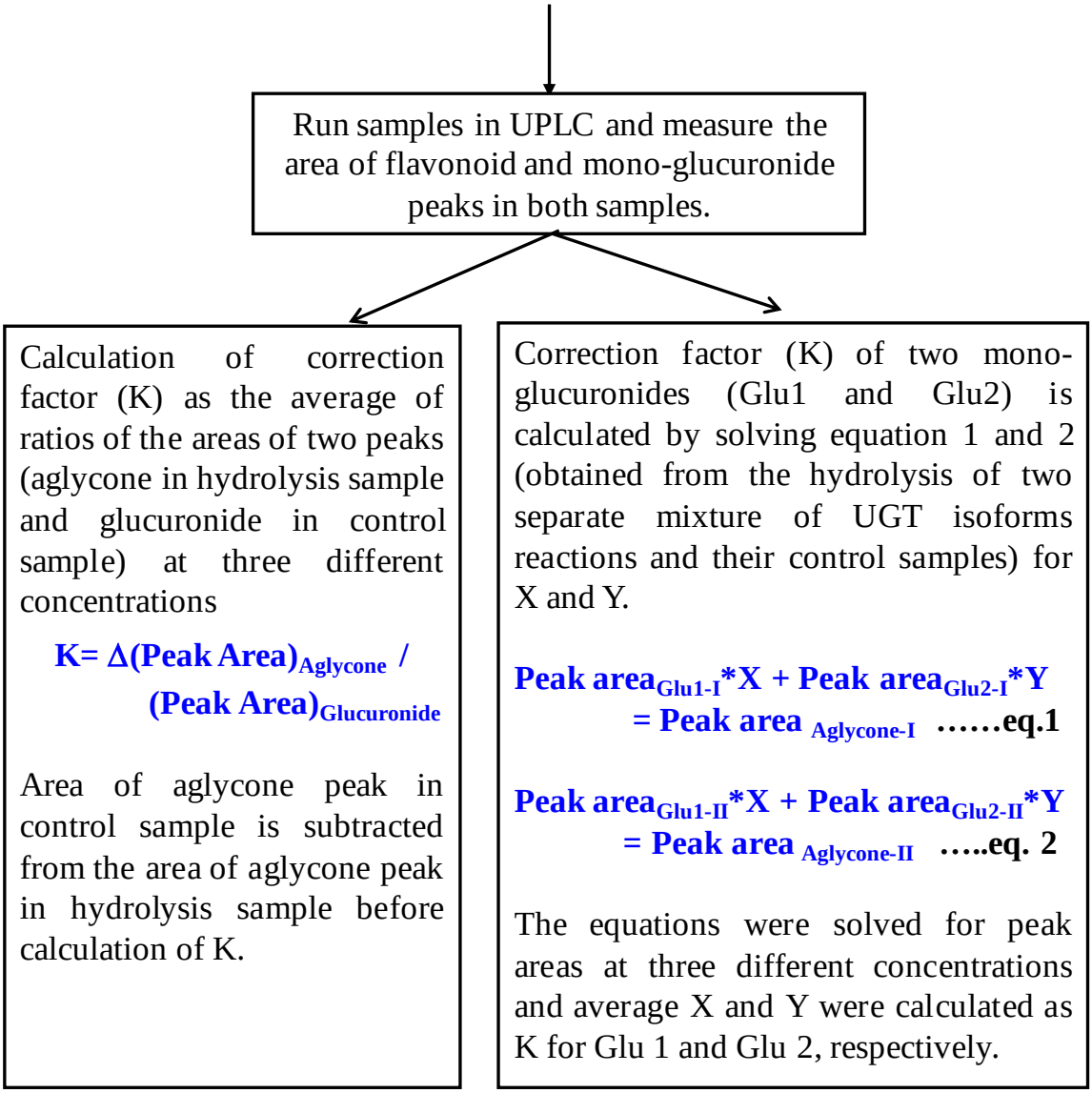

Figure 3. Flow chart of the process of determining the correction factor of single and multiple glucuronides of flavonoids

The peak area of glucuronide(s) before hydrolysis and the peak area of equivalent aglycone after hydrolysis were measured to calculate the correction factors of the glucuronides at the wavelength selected for each compound. In case of single glucuronide, the peak areas of glucuronide at the specified wavelength in the control reaction were measured and compared with the peak areas of the equivalent aglycone produced after hydrolysis. If the extinction coefficients of the glucuronide and flavonoids were the same, for a decrease in glucuronide peak area, a similar increase in the aglycone peak area was observed. If not, an average correction factor (K) was calculated as the ratios of the two peaks (one parent and one glucuronide) areas at three different concentrations (Δ(Peak Area) $_{\text{Aglycone}}$ versus Δ(Peak Area) $_{\text{Glucuronide}}$). Peak areas of aglycone (if found in the control samples) were subtracted from the peak areas of aglycone measured in hydrolysis samples, before the correction factor was calculated. The correction factor was used to make the adjustment in the concentration of glucuronide calculated using the standard curve of the parent aglycone. For each such mixture of glucuronides, equivalent amount of aglycone produced after hydrolysis was measured.

However, in certain cases, if the amount of glucuronide generated by any UGT isoforms was too small to calculate the K for the glucuronide using above method, the standard curve of the parent aglycone had to be used without any correction factor. The extinction coefficients of two or more glucuronides of particular flavonoids can be largely different.

To calculate the extinction coefficients of each individual glucuronide, multiple experiments were run with different UGT isoforms to give different ratios of glucuronides mixture. For each mixture, peak areas of all glucuronides in a control reaction and the equivalent aglycone produced after hydrolysis were measured.

3.6. Data Analysis of Correction Factor for the Extinction Coefficients of Multiple Glucuronides

To calculate the correction factor, each set of the peak areas were represented as an equation. These equations were solved to calculate the correction factors. For example, for a flavonoid with two glucuronides, following two equations can be generated using the peak areas obtained by two separate UGT isoform reactions.

$$\text{Peak area}_{\text{Glu1-I}} * X + \text{Peak area}_{\text{Glu2-I}} * Y = \text{Peak area}_{\text{Aglycone-I}} \qquad \text{eq. 1}$$

$$\text{Peak area}_{\text{Glu1-II}} * X + \text{Peak area}_{\text{Glu2-II}} * Y = \text{Peak area}_{\text{Aglycone-II}} \qquad \text{eq. 2}$$

where Glu1 and Glu2 were the two glucuronides and I and II stood for two separate mixture of UGT isoforms reactions which could form distinctly different ratios of Glu1 and Glu2. Equation 1 and 2 can be solved to obtain the value of X and Y, the correction factor of Glu1 and Glu2, respectively.

3.7. Statistical Analysis for Glucuronidation and Caco-2 Cell Experiments Data

From our previously established work,[87] we typically use one-way ANOVA or an unpaired Student's t-test (GraphPad Prism®, GraphPad software Inc., CA) with or without Tukey-Kramer multiple comparison (posthoc) tests was used to analyze the statistical significance among various data. Two-way ANOVA test (GraphPad Prism®) with Bonferroni (posthoc) tests was used to study the cross-over effect of structure of flavonols on the outcome. The prior level of significance was set at 5%, or $p<0.05$.

UGT1A9, UGT1A8 AND UGT1A1 ARE THE MOST IMPORTANT ISOFORMS RESPONSIBLE FOR THE GLUCURONIDATION OF FLAVONOIDS IN HUMANS

4.1. Abstract

The objectives of this study were to determine the most important human UGT isoforms contributing to the metabolism of flavonoids in first-pass metabolic organs (liver and intestine). We used one compound each from five major sub-classes of flavonoids (apigenin (flavones), genistein (isoflavones), kaempferol (flavonols), naringenin (flavanones) and phloretin (chalcone)); six congeneric compounds of flavonol sub-class; and four congeneric compounds of flavone sub-class. We used 12 recombinant human UGT isoforms, 1A1, 1A3, 1A4, 1A6, 1A7, 1A8, 1A9, 1A10, 2B4, 2B7, 2B15 and 2B17 to do UGT "fingerprinting" of the selected flavonoids at three different concentrations (2.5, 10 and/or 35 μM). We showed that within and across different sub-classes of flavonoids, UGT1A9, followed by 1A8 and 1A1 was the most important isoform contributing to the glucuronidation of most flavonoids. However, the rank-order of isoforms may or may not change based on structure and concentration of substrate. We believe that UGT finger-printing can be successfully used to predict the fate of metabolism of flavonoids in human organs/tissues based on UGT isoforms protein expression levels in different organs/tissues. Glucuronidation of flavonoids by UGT 1A3, 1A6, 1A7, 1A10 and 2B7 was also dependent on the structure and concentration of the

flavonoid. In conclusion, UGT1A9, UGT1A8 and UGT1A1 are the most important UGT isoform responsible for the glucuronidation of vast majority of flavonoids at the tested substrate concentrations. Based on published UGT isoform mRNA expression pattern in human organs, liver and intestine should serve as the major first-pass metabolism organs for flavonoids.

4.2. Introduction

Flavonoids have shown various health benefits such as antioxidants and prevention against cancer and cardiovascular diseases.[1-5] Flavonoids commonly occurs as natural compounds in plants, Vegetables such as spinach,[23] onions,[24] broccoli,[24] and fruits such as apples,[25, 26] pears,[27] grapes,[27] strawberries,[27] cherries,[28] blueberries,[28] and citrus fruits[14, 22] have shown to contain high amounts of flavonoids. Structurally, flavonoids are benzo-pyrone derivatives consisting of phenolic and pyrane rings (Figure 1, pg 5) and are classified according to the degree of oxidation or substitution pattern of their central pyran ring. In and among different sub-classes of flavonoid, compounds usually differ in number and position of hydroxy, methoxy and methyl groups. Over 4000 natural flavonoid compounds have been purified and structurally identified.[161]

Based on their chemical structures backbone, flavonoids can be categorized into seven major sub-classes found in foods, namely, flavones (2-phenylchromen-4-one backbone); isoflavones (3-phenylchromen-4-one backbone); flavonols (3-hydroxy-2-phenylchromen-4-one backbone); flavanones (2,3-dihydro-2-phenylchromen-4-one backbone); flavanols (2-phenyl-3,4-dihydro-2H-chromen-3-ol backbone); chalcone (Phenyl styryl ketone backbone) and anthocyanidins (flavylium (2-phenylchromenylium) ion backbone) (Figure 1, pg 5).

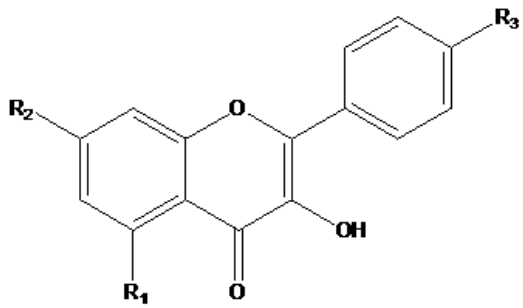

Flavonol	R_1	R_2	R_3
3HF	H	H	H
3,4'DHF	H	H	OH
3,7DHF	H	OH	H
3,7,4'THF	H	OH	OH
3,5,7THF	OH	OH	H
3,5,7,4'QHF	OH	OH	OH

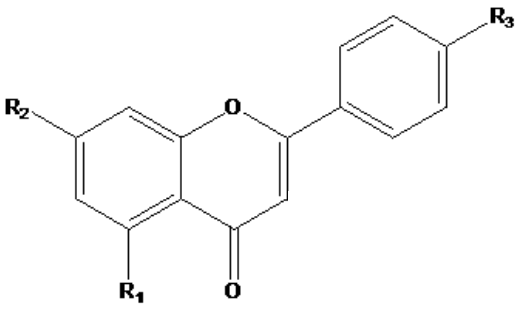

Flavone	R_1	R_2	R_3
4'HF	H	H	OH
5HF	OH	H	H
7HF	H	OH	H
5,4'DHF	OH	H	OH
5,7DHF	OH	OH	H
7,4'DHF	H	OH	OH
5,7,4'THF	OH	OH	OH

Figure 4. Structure of flavonols and flavones used in the study

Research done so far has proved that extensive *in vivo* metabolism by Uridine-5'-diphospho-glucuronyltransferase enzymes (UGTs) is the main reason for the poor *in vivo* bioavailability (< 5%) of flavonoids,[9-11] which poses a challenge in developing them as viable chemopreventive agents.[6-8] Hence, it is important to understand the structural features responsible of flavonoids metabolism that might help to identify the flavonoids with low potential for UGT metabolism and benefit development of flavonoids into chemopreventive agents.

The information about the structure-metabolism relationship (SMR) between flavonoids' structures and UGTs however is limited in nature as the crystal structure of any UGT has not been deduced yet. The reports published have either however discussed the importance of one or more structural features important for glucuronidation using liver and intestinal microsomes, cell cultures and *in situ* animal model[13, 90, 95, 162, 163] or have focused in details on one single isoform.[86] There is however only one or two reports using systematic study of effect of same structural change on different UGTs using recombinant human UGT isoforms.[51, 87, 157]

The objective of this study was to systematically determine the most important UGT isoform(s) responsible for the metabolism of flavonoids based on change in flavonoid structure across and within different sub-classes. Another objective of the study was to observe if the UGT fingerprinting could help to predict the major organ (liver or small

intestine) which might be responsible for glucuronidation of flavonoids based on the *in vivo* expression of major isoforms in human organs.

To understand the effect of change in the backbone of flavonoids on their metabolism by different UGT isoforms, we first studied the glucuronidation of one compound each from five major sub-classes; apigenin (flavones), genistein (isoflavones), kaempferol (flavonols), naringenin (flavanones) and phloretin (chalcone) (Figure 1, pg 5). These compounds were analogs of apigenin in different sub-classes with the hydroxyl group at similar position as in apigenin (C- 5, 7 and 4'). Second, to study the effect of change in position and number of hydroxyl group on the same backbone on the SMR of flavonoids with various UGT isoforms, we used flavones and flavonol sub-classes. Six congeneric compounds of flavonol subclass, 3-hydroxyflavone, 3,4'-dihydroxyflavone, 3,7-dihydroxyflavone, 3,4',7-trihydroxyflavone, 3,5,7-trihydroxyflavone, and 3,5,7,4'-tetrahydoxyflavone; and four congeneric compounds of flavones subclass, 5,4'-dihydroxyflavone, 5,7-dihydroxyflavone, 7,4'-dihydroxyflavone, and 5,7,4'-trihydroxyflavone (Figure 4).

4.3. Materials and Methods

4.3.1. Materials

Genistein (Gen), naringenin (Nar), phloretin (Phlor), 3-hydroxyflavone (3HF), 3,4'-dihydroxyflavone (3,4'DHF), 3,7-dihydroxyflavone (3,7DHF), 5,4'-dihydroxyflavone (5,4'DHF), 5,7-dihydroxyflavone (5,7DHF), 7,4'-dihydroxyflavone (7,4'DHF), 3,7,4'-trihydroxyflavone or resokaempferol (3,7,4'THF) and 3,5,7-trihydroxyflavone or galangin (3,5,7THF), 5,7,4'-trihydroxyflavone or apigenin (Api or 5,7,4'THF), 3,5,7,4'-tetrahydroxyflavone or kaempferol (3,5,7,4'QHF or Kamp), were purchased from Indofine Chemicals (Somerville, NJ). Recombinant human UGT isoforms (Supersomes) were purchased from BD Biosciences (Woburn, MA). Uridine diphosphoglucuronic acid (UDPGA), alamethicin, D-saccharic-1,4-lactone monohydrate, magnesium chloride, and Hanks' balanced salt solution (powder form) were purchased from Sigma-Aldrich (St Louis, MO). All other materials (typically analytical grade or better) were used as received.

4.3.2. Solubility and stability of the tested flavonoids

Solubility and stability of the tested flavonoids were established at the experimental conditions as per the method explained in section 3.1 (Chapter 3).

4.3.3. Glucuronidation activities of recombinant human UGTs

The incubation procedures for measuring UGTs' activities were essentially the same as published before.[51, 52] Briefly, incubation procedures using supersomes were as follows: (1) supersomes (final concentration ≈ in range of 0.013~0.053 mg of protein per mL as optimum for the reaction), magnesium chloride (0.88 mM), saccharolactone (4.4 mM), alamethicin (0.022 mg/mL), different concentrations of substrates in a 50 mM potassium phosphate buffer (pH 7.4), and UDPGA (3.5 mM, add last) were mixed; (2) the mixture (final volume) 200 μL) was incubated at 37°C for a predetermined period of time (30 or 60 min); and (3) the reaction was stopped by the addition of 50μL of 94% acetonitrile/6% glacial acetic acid containing 100 μM of testosterone or 50 μM of 5-hydroxyflavone or formononetin as internal standard. Testosterone was used as internal standard for genistein, phloretin, naringenin, 3,4'DHF, 7,4'THF, 3,7,4'THF, 5,7,4'THF and 3,5,7,4'QHF; formononetin for 3HF, 5,4'DHF, 5,7DHF and 3,5,7THF; and 5-hydroxyflavone for 3,7DHF. Three substrate concentrations, 2.5, 10 and 35 μM were used for the studying the UGT isoforms.

4.3.4. UPLC analysis of flavonoids and their glucuronides

We analyzed flavonoids and their respective glucuronides by using the following common method: system, Waters Acquity UPLC with photodiode array detector and Empower software; column, BEH C_{18}, 1.7 μm, 2.1 × 50 mm; and injection volume, 10μL.

Compound-specific mobile phase, flow rate and gradient conditions are described in table 4. Genistein, naringenin, phloretin, 5,7DHF, 3,5,7THF, 3,5,7,4'QHF and their respective glucuronides were analyzed 254, 286, 286, 268, 263 and 254 nm, respectively. 3HF, 3,4'DHF, 3,7DHF 5,4'DHF, 7,4'DHF, 3,7,4'THF, 5,7,4'THF and their respective glucuronides were analyzed at 340 nm. Testosterone was analyzed at 254, while 5-hydroxyflavone and formononetin were analyzed at 268 nm.

Linearity was established in the range of 0.3-20 μM (total 7 concentrations) for 3,7DHF, 5,4'DHF, 5,7DHF, 7,4'DHF, and 3,5,7THF and 0.16-20 μM (total 8 concentrations) for other compounds. The LLOQ for all compounds was 0.3 μM for 3,7DHF and 3,5,7THF and 0.16 μM for all other compounds. Linearity was established in the range of 0.78-50 μM (total 7 concentrations) for all compounds. Analytical methods for each compound were validated for inter-day and intra-day variation using 6 samples at three concentrations (50, 12.5 and 1.56 μM). Precision and accuracy for all compounds were in acceptable range of 85% to 115%.

4.3.5. Quantification of glucuronides of flavonoids

The quantification of glucuronides of flavonoids was done using the standard curve of the parent compound with a correction factor for difference in extinction coefficient of the compound and its metabolites. The correction factor was measured using the method as explained in section 3.5 and 3.6 (Chapter 3).

Table 4 UPLC conditions for analyzing flavonoids and their glucuronides.

Compounds	Mobile phase A	Mobile phase B	Gradient Condition
Apigenin (5,7,4'THF)	100% aqueous buffer (2.5mM NH_4Ac, pH 3)	100% Acetonitrile	Condition 1
Genistein	100% aqueous buffer (2.5mM NH_4Ac, pH 3)	100% Acetonitrile	Condition 1
Phloretin	100% aqueous buffer (2.5mM NH_4Ac, pH 3)	100% Acetonitrile	Condition 1
Naringenin	100% aqueous buffer (2.5mM NH_4Ac, pH 3)	100% Acetonitrile	Condition 1
3HF	100% aqueous buffer (2.5mM NH_4Ac, pH 3)	100% Acetonitrile	Condition 1
3,4'DHF	100% aqueous buffer (2.5mM NH_4Ac, pH 3)	100% Acetonitrile	Condition 1
3,7DHF	100% aqueous buffer (2.5mM NH_4Ac, pH 3)	100% Acetonitrile	Condition 1
3,7,4'THF	100% aqueous buffer (2.5mM NH_4Ac, pH 3)	100% Acetonitrile	Condition 1
3,5,7THF	100% aqueous buffer (2.5mM NH_4Ac, pH 3)	100% Acetonitrile	Condition 1
Kaempferol (3,5,7,4'QHF)	0.2% Formic acid	100% Methanol	Condition 2
5,4'DHF	100% aqueous buffer (2.5mM NH_4Ac, pH 7.4)	100% Methanol	Condition 2
5,7DHF	100% aqueous buffer (2.5mM NH_4Ac, pH 7.4)	100% Methanol	Condition 2
7,4'DHF	100% aqueous buffer (2.5mM NH_4Ac, pH 7.4)	100% Methanol	Condition 2

Condition 1: 0 to 0.3 min, 10% B, 0.3 to 2.9 min, 10–50%B, 2.9 to 3.2 min, 50-90%B, 3.2 to 4.0 min, 90% B; flow rate = 0.5 ml/min. **Condition 2:** 0 to 2min, 10-20% B, 2 to 3 min, 20–40%B, 3 to 3.5 min, 40–50%B, 3.5 to 4.0 min, 50-70% B, 4.0 to 5.0 min, 70-90% B, 5.0 to 5.5 min, 90-10% B, and 5.5 to 6.0 min, 10% B, flow rate = 0.45 ml/min.

4.3.6. Confirmation of flavonoids glucuronide structure by LC-MS/MS

Flavonoids and their respective glucuronides were separated by the same UPLC system but using slightly different chromatographic conditions because of mass spectrometer requirements. Here, mobile phase A was ammonium acetate buffer (pH 7.5) and mobile phase B was 100% acetonitrile with the gradient as follows: 0-2.0 min, 10–35% B, 2.0-3.0 min, 35–70% B, 3.2-3.5 min, 70–10% B, 3.5-3.7 min, 10% B. The flow rate was 0.5 mL/min. The effluent was introduced into an API 3200 Qtrap triple-quadrupole mass spectrometer (Applied Biosystem/MDS SCIEX, Foster City, CA) equipped with a TurboIonSpray^{TM} source.

The mass spectrometer was operated in negative ion mode to perform the analysis of flavonoids and their respective glucuronides. The main working parameters for the mass spectrometers were set as follows: ion source temperature, 600°C; nebulizer gas (gas1), nitrogen, 40 psi; turbo gas (gas2), nitrogen, 40 psi; curtain gas, nitrogen, 20 psi; DP, -50 V; EP, -10V; CE, -30V; CXP, -3V and IS -4.5KV. Minor adjustments were then made for each flavonoid. Flavonoids mono-*O*-glucuronides were identified by MS and MS2 full scan modes.

The glucuronides were extracted by solid phase extraction from the glucuronidation experiment samples and re-constituted in small amount of 30% acetonitrile in water. The concentrated samples were then used to identify the glucuronides in UPLC/MS/MS.

4.3.7. Data analysis

Rates of metabolism in recombinant human UGT isoforms were expressed as amounts of metabolites formed per min per mg protein or nmol/hr/mg.

4.3.8. Statistical analysis

One-way ANOVA or an unpaired Student's t-test (GraphPad Prism®, GraphPad software Inc., CA) with or without Tukey-Kramer multiple comparison (posthoc) tests was used to analyze the statistical significance among various data. The prior level of significance was set at 5%, or $p<0.05$.

4.4. Results

4.4.1. Confirmation of flavonoid glucuronides structure by LC-MS/MS

We conducted simple LC-MS/MS studies of the metabolites to show that most glucuronides formed during the glucuronidation study were mono-*O*-glucuronides (Figures 1-13, Appendix A). We only found two di-*O*-glucuronides of flavonoid in this study by galangin and kaempferol, but in very small concentrations. Genistein and naringenin formed only one quantifiable mono-*O*-glucuronide (Figures A1b and A1d, Appendix A), while apigenin formed two quantifiable mono-*O*-glucuronides (Figures A2a-A2b, Appendix A). Phloretin and (Figures A3b-A3c, Appendix A) kaempferol (Figures A4a-A4c, Appendix A) formed three quantifiable mono-*O*-glucuronides each. Due to the closely eluting peaks of the three glucuronides of phloretin, we were able to clearly identify only two of the glucuronides (Figures A3b-A3c, Appendix A). We believe the peak of third mono-*O*-glucuronide had been merged with one of the other two mono-*O*-glucuronides, making it undetectable, as MS could not differentiate between two overlapping mono-*O*-glucuronides. Also, the second glucuronides of genistein and naringenin were detectable in concentrated samples in UPLC/MS/MS.

One mono-*O*-glucuronide of 3HF (Figure A5, Appendix A), two mono-*O*-glucuronides of each 3,4’DHF (Figure A6, Appendix

A) and 3,7DHF (Figure A4, Appendix A), and three mono-*O*-glucuronides of each 3,7,4'THF (Figure A7, Appendix A), 3,5,7THF (Figure A8, Appendix A) and 3,5,7,4'QHF (Figure A4, Appendix A) were detected in the glucuronidation samples. Galangin formed one di-*O*-glucuronide with UGT1A7 and 1A9 at 10 and 25µM substrate concentrations, whereas kaempferol formed one di-*O*-glucuronide with UGT1A10 only at the higher concentration (25µM) (LC plots not shown here). Since the concentrations of di-*O*-glucuronides formed in the study were small, we decide not to quantify di-*O*-glucuronides of these compounds in the study. Two mono-*O*-glucuronides was detected for each 5,4'DHF (Figure A11, Appendix A), 5,7DHF (Figure A12, Appendix A), and 7,4'DHF (Figure A13, Appendix A) in the glucuronidation study samples. Figure 10 (Chapter 5, pg 104-107) showed the UPLC chromatograms (left panel) and UV spectra (right panel) of tested flavonols and flavones and their regiospecific glucuronides formed by various UGTs. UV spectra of genistein, naringenin phloretin, and their respective glucuronides were shown in Figure D1 (Appendix D).

4.4.2. Determination of correction factors for glucuronides of flavonoids

Amounts of glucuronides formed were determined using the corrections factors for individual glucuronides of flavonols as described in the method section. UGT isoforms and wavelength used in generation of correction factor and the correction factor for each glucuronides are detailed in Tables C1-C3 (Appendix C). The correction factors were in the range of 0.5 (for 3-*O*-G of 3HF) to 2.5 (for 3-*O*-G for 3,7DHF).

4.4.3. Glucuronidation "fingerprints" of flavonoids across sub-classes by 12 recombinant human UGTs.

We studied the glucuronidation of five flavonoids from different sub-classes by 12 recombinant human UGTs to identify the effect of backbone change with same number and position of hydroxyl group (except kaempferol with an extra hydroxyl group at position C-3) on the selection of most important UGT isoforms contributing to the metabolism of flavonoids (Figure 5).

For most flavonoids across different sub-classes certain selective UGT isoforms were contributing more to the metabolism than others. Genistein (with phenyl side chain at C-3) was the slowest metabolizing compound in the series ($p<0.05$) (Figure 5a), followed by apigenin (Figure 5b) < naringenin (with saturated of C2-C3 double bond) (Figure 5c) < phloretin (with open ring structure) (Figure 5d) < kaempferol (with hydroxyl group at C-3) (Figure 5e) ($p<0.05$). This showed that the addition of hydroxyl group at C-3, saturation of C2-C3 double bond as well as the opening of the ring in the flavone (apigenin) structure improved the overall glucuronidation. Also, most flavonoids except genistein were highly metabolized though at different rates by different UGTs. Below we discussed the top five isoforms primarily glucuronidating these flavonoids.

For genistein (Figure 5a), UGT1A9 (45.28 ± 1.42) and 1A8 (18.99 ± 2.49) were the most important UGT isoforms, followed by its poor glucuronidation by 1A10 (5.93 ± 0.22),

1A1 (4.19 ± 0.43) and 1A3 (2.31 ± 0.23 nmol/hr/mg of protein). For apigenin, the most important isoforms were in the rank order: UGT 1A9 (71.96 ± 7.87) > 1A8 (53.41 ± 7.08) > 1A1 (28.44 ± 2.55) > 1A3 (23.72 ± 0.56) > 1A7 (19.48 ± 3.52) ~ 1A6 (17.02 ± 0.69 nmol/hr/mg of protein) (Figure 5b). This showed that even with flavones and isoflavones backbone difference, the top two isoforms were exactly the same (UGT1A9 and UGT1A8), though at a much higher rate than genistein ($p<0.05$) (Figures 5a-5b).

For naringenin again, the top two isoforms were similar to genistein and apigenin, UGT1A9 (134.26 ± 10.77) and 1A8 (44.82 ± 4.98 nmol/hr/mg of protein) (Figure 5c). However in contrast to apigenin, UGT1A10 (31.16 ± 1.20 nmol/hr/mg of protein) played a more important role in glucuronidation of naringenin and glucuronidated naringenin at least 6 times faster than 1A6 and 1A7 ($p<0.05$) (Figure 5c). This showed that UGT 1A6 and 1A7 did not prefer the saturation of C2-C3 double bond in naringenin structure, whereas IA10 did. The next two equally important isoforms for naringenin were UGT 1A1 (17.95 ± 0.29) and 1A3 (21.68 ±1.30 nmol/hr/mg of protein) (Figure 5c).

In case of kaempferol, which was the highest glucuronidated flavonoid in the series, the top two isoforms were again UGT1A9 (374.43 ± 8.96) and 1A8 (105.37 ± 2.26 nmol/hr/mg of protein) (Figure 5e). For kaempferol, UGT1A7 (42.53 ± 2.60 nmol/hr/mg of protein) was important but UGT1A3 and 1A6 were not. Like naringenin, UGT1A10 played an important role in glucuronidation of kaempferol (30.95 ± 1.14 nmol/hr/mg of protein) (Figure 5e).

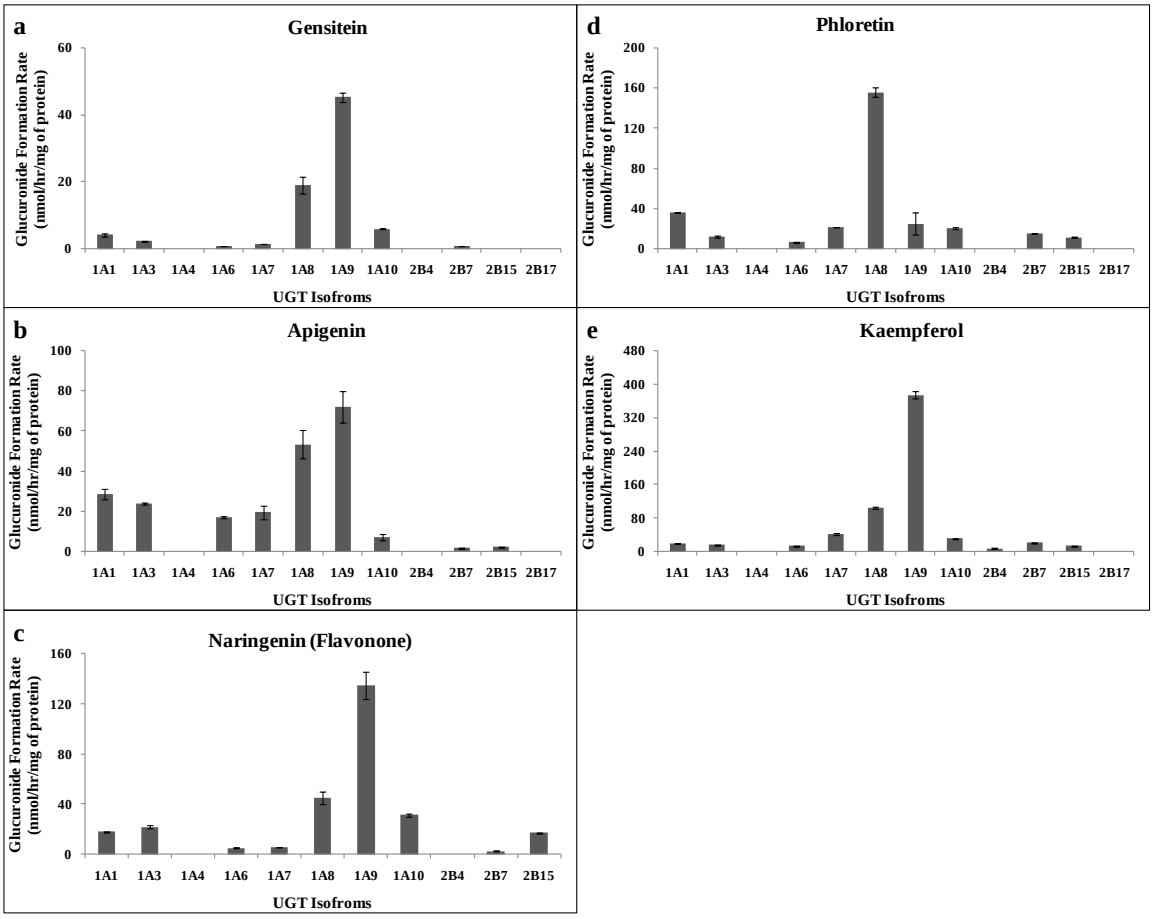

Figure 5. Glucuronidation of flavonoids from five sub-classes by 12 recombinant human UGTs.

Genistein (isoflavone) (a), apigenin (flavone) (b), naringenin (flavonone) (c), phloretin (chalcone) (d) and kaempferol (flavonol) (e) at 10 µM concentration were incubated at 37 ºC for 1 (or 0.5) hr with each UGT isoform (using optimum final protein concentration ~ 0.25, 0.5 or 1 mg/ml). The amounts of mono-glucuronide(s) formed were measured using UPLC. Rates of glucuronide(s) formation were calculated as nmol/hr/mg of protein. In case of both phloretin and kaempferol, rates of glucuronide formation were calculated as the sum of rates of formation of three mono-glucuronides of phloretin and kaempferol, respectively. Each bar is the average of three determinations, and the error bars are the standard deviations of the mean (n=3).

UGT 1A1 (19.06 ± 0.66) and 2B7 (21.54 ± 0.98 nmol/hr/mg of protein) metabolized kaempferol comparably but poorly (Figure 5e). For phloretin (an open ring flavonoid), ranking of top five isoforms was completely different from other flavonoids. The most important and highest contributing isoform was UGT1A8 (155.98 ± 2.29), followed by 1A1 (36.07 ± 2.18 nmol/hr/mg of protein), which glucuronidated phloretin more than 4 times slower than 1A8 ($p<0.05$) (Figure 5d). The next three equally and poorly contributing isoforms for phloretin were 1A9 (25.12 ± 1.67), 1A7 (21.82 ± 0.63) and 1A10 (20.56 ± 1.67) ($p<0.05$) (Figure 5d).

In general, UGT 1A9 and 1A8 were the two most important isoform for all compounds from different sub-classes of flavonoids, except phloretin which was glucuronidated most importantly by UGT 1A8, followed by 1A1 and 1A9. Apart from UGT1A9 and 1A8, UGT1A1 and UGT1A10 were the only isoform present among the top five isoforms for all selected flavonoids.

4.4.4. Glucuronidation "fingerprints" of flavonol sub-class by 12 recombinant human UGTs.

We studied the congeneric series of compounds in flavonol sub-class to see the effect of change in number and position of hydroxyl group on the same backbone, on the selection of most important UGT isoforms contributing to the metabolism of flavonoids (Figure 6).

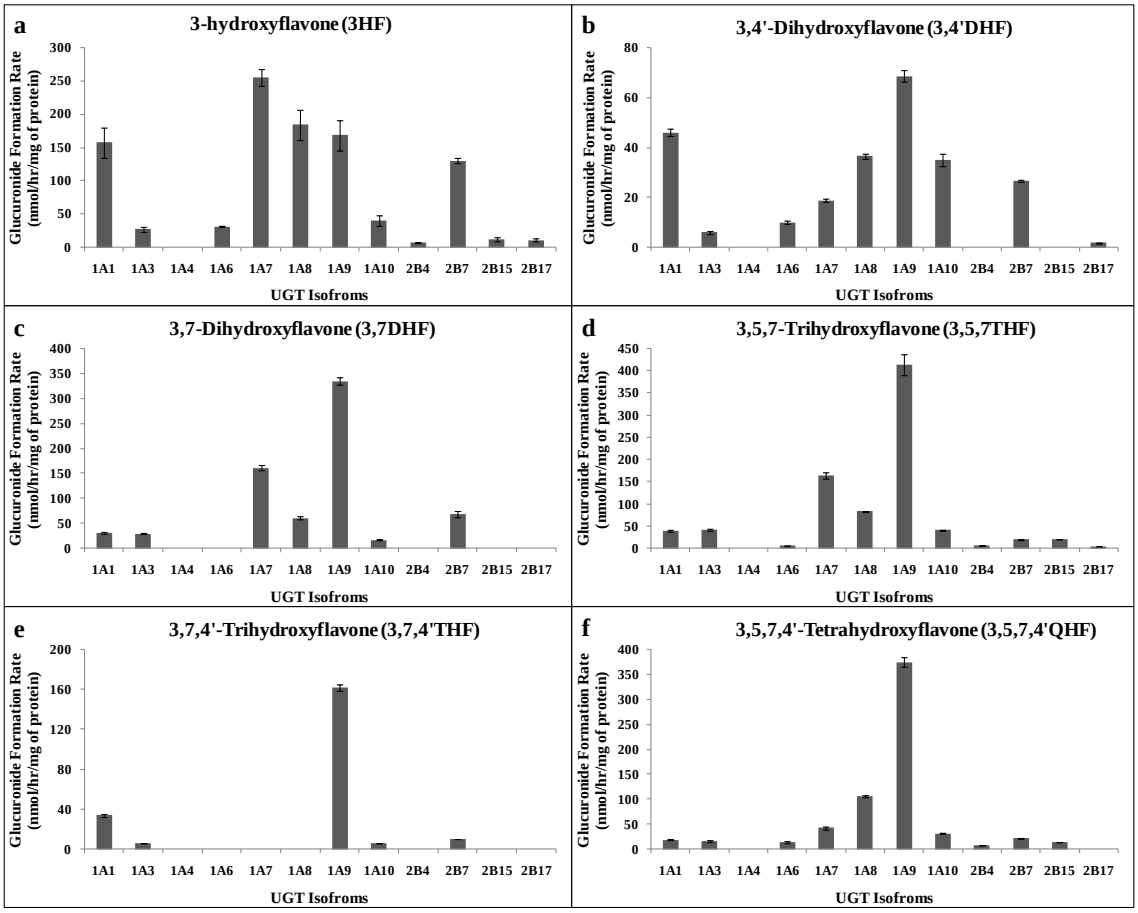

Figure 6. Glucuronidation of flavonols by 12 recombinant human UGTs.
3-hydroxyflavone (3HF) (a), 3,4'-dihydroxyflavone (3,4'DHF) (b), 3,7-dihydroxyflavone (3,7DHF) (c), 3,7,4'-trihydroxyflavone (3,7,4'THF) (d), 3,5,7-trihydroxyflavone (3,5,7THF) (e) and 3,5,7,4'-tetrahydroxyflavone (3,5,7,4'QHF) (f) at 10 µM concentration were incubated at 37 ºC for 1 (or 0.5) hr with each UGT isoform (using optimum final protein concentration ~ 0.25, 0.5 or 1 mg/ml). The amounts of mono-glucuronide(s) formed were measured using UPLC. In case of flavonols with two or three mono-glucuronides, rates of glucuronide formation were calculated as the sum of rates of formation of two or three mono-glucuronides of flavonols, respectively. Each bar is the average of three determinations, and the error bars are the standard deviations of the mean (n=3).

3HF was the fastest metabolizing compound by most UGT isoforms whereas 3,7,4'THF was the slowest ($p < 0.05$). The rank order of top five UGT isoforms for the glucuronidation of 3HF was UGT 1A7 (255.40 ± 12.84) < 1A8 (184.32 ± 22.99) ~1A9 (168.75 ± 22.9) ~1A1 (157.44 ± 22.79) < 2B7 (130.13 ± 4.01 nmol/hr/mg of protein) (Figure 6a). UGT 1A3, 1A6 and 1A10 metabolized 3HF relatively poorly, about 4 times lower than UGT2B7 (Figure 6a). For 3,4'DHF, the rank order of top five UGT isoforms was also different from the rank order of 3HF: UGT 1A9 (68.65 ± 2.22) < 1A1 (46.02 ± 1.51) < 1A8 (36.60 ± 1.06) ~ 1A10 (35.04 ± 2.49) < 2B7 (26.80 ± 0.44 nmol/hr/mg of protein) (Figure 6b). Whereas, the rank order of top UGT isoforms for glucuronidation of 3,7DHF was: UGT 1A9 (334.56 ± 7.42) < 1A7 (160.90 ± 4.93) < 2B7 (69.09 ± 6.41) ~ 1A8 (60.66 ± 3.06) < 1A1 (30.33 ± 1.83) ~ 1A3 (29.57 ± 0.71 nmol/hr/mg of protein) (Figure 6c).

There were only five UGT isoforms which glucuronidated 3,7,4'THF in the following rank order: UGT 1A9 (162.10 ± 3.08) < 1A1 (33.88 ± 1.67) < 2B7 (10.21 ± 0.20) < 1A3 (5.97 ± 0.29) ~ 1A10 (5.57 ± 0.12 nmol/hr/mg of protein) (Figure 6d). The rank order of top UGT isoforms for glucuronidation of 3,5,7THF was almost similar to the rank order of 3,7DHF with only one difference: UGT 1A9 (413.42 ± 23.89) < 1A7 (163.61 ± 6.28) < 1A8 (82.86 ± 1.81) < 1A3 (41.82 ± 2.22) ~ 1A10 (40.66 ± 1.74) ~ 1A1 (38.74 ± 2.55 nmol/hr/mg of protein). UGT2B7 did not glucuronidate 3,5,7THF well (Figure 6e). The rank order of top UGT isoforms for glucuronidation of 3,5,7,4'QHF was: UGT 1A9

(374.43 ± 8.96) < 1A8 (105.37 ± 2.26) < 1A7 (42.53 ± 2.60) < 1A10 (30.95 ± 1.14) < 2B7 (21.54 ± 0.98) ~ 1A1 (19.06 ± 0.66 nmol/hr/mg of protein) (Figure 6f).

The above data suggested that UGT1A9 was the most important isoform for the glucuronidation of flavonols except for 3HF where 1A7 was more important than 1A9. After UGT1A9, 1A8 and 1A1 were the most important isoforms, which were among the top five glucuronidating isoform for all flavonols except for 3,7,4'THF, which was not a substrate of UGT1A8. UGT1A7 was among the top three isoforms for all flavonols except for 3,4'DHF and 3,7,4'DHF. Rest of the UGT isoforms (1A3, 1A10 and 2B7) varied in their importance for each flavonol.

4.4.5. Glucuronidation "fingerprints" of flavone sub-class by 12 recombinant human UGTs.

We also studied the congeneric series of compounds in flavone sub-class (5,4'DHF, 5,7DHF, 7,4'DHF and 5,7,4'THF) to observe if the selection of most important UGT isoforms contributing to the metabolism of flavonoids, based on number and position of hydroxyl group, was dependent on the sub-class or backbone structure (Figures 3b and 5d-5e). We also re-plotted the data of mono-hydroxyflavones, 4'HF, 5HF and 7HF from Tang *et al.* (2010)[157] here for comparison (Figure 7). 5,7DHF was the fastest whereas 5HF was the slowest metabolizing compound in the series, followed by 7,4'DHF (Figure 7).

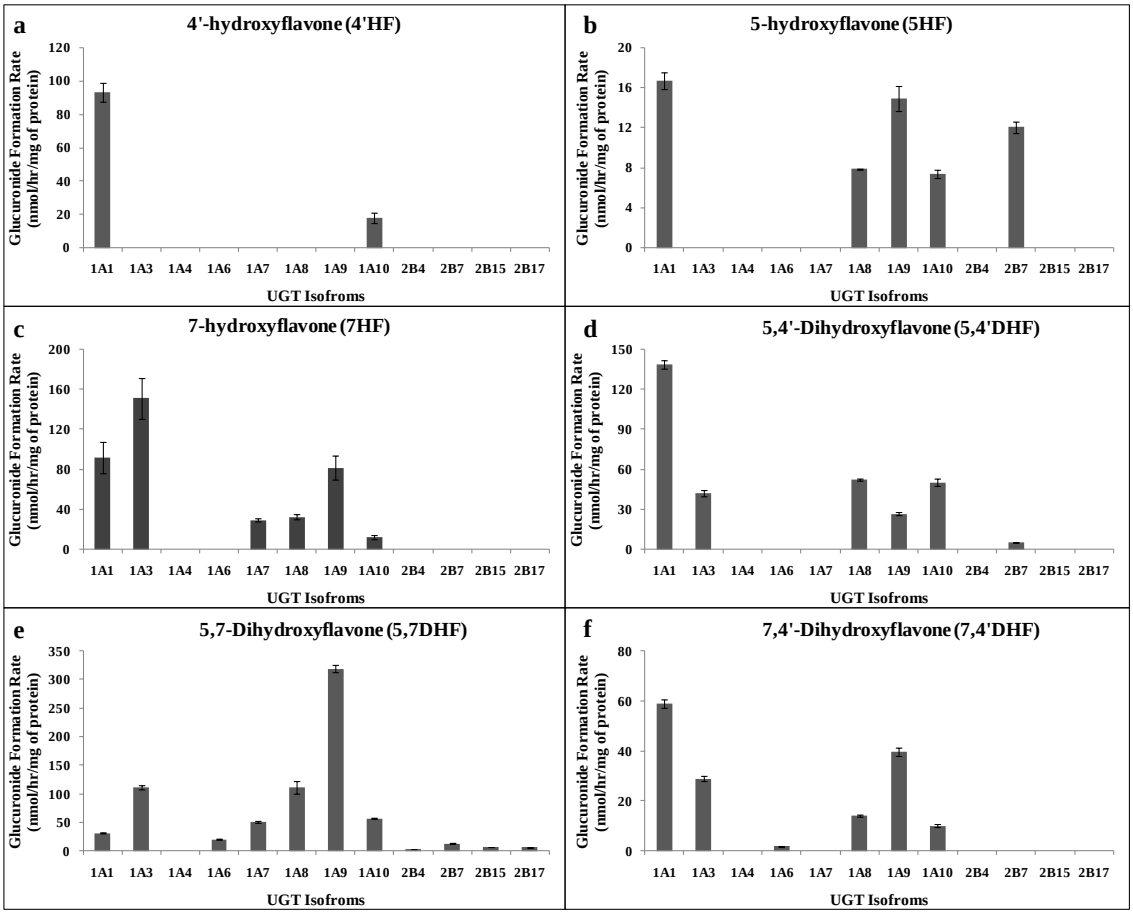

Figure 7. Glucuronidation of Flavones by 12 recombinant human UGTs.
4'-hydroxyflavone (4'HF) (a), 5-hydroxyflavone (5HF) (b), 7-hydroxyflavone (7HF) (c), 5,4'-dihydroxyflavone (5,4'DHF) (d), 5,7-dihydroxyflavone (5,7DHF) (e) and 7,4'-dihydroxyflavone (7,4'DHF) (f) at 10 µM concentration were incubated at 37 ºC for 1 (or 0.5) hr with each UGT isoform (using optimum final protein concentration ~ 0.25, 0.5 or 1 mg/ml). The amounts of mono-glucuronide(s) formed were measured using UPLC. In case of flavones with two mono-glucuronides, rates of glucuronide formation were calculated as the sum of rates of formation of two mono-glucuronides of flavones. Each bar is the average of three determinations, and the error bars are the standard deviations of the mean (n=3). The data of 4'-hydroxyflavone (4'HF), 5-hydroxyflavone (5HF) and 7-hydroxyflavone (7HF) has been re-plotted for comparison from Tang *et al.* (2010).[157]

5,4'DHF was better glucuronidated than 4'HF or 5HF by most UGT isoforms (Figure 7a, 7b and 7d). The rank order of top five UGT isoforms for glucuronidation of 5,4'DHF was: UGT 1A1 (138.98 ± 3.14) < 1A8 (52.37 ± 1.02) ~ 1A10 (50.19 ± 2.60) < 1A3 (42.42 ± 2.30) < 1A9 (26.75 ± 1.14 nmol/hr/mg of protein) (Figure 7d). 5,7DHF was the fastest metabolizing compound in the series by most isoforms ($p<0.05$) (Figure 7e). The rank order of top five UGT isoforms for glucuronidation of 5,7DHF was almost the reverse of the rank order of 5,4'DHF: UGT 1A9 (318.41 ± 6.15) < 1A3 (111.86 ± 3.69) ~1A8 (111.08 ± 10.84) < 1A10 (56.58 ± 0.69) < 1A7 (50.76 ± 2.49 nmol/hr/mg of protein) (Figure 7d).

The rates of glucuronidation of 7,4'DHF by all metabolizing UGT isoforms were slower that the rates of glucuronidation of 4'HF and 7HF ($p<0.05$) (Figures 7b, 7c and 7f). The rank order of top five UGT isoforms for glucuronidation of 7,4'DHF was: UGT 1A1 (58.85 ± 1.83) < 1A9 (39.52 ± 1.72) < 1A3 (28.90 ± 1.12) < 1A8 (14.12 ± 0.59) < 1A10 (10.07 ± 0.64 nmol/hr/mg of protein) (Figure 7f). As discussed in section 4.4.4., for 5,7,4'THF (apigenin), the rank order of the most important isoforms was: UGT 1A9 (71.96 ± 7.87) > 1A8 (53.41 ± 7.08) > 1A1 (28.44 ± 2.55) > 1A3 (23.72 ± 0.56) > 1A7 (19.48 ± 3.52) ~ 1A6 (17.02 ± 0.69 nmol/hr/mg of protein) (Figure 5b).

The above results showed that UGT 1A1 and 1A10 were the only isoforms which could metabolize all flavonols. UGT1A8 and 1A9 were able to glucuronidate all flavonols

except 4'HF, whereas UGT1A3 glucuronidated all flavones except two mono-hydroxyflavones, 4'HF and 5HF (Figures 5b and 7a-7f). UGT1A6 was only important for 5,7DHF and 5,7,4'THF. Most flavones were either not glucuronidated by UGT2B7 or glucuronidated poorly (Figures 5b and 7a-7f). Also, the ranking of top five isoforms for all tested flavones were different.

In contrast to flavonols, there was no single isoform which metabolized all compounds at the fastest rate. However, for all flavones either UGT1A1 or UGT1A9 was the top isoform. This suggested that whether all compounds would share the similar most important UGT isoforms was dependent on the flavonoid sub-class.

4.4.6. Concentration-dependent glucuronidation of flavonoids across sub-classes by six most important recombinant human UGT isoforms.

We studied the rates of glucuronidation of five flavonoids with six major UGT isoforms (1A1, 1A3, 1A7, 1A8, 1A9 and 1A10) at three different substrate concentrations (2.5, 10 and 35 µM) to see the effect of substrate concentration on the selection of the most important isoform(s). The data suggested that the rank order of most important isoforms for flavonoids changed with substrate concentrations (Figure 8).

For genistein, at 2.5µM substrate concentration, UGT 1A9 (46.87 ± 5.88) and 1A1 (18.79 ± 0.84) were most important isoforms, whereas at 10µM, after UGT1A9, 1A8 (18.99 ± 2.49) was more important than 1A1 (4.19 ± 0.43 nmol/hr/mg of protein). However, at

35µM substrate concentration, UGT1A8 (118.78 ± 5.38) became the most important isoform, followed by 1A9 (70.67 ± 2.88) and 1A10 (48.52 ± 6.20 nmol/hr/mg of protein) (Figure 8a).

Similar behavior was shown by apigenin, where 2.5µM substrate concentration, UGT 1A9 (102.7 ± 2.61) and 1A1 (26.92 ± 3.48) were most important isoforms, whereas at 10µM, after UGT1A9, 1A8 (53.41 ± 7.08) was more important than 1A1 (28.44 ± 2.55 nmol/hr/mg of protein). However, in this case, at 35µM substrate concentration, UGT1A8 (80.30 ± 2.26) became almost as important as 1A9 (99.12 ± 8.17), followed by 1A6 (43.23 ± 6.05 nmol/hr/mg of protein) (Figure 8b).

In case of naringenin, the top two isoforms, UGT1A9 and 1A8, maintain the same rank order at all the three substrate concentrations, although UGT1A3 became more important at higher substrate concentrations (Figure 8c). For phloretin, rank order was almost maintained the same at all the three substrate concentrations, UGT1A8 as the fastest metabolizing isoform, followed by 1A1 and 1A9 (Figure 8d). For kaempferol, the rank order at 35µM was exactly similar to that at 10µM, but changed at lower substrate concentration, where after UGT 1A9, 1A1 (99.96 ± 2.46) and 1A7 (63.01 ± 2.65) were more important isoforms than 1A8 (52.99 ± 5.09 nmol/hr/mg of protein) (Figure 8e).

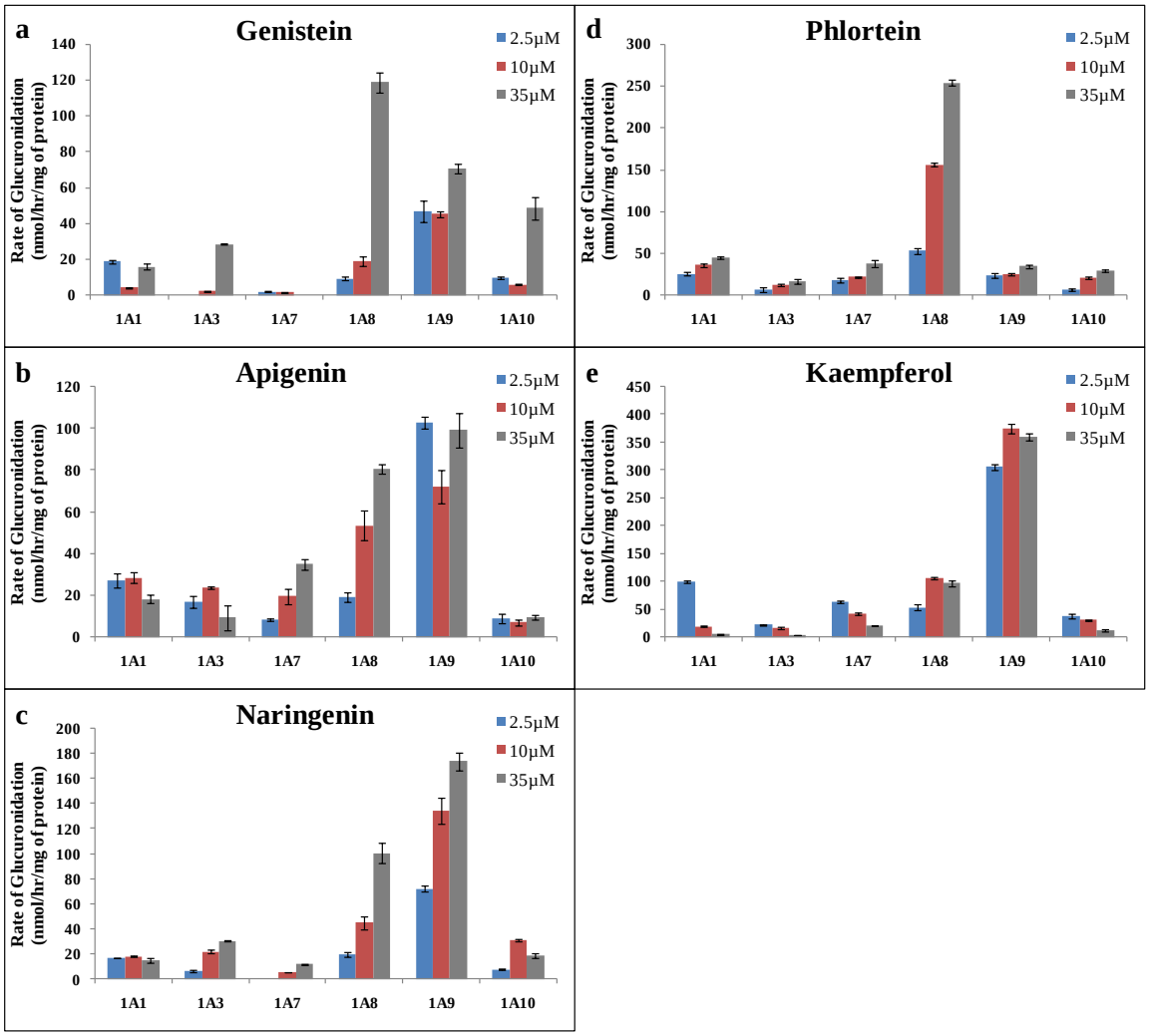

Figure 8. Glucuronidation of flavonoids at three different concentrations from five sub-classes by 6 major human UGT isoforms.

Genistein (isoflavone) (a), apigenin (flavones) (b), naringenin (flavonone) (c), phloretin (chalcone) (d) and kaempferol (flavonol) (e) (at 2.5, 10 and 35 µM concentration) were incubated at 37 ºC for 1 (or 0.5) hr with each UGT isoform (using optimum final protein concentration ~ 0.25, 0.5 or 1 mg/ml). The amounts of mono-glucuronide(s) formed were measured using UPLC. Rates of glucuronide(s) formation were calculated as nmol/hr/mg of protein. In case of both phloretin and kaempferol, rates of glucuronide formation were calculated as the sum of rates of formation of three mono-glucuronides of phloretin and kaempferol, respectively. Each bar is the average of three determinations, and the error bars are the standard deviations of the mean (n=3).

In general, UGT1A9 was the most important isoform for all flavonoids at all the three substrate concentrations, except phloretin which was glucuronidated most importantly by 1A8 at all the three substrate concentrations (Figure 8). Moreover, for all compounds except phloretin and naringenin, UGT 1A1 and 1A8 changed ranks at highest substrate concentration. In general, after UGT1A9, UGT1A1 was the second most important isoforms at lowest substrate concentration (2.5μM) whereas 1A8 was the most important isoforms at highest substrate concentration (35μM) (Figure 8).

4.4.7. Concentration-dependent glucuronidation of flavonols across sub-classes by six most important recombinant human UGT isoforms.

We also studied the rates of glucuronidation of six flavonols with their respective six major UGT isoforms (1A1, 1A3, 1A7, 1A8, 1A9, 1A10) at three different substrate concentrations (2.5, 10 and 35 μM) to see the effect of substrate concentration on the selection of the most important isoform(s). The data suggested that the rank order of most important isoforms for flavonols changed with concentration (Figure 9).

At 2.5μM substrate concentration, 3HF was metabolized fast only by UGT1A1 (53.51 ± 9.42), and poorly by UGT1A8 (5.61 ± 0.84), 1A9 (5.78 ± 0.12) and 2B7 (13.92 ± 0.12 nmol/hr/mg of protein) (Figure 9a). But at 10μM substrate concentration, it was metabolized by all isoforms except UGT1A4.

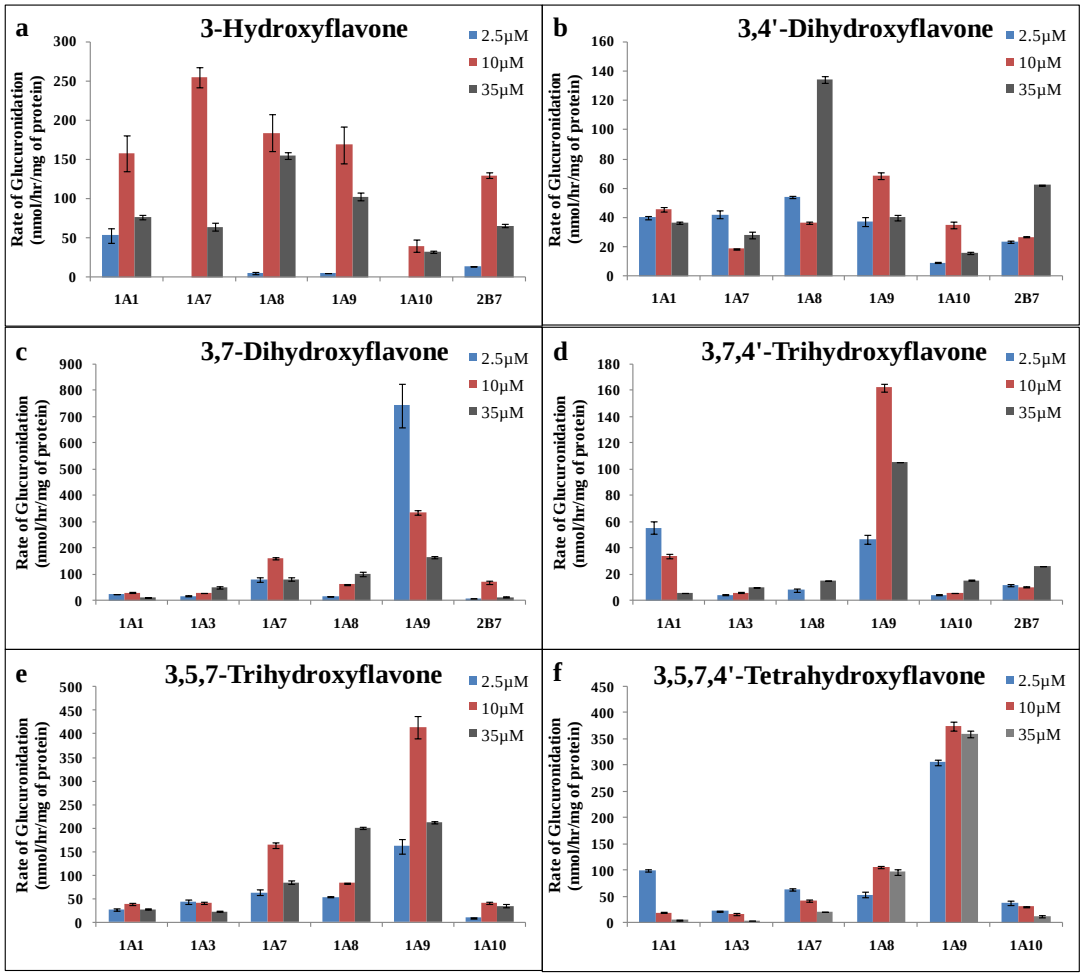

Figure 9. Glucuronidation of flavonols at three different concentrations by 6 major human UGT isoforms.

3-hydroxyflavone (3HF) (a), 3,4'-dihydroxyflavone (3,4'DHF) (b), 3,7-dihydroxyflavone (3,7DHF) (c), 3,7,4'-trihydroxyflavone (3,7,4'THF) (d), 3,5,7-trihydroxyflavone (3,5,7THF) (e) and 3,5,7,4'-tetrahydroxyflavone (3,5,7,4'QHF) (f) (at 2.5, 10 and 35 µM concentration) were incubated at 37 ºC for 1 (or 0.5) hr with each UGT isoform (using optimum final protein concentration ~ 0.25, 0.5 or 1 mg/ml). The amounts of mono-glucuronide(s) formed were measured using UPLC. Rates of glucuronide(s) formation were calculated as nmol/hr/mg of protein. In case of flavonols with multiple glucuronides, rates of glucuronides formation were calculated as the sum of rates of formation of all mono-glucuronides. Each bar is the average of three determinations, and the error bars are the standard deviations of the mean (n=3).

At 35µM substrate concentration, except for UGT1A7 which was came last, the rank orders of important isoforms of 3HF was similar to their rank order at 10µM (Figure 9a).

In case of 3,4'DHF, all the three different concentrations have different rank order of important isoforms, with UGT 1A1 and 1A8 as top two most important isoforms at lowest substrate concentration (2.5µM); UGT1A9 and 1A1 at middle substrate concentration (10µM); and UGT1A8 and 2B7 at highest substrate concentrations (35µM) (Figure 9b).

At 2.5µM substrate concentration, 3,7DHF was glucuronidated by UGT1A9 (2143.10 ± 252.96) about ~100 times faster than by UGT1A1 (24.33 ± 1.44), and ~25 times faster than by UGT1A7 (79.95 ± 9.05 nmol/hr/mg of protein) ($p<0.05$) (Figure 9c). Also, the glucuronidation of 3,7DHF at 2.5µM substrate concentration by UGT1A9 was about 6-10 times faster than its glucuronidation at 10 and 35µM ($p<0.05$) (Figure 9c).

For 3,7DHF, UGT1A9 was the most important isoform at all the three substrate concentrations, followed by UGT1A7 at 2.5 and 10 µM substrate concentrations, whereas by UGT1A8 at 35µM substrate concentration (Figure 9c). Similarly, for 3,5,7THF also UGT1A9 was the most important isoform at all the three substrate concentrations followed by UGT1A7 at 2.5 and 10 µM substrate concentrations, whereas by UGT1A8 became as important as UGT1A9 at 35µM substrate concentration (Figure 9e).

In case of 3,7,4'THF, the rank order at 2.5μM substrate concentration was exactly similar to that at 10μM, but changed at higher concentration. UGT1A9 was again the most important isoform at all the three substrate concentrations followed by UGT1A1 at 2.5 and 10 μM substrate concentrations, whereas by UGT2B7 at 35μM substrate concentration (Figure 9d). For 3,5,7,4'QHF (kaempferol), the rank order at 35μM was exactly similar to that at 10μM, but changed at lower substrate concentration, where after UGT1A9, 1A1 (99.96 ± 2.46) and 1A7 (63.01 ± 2.65) were more important isoforms than 1A8 (52.99 ± 5.09 nmol/hr/mg of protein) (Figure 9e).

In summary, the change in substrate concentration showed a greater effect on the most important UGT isoform within specific sub-class rather than across sub-classes. UGT1A9 was the most important isoform for all flavonols at 10μM substrate concentration, but not necessarily at 2.5 and 35μM. At 2.5μM substrate concentrations, the first most important isoform was either UGT 1A1 (3HF and 3,7,4'THF) or 1A8 (3,4'DHF) or 1A9 (3,7DHF, 3,5,7THF, and 3,5,7,4'QHF). At 35μM substrate concentrations, the top two most important isoform was either 1A8 (for 3HF and 3,4'THF) or 1A9 (for 3,7DHF, 3,5,7THF, 3,7,4'THF and 3,5,7,4'QHF), except for 3,7,4'THF which was not a good substrate of UGT1A8. The rank order of most important UGT isoform at 35μM for most flavonols was different from the rank order at 2.5μM substrate concentration.

4.5. Discussion

UGT1A9, UGT1A8 and UGT1A1 are the most important isoforms that can glucuronidate vast majority of tested flavonoids. Based on published UGT isoform mRNA expression pattern in human organs, liver and intestine should serve as the major first-pass metabolism organs for flavonoids. These UGT isoforms were able to efficiently (faster rates) glucuronidate diverse types of flavonoid structures. This can be supported by the fact that UGT 1A9 and UGT1A8 were the top two metabolizing isoforms for the flavonoids (at 10μM substrate concentration) from different sub-classes, flavone (apigenin), isoflavone (genistein), flavonone (naringenin) and flavonol (kaempferol) (Figure 5). Only for the glucuronidation of compound from chalcone sub-class (phloretin), which has open ring structure, UGT1A8 was the most important isoform, followed by UGT1A1 (Figure 5). This strongly indicated that except phloretin, all flavonoids with same numbers and positions of hydroxyl groups at different backbones were glucuronidated by UGT1A9 exclusively expressed in liver and kidney,[61] and UGT1A8 exclusively expressed in small intestine in humans.[61]

It is also be supported by the fact that within flavonol sub-class, compounds with different numbers and positions of hydroxyl groups on the same backbone, were glucuronidated fastest by UGT1A9, except for 3HF, where 1A7 was faster than 1A9 (Figure 6). After UGT1A9, 1A8 and 1A1 were the only two isoforms which were among the top five glucuronidating isoform for all flavonols except for 3,7,4'THF, which was

not a substrate of UGT1A8. On the other hand, either UGT1A1 or UGT1A9 was the most important isoform for the compounds within flavone sub-class, except for 7HF (Figures 5e and 7). UGT1A8 was also an important isoform for all flavones except 4'HF (Figure 7). This suggested that main metabolizing isoform was more affected by the numbers and position of hydroxyl group in the structure than the backbone change.

Another evidence in support of the conclusion is that UGT1A9 was the most important isoform for all the selected flavonoids across different sub-classes at all the three substrate concentrations (2.5, 10 and 35μM), except for phloretin which was glucuronidated most importantly by UGT1A8 at all the three substrate concentrations (Figure 8). In general, for all flavonoids except phloretin, UGT1A1 was the second most important isoform at lower substrate concentration (2.5μM), while UGT1A8 was the second most important isoform at higher substrate concentration (35μM) (Figure 8).

Similarly, in case of flavonol sub-class, at lower substrate concentration (2.5μM), the most important isoform was either UGT1A1, or UGT1A8 or UGT1A9 (Figure 9). Whereas, at higher substrate concentration (35μM), the top two most important isoform was either UGT1A8 or UGT1A9, except for 3,7,4'THF which was not a good substrate of UGT1A8 (Figure 9). This again suggested that the concentration-dependent rank order of the important isoforms was more visible in case of change in numbers and position of hydroxyl group in the structure than in case of the backbone change.

Our conclusion is also supported by the published reports on glucuronidation of various flavonoids by UGT isoforms. Recently published report by Tang *et al.* (2009) on UGT "fingerprinting" of isoflavones, also showed that in general, UGT 1A1, 1A8, 1A9 and 1A10 were the most important isoforms for glucuronidating isoflavones.[87] As per the published report on comparable mRNA expression of UGT1A1 and 1A9 in human liver,[164] the sum of rates of glucuronidation of isoflavones by recombinant human UGT1A1 and UGT1A9 showed good correlation well with their corresponding rates of glucuronidation by human liver microsomes.[87] This suggested that UGT fingerprinting of flavonoids can be used to predict the metabolism of flavonoids by major metabolic organs/tissues such as liver, intestine, kidney etc. based on their UGT isoforms expression levels.

Another reports showed that most mono-hydroxyflavones were glucuronidated fastest by UGT1A1, 1A8 and 1A9 at three substrate concentrations (2.5, 10 and 35μM), whereas UGT1A10 slowly glucuronidated all mono-hydroxyflavones at substrate concentrations of 10 and 35 μM.[157] Boersma *et al.* (2002) also showed that at 100μM substrate concentration, luteolin (a flavone) was mainly metabolized by UGT1A1, 1A6, 1A8 and 1A9, whereas quercetin (a flavonol) was mainly metabolized by UGT1A1, 1A3, 1A8 and UGT1A9.[89]

Mizuma (2009) reported that the UGT1A1, UGT1A8, UGT1A9, and UGT1A10 were responsible for raloxifene (a polyphenolic compound like flavonoids) glucuronidation

and suggested that intestinal glucuronidation by UGT1A8 and 1A10 were mainly responsible for low bioavailability of raloxifene.[165] The present results also showed that UGT 1A3, 1A6, 1A7, 1A10 and 2B7 played flavonoid structure-, substrate concentration- and sub-class- dependent role in glucuronidating the flavonoids (Figures 5-9). This can also be supported by various published reports.[87, 89, 157]

In conclusion, UGT1A9, UGT1A8 and UGT1A1 are the most important UGT isoform responsible for the glucuronidation of vast majority of flavonoids at the tested substrate concentrations. Based on published UGT isoform mRNA expression pattern in human organs, liver and intestine should serve as the major first-pass metabolism organs for flavonoids. This study allowed us to choose the important UGT isoforms for further investigation of regiospecific and substrate-selective glucuronidation of flavonoids. It further gave us the rationale for choosing the isoforms for the purpose of developing UGT isoform-specific *in silico* prediction models for flavonoid glucuronidation.

UGT ISOFORM-DEPENDENT REGIOSPECIFICITY AND SUBSTRATE SELECTIVITY OF GLUCURONIDATION OF FLAVONOIDS

5.1. Abstract

The objective of this study was to determine the regiospecificity and substrate selectivity of the most important UGT isoforms responsible for the glucuronidation of flavones and flavonols. We systematically studied the glucuronidation of 13 flavonoids (7 flavones and 6 flavonols, with hydroxyl group at C-3, C-4', C-5, and/or C-7 positions) at a substrate concentration of 10μM by 8 recombinant human UGT isoforms mainly responsible for metabolism of flavonoids, UGT 1A1, 1A3, 1A6, 1A7, 1A8, 1A9, 1A10 and 2B7. We showed that at 10μM substrate concentration, different UGT isoforms gave different regiospecific glucuronidation patterns. UGT1A1 equally glucuronidated 3-*O*, 7-*O* and 4'-*O*, whereas UGT1A8 and 1A9 preferably glucuronidated only 3-*O* and 7-*O* positions. UGT1A1 showed no regiospecificity for glucuronidating any position, whereas, UGT1A8 and UGT1A9 showed dominant, preferred or weak regiospecificity for 3-*O* or 7-*O* position, depending on the structure of the compound. We showed that the rates of glucuronidation of 3-*O* and 7-*O* positions in flavones and flavonols were affected by the addition of multiple hydroxyl groups at different positions as well as by the substrate concentrations (2.5, 10 and 35μM). We showed that in general, for flavones and flavonols, the rates of glucuronidation by UGT1A1 reduced as number of hydroxyl group in the structure increased, with few exceptions. We also showed that the addition of

hydroxyl group at C-4’ reduced, whereas the addition of hydroxyl group at C-3, C-5 and/or C-7 improved the rates of glucuronidation of flavonoids by UGT1A8 and 1A9. In conclusion, regiospecificity and substrate-selectivity was isoform-dependent. UGT1A8 and UGT1A9 preferred glucuronidation at 3-*O* position followed by 7-*O*, whereas UGT1A1 showed no preference to glucuronidate any specific position. UGT1A1 activities towards flavonoids usually decreased with increasing number of hydroxyl groups. On the other hand, UGT1A8 and UGT1A9 activities increased with addition of hydroxyl group at 3-*O*, 5-*O* and/or 7-*O* positions, while decreased with addition of hydroxyl group at 4’-*O* position.

5.2. Introduction

UGTs utilize UDP-glucuronic acid as cofactor and transfer glucuronic acid to the usually lipophilic substrates, forming hydrophilic conjugates called glucuronides. Substrates of UGTs include endogenous compounds such as steroids, bile acids, bilirubin, hormones, dietary constituents like flavonoids, xenobiotics such as morphine and valproic acid, the products of phase I metabolism, and environmental toxins and carcinogens such as PhIP.[43, 45, 49] UGT-catalyzed glucuronidation reactions are responsible for 35% of all drugs metabolized by phase II enzymes.[50] Despite the important role of UDP-glucuronosyltransferases (UGT) in the metabolism of drugs, environmental chemicals and endogenous compounds, the structural features of these enzymes responsible for substrate binding and selectivity remain poorly understood.[60, 166]

For the glucuronidation reaction, the substrates typically possess hydroxyl group (alcoholic, phenolic), carboxyl, sulfuryl, carbonyl, or amino (primary, secondary, or tertiary) group in their structure. *O*-glucuronidations are more common than N- and C-glucuronidation.[43, 45, 49] The UGT superfamily is comprised of 4 families (UGT1, UGT2, UGT3 and UGT8) and 5 subfamilies (UGT1A, UGT2A, UGT2B, UGT3A, and UGT8A).[55] So far, 19 human UGT proteins have been isolated: UGT 1A1, 1A3, 1A4, 1A6, 1A7, 1A8, 1A9, 1A10, 2B4, 2B7, 2B10, 2B11, 2B15, 2B17, 2B28, 8A1, 3A1 and 3A2.[55, 60] Unlike CYP-450 isoforms which have shown to exhibit broad but specific

substrate selectivities, UGT isoforms usually exhibit distinct but significantly overlapping substrate selectivities.[45, 147, 167]

The metabolic clearance of flavonoids via glucuronidation may vary considerably owing to factors including genetic polymorphism and drug interaction due to UGT enzyme as well as efflux transporters involved in excretion of glucuronides.[45, 50, 97, 108, 168, 169] Such factors affecting the metabolic clearance of flavonoids are important in regards to development of flavonoids as chemopreventive agents as well as rationalizing and optimizing dosage regimens of the established drugs co-administered with flavonoids. Reaction phenotyping, i.e. the identification of the specific isoform(s) primarily responsible for the metabolism of a compound, allows semi-quantitative prediction of factors altering metabolic clearance *in vivo*.[122] Reaction phenotyping is readily achieved *in vitro* using kinetic and inhibitor approaches for CYP-450-catalyzed drug biotransformation.[122, 123] However, *in vitro* reaction phenotyping of glucuronidated compounds is less advanced because of the limited availability of UGT isoform selective substrates and inhibitors.[122, 141]

In addition to overlapping substrate selectivities, various UGT isoforms exhibit regiospecificity in glucuronidation of various compounds. However, there is very limited information available in literature on the regiospecificity of glucuronidation of compounds in general and flavonoid in specific.[51, 87, 96, 100, 157, 160, 170] The regiospecific glucuronides of certain flavonoids have shown to exhibit different pharmacological

actions *in vivo*.[80, 82] Also, it has been proposed that glucuronides in systemic circulation or after uptake into an organ such as liver, intestine and neutrophils may hydrolyze back into aglycone by β-glucuronidase enzyme for pharmacological action. However, the rate of flavonoid glucuronides hydrolysis depends on the position of conjugation, which could affect the subsequent re-conjugation rate.[78, 85] Therefore, it becomes important to understand the regiospecificity of various UGT isoforms, as based on different expression levels of UGTs in various metabolic organs and mode of administration of drug, the exposure of regiospecific glucuronides to an organ may differ extensively.

In the previous chapter, we showed that certain UGT isoforms were important for the glucuronidation of most flavonoids from different sub-classes. This provided evidence that UGT isoforms showed over-lapping substrate selectivity for flavonoids. However, different UGT isoforms showed differences in their rate and position of glucuronidation of flavones and flavonols. Therefore, we decided to study all major UGT isoforms for the preference of structure and position of glucuronidation using 13 flavonoids (7 flavones and 6 flavonols) (Figure 4, pg 65) with hydroxyl groups at C-3, C-4', C-5 and C-7 positions. This will help us to identify the compounds or structural features which might be specific or better substrate of a particular UGT isoform. Additionally, it will give insight into regiospecificity of various UGT isoforms and based on expression levels of various metabolic organs such as liver and intestine, we might be able to predict the relative occurrence of various regiospecific glucuronides of flavonoids.

5.3. Materials and Methods

5.3.1. Materials

3-hydroxyflavone (3HF), 3,4'-dihydroxyflavone (3,4'DHF), 3,7-dihydroxyflavone (3,7DHF), 5,4'-dihydroxyflavone (5,4'DHF), 5,7-dihydroxyflavone (5,7DHF), 7,4'-dihydroxyflavone (7,4'DHF), 3,7,4'-trihydroxyflavone or resokaempferol (3,7,4'THF) and 3,5,7-trihydroxyflavone or galangin (3,5,7THF), 5,7,4'-trihydroxyflavone or apigenin (Api or 5,7,4'THF), 3,5,7,4'-tetrahydroxyflavone or kaempferol (3,5,7,4'QHF or Kamp), were purchased from Indofine Chemicals (Somerville, NJ). 8 commercially available recombinant human UGT isoforms (Supersomes), UGT 1A1, 1A3, 1A6, 1A7, 1A8, 1A9, 1A10, and 2B7, were purchased from BD Biosciences (Woburn, MA). Uridine diphosphoglucuronic acid (UDPGA), alamethicin, D-saccharic-1,4-lactone monohydrate, magnesium chloride, and Hanks' balanced salt solution (powder form) were purchased from Sigma-Aldrich (St Louis, MO). All other materials (typically analytical grade or better) were used as received.

5.3.2. Identification of position of glucuronidation in the structure of flavones and flavonols by UV shift method

The sites of glucuronic acid substitutions in flavones and flavonols were established based on the online UV spectral shift method, optimized and validated in our lab based on the published literature.[171, 172] Briefly, substitution of a single hydroxyl group by

glucuronic acid in the structure of flavone at a specific position would result in diagnostic shifts or no shift in λ_{max} of Band I (300-380 nm) and/or Band II (240-280 nm) in the UV spectrum of the resulting glucuronide as compared to the UV spectrum of parent compound. Based on these differentiating diagnostic shifts for each position of glucuronidation, structure of a glucuronide can be estimated. The details of the method and its validation can be found in Singh *et al.* (2010).[173]

5.3.3. Methods

All other methods used in this chapter were exactly similar to the ones described in Chapter 4, sections 4.3.2 to 4.3.7, pg 68-73.

5.4. Results

5.4.1. Confirmation of flavones and flavonols glucuronides structure by LC-MS/MS

We conducted simple LC-MS/MS studies of the glucuronides of flavonoids to identify the degree of conjugation (mono- or di-) of glucuronides (Figures 1-13, Appendix A). All the results obtained were same as described in the section 4.4.1 of Chapter 4.

5.4.2. Position of glucuronides in the structure of flavones and flavonols by UV shift method

We determined the position of glucuronidation based on the diagnostic shift in λ_{max} of Band I and Band II of UV spectra of glucuronides (Figure 10). Tables B1-B3 (Appendix B) showed the λ_{max} of Band I and II of the selected flavones, flavonols and their glucuronides and shift in λ_{max} of Band I and Band II of the glucuronides as compared to their corresponding aglycone. We do not yet have methods to identify the position of glucuronidation of isoflavones (genistein), flavonone (naringenin) and chalcone (phloretin), hence these are not reported here.

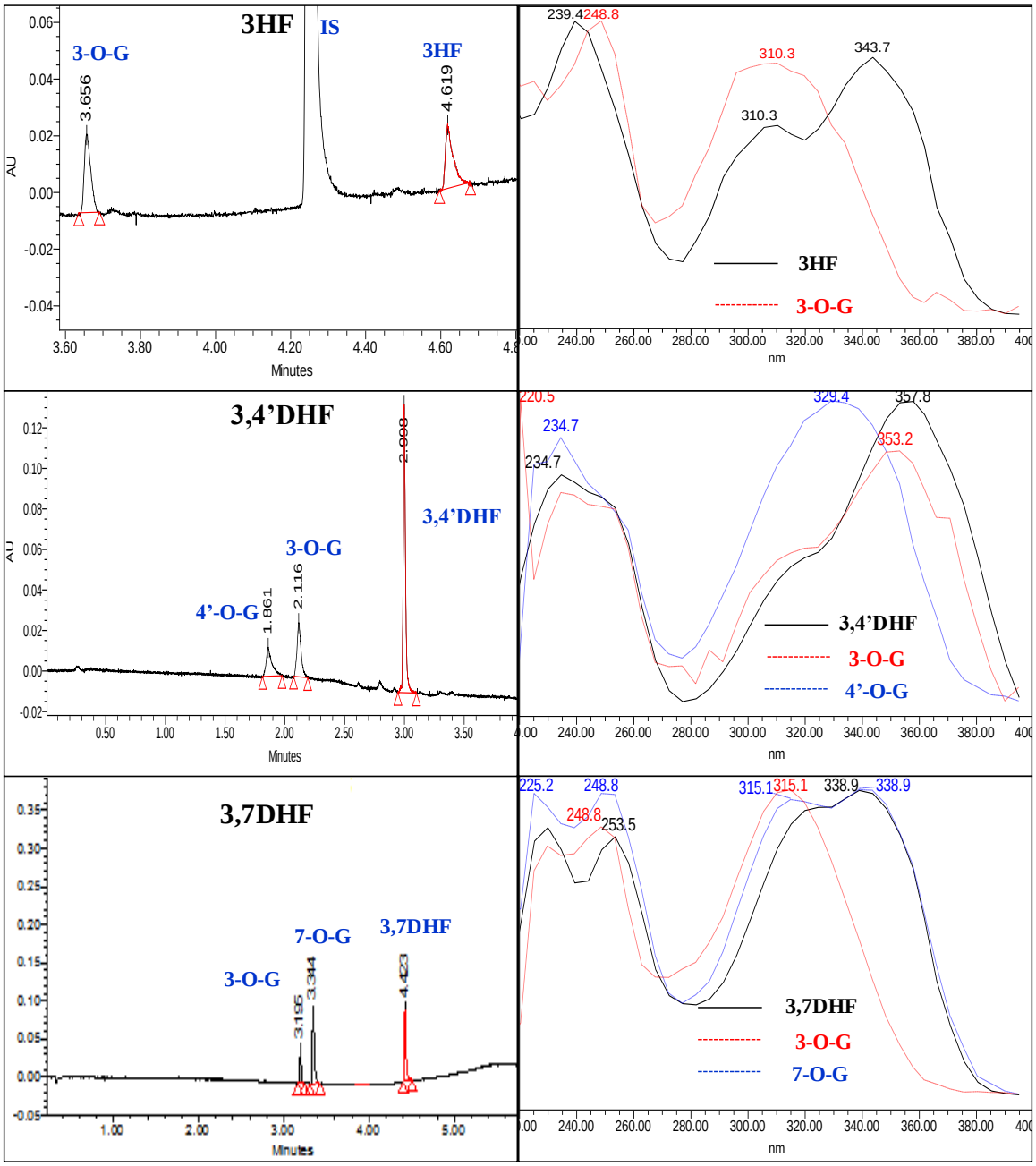
3HF
IS
3-O-G
3HF
3.656
4.619
AU
Minutes
239.4
248.8
310.3
343.7
310.3
3HF
3-O-G
nm
3,4'DHF
2.998
3,4'DHF
3-O-G
4'-O-G
1.861
2.116
220.5
234.7
234.7
329.4
357.8
353.2
3,4'DHF
3-O-G
4'-O-G
3,7DHF
7-O-G
3,7DHF
3-O-G
3.195
3.344
4.423
225.2
248.8
248.8
253.5
315.1
315.1
338.9
338.9
3,7DHF
3-O-G
7-O-G

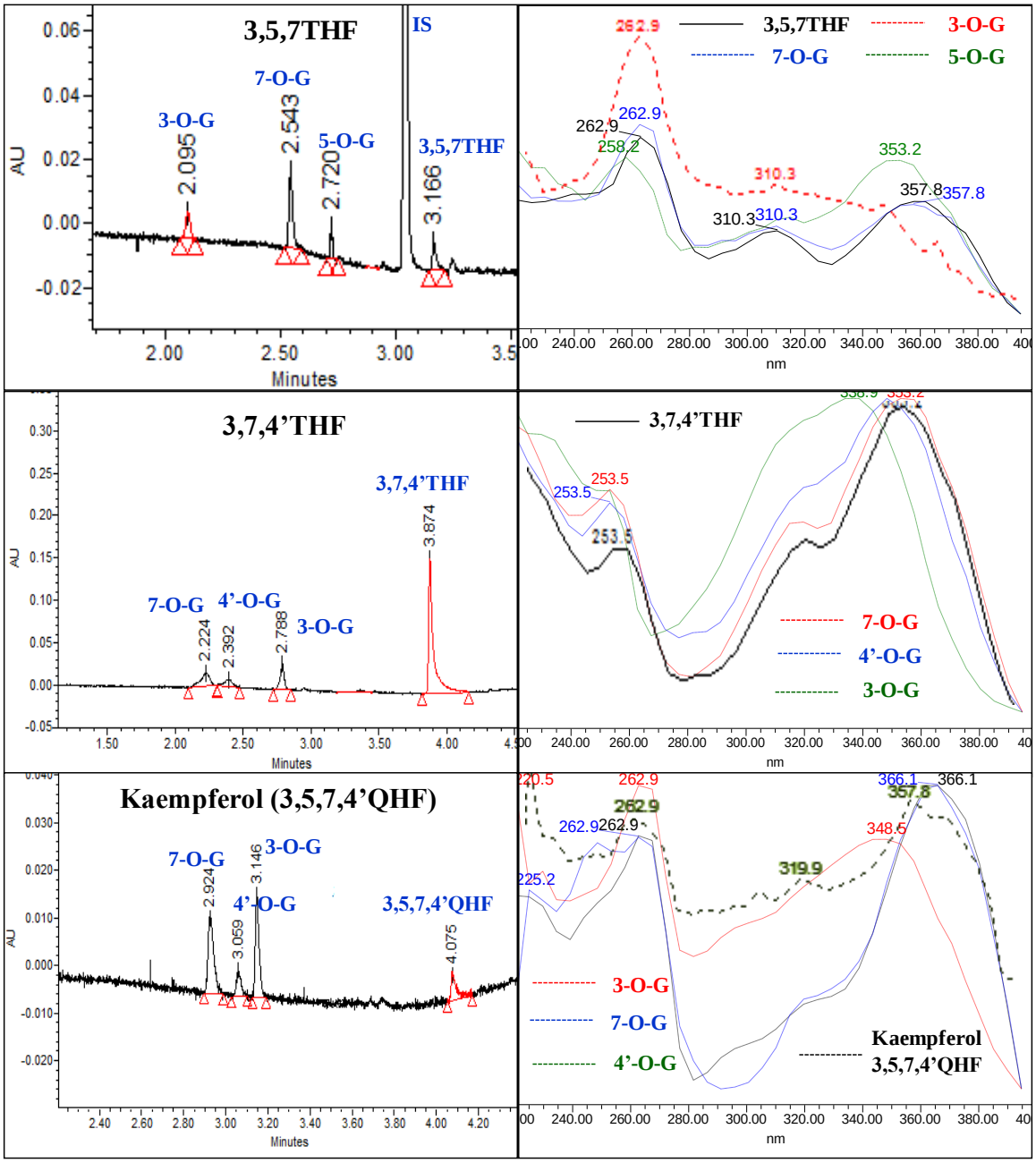
3,5,7THF
IS
7-O-G
3-O-G
5-O-G
3,5,7THF
2.095
2.543
2.720
3.166
AU
Minutes
3,5,7THF
3-O-G
7-O-G
5-O-G
262.9
258.2
310.3
353.2
357.8
nm
3,7,4'THF
3,7,4'THF
7-O-G
4'-O-G
3-O-G
2.224
2.392
2.788
3.874
253.5
Kaempferol (3,5,7,4'QHF)
7-O-G
3-O-G
4'-O-G
3,5,7,4'QHF
2.924
3.059
3.146
4.075
220.5
225.2
319.9
348.5
366.1
Kaempferol
3,5,7,4'QHF

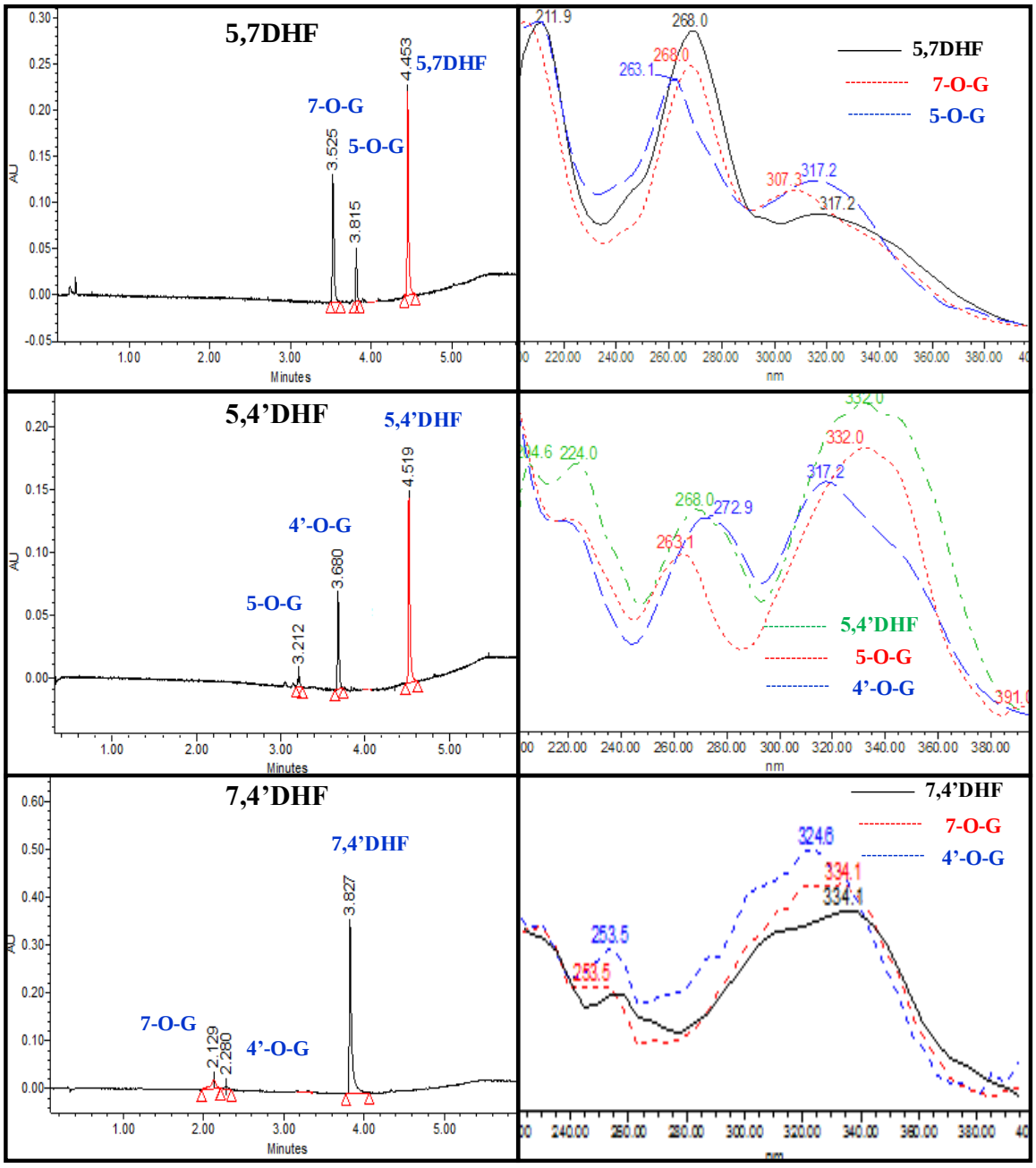
5,7DHF
5,7DHF
7-O-G
5-O-G
4.453
3.525
3.815
AU
Minutes
211.9
268.0
263.1
268.0
307.3
317.2
317.2
5,7DHF
7-O-G
5-O-G
nm
5,4'DHF
5,4'DHF
4'-O-G
5-O-G
4.519
3.680
3.212
AU
Minutes
224.0
332.0
317.2
268.0
272.9
263.1
5,4'DHF
5-O-G
4'-O-G
nm
7,4'DHF
7,4'DHF
7-O-G
4'-O-G
3.827
2.129
2.280
AU
Minutes
324.6
334.1
253.5
253.5
7,4'DHF
7-O-G
4'-O-G
nm

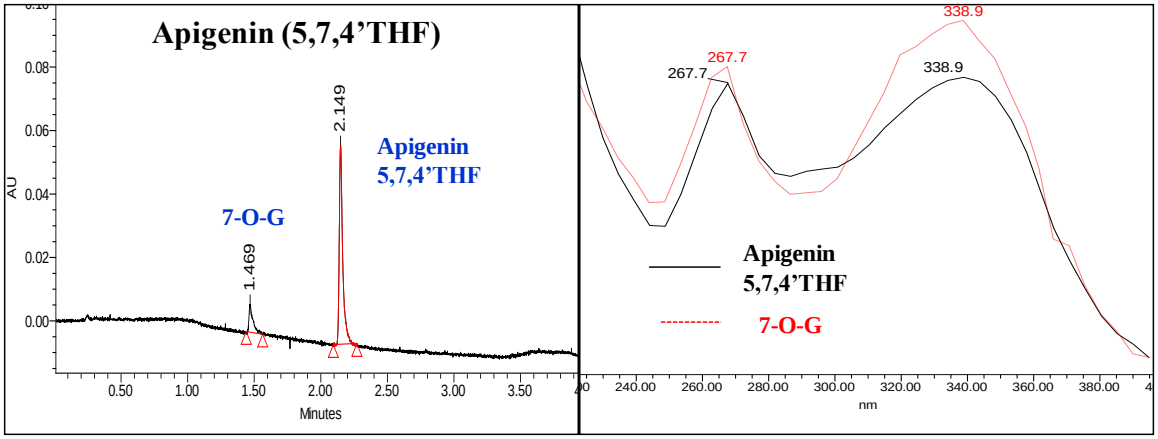

Figure 10. UPLC chromatograms (left panel) and UV spectra (right panel) of flavonoids and their regiospecific glucuronides.
Aglycone and regiospecific glucuronides of 3-hydroxyflavone (3HF), 3,4'-dihydroxyflavone (3,4'DHF), 3,7-dihydroxyflavone (3,7DHF), 3,5,7-trihydroxyflavone (3,5,7THF), 3,7,4'-trihydroxyflavone (3,7,4'THF), kaempferol or 3,5,7,4'-tetrahydroxyflavone (3,5,7,4'QHF), 5,7-dihydroxyflavone (5,7DHF), 5,4'-dihydroxyflavone (5,4'DHF), 7,4'-dihydroxyflavone (7,4'DHF), apigenin or 5,7,4'-trihydroxyflavone (5,7,4'THF) formed by various recombinant human UGT isoforms.

For 3,4'DHF, the first glucuronide was 4'-*O*-G while the second glucuronide was 3-*O*-G, whereas for 3,7 DHF, the first glucuronide was 3-*O*-G, while the second glucuronide was glucuronidated at position C-7 (Figure 10). In case of 3,5,7THF, the position of glucuronidation of first, second and third glucuronides were 3-*O*-G, 7-*O*-G, and 5-*O*-G, respectively (Figure 10). In case of both 3,7,4'THF and 3,5,7,4'QHF (kaempferol), the position of glucuronidation of first, second and third glucuronides were 7-*O*-G, 4'-*O*-G, and 3-*O*-G, respectively (Figure 10).

First and second glucuronide of 5,4'DHF was 5-*O*-G and 4'-*O*-G respectively. Similarly for 5,7DHF, the first glucuronide was 5-*O*-G, while the second glucuronide was 7-*O*-G (Figure 10). In case of 7,4'DHF, the position of conjugation of first and second glucuronides were 7-*O*-G, 4'-*O*-G, respectively, whereas, only one quantifiable glucuronide was observed in case of 5,7,4'THF (apigenin), glucuronidated at C-7 (Figure 10).

5.4.3. Determination of correction factors for glucuronides of flavones and flavonols

Amounts of glucuronides formed were determined using the corrections factors for individual glucuronides of flavonols and flavones as described in the method section. UGT isoforms and wavelength used in generation of correction factor and the correction factor for each glucuronides are detailed in Tables C2-C3 (Appendix C). The correction factors were in the range of 0.5 (for 3-*O*-G of 3HF) to 2.5 (for 3-*O*-G for 3,7DHF).

5.4.4. Regiospecificity of flavonoids glucuronidation by UGTs

We studied the regiospecificity of flavonols and flavones glucuronidation, i.e. preference of glucuronidating a particular hydroxyl group position by UGT 1A1, 1A3, 1A6, 1A7, 1A8, 1A9, 1A10 and 2B7. For the ease of understanding the data, the regiospecificity here is randomly defined into four categories: dominant, preferred, weak and none. *Dominant regiospecificity* means that one hydroxyl group position in the structure is dominantly glucuronidated, such as the ratio of the dominant glucuronide to other glucuronide(s) is equal to or more than 9:1. *Preferred regiospecificity* means that either hydroxyl group at only one position is glucuronidated and no other, or one or two hydroxyl group(s) are preferably glucuronidated in comparison to other(s), such that the ratio of preferred to other(s) glucuronide is equal to or more than 3:1.

Weak regiospecificity means that the glucuronidation of one hydroxyl group was weakly preferred to other, such that the ratio of preferred to other glucuronide is equal to or more than 2:1, whereas *no regiospecificity* means that glucuronidation of no hydroxyl group(s) is significantly preferred to other(s), such that such that the ratio of one to other glucuronide(s) is less than 1:2. All UGT isoforms were studied for their regiospecificity for each compound based into these random categories.

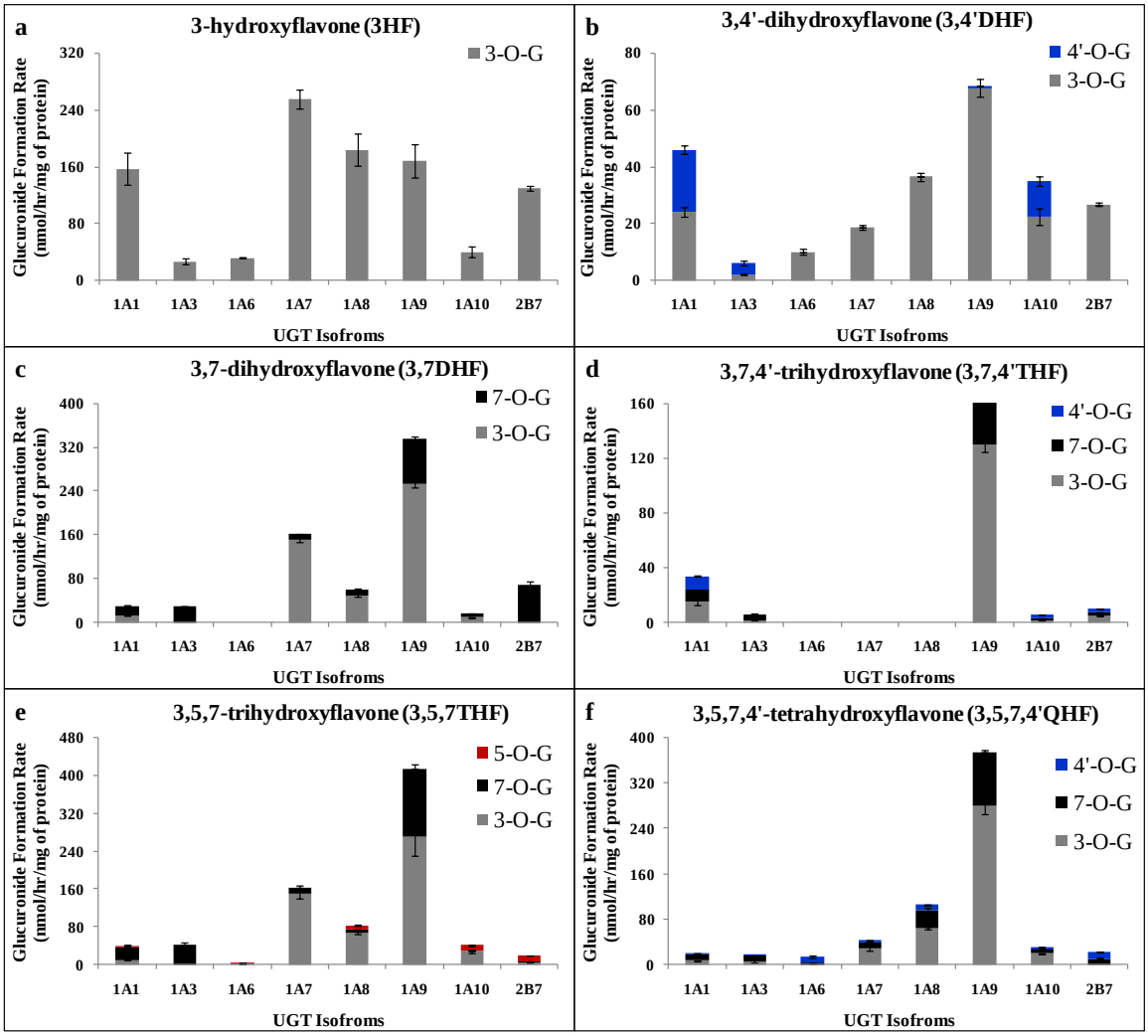

Figure 11. Regiospecific glucuronidation of flavonols by UGTs.
Rate of glucuronidation of regiospecific glucuronides of 3HF (a), 3,4'DHF (b), 3,7DHF (c), 3,7,4'THF (d), 3,5,7THF (e) and 3,5,7,4'QHF (f) with UGT 1A1, 1A3, 1A6, 1A7, 1A8, 1A9, 1A10 and 2B7. Flavonols (at 10 µM concentration) were incubated at 37 ºC for 1 (or 0.5) hr with UGTs (using optimum final protein concentration ~ 0.25, 0.5 or 1 mg/ml). The amounts of each regiospecific mono-glucuronide formed were measured using UPLC. Rates of mono-glucuronide formation were calculated as nmol/hr/mg of protein. Each bar is the average of three determinations, and the error bars are the standard deviations of the mean (n=3).

Flavonols: In general, most isoforms preferably glucuronidated 3-*O* position in the structure of flavonols, followed by glucuronidation of 7-*O* position, except 1A3, which exclusively preferred glucuronidation of 7-*O* position. However, different isoforms might fall in different categories of regiospecificity depending upon structure of compounds. In case of 3,4'DHF, all isoforms showed dominant regiospecificity by glucuronidating almost only the 3-*O* position, except UGT1A1, 1A3 and 1A10 which showed no regiospecificity and glucuronidated both hydroxyl groups at C-4'position and C-3 positions comparably (Figure 11b).

In case of 3,7DHF, different isoforms showed greater differences in their regiospecificity. UGT1A3 and 2B7 were dominantly regiospecific by glucuronidating hydroxyl group only at C-7 position, whereas UGT1A7 dominantly glucuronidated hydroxyl group at C-3 position, which glucuronidated 16 times faster than 7-*O* position. UGT1A1 and 1A10 showed no regiospecificity and glucuronidated both positions comparably, whereas, UGT1A8 and 1A9 showed preferred regiospecificity by preferring glucuronidation of 3-*O* than 7-*O* position (Figure 11c).

In case of 3,7,4'THF, UGT1A1, 1A10 and 2B7 glucuronidated all the three hydroxyl groups and showed no regiospecific preference for any position, whereas 1A3 and 1A9 glucuronidated hydroxyl groups at C-3 and C-7 positions only, with 3-*O* as more favored position of glucuronidation (Figure 11d). UGT1A9 showed preferred regiospecificity by

preferring glucuronidation of 3-*O* than 7-*O* position, whereas UGT1A3 showed weak regiospecificity by preferring glucuronidation of 7-*O* than 3-*O* position (Figure 11d).

In case of 3,5,7THF, UGT1A1 preferred glucuronidation of 3-*O* and 7-*O* positions only, but the glucuronidation of 7-*O* was only weakly preferred over 3-*O* position. UGT1A3 was dominantly regiospecific by glucuronidating hydroxyl group at C-7 position only, whereas UGT1A7 dominantly glucuronidated hydroxyl group at C-3 position, which glucuronidated 10 times faster than 7-*O* position (Figure 11e). UGT1A6 and 1A10 glucuronidate only 3-*O* and 5-*O* positions, in which 1A6 did not show any regiospecificity whereas 1A10 weakly preferred 3-*O* to 5-*O* position. UGT2B7 glucuronidated all the three positions in the following approximate ratio: 8 (5-*O*): 3 (3-*O*): 1 (7-*O*) (Figure 11e). UGT1A8 also glucuronidated all the three positions but showed dominant regiospecificity for 3-*O* position, which glucuronidated 8 times faster than both 7-*O* and 5-*O*. UGT1A9 glucuronidated only 3-*O* and 7-*O* positions but showed no regiospecific preference for any of the positions (Figure 11e).

In case of 3,5,7,4'QHF, no isoforms showed any dominant regiospecificity for any position. UGT 1A1, 1A3, 1A7, 1A8 and 1A9 preferred the glucuronidation of 3-*O* and 7-*O* positions over 4'-*O* position. However, between 3-*O* and 7-*O*, UGT 1A1, 1A3 showed no regiospecific preference, whereas 1A7, 1A8 and 1A9 only weakly preferred 3-*O* position (Figure 11f).

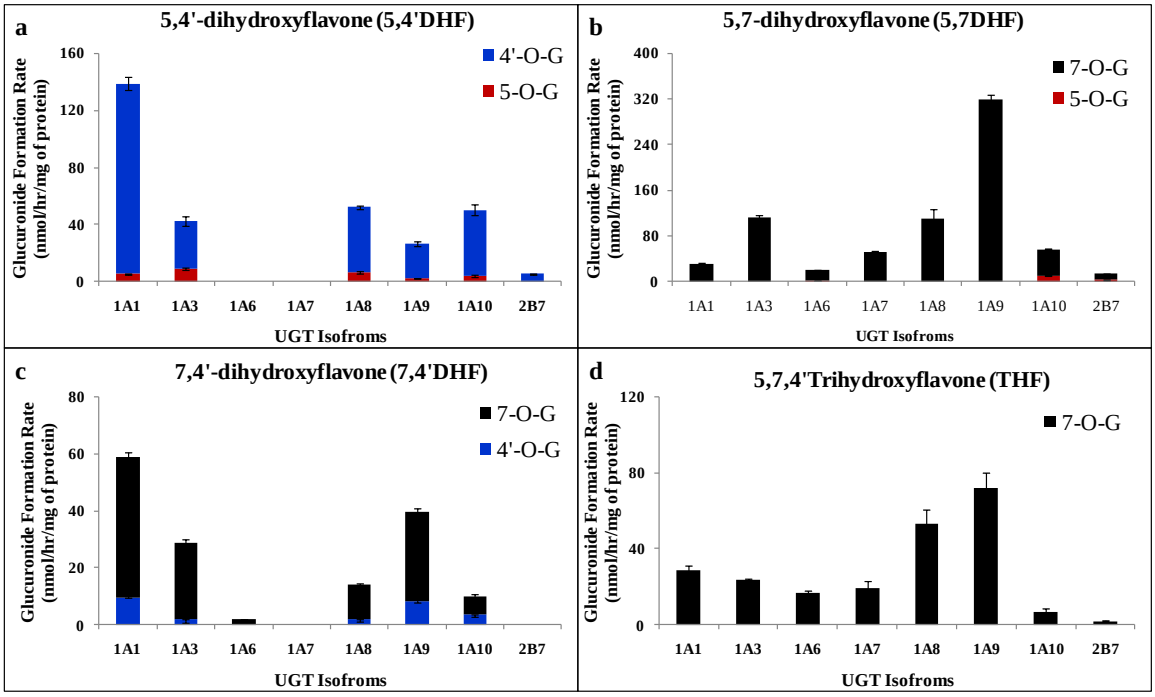

Figure 12. Regiospecific glucuronidation of flavones by UGTs.
Rate of glucuronidation of regiospecific glucuronides of 5,4'DHF (a), 5,7DHF (b), 7,4'DHF (c), and 5,7,4'THF (d) with UGT 1A1, 1A3, 1A6, 1A7, 1A8, 1A9, 1A10 and 2B7. Flavones (at 10 µM concentration) were incubated at 37 ºC for 1 (or 0.5) hr with UGTs (using optimum final protein concentration ~ 0.25, 0.5 or 1 mg/ml). The amounts of each regiospecific mono-glucuronide formed were measured using UPLC. Rates of mono-glucuronide formation were calculated as nmol/hr/mg of protein. Each bar is the average of three determinations, and the error bars are the standard deviations of the mean (n=3).

UGT 1A6 and 2B7 glucuronidated only 7-*O* and 4'-*O* position, where UGT1A6 preferred regiospecific glucuronidation of 4'-*O* position, whereas, 2B7 showed no preference at all (Figure 13f). UGT1A10 glucuronidated all the three position in the following ratio: 6 (3-*O*): 2 (7-*O*): 1 (4'-*O*) (Figure 11f).

In general, UGT1A1, 1A6, 1A10 and 2B7 did not show any dominant regiospecificity for any position, however in some cases, preferred or weak regiospecificity can be seen for glucuronidation of different positions of flavonols. UGT1A3 showed dominant regiospecificity for 7-*O* position, whereas 1A7 showed dominant regiospecificity for 3-*O* position. UGT1A8 and 1A9 preferably glucuronidated 3-*O* and 7-*O* positions only, with preferred or weak regiospecificity for 3-*O* position in most cases.

Flavones: In general, most isoforms preferably glucuronidated 7-*O* position in the structure of flavonols, followed by glucuronidation of 4'-*O* position to some extent (Figure 12). In case of 5,4'DHF, except UGT2B7, all metabolizing isoforms glucuronidated both hydroxyl groups at both C-5 and C-4', though 4'-*O* was the preferred position of glucuronidation in all cases. UGT1A1, 1A9 and 1A10 showed dominant regiospecificity, whereas, 1A3 and 1A8 showed preferred regiospecificity for 4'-*O* position (Figure 12a). In 5,7DHF, UGT1A1, 1A3, 1A8 and 1A9 glucuronidated 7-*O* position only and hence showed dominant regiospecificity towards 7-*O* position (Figure

12b). On the other hand, UGT1A6, 1A10 and 2B7 glucuronidated both 7-*O* and 5-*O* positions, but showed only preferred regiospecificity towards 7-*O* position (Figure 12b).

In case of 7,4'DHF, except UGT1A6, all metabolizing isoforms glucuronidated both hydroxyl groups at C-7 and C-4' positions. UGT 1A3 and 1A6 showed dominant regiospecificity for glucuronidation of 7-*O* position, whereas UGT1A1, 1A8 and 1A9 showed only preferred regiospecificity for glucuronidation of 7-*O* position (Figure 12c). UGT1A10 did not show any regiospecificity and glucuronidated both positions comparably (Figure 14c). In case of 5,7,4'THF, all isoforms showed dominant regiospecific glucuronidation of hydroxyl group at C-7 position only (Figure 12-D).

In summary, for flavones with hydroxyl group at C-7 position, most UGT isoforms showed either dominant or preferred regiospecificity for glucuronidating 7-*O* position over 4'-*O* and 5-*O* position. In absence of hydroxyl group at C-7 position, most UGT isoforms showed either dominant or preferred regiospecificity for glucuronidating 4'-*O* position over 5-*O* position.

5.4.5. Regiospecificity of UGT 1A1, 1A8 and 1A9 for flavonoids glucuronidation

We studied in detail the effect of differences in numbers and positions of hydroxyl groups in the structure of flavonoids, on the regiospecific glucuronidation of flavonoids, specifically the glucuronidation of 3-*O* and 7-*O* positions.

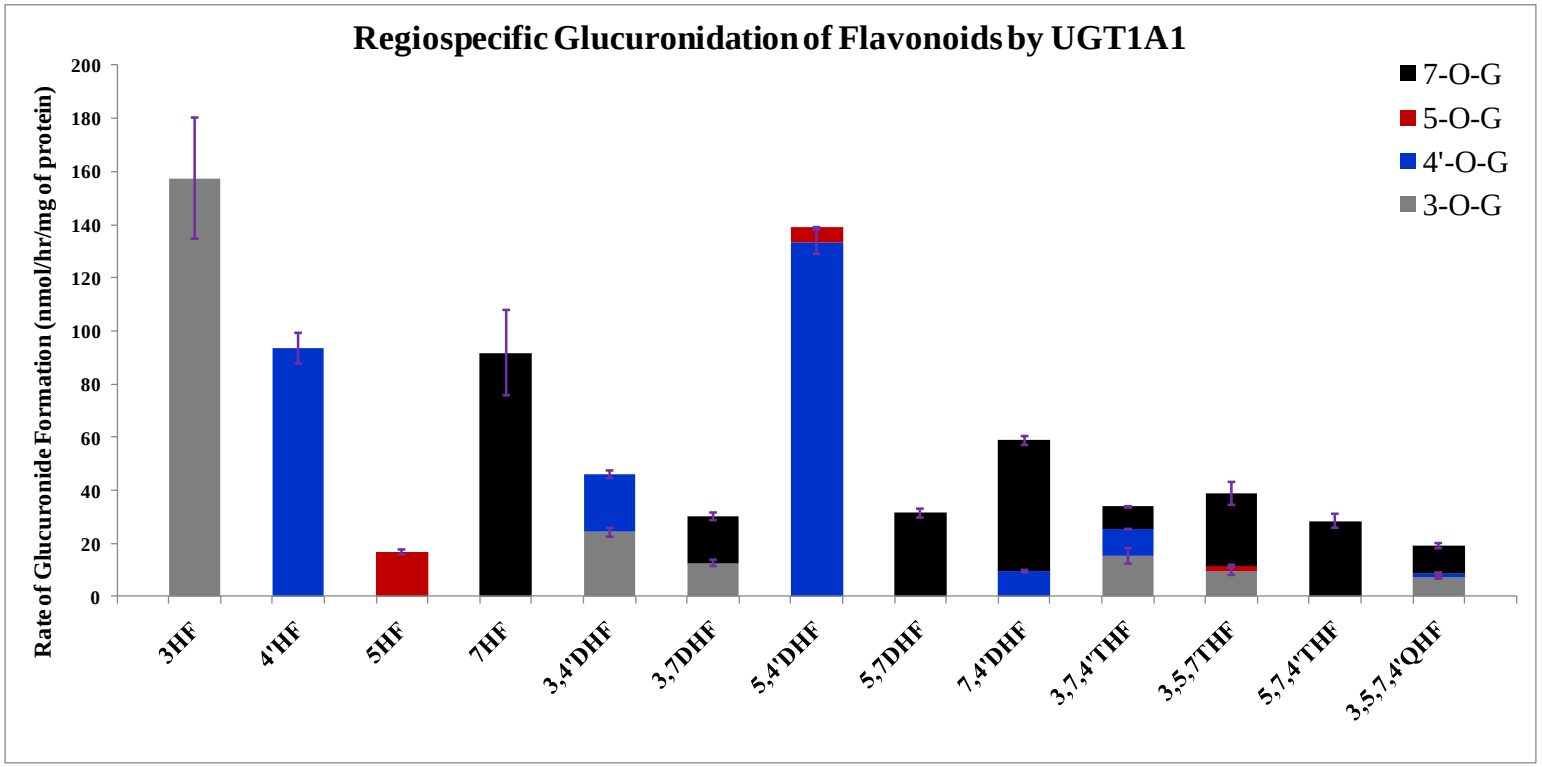

Figure 13. Regiospecific glucuronidation of flavonoids by UGT1A1.
Flavonoids (flavones and flavonols at 10 µM concentration) were incubated at 37 ºC for 1 (or 0.5) hr with UGT1A1 (using optimum final protein concentration ~ 0.25, 0.5 or 1 mg/ml). The amounts of mono-glucuronide(s) formed were measured using UPLC. The amounts of each regiospecific mono-glucuronide formed were measured using UPLC. Rates of mono-glucuronide formation were calculated as nmol/hr/mg of protein. Each bar is the average of three determinations, and the error bars are the standard deviations of the mean (n=3). The data of 4'-hydroxyflavone (4'HF), 5-hydroxyflavone (5HF) and 7-hydroxyflavone (7HF) has been re-plotted for comparison from Tang *et al.* (2010) [157]. The regiospecific data of other flavonoids has been re-plotted from Figures 11 and 12.

UGT1A1: UGT1A1 was able to effectively glucuronidate 3-*O*, 4'-*O* and 7-*O* position in selected flavonoids, but 5-*O* position was not favored (Figure 13). In case of di-hydroxyflavones, UGT1A1 did not show any regiospecific preference of glucuronidation between 3-*O* and 4'-*O* or 3-*O* and 7-*O* positions (Figure 13). However, between 7-*O* and 4'-*O*, UGT1A1 showed preferred regiospecificity for 7-*O* position, whereas between 5-*O* and 7-*O*, it showed dominant regiospecificity for 7-*O* position (Figure 13). Between 5-*O* and 4'-*O*, 4'-*O* was dominantly preferred position of glucuronidation (Figure 13).

In case of tri- and tetra- hydroxyflavones, in absence of hydroxyl group at C-3 position (i.e. 5,7,4'THF), 7-*O* was dominantly preferred position of glucuronidation (Figure 13). In presence of hydroxyl group at C-3, UGT1A1 showed either no or weak regiospecificity for any position (Figure 13).

In general, rates of glucuronidation of hydroxyl group at C-3 and C-7 position by UGT1A1 reduced as the number of hydroxyl groups increase in the structure of flavonols and flavones, although the magnitude of reduction was more when the hydroxyl group was added at C-7 and/or C-5 positions than at C-4' position ($p < 0.05$) (Figure 13).

UGT1A8: UGT1A8 preferably glucuronidated 3-*O* position when hydroxyl group is present at C-3. In cases where there was no hydroxyl group at C-3 position, 7-*O* was the preferred position of glucuronidation. In general, glucuronidation of 4'-*O* and 5-*O* was not much favored by UGT1A8 (Figure 14).

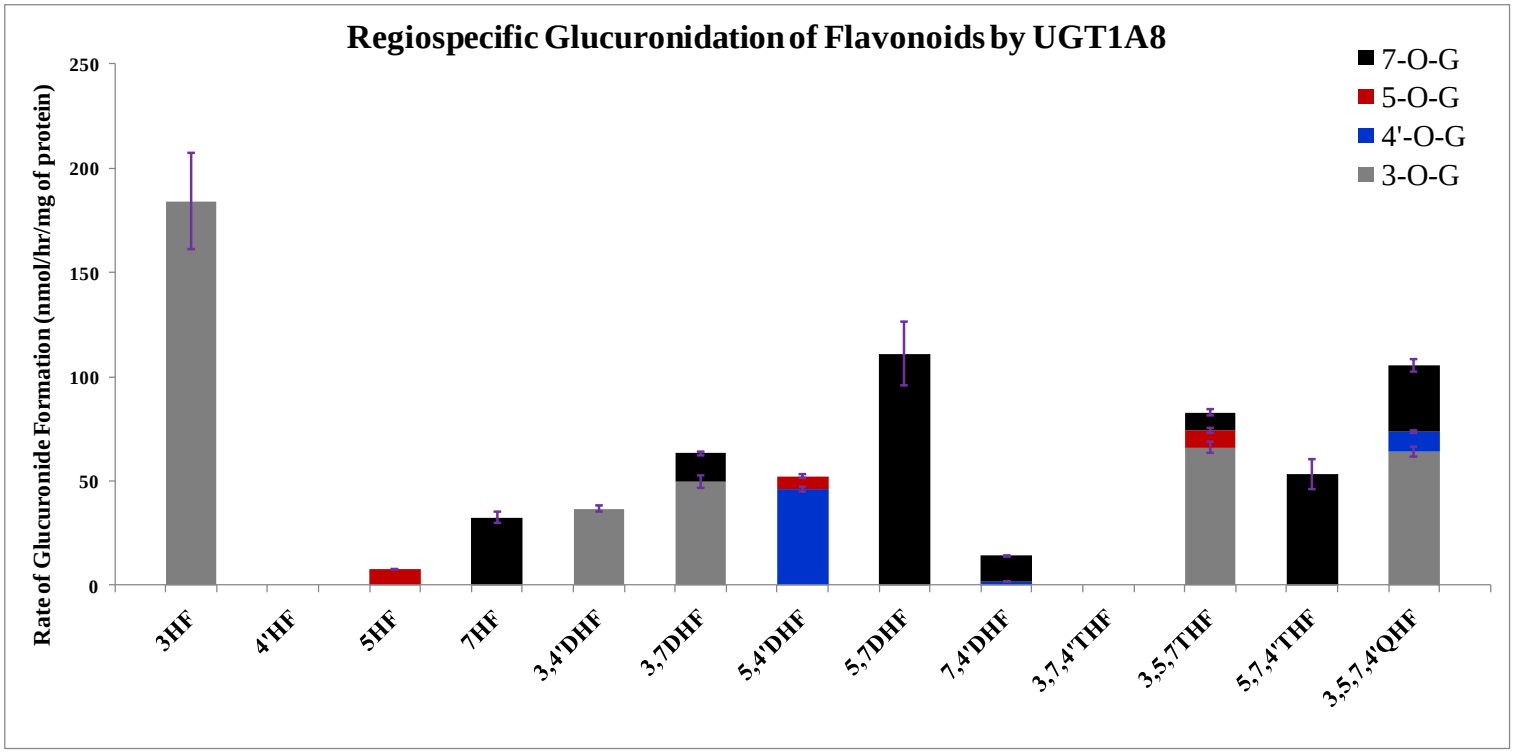

Figure 14. Regiospecific glucuronidation of flavonoids by UGT1A8.
Flavonoids (flavones and flavonols at 10 µM concentration) were incubated at 37 ºC for 1 (or 0.5) hr with UGT1A8 (using optimum final protein concentration ~ 0.25, 0.5 or 1 mg/ml). The amounts of mono-glucuronide(s) formed were measured using UPLC. The amounts of each regiospecific mono-glucuronide formed were measured using UPLC. Rates of mono-glucuronide formation were calculated as nmol/hr/mg of protein. Each bar is the average of three determinations, and the error bars are the standard deviations of the mean (n=3). The data of 4'-hydroxyflavone (4'HF), 5-hydroxyflavone (5HF) and 7-hydroxyflavone (7HF) has been re-plotted for comparison from Tang *et al.* (2010) [157]. The regiospecific data of other flavonoids has been re-plotted from Figures 11 and 12.

In case of di-hydroxyflavones, UGT1A8 showed dominant regiospecific preference for glucuronidation of 3-*O* and 7-*O* position in 3,4'DHF and 5,7DHF, respectively (Figure 14). UGT1A8 showed preferred regiospecificity for glucuronidating 3-*O*, 4'-*O* and 7-*O* position in 3,7DHF, 5,4'DHF and 7,4'DHF, respectively (Figure 14).

In case of tri- and tetra- hydroxyflavones, in absence of hydroxyl group at C-3 position (i.e. 5,7,4'THF), 7-*O* was dominantly preferred position of glucuronidation by UGT1A8 In presence of hydroxyl group at C-3, regiospecificity of UGT1A8 was dependent on the compound structure. 3,7,4'THF was not glucuronidated at all. For 3,5,7THF, UGT1A8 showed dominant regiospecificity for 3-*O* position over 7-*O* and 5-*O* position, whereas 3,5,7,4'QHF showed dominant regiospecificity for 3-*O* and 7-*O* positions over 4'-*O* position, but only weakly preferred 3-*O* over 7-*O* position (Figure 14).

In general, the rates of glucuronidation of 3-*O* and 7-*O* by UGT1A8 usually reduced by the addition of hydroxyl group at C-4' and/or C-7 positions, while improved by the addition of hydroxyl group at C-5 ($p < 0.05$) (Figure 14).

UGT1A9: Similar to UGT1A8, UGT1A9 also mainly glucuronidated 3-*O* and 7-*O* positions, though the glucuronidation of 7-*O* position by UGT1A9 was faster than by UGT1A8. 3-*O* was more favored position than 7-*O* for glucuronidation. 7-*O* was the most preferred position of glucuronidation in absence of 3-*O* glucuronidation. Glucuronidation of 4'-*O* and 5-*O* was not favored at all by UGT1A9 (Figure 15).

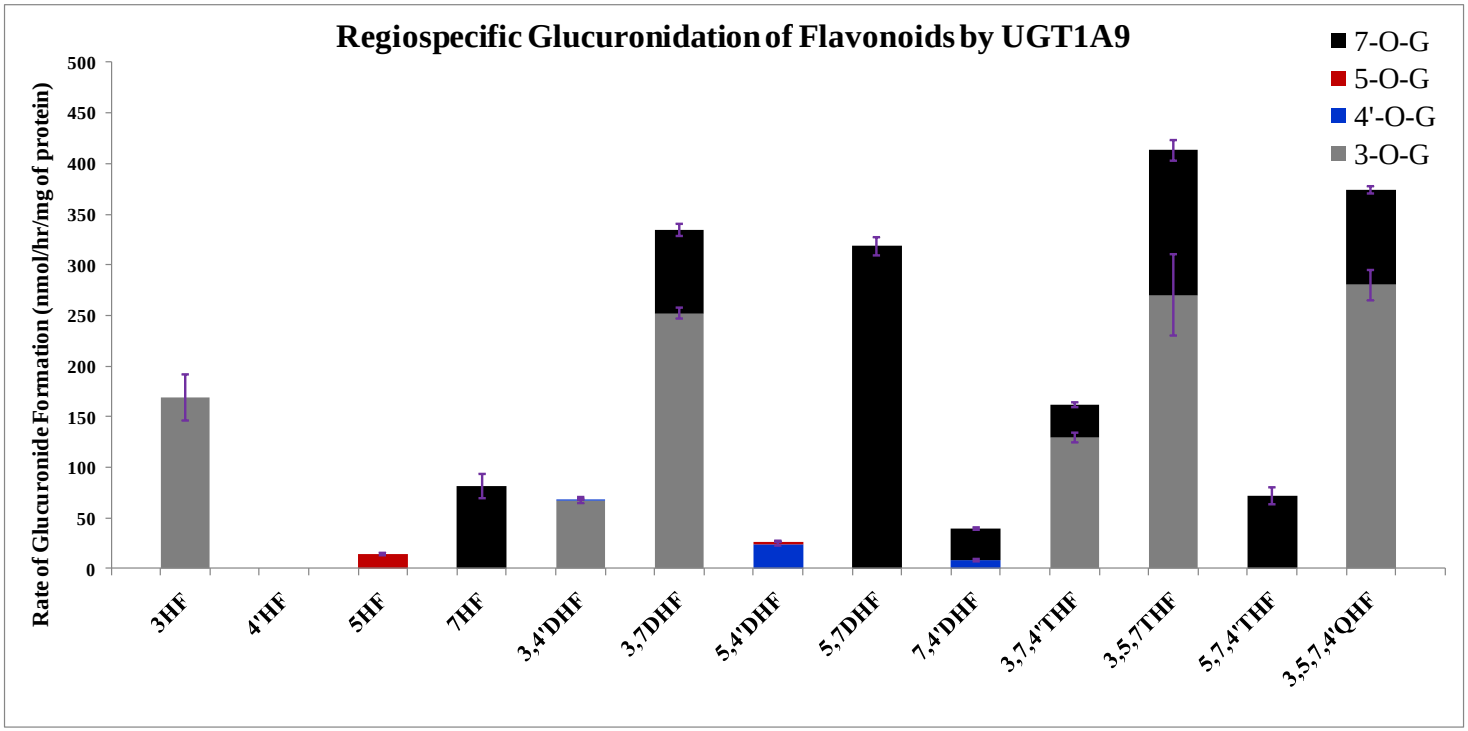

Figure 15. Regiospecific glucuronidation of flavonoids by UGT1A9.
Flavonoids (flavones and flavonols at 10 µM concentration) were incubated at 37 ºC for 1 (or 0.5) hr with UGT1A9 (using optimum final protein concentration ~ 0.25, 0.5 or 1 mg/ml). The amounts of mono-glucuronide(s) formed were measured using UPLC. The amounts of each regiospecific mono-glucuronide formed were measured using UPLC. Rates of mono-glucuronide formation were calculated as nmol/hr/mg of protein. Each bar is the average of three determinations, and the error bars are the standard deviations of the mean (n=3). The data of 4'-hydroxyflavone (4'HF), 5-hydroxyflavone (5HF) and 7-hydroxyflavone (7HF) has been re-plotted for comparison from Tang *et al.* (2010) [157]. The regiospecific data of other flavonoids has been re-plotted from Figures 11 and 12.

In case of di-hydroxyflavones, UGT1A9 showed dominant regiospecific preference for glucuronidation of 3-*O*, 7-*O* and 4'-*O* position in 3,4'DHF, 5,7DHF and 5,4'DHF respectively (Figure 15). UGT1A9 showed preferred regiospecificity for glucuronidating 3-*O* and 7-*O* position in 3,7DHF and 7,4'DHF, respectively (Figure 15).

In case of tri- and tetra- hydroxyflavones, in absence of hydroxyl group at C-3 position (i.e. 5,7,4'THF), 7-*O* was dominantly preferred position of glucuronidation by UGT1A9, similar to UGT1A1 and 1A8 (Figure 15). However, in presence of hydroxyl group at C-3, regiospecificity of UGT1A9 was different from UGT1A1 and 1A8. UGT1A9 showed preferred regiospecificity for glucuronidating 3-*O* position in 3,7,4'THF and 3,5,7,4'QHF, whereas, showed weak regiospecificity for glucuronidating 3-*O* position in 3,5,7THF (Figure 15).

In general, in di-hydroxyflavones, the rates of glucuronidation of 3-*O* by UGT1A9 usually was reduced by the addition of hydroxyl group at C-4' position, while improved by the addition of hydroxyl group at C-7 ($p<0.05$) (Figure 15). In di-hydroxyflavones, the rates of glucuronidation of 7-*O* by UGT1A9 was reduced by the addition of hydroxyl group at C-4' position, while improved by the addition of hydroxyl group at C-5 ($p<0.05$) (Figure 15). In tri- and tetra-hydroxyflavones, the rates of glucuronidation of 3-*O* and 7-*O* by UGT1A9 was reduced by the addition of hydroxyl group at C-4' position, while did not change significantly by the addition of hydroxyl group at C-5 ($p<0.05$) (Figure 15).

5.4.6. Effect of concentration on the regiospecificity of UGT 1A1, 1A8 and 1A9

We also studied the effect of substrate concentration (2.5, 10 and 35µM) of the regiospecificity of the three isoforms, UGT1A1, 1A8 and 1A9. Figure 18 represented the data of a di-hydroxyflavone (3,7DHF) and a tetra-hydroxyflavone (3,5,7,4'QHF) as examples. We found that the ratio of rates of glucuronidation of 3-*O* and 7-*O* positions in 3,7DHF and 3,5,7,4'QHF by UGT1A1, 1A8 and 1A9 significantly changed with the concentration ($p<0.05$) (Figure 16A-16B).

UGT1A1 weakly preferred the glucuronidation of 7-*O* position at 2.5 and 10µM, but showed no regiospecificity at 35µM substrate concentration (Figure 16A). UGT1A8 showed preferred regiospecificity at 2.5 and 35µM for 3-*O* position, while weak regiospecificity for 3-*O* position at 10µM substrate concentration (Figure 16A). UGT1A9 showed preferred regiospecificity at 2.5µM for 3-*O* position, whereas no regiospecificity at 10 and 35µM substrate concentration (Figure 16A).

In case of 3,5,7,4'QHF, preferred position of glucuronidation by UGT1A8 and 1A9 changed with concentration (Figure 16B). UGT1A1 showed no regiospecific preference for either 3-*O* or 7-O at any tested substrate concentrations (Figure 16B). UGT1A8 only showed weak regiospecificity at all the three concentrations; however 7-*O* was the preferred position of glucuronidation at 2.5 and 35 µM, while 3-*O* was the preferred position at 10µM substrate concentration (Figure 16B).

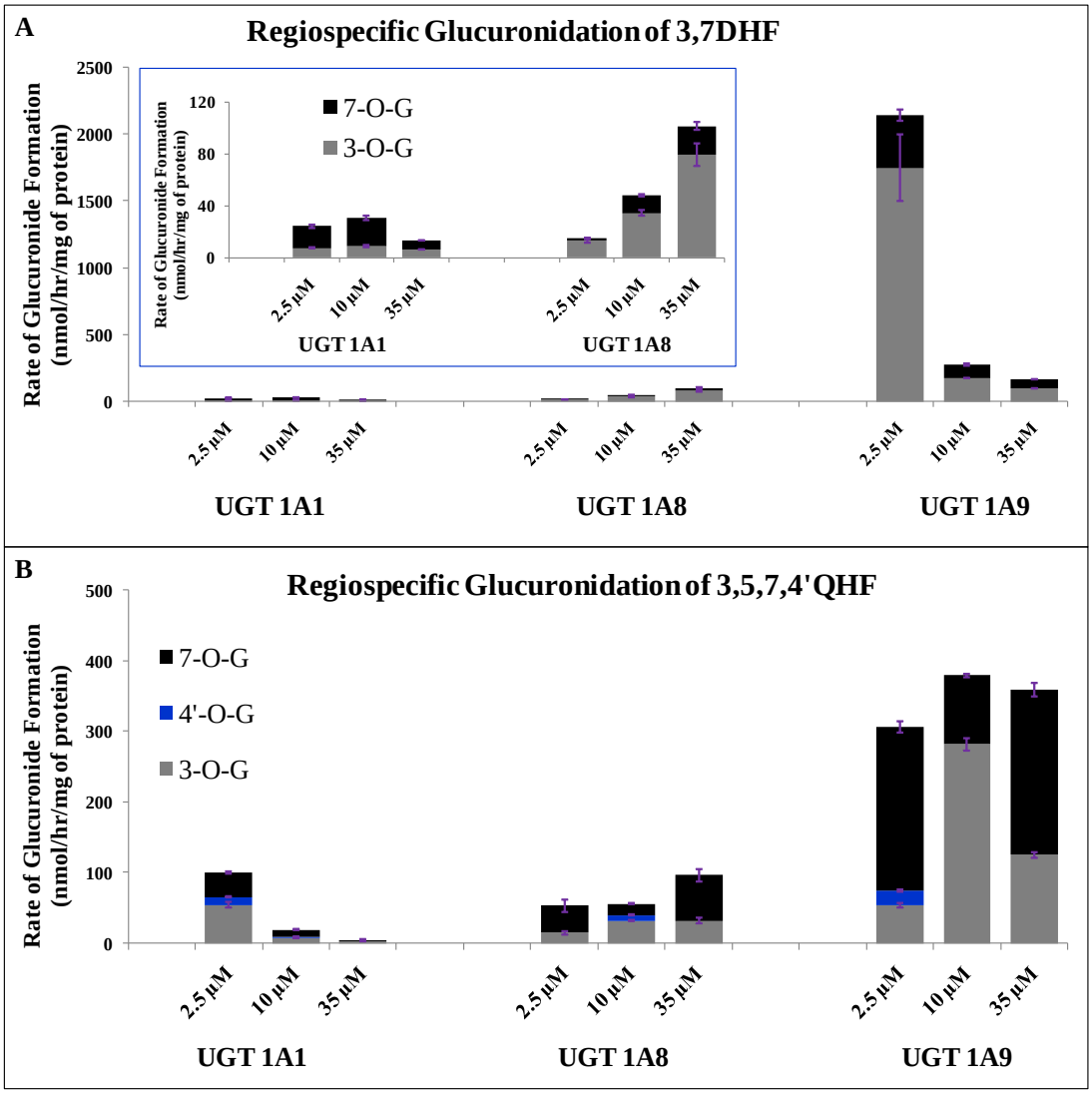

Figure 16. Concentration-dependent regiospecific glucuronidation of 3,7DHF (A) and 3,5,7,4'QHF (B) by UGT 1A1, 1A8 and 1A9.

3,7DHF and 3,5,7,4'QHF (at 2.5, 10 and 35 µM concentration) were incubated at 37 ºC for 1 (or 0.5) hr with UGT1A1, 1A8 or 1A9 (using optimum final protein concentration ~ 0.25, 0.5 or 1 mg/ml). The amounts of mono-glucuronide(s) formed were measured using UPLC. The amounts of each regiospecific mono-glucuronide formed were measured using UPLC. Rates of mono-glucuronide formation were calculated as nmol/hr/mg of protein. Each bar is the average of three determinations, and the error bars are the standard deviations of the mean (n=3).

UGT1A9 showed preferred regiospecificity for glucuronidation of 7-*O* position at 2.5µM, while weak regiospecificity for glucuronidation of 3-*O* position at 10µM substrate concentration. UGT1A9 did not show any regiospecificity for glucuronidation of either 3-*O* or 7-*O* position at 35µM substrate concentration (Figure 16B).

5.4.7. Substrate-selectivity of flavonoids glucuronidation by UGTs

For Flavonols: There was no significant difference between overall glucuronidation rates of 3HF by UGT 1A1, 1A8 and 1A9 ($p<0.05$), suggesting that the basic flavonol structure was the equally favorable structure for these isoforms (Figure 11). However, addition of a hydroxyl group at C-4' in the structure of 3HF i.e. 3,4'DHF, reduced the rates of overall glucuronidation by most isoforms, suggesting that for most isoforms, presence of hydroxyl group at C-4' position was not a favorable feature for glucuronidation of compounds ($p<0.05$) (Figure 11).

Again, addition of a hydroxyl group at C-7 in the structure of 3HF i.e. 3,7DHF reduced the rates of overall glucuronidation by most isoforms, except UGT1A9, which showed higher rates of overall glucuronidation for 3,7DHF than for 3HF ($p<0.05$) (Figure 17). This suggested that presence of hydroxyl group at C-7 position was favored by UGT1A9 but not by any other isoform in glucuronidating the compound.

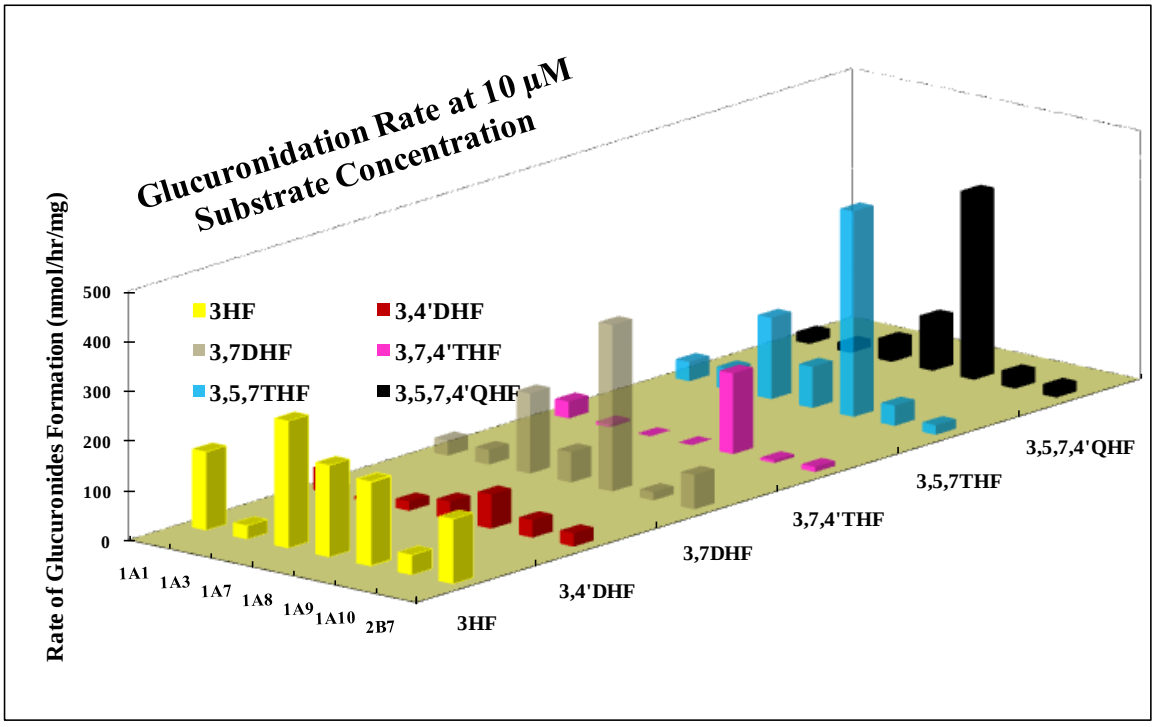

Figure 17. Substrate-selectivity of UGTs for flavonols.
Flavonols (at 10 µM concentration) were incubated at 37 ºC for 1 (or 0.5) hr with UGT 1A1, 1A3, 1A7, 1A8, 1A9, 1A10 or 2B7 (using optimum final protein concentration ~ 0.25, 0.5 or 1 mg/ml). The amounts of total glucuronides formed for every flavonols were measured using UPLC. Rates of glucuronide(s) formation were calculated as nmol/hr/mg of protein. This data has been re-plotted here from Figures 6a-6f (Chapter 4).

Addition of another hydroxyl group in the structure of 3,4'DHF at C-7 or 3,7DHF at C-4' i.e. 3,7,4'THF further made the compound a poorer substrate for glucuronidation by all isoforms ($p<0.05$), however UGT1A1 and UGT1A9 still glucuronidated 3,7,4'THF decently (Figure 17). This indicated that UGT 1A1 and 1A9 were more inclusive for variety of flavonol structures as compared to other isoforms.

3,5,7THF was a faster glucuronidating compound as compared to 3,4'DHF, 3,7DHF and 3,7,4'THF for most isoforms and even faster than 3HF for UGT1A9 ($p<0.05$), suggesting that addition of a hydroxyl group at C-5 position in structure of 3,7DHF improved the glucuronidation of compound (Figure 17). Addition of a hydroxyl group at C-5 position in 3,7,4'THF i.e. 3,5,7,4'QHF again made the resulting compound a better substrate for most UGT isoforms, whereas addition of hydroxyl group at C-4' position in 3,5,7THF i.e. 3,5,7,4'QHF reduced the glucuronidation ($p<0.05$) (Figure 17).

In general, addition of a hydroxyl group at C-5 position in and 3,7DHF and 3,7,4'THF, i.e. 3,5,7THF and 3,5,7,4'QHF, respectively, improved the glucuronidation of compound by most UGT isoforms, strongly suggesting that addition of hydroxyl group at C-5 position in compounds already with a hydroxyl group at C-4' and/or C-7 position would always favor the glucuronidation of compound.

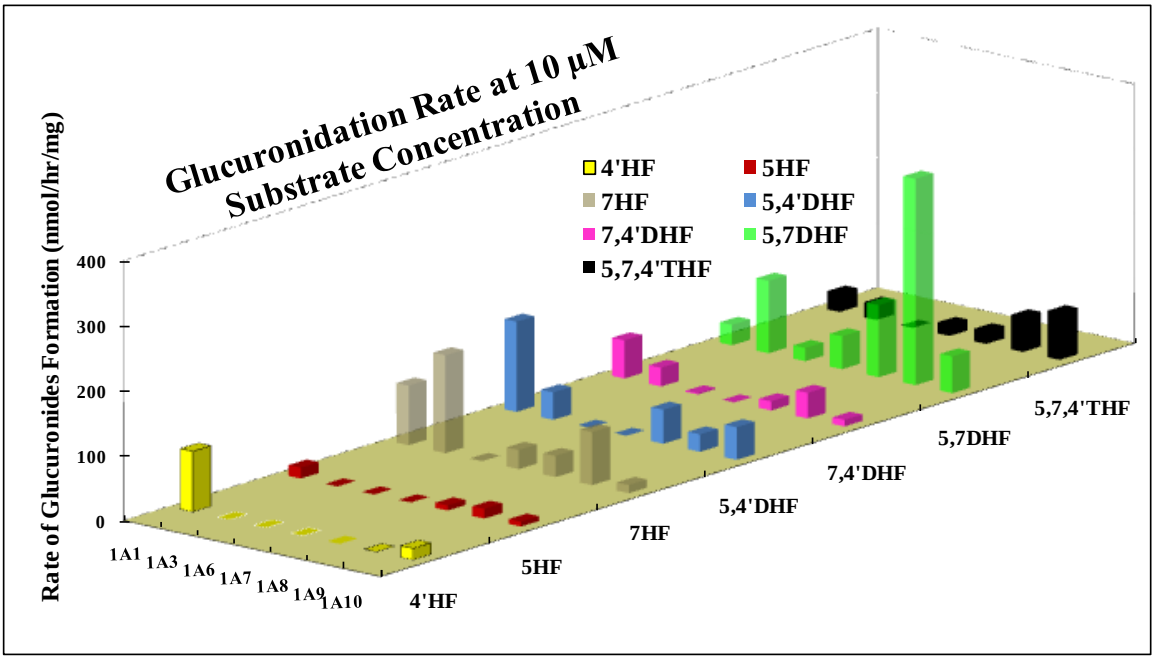

Figure 18. Substrate-selectivity of UGTs for flavones.
Flavones (at 10 µM concentration) were incubated at 37 ºC for 1 (or 0.5) hr with UGT 1A1, 1A3, 1A6, 1A7, 1A8, 1A9 or 1A10 (using optimum final protein concentration ~ 0.25, 0.5 or 1 mg/ml). The amounts of total glucuronides formed for every flavone were measured using UPLC. Rates of glucuronide(s) formation were calculated as nmol/hr/mg of protein. This data has been re-plotted here from Figures 5b and 7a-7f (Chapter 4). The data of 4'-hydroxyflavone (4'HF), 5-hydroxyflavone (5HF) and 7-hydroxyflavone (7HF) has been re-plotted for comparison from Tang *et al.* (2010) [157].

On the other hand, addition of a hydroxyl group at C-4' position in 3HF, 3,7DHF or 3,5,7THF resulting in 3,4'DHF, 3,7,4'THF or 3,5,7,4'QHF, respectively, always reduced the glucuronidation of the resulting compound as compared to the parent analog, again suggesting that addition of hydroxyl group at C-4' position was not favored by UGTs in general.

For Flavones: 5,7DHF was the fastest glucuronidating compound, whereas 5HF was the slowest glucuronidating compounds in the series ($p<0.05$) (Figure 18). Addition of a hydroxyl group at C-5 in the structure of 4'HF i.e. 5,4'DHF, made the resulting compound a better substrate for most isoform ($p<0.05$), as 4'HF was glucuronidated only by UGT 1A1 and 1A10 (Figure 18). Similarly, addition of a hydroxyl group at C-4' in the structure of 5HF i.e. 5,4'DHF, also improved the glucuronidation by all metabolizing isoforms, except UGT2B7 ($p<0.05$) (Figure 18).

In case of 7HF, addition of a hydroxyl group at C-4' position i.e. 7,4'DHF, made the resulting compound a poorer substrate for all isoforms (Figure 18) whereas addition of a hydroxyl group at C-5 position i.e. 5,7DHF improved the glucuronidation by all isoforms, except 1A3 ($p<0.05$). In case of 5HF, addition of a hydroxyl group at C-4' i.e. 5,4'DHF or C-7 i.e. 5,7DHF, improved glucuronidation by all isoforms ($p<0.05$). However, increase was much higher in the latter case except for 1A1, which glucuronidated 5,4'DHF faster than 5,7DHF ($p<0.05$) (Figure 18).

For 7,4'DHF, addition of a hydroxyl group at C-5 position i.e. 5,7,4'THF improved the glucuronidation by UGT 1A6, 1A7, 1A8 and 1A9, whereas reduced the glucuronidation by UGT 1A1 and 1A10 ($p<0.05$) . On the other hand, for 5,7DHF, addition of a hydroxyl group at C-4' position i.e. 5,7,4'THF reduced the glucuronidation by all UGT isoforms ($p<0.05$), though the magnitude of reduction varies for various isoforms (Figure 18).

The above results showed that similar to flavonols, the addition of hydroxyl group at C-4' in the structure of 7HF i.e. 7,4'DHF and 5,7DHF i.e. 5,7,4'THF, reduced the glucuronidation by UGT isoforms. Also, similar to flavonols, in general the addition of hydroxyl group at C-5 in the structure of 7HF i.e. 5,7DHF and 7,4'DHF i.e. 5,7,4'THF, improved the glucuronidation by UGT isoforms.

5.4.8. Substrate-selectivity of UGT1A1, 1A8 and 1A9 for flavonoids glucuronidation

We also studied in detail the effect of the number and position of hydroxyl groups on the substrate-selectivity of UGT1A1, 1A8 and 1A9 in the glucuronidating the flavonoids.

UGT1A1: Addition of a hydroxyl group in the structure of all mono-hydroxyflavone (except 5HF) at any position reduced the rates of glucuronidation of the resulting di-hydroxyflavones as compared to mono-hydroxyflavones ($p<0.05$). In case of 5HF, addition of a hydroxyl group at any position improved the rates of glucuronidation of the resulting di-hydroxyflavones ($p<0.05$) (Figure 13).

Addition of another hydroxyl group in the structure of 3,4'DHF and 5,4'DHF at C-7 position or 3,7DHF and 7,4'DHF at C-5 position further reduced the rates of glucuronidation of the resulting tri-hydroxyflavones ($p<0.05$) as compared to mono- and di- hydroxyflavones (Figure 13). However, addition of another hydroxyl group in the structure of 3,7DHF and 5,7DHF at C-4' position did not significantly affect the rates of glucuronidation of the resulting tri-hydroxyflavone as compared to di- hydroxyflavones ($p<0.05$) (Figure 13). Addition to another hydroxyl group in any of the tri-hydroxyflavones at any position, significantly reduced the rates of glucuronidation of the resulting compound (i.e. 3,5,7,4'QHF) as compared to tri-hydroxyflavones ($p<0.05$) (Figure 13). In summary, the rates of glucuronidation by UGT1A1 generally reduced as the number of hydroxyl groups in the structure increased.

UGT1A8: Addition of a hydroxyl group in the structure of 3HF at any position reduced the rates of glucuronidation of the resulting di-hydroxyflavones (i.e. 3,4'DHF and 3,7DHF) as compared to 3HF ($p<0.05$) (Figure 14). In case of 4'HF and 5HF, addition of a hydroxyl group at any position improved the rates of glucuronidation of the resulting di-hydroxyflavones ($p<0.05$) (Figure 14). In case of 7HF, addition of a hydroxyl group at C-5 position improved, whereas, at C-4' or C-3 position reduced the rates of glucuronidation of the resulting di-hydroxyflavones ($p<0.05$) (Figure 14).

Addition of another hydroxyl group in the structure of 3,4'DHF at C-7 position or 3,7DHF and 5,7DHF at C-4' position drastically reduced the rates of glucuronidation of the resulting tri-hydroxyflavones ($p<0.05$) as compared to mono- and di-hydroxyflavones (Figure 14). However, addition of another hydroxyl group in the structure of 3,7DHF and 7,4'DHF at C-5 position significantly improved the rates of glucuronidation of the resulting tri-hydroxyflavones as compared to di- hydroxyflavones ($p<0.05$) (Figure 14). Addition of another hydroxyl group in the structure of 5,4'DHF at C-7 position did not change the rate of glucuronidation of resulting compound (5,7,4'THF) as compared to 5,4'DHF ($p<0.05$) (Figure 14).

Addition of another hydroxyl group in any of the tri-hydroxyflavones, significantly improved the rates of glucuronidation of the resulting compound (i.e. 3,5,7,4'QHF) as compared to all mono-, di-, and tri-hydroxyflavones except 3HF and 5,7DHF ($p<0.05$). 3HF was glucuronidated much faster than 3,5,7,4'QHF, whereas, 5,7DHF showed similar rates of glucuronidation as 3,5,7,4'QHF by UGT1A8 ($p<0.05$) (Figure 14).

In summary, the rates of glucuronidation of di- and tri-hydroxyflavones by UGT1A8 always reduced as one or more hydroxyl group(s) are added in the structure of mono-hydroxyflavones at C-4' and/or C-7 position, except for the addition of hydroxyl group at C-7 position in 4'HF and C-4' position in 5HF. On the other hand, the rates of glucuronidation of di- and tri-hydroxyflavones by UGT1A8 always improved as hydroxyl group is added in the structure of mono-hydroxyflavones at C-5 position, except for the

addition of hydroxyl group at C-5 position in 3HF (data published)[157]. Addition of fourth hydroxyl group in any of the tri-hydroxyflavones always improved the rates of glucuronidation tetra-hydroxyflavone as compared to tri-hydroxyflavone.

UGT1A9: Addition of a hydroxyl group in the structure of 3HF at C-4' position reduced, whereas, at C-7 position improved the rates of glucuronidation of the resulting di-hydroxyflavones as compared to 3HF ($p<0.05$) (Figure 15). In case of 4'HF and 5HF, addition of a hydroxyl group at any position improved the rates of glucuronidation of the resulting di-hydroxyflavones ($p<0.05$) (Figure 15). In case of 7HF, addition of a hydroxyl group at C-5 or C-3 position improved, whereas, at C-4' position reduced the rates of glucuronidation of the resulting di-hydroxyflavones ($p<0.05$) (Figure 15).

Addition of another hydroxyl group in the structure of 3,4'DHF and 5,4'DHF at C-7 position or 3,7DHF at C-4' position or 7,4'DHF at C-5 position significantly improved the rates of glucuronidation of the resulting tri-hydroxyflavones ($p<0.05$) as compared to di-hydroxyflavones (Figure 15). However, addition of another hydroxyl group in the structure of 5,7DHF at C-4' position significantly reduced the rates of glucuronidation of 5,7,4'THF as compared to 5,7DHF ($p<0.05$) (Figure 15).

Addition of another hydroxyl group in any tri-hydroxyflavone at any position significantly improved the rates of glucuronidation of the resulting compound (i.e. 3,5,7,4'QHF) as compared to all mono-, di-, and tri-hydroxyflavones except for addition

of hydroxyl group at C-4' position in 3,5,7THF, which showed faster rates of glucuronidation than 3,5,7,4'QHF by UGT1A9 ($p<0.05$) (Figure 15).

In summary, the rates of glucuronidation of di- and tri-hydroxyflavones by UGT1A9 always improved as one or more hydroxyl group(s) is added in the structure of mono-hydroxyflavones at C-7 and/or C-5 position, except for the addition of hydroxyl group at C-5 position in 3HF (data published)[157]. On the other hand, the rates of glucuronidation of di-, tri- and tetra- hydroxyflavones by UGT1A9 always reduced as hydroxyl group is added in the structure of mono-hydroxyflavones at C-4' position, except for the addition of hydroxyl group at C-4' position in 5HF. The rates of glucuronidation of 3,5,7,4'QHF was faster than 3,7,4'THF and 5,7,4'THF by UGT1A9.

5.6. Discussion

We concluded that regiospecificity and substrate-selectivity was isoform-dependent. For isoform-specific regiospecificity, we concluded that UGT1A1 usually showed no preference, whereas UGT1A8 and UGT1A9 showed preference (3-*O* position was glucuronidated faster than other positions) (Figure 13-14). For isoform-specific substrate-selectivity, we concluded that the susceptibility of flavonoids to be glucuronidated by UGT1A1 decreased with increasing number of hydroxyl groups, with few exceptions, for e.g. 3,5,7THF glucuronidated faster than 5,7DHF (Figures 17-18). On the other hand, the susceptibility of flavonoids to be glucuronidated by UGT1A8 and UGT1A9 increased with addition of hydroxyl group at 3-*O*, 5-*O* and/or 7-*O* position, except for 3,7,4'THF, while decreased with addition at 4'-*O* position (Figures 17-18).

This is the first time that a study has demonstrated a UGT isoform-specific regiospecificity in glucuronidation of flavonoids. At 10μM substrate concentration, different UGT isoforms gave different regiospecific glucuronidation patterns (Figures 11-12). Most isoforms preferred glucuronidation of 3-*O* position followed by 7-*O* position over 4'-*O* position and 5-*O* position was hardly glucuronidated (Figures 11-12). UGT1A3 showed dominant regiospecificity for glucuronidation at 7-*O* position, whereas UGT1A7 showed dominant regiospecificity for glucuronidation at 3-*O* position (Figures 11-12). UGT1A1 generally showed no regiospecificity for any position (Figure 13). Among all hydroxyl group positions, UGT1A8 and UGT1A9 dominantly glucuronidated 3-*O* and 7-

O positions over glucuronidation of 4'-*O* and 5-*O*. Between 3-*O* and 7-*O* position, UGT1A8 and UGT1A9 showed either dominant, preferred or weak regiospecificity depending on the compound structure (Figures 14-15). Similar to UGT1A1, UGT1A6, 1A10 and 2B7 showed no regiospecificity for any position (Figures 11-12).

Our findings on regiospecificity are also supported by many published reports.[88, 160, 174, 175] The hydroxyl group on C-5 position did not seem to be a site for glucuronidation.[88] Chen *et al.* (2005) showed that the catalytic efficiency order for regiospecific glucuronidation of quercetin (3,5,7,3',4'-pentahydroxyflavone) by UGT1A9 was 3- > 7- > 3′- > 4′-*O*-glucuronide.[174] Otake *et al.* (2002) published a report on regiospecific glucuronidation of 3,5,7THF (galangin) by UGT1A1 and 1A9 also matched with our data.[160] However, the published data on quercetin regiospecific glucuronidation by UGT1A1 did not match with our findings. The major glucuronides of quercetin formed in that study was 3'-*O*-G.[175] Since none of the compound used in the study had hydroxyl group at C-3', we cannot comment on this difference in result.

We also showed that the rate of formation of main regiospecific glucuronide(s) (3-*O*-G and 7-*O*-G) by UGT1A1, 1A8 and 1A9 is affected by the addition of hydroxyl group(s) at different positions in the structure of flavones and flavonols. Increase in the number of hydroxyl group(s) in the structure of mono-hydroxyflavones (3HF, 7HF and 4'HF) always slowed down the rates of glucuronidation at 3-*O* or 7-*O* positions by UGT1A1 as compared to the rates of glucuronidation of mono-hydroxyflavones (Figure 13). The rates

of glucuronidation of 3-*O* and 7-*O* by UGT1A8 was generally reduced by the addition of hydroxyl group at C-4' and/or C-7 positions, but was improved by the addition of hydroxyl group at C-5 position (Figure 14). The rates of glucuronidation of 3-*O* and 7-*O* by UGT1A9 was reduced by the addition of hydroxyl group at C-4' position in flavones and flavonols. However, the addition of hydroxyl group at C-5 and/or C-7 position might or might not significantly change the rates of glucuronidation at 3-*O* or 7-*O* by UGT1A9 (Figure 15).

We additionally showed that the regiospecificity of glucuronidation by UGT isoforms was also dependent on the concentration of substrate (Figure 16). For examples, UGT1A8 showed preferred regiospecificity for 3-*O* position in 3,7DHF at 2.5 and 35µM, where as weak regiospecificity for 3-*O* position at 10µM substrate concentration (Figure 16A). In 3,5,7,4'QHF, UGT1A9 regiospecificity changed from preferred regiospecificity for 7-*O* position at 2.5 µM, to weak regiospecificity for 3-*O* position at 10 µM, to no regiospecificity for any position at 35µM substrate concentration (Figure 16B).

The above results suggests that the formation of major regiospecific glucuronide(s) *in vivo* will be determined based on the exposure of substrate concentration and the UGT isoform expression level of an organ/tissue. For example, UGT1A9 is exclusively expressed in liver and kidney; UGT1A3 in liver; UGT1A7 in stomach; UGT1A1 in liver and intestine; whereas UGT1A8 and 1A10 is exclusively expressed in intestine. Also, during oral administration intestine is exposed to highest concentration of flavonoid (10-

50 μM based on solubility), whereas liver is exposed to a much lower concentration of flavonoid (≤ 2.5μM). This indicates that the regiospecific glucuronides of a particular flavonoid might be formed in different ratio in human liver and intestine.

Also, the dominant and preferred regiospecificity of glucuronidation shown by different UGT isoforms can be useful in predicting the major glucuronide(s) formed in human, but not useful if UGT isoforms showed weak or no regiospecific preference. For example, after oral intake of kaempferol (3,5,7,4'QHF) in human, 3-*O*-glucuronide of kaempferol was found to be the predominant form in plasma,[163] which matched with prediction based on the regiospecific glucuronidation of 3,5,7,4'QHF in our study. However, it should be noted that if the main UGT isoforms responsible for the glucuronidation of flavonoids in an organ/tissue, showed opposite preference for a particular regiospecificity, then it might again be difficult to predict the *in vivo* metabolic outcome.

In support of the conclusion for isoform-specific substrate-selectivity, we showed that substrate-selectivity was dependent on the UGT isoforms and the number and position of hydroxyl groups (Figures 17-18). UGT1A1 activities towards flavonoids usually decreased with increasing number of hydroxyl groups with few exceptions, for e.g. 3,5,7THF glucuronidated faster than 5,7DHF (Figures 17-18). On the other hand, UGT1A8 and UGT1A9 activities increased with addition of hydroxyl group at 3-*O*, 5-*O* or 7-*O* positions except for 3,7,4'THF, which was a poor substrate of UGT1A8. However, similar to UGT1A1, UGT1A8 and UGT1A9 activities decreased with addition

of hydroxyl group at 4'-*O* position. The only exception was the addition of hydroxyl group to 5HF at C-4', which improved the glucuronidation of resulting di-hydroxyflavone, 5,4'DHF (Figures 17-18).

We also showed that adding multiple hydroxyl groups in the flavonol structure reduced glucuronidation rates whereas adding the same groups in the flavone structure improved the glucuronidation rates by most UGT isoforms (Figure 17-18). Substrate selectivity data of UGT isoforms also suggested that as compared to 3HF, which can be highly glucuronidated by the liver as well as intestine, flavonols with multi-hydroxyl groups will be glucuronidated more effectively in liver than in intestine (Figure 17). However, depending on the substrate structure, both hepatic (UGT1A1, 1A3 and 1A9) and extra-hepatic (UGT1A1, UGT1A8 and 1A10) UGT isoforms can equally contribute to the metabolism of mono and multi-hydroxyflavones (Figure 18).

In conclusion, regiospecificity and substrate-selectivity was isoform-dependent. UGT1A8 and UGT1A9 preferred glucuronidation at 3-*O* position followed by 7-*O*, whereas UGT1A1 showed no preference to glucuronidate any specific position. UGT1A1 activities towards flavonoids usually decreased with increasing number of hydroxyl groups. On the other hand, UGT1A8 and UGT1A9 activities increased with addition of hydroxyl group at 3-*O*, 5-*O* and/or 7-*O* positions, while decreased with addition of hydroxyl group at 4'-*O* position.

ISOFORM-SPECIFIC PHARMACOPHORE-BASED SMR MODELS FOR PREDICTING GLUCURONIDATION OF FLAVONOIDS BY UGT1A9

6.1. Abstract

The objective of the study was to develop isoform-specific pharmacophore-based 3-D structure-metabolism relationship (SMR) prediction models for the glucuronidation of flavonoids by UGT1A8 and UGT1A9 with the predictive ability of more than 75%. Another objective was to develop 2-D/3-D quantitative SMR prediction model for the glucuronidation of flavonoids by UGT1A8 and UGT1A9. We used "Hypogen" module for the generation of pharmacophores and Partial Least Square (PLS) regression for the generation of 2-D/3-D QSAR models in the Discovery Studio software of Accelrys'. We developed four three-featured and one four-featured pharmacophores models using 5 different randomized group divided into training and test set. There were four three-featured pharmacophores with one hydrogen bond acceptor (HBA), one hydrogen bond donor (HBD), and one aromatic ring or hydrophobic center. Only one four-featured pharmacophore was developed with two HBA, one HBD and one hydrophobic center. All pharmacophores could correctly predict at least 60% of the training and test compounds as lowly (with $Cl_{int} < 3 \times 10^5$ ml per min per mg of protein or highly metabolizing (with $Cl_{int} \geq 3 \times 10^5$) compounds, and one three-featured pharmacophore showed >75% predictive ability. But there was no correlation found between the Cl_{int} values estimated by pharmacophores and experimentally derived Cl_{int} values. We could also develop four

semi-quantitative pharmacophores based 3-D SMR prediction models for UGT1A8 which could rightly predict > 60% training as low (with $Cl_{int} < 1 \times 10^5$ ml per min per mg of protein) or high metabolizing (with $Cl_{int} \geq 1 \times 10^5$) compounds. But none of the models could correctly predict at least 60% the test compounds. Also, no 2-D and/or 3-D QSMR models with $r^2 > 0.6$ (correlation of estimated vs experimental Cl_{int} values) and average squared error < 50 could be successfully developed for UGT1A8 and UGT1A9. In conclusion, semi-quantitative pharmacophore-based 3-D SMR prediction models could be developed for UGT1A9 with the predictive ability of more than 75%.

6.2. Introduction

Flavonoids are polyphenolic compounds of plant origin that have shown beneficial effects against a variety of disease conditions such as prostate and breast cancer, aging-related and hormone-dependent disorders as well as cardiovascular diseases.[2-5, 176-178] Despite reports of various biological activities *in vitro*, *in vivo* studies in animals and humans, flavonoids have poor bioavailabilities (generally in the range of less than 5%) that are highly variable.[1, 6-8, 39, 40] Flavonoids found in the plasma are present as conjugates (metabolites) with *in vivo* aglycone (drug molecule) plasma concentrations of 0.01 to 0.4 μM.[6, 40] These *in vivo* concentrations are significantly less than the IC_{50} or EC_{50} values (5 to 50 μM) commonly reported for its anticancer effects *in vitro*.[1, 3, 41] Hence, use of flavonoids as an anticancer agent is limited by their poor bioavailability, which is mainly due to their high intestinal glucuronidation by UGTs.[9-11]

In order to exploit the beneficial effects, flavonoids with low UGT metabolism need to be screened from naturally occurring flavonoids and/or their synthetic analogues and developed into chemopreventive agents. To screen for the better compounds in terms of desired metabolic outcome (higher bioavailability or higher metabolism of aglycone) and lower drug-drug interactions, UGT "fingerprinting" can be used. But, it is difficult to experimentally test every naturally available (~4000 compounds) and synthetically designed flavonoid using the whole range of UGT isoforms. 16 human UGT isoforms

have been reported and but only 12 are available so far. Therefore, there is a need to use more economic and time saving screening tools, such as quantitative structure-metabolism relationship (QSMR) prediction models. However, based on direct analysis of the experimental data from UGT isoforms or human liver or intestinal microsomes, it is somewhat difficult to develop good QSMR models, so better computational (*in silico*) tools are required to develop QSMR models with good predictive ability.[139, 140]

Homology and pharmacophore modeling and two-/ three- dimensional quantitative structure activity relationships (2-D/ 3-D QSAR) are few of the *in silico* approaches that can be used to establish QSMR.[139-145] Until now, it's been impossible to use homology model for predicting glucuronidation because of the poorly understood structure-function relationship of UGT and lack of availability of a 3-D X-ray crystal structure of an enzyme homologous to human UGT.[142, 146, 147] *In silico* modeling for glucuronidation therefore has mainly focused on pharmacophore-based 3-D QSAR and descriptors based 2-D/3-D QSAR modeling to develop a QSMR. A pharmacophore is a defined 3-D geometrical arrangement of those interactive functional groups in the structure of a molecule, which is recognized at the receptor (i.e. enzyme interaction) site and is responsible for the biological activity (i.e. glucuronidation) of that molecule. Pharmacophore modeling uses pharmacophore(s) of substrate and non-substrates of the target protein to develop a QSMR, whereas 2-D and 3-D QSMR uses 2-D and 3-D descriptors of the ligand molecules.[141, 147] Various statistical tools such as partial least

square (PLS), genetic function approximation (GFA), multiple regression analysis, neural network can be utilized to generate the 2-D and 3-D QSMR models.

Sorich *et al*. (2002) presented the first generalized 2-D and 3-D QSMR and pharmacophore models developed for UGT.[92] Different methodologies were used to develop models which predicted the substrate selectivity and binding affinity toward UGT1A1. The substrate affinity (as reflected by low apparent inhibitor constant ($K_{i,app}$) was in the order: quercetin ~ naringenin >> 3-HF; this was consistent with the substrate selectivity study on UGT1A1 mentioned above.[153] Another study on UGT1A9 indicated that the substrate affinity is in the order: quercetin ~ 3-HF >> naringenin[154], which is different from that observed for UGT1A1.

However, it is important to note that these models are for predicting substrate selectivity and binding affinity, rather than the glucuronidation efficiencies. It is very much possible that a bulky flavonoid substrate might fit in the active site, but might not be glucuronidated, or only weakly glucuronidated. A QSMR study for UGTs 1A6 and 1A9 on simple phenols was done to study the effects of 4-substutients (i.e., *para* position) on phenol glucuronidation. The authors found that in UGTs 1A6 and 1A9, V_{max} decreased as substrates' molecular volume increased, which means that bulky flavonoids might act as UGTs inhibitors instead of substrates.[155] These models have shown reasonably good predictive ability (in range of 60-80%). But, so far no UGT QSMR model has been

developed which focuses on predicting the level of metabolism of substrates, which is of great interest to us in the case of flavonoids.

K_m and C_{lint} are two important kinetic parameters that can be used to explain the relationship between enzyme activity and substrate structure. An enzymatic reaction that converts a substrate into the product can be explained by a two step reaction, first the binding of substrate to the enzyme and second the conversion of substrate to the product. Since it's a two step process, the overall outcome depends upon the rates of both steps. K_m is an intrinsic property of an enzyme related to the binding constant for forming the ES complex and can be defined as $K_m = (k_2 + k_3)/k_1$, which means that K_m reflects both binding of enzyme to substrate and also the catalytic constant of the enzyme catalyzed reaction or turnover constant (k_3 or k_{cat}). The maximum velocity of the enzyme catalyzed reaction (V_{max}) is also dependent on the catalytic constant: $V_{max} = k_{cat}$ [E].

On the other hand, C_{lint} is the ratio V_{max}/K_m, which measures the efficiency of an enzyme and is independent of physiological factors such as the liver blood flow or drug binding in the blood. When the drug concentration is much smaller than K_m, Cl_{int} becomes V/C_s, where C_s is the concentration of the unbound drug at the enzyme site. So, using a low concentration such as 2.5 µM, an approximate Cl_{int} can be obtained using lesser time and resources than obtaining K_m and V_{max} values. Also, since K_m is a parameter for individual enzyme, it is usually different among different species and cannot be used for inter-species scaling, while Cl_{int} can be related to tissue or organ level metabolism and if

required can be used for inter-species scaling. The values of Cl_{int} predicted by QSMR models can be compared to data obtained in sub-cellular fractions, cell lines, hepatocytes and *in situ* and *in vivo* experimental data on metabolism. Hence in our study, approximate Cl_{int} values of flavonoids with specific UGT isoform will be used as metabolism activity establishing structure-metabolism relationship.

In the current study, we aim to generate QSMR models for predicting flavonoids glucuronidation by specific UGT isoforms, with the predictive ability of equal to or more than 75%, i.e. it could correctly predict 3 out of 4 compounds. We used the various modeling approaches, such as, pharmacophore-based 3-D QSAR, 2-D and 3-D QSAR modeling using 2-D and 3-D descriptors individually and in combination using PLS statistical technique, for developing the models and testing the proposed hypothesis. Based on our findings in Chapter 4, we choose to use the two most important isoforms, UGT1A8 (isoform exclusively expressed in intestine) and UGT1A9 (isoform exclusively expressed in liver and kidney) to develop the QSMR models. We experimentally generated approximate intrinsic clearance (Cl_{int}) values for 48 flavonoids by UGT1A8 and UGT1A9 in our lab only in order to avoid any variation in data due to different experimental conditions between labs.

6.3. Materials and Methods

6.3.1. Materials

Genistein, biochanin A, formononetin, prunetin, glycitein, daidzein, phlortein, naringenin (Figure 19) were purchased from Indofine Chemicals (Somerville, NJ). Additionally, 24 flavones and 16 flavonols (Figure 19, Table 5) were also purchased from Indofine Chemicals (Somerville, NJ). Recombinant human UGT1A8 and UGT1A9 (Supersomes™) were purchased from BD Biosciences (Woburn, MA). Uridine diphosphoglucuronic acid (UDPGA), alamethicin, D-saccharic-1,4-lactone monohydrate, magnesium chloride, and Hanks' balanced salt solution (powder form) were purchased from Sigma-Aldrich (St Louis, MO). All other materials (typically analytical grade or better) were used as received.

Random Allocation Software, a free tool developed by M. Saghaei, MD., Department of Anesthesia, Isfahan University of Medical Sciences, Isfahan, Iran, was used to divide molecules into training and test sets. Discovery Studio and Discovery Studio Visualizer (Version 2.5) by Accelrys, Inc., San Diego, CA were used for *in silico* modeling. Discovery Studio® is a modeling and simulation suite of applications that has various modules or utilities which can be used to draw structures of compounds, develop conformers, develop semi-quantitative and quantitative pharmacophore models.

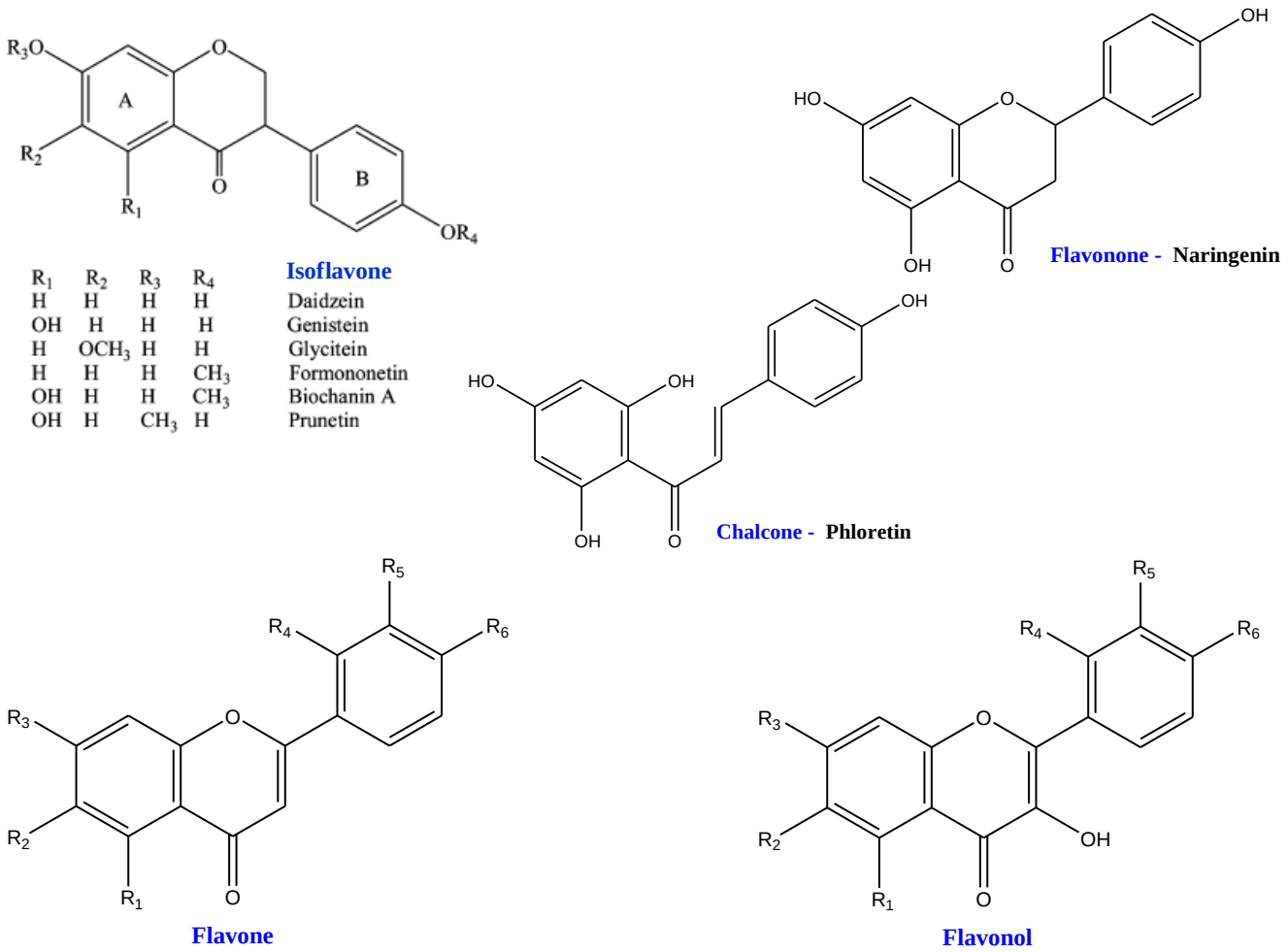

Figure 19. Structure of flavonoids used in *in silico* QSMR modeling

Table 5 Details of hydroxyl and methoxyl substitutions in the structure of flavones and flavonols used in the study

Compounds (Abbreviation)	Substitutions at various position in the structure					
	R1	R2	R3	R4	R5	R6
Flavones						
2'-Hydroxyflavone (2'HF)	-H	-H	-H	-OH	-H	-H
3'-Hydroxyflavone (3'HF)	-H	-H	-H	-H	-OH	-H
4'-Hydroxyflavone (4'HF)	-H	-H	-H	-H	-H	-OH
5-Hydroxyflavone (5HF)	-OH	-H	-H	-H	-H	-H
6-Hydroxyflavone (6HF)	-H	-OH	-H	-H	-H	-H
7-Hydroxyflavone (7HF)	-H	-H	-OH	-H	-H	-H
4'-Hydroxy-5-methoxyflavone (4'H5MF)	-OMe	-H	-H	-H	-H	-OH
4'-Hydroxy-6-methoxyflavone (4'H5MF)	-H	-OMe	-H	-H	-H	-OH
4'-Hydroxy-7-methoxyflavone (4'H7MF)	-H	-H	-OMe	-H	-H	-OH
5-Hydroxy-7-methoxyflavone (5H7MF)	-OH	-H	-OMe	-H	-H	-H
6-Hydroxy-4'-methoxyflavone (6H4'MF)	-H	-OH	-H	-H	-H	-OMe
6-Hydroxy-7-methoxyflavone (6H7MF)	-H	-OH	-OMe	-H	-H	-H
7-Hydroxy-4'-methoxyflavone (7H4'MF)	-H	-H	-OH	-H	-H	-OMe
5,4'-Dihydroxyflavone (5,4'DHF)	-OH	-H	-H	-H	-H	-OH
5,6-Dihydroxyflavone (5,6DHF)	-OH	-OH	-H	-H	-H	-H
5,7-Dihydroxyflavone (5,7DHF)	-OH	-H	-OH	-H	-H	-H
6,4'-Dihydroxyflavone (6,4'DHF)	-H	-OH	-H	-H	-H	-OH
6,7-Dihydroxyflavone (6,7DHF)	-H	-OH	-OH	-H	-H	-H
7,4'-Dihydroxyflavone (7,4'DHF)	-H	-H	-OH	-H	-H	-OH
5,4'-Dihydroxy-7-methoxyflavone (5,4'DH7MF)	-OH	-H	-OMe	-H	-H	-OH
5,6-Dihydroxy-7-methoxyflavone (5,6DH7MF)	-OH	-OH	-OMe	-H	-H	-H

Compounds (Abbreviation)	**Substitutions at various position in the structure**					
	R1	**R2**	**R3**	**R4**	**R5**	**R6**
Apigenin (5,7,4'THF)	-OH	-H	-OH	-H	-H	-OH
Baicalein (5,6,7THF)	-OH	-OH	-OH	-H	-H	-H
Leutolin (5,7,3',4'QHF)	-OH	-H	-OH	-H	-OH	-OH
Flavonols						
3-Hydroxyflavone (3HF)	-H	-H	-H	-H	-H	-H
3,4'-Dihydroxyflavone (3,4'DHF)	-H	-H	-H	-H	-H	-OH
3,5-Dihydroxyflavone (3,5DHF)	-OH	-H	-H	-H	-H	-H
3,6-Dihydroxyflavone (3,6DHF)	-H	-OH	-H	-H	-H	-H
3,7-Dihydroxyflavone (3,7DHF)	-H	-H	-OH	-H	-H	-H
3-Hydroxy-4'-methoxyflavone (3H4'MF)	-H	-H	-H	-H	-H	-OMe
3-Hydroxy-5-methoxyflavone (3H5MF)	-OMe	-H	-H	-H	-H	-H
3-Hydroxy-6-methoxyflavone (3H6MF)	-H	-OMe	-H	-H	-H	-H
3-Hydroxy-7-methoxyflavone (3H7MF)	-H	-H	-OMe	-H	-H	-H
5,7-Dimethody-3-hydroxyflavone (5,7DM3HF)	-OMe	-H	-OMe	-H	-H	-H
7,4'-Dimethody-3-hydroxyflavone (7,4'DM3HF)	-H	-H	-OMe	-H	-H	-OMe
3,7,4'-Trihydroxyflavone (3,7,4'THF)	-H	-H	-OH	-H	-H	-OH
3,5,7-Trihydroxyflavone (3,5,7THF)	-OH	-H	-OH	-H	-H	-H
3,6,4'-Trihydroxyflavone (3,6,4'THF)	-H	-OH	-H	-H	-H	-OH
Kaempferol (3,5,7,4'QHF)	-OH	-H	-OH	-H	-H	-OH
Quercetin (3,5,7,3',4'PHF)	-OH	-H	-OH	-H	-OH	-OH

Additionally, Discovery studio can calculate molecular descriptors (or properties), and develop 2-D and 3-D QSAR models using various statistical tools.

6.3.2. Solubility and stability of the tested flavonoids

Solubility and stability of the tested flavonoids were established at the experimental conditions as per the method explained in section 3.1 (Chapter 3).

6.3.3. Determining approximate intrinsic clearance values of selected flavonoids for UGT1A8 and UGT1A9

Glucuronidation activities of recombinant human UGT1A8 and UGT1A9: The incubation procedures for measuring UGTs' activities were essentially the same as described in section 4.3.3 (Chapter 4). Substrate concentration of 2.5 μM was used to measure the rate of glucuronidation by UGT1A8 and 1A9. UGT1A8 and 1A9 could generate multiple mono-*O*-glucuronides for certain flavonoids. For calculating the approximate Cl_{int}, rates of formation of all glucuronides of a compound was added together and divided with the substrate concentration.

UPLC analysis of flavonoids and their glucuronides: We analyzed flavonoids and their respective glucuronides by using the same system and method as described in section 4.3.4 (Chapter 4). For genistein, naringenin, phloretin, 3HF, 3,4'DHF, 3,7DHF 5,4'DHF, 5,7DHF, 7,4'DHF, 3,7,4'THF, 5,7,4'THF, 3,5,7THF, 3,5,7,4'QHF and their respective

glucuronides measuring wavelength and internal standards and method validation were the same as mentioned in section 4.3.4 (Chapter 4) Rest of the flavonoids and their respective glucuronides were analyzed using the following common method: system, Waters Acquity UPLC with photodiode array detector and Empower software; column, BEH C_{18}, 1.7 μm, 2.1 × 50 mm; mobile phase A, 100% aqueous buffer (2.5mM NH_4Ac, pH 3); mobile phase B, 100% acetonitrile; gradient, 0 to 0.3 min, 10% B, 0.3 to 2.9 min, 10–50%B, 2.9 to 3.2 min, 50-90%B, 3.2 to 4.0 min, 90% B; flow rate, 0.5 ml/min; and injection volume, 10μL.

Testosterone (254 nm) was used as internal standard for analyzing 3H4'MF (340 nm), 3H7MF (340 nm), 4'H6MF (330 nm), 4'H7M (330 nm), 5H7MF (268 nm), 6H4'MF (330 nm), 6H7MF (263 nm), 7H4'MF (330 nm), 6,4'DHF (330 nm), 6,7DHF (263 nm), baicalein (277 nm), quercetin (254 nm) and their respective glucuronides at the wavelength given in bracket. Formononetin (254 nm) was used as internal standard for analyzing 3H5MF (340 nm), 3H6MF (340 nm), 4'H5MF (340 nm), 3,5DHF (263 nm), 3,6DHF (340 nm), 5,6DHF (282 nm), 5,7DM3HF (354 nm), 7,4'DM3HF (354 nm), 5,4'DH7MF (354 nm), and 5,6DH7MF (354 nm), 3,6,4'THF (354 nm), luteolin (354 nm), and their respective glucuronides at the wavelength given in bracket. Linearity was established in the range of 0.63-10 μM (total 5 concentrations) for these compounds.

Quantification of glucuronides of flavonoids: The quantification of glucuronides of flavonoids was done using the standard curve of the parent compound with a correction

factor (where determined) for the difference in extinction coefficient of the compound and its glucuronides. The correction factor of the glucuronides was measured using the method as explained in section 3.5 and 3.6 (Chapter 3). The correction factor were not determined for the glucuronide(s) of the following flavonoids: 3,6DHF, 5,6DHF, 6,4'DHF, 6,7DHF, 3,6,4'THF, luteolin, quercetin, baicalein, 4'H6MF, 4'H7MF, 5H7MF, 6H4'MF, 6H7MF, 7H4'MF, 5,7DM3HF, 7,4'DM3HF, 5,4'DH7MF and 5,6DH7MF. Hence, standard curve of the parent compound without any correction factor was used for quantifying the glucuronides of these compounds.

Confirmation of flavonoids glucuronide structure by LC-MS/MS: Glucuronides of the flavonoids were confirmed using the same method for LC-MS/MS as described in section 4.3.6 (Chapter 4).

Data analysis: Rates of metabolism in recombinant human UGT isoforms were expressed as amounts of metabolites formed per min per mg protein or pmol/min/mg. Intrinsic clearance values (ml per min per mg of protein) were expressed as the ratio of the measured rate of glucuronidation to the substrate concentration (2.5 µM).

6.3.4. Dividing compounds into training and test sets

The compounds were randomly divided into training (80% of total compounds) and test set (20% of total compounds) using Random Allocation Software to avoid any bias. Different training and test sets were created for UGT1A8 and UGT1A9.

Table 6 Approximate Intrinsic clearance (Cl_{int}) values presented as average (Avg) of n=3 determination with standard deviation (SD), activity as inverse of Cl_{int} values (*Activ*) and uncertainty of activity (*Uncert*) as input for *in silico* modeling for UGT1A8 and UGT1A9.

Compound	*Activ* for Pharmacophore Modeling (Cl_{int} values for UGT1A8 (ml per min per mg of protein)		*Activ* for 2-D/3-D QSAR Modeling (1/ Cl_{int})	*Uncert*
	Avg	SD		
Genistein	6.23E+04	7.32E+03	1.60E-05	1.13
Glycitein	2.72E+05	1.33E+04	3.67E-06	1.05
Prunetin	5.18E+04	1.81E+04	1.93E-05	1.44
2'HF	4.72E+05	1.04E+05	2.12E-06	1.25
3'HF	1.06E+05	6.28E+03	9.40E-06	1.06
3HF	2.12E+05	1.73E+03	4.72E-06	1.01
5HF	1.12E+05	1.69E+04	8.92E-06	1.16
6HF	3.48E+05	4.71E+04	2.88E-06	1.15
7HF	9.25E+04	1.28E+04	1.08E-05	1.15
3,4'DHF	6.32E+04	4.76E+03	1.58E-05	1.08
3,5DHF	5.64E+04	9.23E+02	1.77E-05	1.02
3,6DHF	5.66E+05	4.07E+04	1.77E-06	1.07
3,7DHF	6.30E+04	6.01E+03	1.59E-05	1.10
5,4'DHF	6.29E+04	1.40E+04	1.59E-05	1.25
5,6DHF	1.98E+06	9.74E+04	5.05E-07	1.05
5,7DHF	2.98E+05	1.07E+04	3.35E-06	1.04
6,4'DHF	8.30E+04	2.98E+03	1.21E-05	1.04
6,7DHF	1.81E+05	2.82E+04	5.53E-06	1.17
7,4'DHF	1.50E+04	1.08E+03	6.68E-05	1.08
Luteolin	7.06E+05	4.23E+04	1.42E-06	1.06
Quercetin	2.29E+05	3.23E+04	4.37E-06	1.15
Baicalein	1.19E+06	1.33E+05	8.42E-07	1.12
Kaempferol	1.83E+05	9.51E+03	5.48E-06	1.05
Naringenin	2.99E+05	3.32E+04	3.35E-06	1.12
Apigenin	1.27E+05	1.48E+04	7.85E-06	1.12
Phlortein	3.54E+05	2.69E+04	2.83E-06	1.08

Compound	***Activ* for Pharmacophore Modeling (Cl_{int} values for UGT1A8 (ml per min per mg of protein)**		***Activ* for 2-D/3-D QSAR Modeling (1/ Cl_{int})**	***Uncert***
	Avg	**SD**		
Galangin	2.01E+05	3.63E+03	4.98E-06	1.02
3,6,4'THF	1.75E+04	2.57E+03	5.71E-05	1.16
3H4'MF	9.06E+04	5.15E+03	1.10E-05	1.06
3H5MF	5.20E+04	7.22E+03	1.92E-05	1.15
3H6MF	1.43E+05	1.53E+04	6.97E-06	1.12
3H7MF	6.28E+04	8.08E+03	1.59E-05	1.14
4'H6MF	9.35E+03	2.21E+03	1.07E-04	1.27
4'H7MF	1.38E+04	7.24E+02	7.27E-05	1.05
6H4'MF	7.24E+04	1.35E+04	1.38E-05	1.21
6H7MF	4.33E+04	4.94E+03	2.31E-05	1.12
7H4'MF	7.48E+04	9.18E+03	1.34E-05	1.13
5,7DM3HF	3.22E+04	6.06E+03	3.11E-05	1.21
7,4'DM3HF	1.83E+05	1.26E+04	5.48E-06	1.07
5,6DH7MF	5.32E+05	2.08E+04	1.88E-06	1.04
Compound	***Activ* for Pharmacophore Modeling Cl_{int} values for UGT1A9 (ml per min per mg of protein)**		***Activ* for 2-D/3-D QSAR Modeling (1/ Cl_{int})**	***Uncert***
	Avg	**SD**		
Genistein	3.13E+05	3.92E+04		
Glycitein	4.59E+05	1.47E+04	2.18E-06	1.03
Diadzein	2.94E+05	4.90E+04	3.41E-06	1.18
Biochanin A	5.94E+04	7.71E+03	1.68E-05	1.14
Prunetin	8.31E+04	3.71E+03	1.20E-05	1.05
2'HF	1.74E+05	2.45E+04	5.76E-06	1.15
3'HF	1.90E+05	5.06E+04	5.25E-06	1.31
3HF	7.31E+05	4.22E+04	1.37E-06	1.06
4'HF	9.46E+04	4.57E+03	1.06E-05	1.05
5HF	1.16E+05	2.36E+03	8.65E-06	1.02
6HF	3.86E+04	2.18E+03	2.59E-05	1.06
7HF	5.21E+05	3.73E+04	1.92E-06	1.07
3,4'DHF	5.44E+05	5.18E+04	1.84E-06	1.10
3,5DHF	6.10E+05	2.82E+04	1.64E-06	1.05
3,6DHF	2.21E+06	5.77E+04	4.52E-07	1.03
3,7DHF	2.69E+07	2.99E+06	3.72E-08	1.12

Compound	*Activ* for Pharmacophore Modeling Cl_{int} values for UGT1A9 (ml per min per mg of protein)		*Activ* for 2-D/3-D QSAR Modeling (1/ Cl_{int})	*Uncert*
	Avg	SD		
5,4'DHF	2.19E+05	1.90E+04	4.57E-06	1.09
5,6DHF	2.88E+05	5.95E+04	3.47E-06	1.23
5,7DHF	1.82E+06	1.19E+05	5.50E-07	1.07
6,4'DHF	3.14E+05	1.59E+04	3.19E-06	1.05
6,7DHF	3.80E+05	7.25E+04	2.63E-06	1.21
7,4'DHF	1.29E+05	3.07E+03	7.76E-06	1.02
Luteolin	1.30E+06	1.87E+04	7.67E-07	1.01
Quercetin	1.49E+06	2.82E+04	6.72E-07	1.02
Baicalein	1.99E+06	2.39E+04	5.03E-07	1.01
Kaempferol	2.95E+06	1.18E+05	3.39E-07	1.04
Naringenin	4.79E+05	1.66E+04	2.09E-06	1.04
Apigenin	6.85E+05	1.74E+04	1.46E-06	1.03
Phlortein	1.67E+05	1.11E+04	5.97E-06	1.07
Resokaempferol	4.21E+05	1.07E+04	2.38E-06	1.03
Galangin	1.47E+06	2.72E+04	6.78E-07	1.02
3,6,4'THF	5.66E+05	1.11E+04	1.77E-06	1.02
3H4'MF	2.94E+05	2.78E+04	3.41E-06	1.10
3H5MF	4.77E+05	3.14E+04	2.10E-06	1.07
3H6MF	3.13E+05	2.68E+04	3.19E-06	1.09
3H7MF	7.22E+05	7.93E+03	1.39E-06	1.01
4'H6MF	6.61E+03	2.20E+03	1.51E-04	1.42
4'H7MF	1.73E+04	1.72E+03	5.78E-05	1.11
5H7MF	2.29E+04	9.79E+02	4.37E-05	1.04
6H4'MF	1.87E+04	3.16E+03	5.36E-05	1.19
6H7MF	1.28E+05	9.22E+02	7.79E-06	1.07
7H4'MF	8.22E+04	1.07E+04	1.22E-05	1.14
5,7DM3HF	1.04E+05	2.49E+03	9.65E-06	1.02
7,4'DM3HF	6.09E+05	3.32E+04	1.64E-06	1.06
5,4'DH7MF	4.95E+04	3.07E+03	2.02E-05	1.06
5,6DH7MF	1.96E+05	2.31E+04	5.11E-06	1.13

HF = hydroxyflavone; DHF = dihydroxyflavone; THF = trihydroxyflavone; H-MF = hydroxyl-methoxyflavone; DH-MF = dihydroxy-methoxyflavone; and DM-HF = dimethoxy- hydroxyflavone

Training set molecules were used to develop the QSMR models and test set molecules were used to test the predictive ability of the models. Ten such randomized groups of training and test set were formed for UGT1A8 and UGT1A9 each for the *in silico* modeling. The molecules in the training and test set of the ten randomized groups for UGT1A8 and UGT1A9 are shown in Table E1 and Table E2 of Appendix E.

6.3.5. Entering intrinsic clearance values

Structure of selected 48 flavonoids (Figure 19, Table 5) was drawn/ sketched using Catalyst® or Discover Studio software by Accelrys, Inc., San Diego, CA. Once the structure is sketched, it is subjected to clean up, to optimize the bond length and angles, using minimization of energy. The file was saved as .sd or .mol file. Using a "spreadsheet" feature in the software, desired compounds were added to the each training and test set spreadsheet. Different spreadsheets were created for the training and test set of each randomized group of UGT1A8 and UGT1A9.

For pharmacophore-based QSMR modeling, the activity values (inverse of approximate intrinsic clearance values) for the molecules were entered in the *Activ* attributes (column) of the spreadsheets. Uncertainty in the activity values was calculated using the experimental standard deviation of the activity values as the average of {(Mean activity + SD)/ Mean activity} and {(Mean activity / (Mean activity-SD)}. Uncertainty values were entered in the *Uncert* attributes (column) of the spreadsheet. Intrinsic clearance and uncertainty values of flavonoids for UGT1A8 and 1A9 were given in Table 6. For 2-D/3-

D QSMR modeling, n=3 individual experimentally derived Cl_{int} values for UGT1A8 and 1A9 were input as activity in the spreadsheet.

6.3.6. Generation of conformers and calculation of molecular descriptors

Since, there is no information in literature about the active conformation of flavonoid molecules in the UGT enzyme cavity; hence, we generated the maximum number of conformers (3-D configuration of a particular molecular structure) possible for the molecules. All possible (maximum 255) conformations of a molecule with 20 Kcal/mol cut off above minimum energy were generated using the "Best" function of Discovery studio to ensure the widest possible conformer coverage. Each spreadsheet was used for generating the maximum conformers of all the molecules in it. The output file with all the confirmations for each spreadsheet was further used to calculate the 2-D and 3-D molecular descriptors of all the molecules in the spreadsheet. Broad groups of 2-D descriptors calculated were AlogP, estate keys, molecular properties, molecular property counts, topological descriptors, surface area and volume. Broad groups of 3-D descriptors calculated were dipole, Jurs descriptors, molecular properties, principle moment of inertia, shadow indices and molecular volume.

6.3.7. Pharmacophore-based 3-D QSMR modeling

Feature mapping for all the compounds were done using "Feature Mapping" tool of the Discovery Studio. Hydrophobic region (HR), hydrogen bond acceptors (HBA), hydrogen bond donors (HBD), and ring aromatic (AR) (which might and might not be

hydrophobic) were the only features found in all the molecules. "3-D QSAR Pharmacophore Generation (Hypogen module)" tool of the Discovery Studio was used to develop the pharmacophores using training set molecules. Output file obtained from the conformer generation step in section 6.3.6 was used as input file in this step. Software generated the 10 best pharmacophores as output, also referred as "hypotheses". These pharmacophores were further used to predict the activity of molecules of test set. The predictive ability of each pharmacophore and the correlation between experimental and estimated values of the molecules were calculated to select the best pharmacophore. This exercise was repeated for each randomized group of both UGT1A8 and UGT1A9.

6.3.8. 2-D/3-D QSMR modeling

Out of the total 361 2-D (237) and 3-D (58) descriptors calculated in section 9.2.6, 80 2-D or 58 3-D descriptors molecular descriptors were used to generate 2-D or 3-D QSMR models, respectively in the Discovery Studio. Certain low-variable (almost constant) descriptors that were different from a constant only for a few (2-3) compounds in the training set, were also eliminated while building the model, because such descriptors could not provide useful statistical information and decreased the model predictive ability. 157 such 2-D descriptors were not used for model building. 2-D and 3-D molecular descriptors were also used in combination (total 135 descriptors) to develop 2-D/3-D QSAR models. Multiple 2-D and/or 3-D molecular descriptors as independent variables and Cl_{int} as dependent variable were used to develop the predictive models.

Partial least square (PLS) regression technique was used in modeling as the number of descriptors was much greater than number of compounds (data points). PLS regression uses transformation of large number of independent variables into small number of principle components. These principal components were mutually independent linear combinations of original descriptors and were chosen in such a way as to provide maximum correlation with dependent variable. The number component should be maximum 3 times the number of compounds used for building the model. For UGT 1A8 (32 compounds in training set), n = 10 principle components and for UGT1A9 (37 compounds in training set), n = 15 principle components were selected to build the models.

6.3.9. Data analysis

Each pharmacophore-based 3-D QSMR model developed using a particular training set was analyzed for its ability to semi-quantitatively (high versus low metabolizing compounds) or quantitatively (approximate Cl_{int} values) predict the activity of the compounds in the corresponding test set. Predictive ability of the model was defined as the percentage of compounds of the test set which were correctly predicted using the model. Similarly, each 2-D QSMR, 3-D QSMR, and 2-D/3-D QSMR model developed using a particular training set was analyzed for its ability to quantitatively (approximate Cl_{int} values) predict the activity of compounds in the corresponding test set. r^2 value of correlation between experimental and estimated value by PLS model was calculated.

Additionally, average squared error was calculated as Average [{(Experimental Cl_{int} – Estimated Cl_{int})/ Experimental Cl_{int}}^{2}] for both training and test set.

6.4. Results

6.4.1. Confirmation of flavonoid glucuronides structure by LC-MS/MS

We conducted simple LC-MS/MS studies of the metabolites to confirm the (mono- and di-) glucuronides peaks for all flavonoids.

6.4.2. Determination of correction factors for glucuronides of flavonoids

Amounts of glucuronides of certain flavonoids formed were determined using the corrections factors for individual glucuronides of flavonoids as described in the method section. UGT isoforms and wavelength used in generation of correction factor and the correction factor for each glucuronides are detailed in Tables C1-C4 (Appendix C). The correction factors were in the range of 0.5 (for 3-*O*-G of 3HF) to 2.5 (for 3-*O*-G for 3,7DHF).

6.4.3. Pharmacophore-based 3-D semi-quantitative SMR models

We tried to develop isoform-specific pharmacophore-based 3-D QSMR model. We found that there was no correlation between the experimentally obtained and pharmacophore estimated Cl_{int} values for UGT1A8 and UGT1A9. Hence, it was not possible to do quantitative prediction using pharmacophore models. However, when we divided the compounds into two classes of high and low metabolizing compounds (cut off was

arbitrarily set at Cl_{int} value of 3 x 10^5 ml per min per mg of protein for UGT1A9 and 3 x 10^5 ml per min per mg of protein for UGT1A8), generated models were able to reasonably predict the compounds in the right class. Pharmacophores with predictive ability of more than 60% for both training and test set were reported here.

Discovery Studio generated 10 pharmacophores using training sets of each randomized group (total 10 sets). For each group, out of 10 pharmacophores, best pharmacophore model was chosen based on the following criteria for selection. (1) Ability of each pharmacophore of a randomized group for predicting the compounds of training set into right class was calculated. Pharmacophores with predictive ability of less than 60% for training set were discarded. (2) For rest of the pharmacophores were mapped with compounds of test set and estimated Cl_{int} values were generated. Only pharmacophores which were able to map all test set substrates were selected here. If no pharmacophore could map all test set compounds, then pharmacophore which could map maximum number of compounds were selected. (3) Then, the ability of the pharmacophores to correctly predict the compounds from test set into the right class were calculated. If a compound was not mapped by the pharmacophores, it was considered as falsely predicted. Pharmacophores with predictive ability of less than 60% for test set were discarded. (4) Out of the remaining pharmacophores, one single (best) pharmacophore was chosen for each randomized group, based on which pharmacophore more correctly predicted the compounds at the extremes of the activity range.

Based on these selection criteria, for UGT1A8, out of the ten randomized groups' training sets, only 4 (III, V, VIII and IX) were able to generate pharmacophores which had the predictive power of 60-80% for the training sets, but only VIII and IX groups' pharmacophores predicted equal to or more that 60% of the test set compounds correctly. However, we observed that each of these pharmacophores wrongly predicted the low metabolizing compounds (only 2 in each test set) as high metabolizing. Both pharmacophores over-estimated all activity values. Hence, we did not approve the two pharmacophores as the right predictive models. So, we could not get any valid predictive model for UGT1A8.

On the other hand, for UGT1A9, all of the ten randomized groups' training sets were able to generate pharmacophores which had the predictive power of 60-90% for the training sets. But out of these ten, only five (II, III, V, IX and X) randomized groups' pharmacophores had the predictive power of more than 60% for both training and test set. The data for each of the pharmacophore estimated Cl_{int} values and predicted class of the compounds of training and test set were listed in table E3-E6 (Appendix E).

UGT1A9_pharmacophore_Group II: Group II was the only group to be able to generate four-feature pharmacophore which passed the cut of >60% predictive ability. Rest of the groups generated only three-feature pharmacophores. The best pharmacophore had the following features: two hydrogen bond acceptors (HBA), one hydrogen bond donor (HBD) and one hydrophobic region.

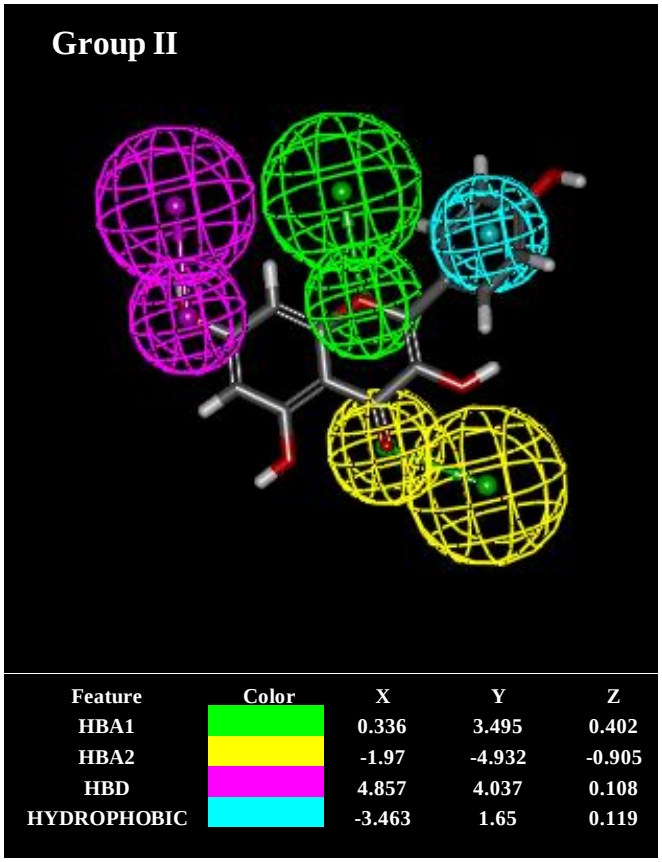

Figure 20. UGT1A9 Pharmacophore for Group II.

Four-feature pharmacophore with two hydrogen bond acceptors (HBA), one hydrogen bond donor (HBD) and one hydrophobic region in a defined 3-D space was generated by Discovery Studio using the training set compounds in group II. The pharmacophore shown here was the best pharmacophore chosen based on the selection criteria defined in section 9.4.3. The figure shows the mapping of substrate kaempferol with the pharmacophore for Group II.

The X, Y, Z coordinates of the features were shown in Figure 20. When kaempferol (a high metabolizing substrate of UGT1A9) was mapped with the pharmacophore, hydroxyl group at 7-C position mapped with HBD and phenyl side chain mapped with hydrophobic region. The one HBA mapped with the carbonyl group oxygen and the other HBA mapped with oxygen of the pyran ring (Figure 20).

The predictive abilities of this pharmacophore for the training and test set were 65% and 67%, respectively. Out of the 9 test set compounds, the pharmacophore was able to map only eight compounds and wrongly predicted high metabolizing compounds 3,5DHF and 3H5MF into low metabolizing class (Table E3, Appendix E).

UGT1A9_pharmacophores_Group III and IX: Training sets of both groups III and IX, generated three-feature pharmacophores with one HBA, one HBD and one hydrophobic region each. However, location constrains between the three features of the two pharmacophores were totally different (Figure 21). Mapping with kaempferol showed that HBAs of the two pharmacophores were located at different point in 3-D space (Figure 21). In the pharmacophore of group III, HBA mapped with the oxygen of pyrane ring, whereas, in the pharmacophore of group IX, HBA mapped with the carbonyl oxygen. The center of hydrophobic region of both pharmacophores mapped with the phenyl side chain. The HBD both pharmacophores also mapped for 7-OH group but the direction of vector was different, which means that the interaction space of the groups mapping with HBD lies in different direction and space.

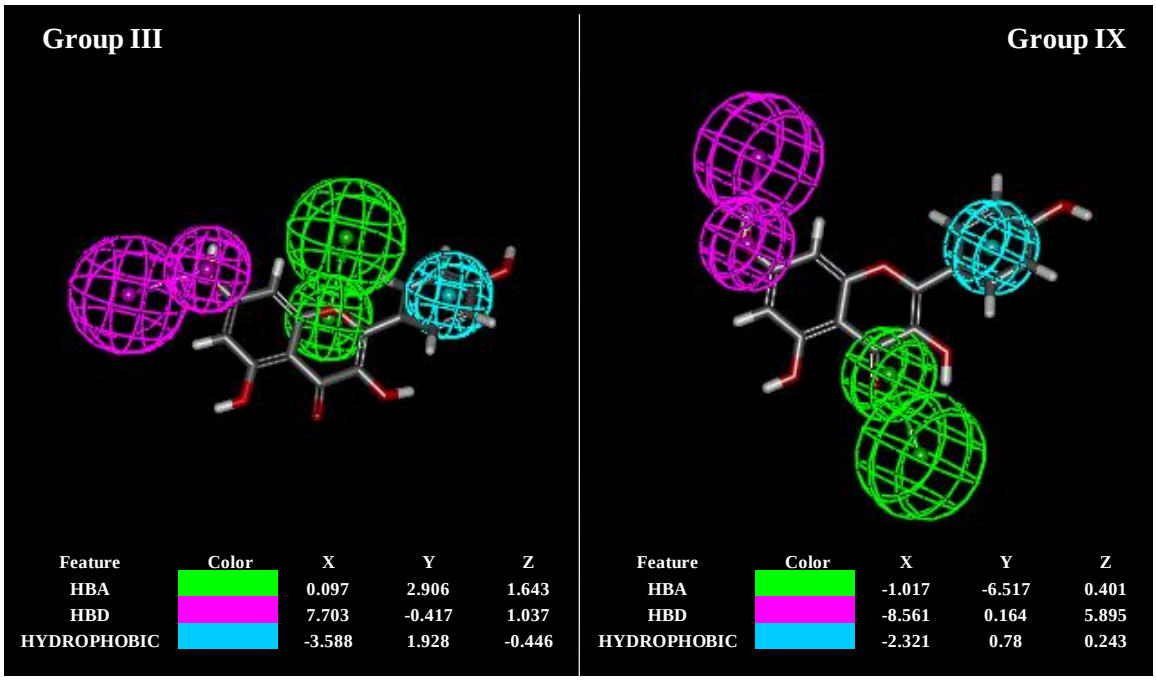

Figure 21. UGT1A9 Pharmacophores for Group III and IX.

Three-feature pharmacophores with one hydrogen bond acceptor (HBA), one hydrogen bond donor (HBD) and one hydrophobic region in a defined 3-D space was generated by Discovery Studio using the training set compounds in group II and IX. The pharmacophores shown here were the best pharmacophores chosen based on the selection criteria defined in section 9.4.3. The figure shows the mapping of substrate kaempferol with the pharmacophores for Group III and IX.

The predictive abilities of pharmacophore of group III for the training and test set was 78% and 67%, respectively. On the other hand, pharmacophore of group IX showed better predictive ability for the test set than all other groups' pharmacophore, with 73% and 78% correct predictions for training and test set, respectively (Table E5, Appendix E). Similar to the pharmacophore of group II, group III pharmacophore also wrongly predicted high metabolizing compounds 3HF, 3,5DHF and 3H5MF into low metabolizing class (Table E4, Appendix E). Both pharmacophores mapped all the nine substrates of the respective test set.

UGT1A9_pharmacophores_Group V and X: Training sets of both groups V and X generated three-feature pharmacophores with one HBA, one HBD and one aromatic ring each. Similar to the case above, location constrains between the three features of the two pharmacophores were different (Figure 22). Mapping with kaempferol showed that HBA in the pharmacophore of group V mapped with the oxygen of pyrane ring, whereas, HBA in the pharmacophore of group X mapped with the carbonyl oxygen (Figure 22). The HBD both pharmacophores also mapped for 7-OH group and the vectors were also in the same directions. The centeroids of the aromatic rings of both pharmacophores mapped with the phenyl side chain, but the interaction space were in the opposite directions (Figure 22).

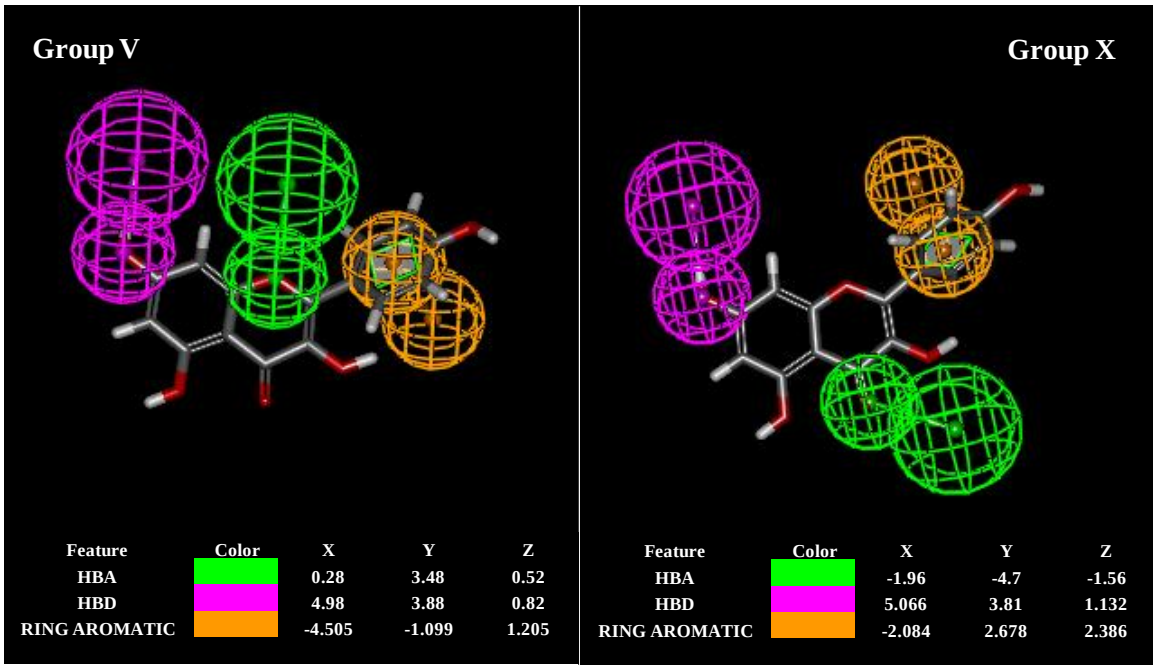

Figure 22. UGT1A9 Pharmacophores for Group V and X.

Three-feature pharmacophores with one hydrogen bond acceptor (HBA), one hydrogen bond donor (HBD) and one aromatic ring in a defined 3-D space was generated by Discovery Studio using the training set compounds in group V and X. The pharmacophores shown here were the best pharmacophores chosen based on the selection criteria defined in section 9.4.3. The figure shows the mapping of substrate kaempferol with the pharmacophores for Group V and X.

The predictive abilities of pharmacophore of group V for the training (65%) and test set (67%) were exactly similar to the pharmacophore of group II, whereas, predictive abilities of pharmacophore of group V were for the training and test set were 73% and 67%, respectively (Tables E5-E7, Appendix E). Group X pharmacophore wrongly predicted low metabolizing compounds 7,4'DHF, 7H4'MF and phloretin of the test set into high metabolizing class (Table E7, Appendix E).

6.4.4. Pharmacophores comparison

We compared all the five pharmacophores to understand the differences and similarity between them. The HBA and HBD features of one pharmacophore were mapped to the HBA and HBD features of another pharmacophore, respectively. Similarly, "hydrophobic" and "ring aromatic" features of one pharmacophore were mapped to the "hydrophobic" and "ring aromatic" features of another pharmacophore, respectively. However, "hydrophobic" feature of one pharmacophore was not mapped to the "ring aromatic" feature of another pharmacophore.

The displacement value of individual features were calculated and used to calculate root-mean-square (RMS) displacement values for each pair of pharmacophores. No displacement values by mapping "hydrophobic" to "ring aromatic" feature was calculated, hence only HBA and HAD displacement values were used to calculate RMS in these pairs of pharmacophores.

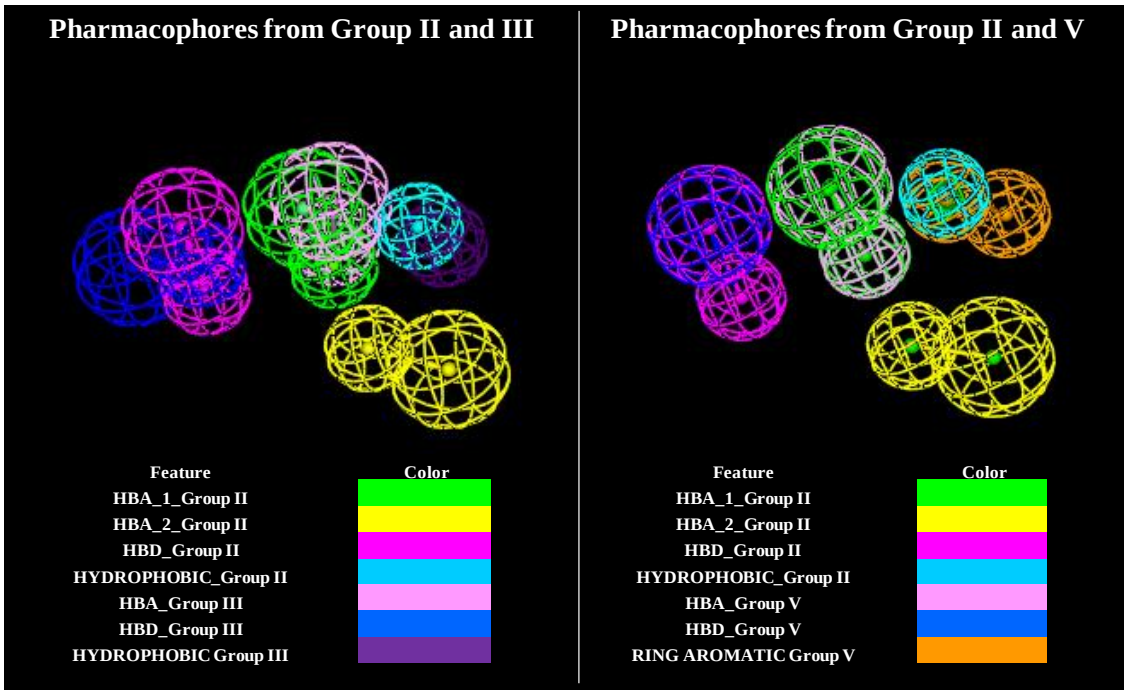

Figure 23. Comparison of UGT1A9 Group II Pharmacophore with Group III and Group V Pharmacophore.

Group II and III: Location constraint “hydrophobic” was mapped to “hydrophobic” (displacement = 1.08 Å). Location constraint "HBD (smaller sphere)" mapped to "HBD (smaller sphere)" (displacement = 1.80 Å). Location constraint "HBD (bigger sphere)" mapped to "HBD (bigger sphere)" (displacement = 2.96 Å). Location constraint "HBA1 (smaller sphere)" mapped to "HBA (smaller sphere)" (displacement = 0.85 Å). Location constraint "HBA1 (bigger sphere)" mapped to "HBA (bigger sphere)" (displacement = 1.19 Å). RMS displacement = 1.75 Å. **Group II and V:** Location constraint "HBD (smaller sphere)" mapped to "HBD (smaller sphere)" (displacement = 0.12 Å). Location constraint "HBD (bigger sphere)" mapped to "HBD (bigger sphere)" (displacement = 0.12 Å). Location constraint "HBA1 (smaller sphere)" mapped to "HBA (smaller sphere)" (displacement = 0.11 Å). Location constraint "HBA1 (bigger sphere)" mapped to "HBA (bigger sphere)" (displacement = 0.17 Å). RMS displacement: 0.13 Å. Hydrophobic feature in pharmacophore of group II was not mapped to ring aromatic feature in pharmacophore of group V.

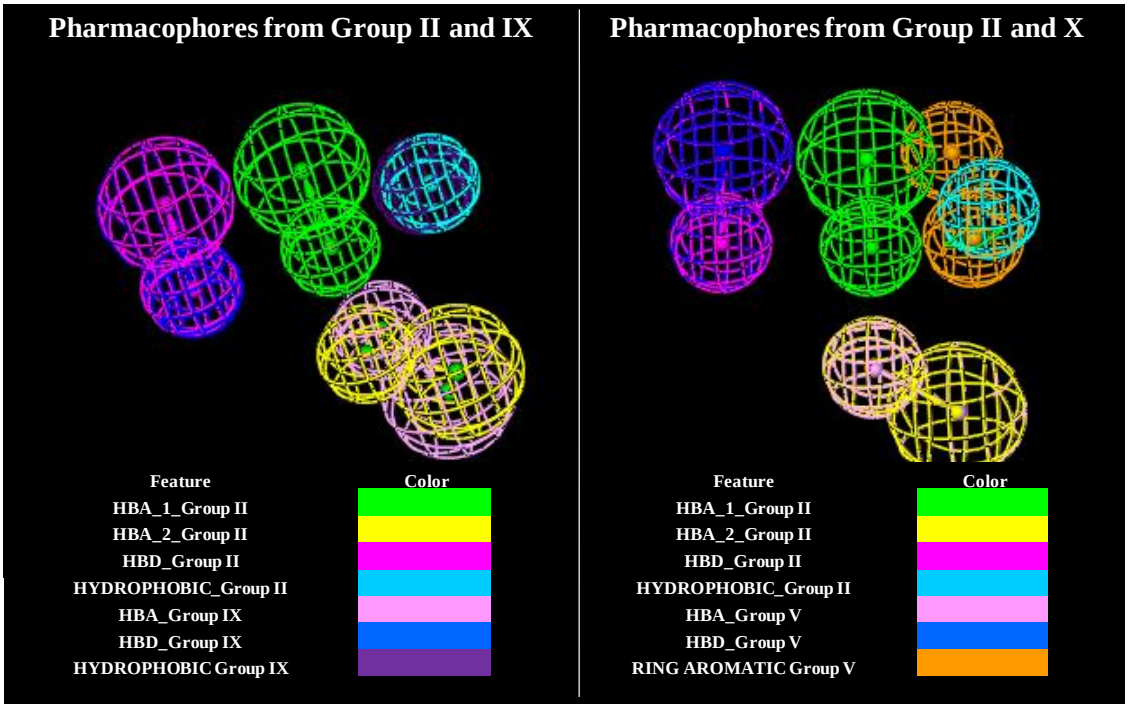

Figure 24. Comparison of UGT1A9 Group II Pharmacophore with Group IX and Group X Pharmacophore.

Group II and IX: Location constraint “hydrophobic” was mapped to “hydrophobic” (displacement = 0.29 Å). Location constraint "HBD (smaller sphere)" mapped to "HBD (smaller sphere)" (displacement = 0.18 Å). Location constraint "HBD (bigger sphere)" mapped to "HBD (bigger sphere)" (displacement = 0.13 Å). Location constraint "HBA2 (smaller sphere)" mapped to "HBA (smaller sphere)" (displacement = 0.95 Å). Location constraint "HBA2 (bigger sphere)" mapped to "HBA (bigger sphere)" (displacement = 0.72Å). RMS displacement = 0.56 Å. **Group II and X:** Location constraint "HBD (smaller sphere)" mapped to "HBD (smaller sphere)" (displacement = 0.07 Å). Location constraint "HBD (bigger sphere)" mapped to "HBD (bigger sphere)" (displacement = 0.03Å). Location constraint "HBA2 (smaller sphere)" mapped to "HBA (smaller sphere)" (displacement = 0.07 Å). Location constraint "HBA2 (bigger sphere)" mapped to "HBA (bigger sphere)" (displacement = 0.05 Å). RMS displacement: 0.06 Å Hydrophobic feature in pharmacophore of group II was not mapped to ring aromatic feature in pharmacophore of group X.

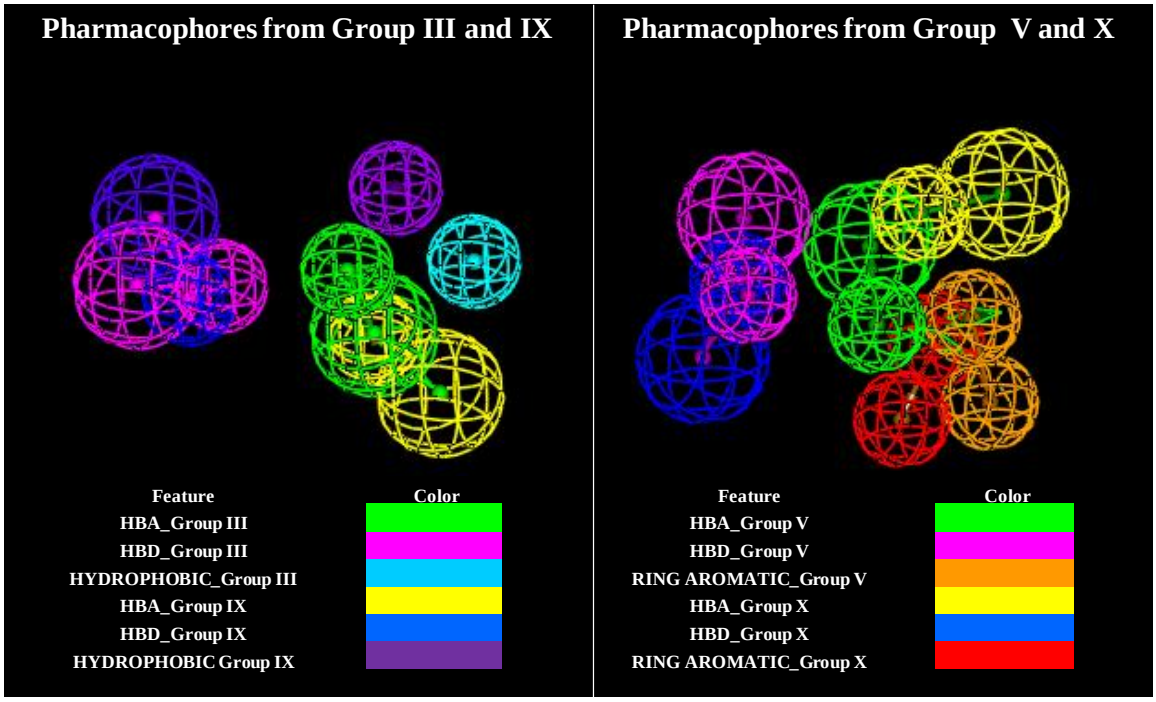

Figure 25. Comparison of UGT1A9 Pharmacophore of Group III with Group IX and Group V with Group X.

Group III and IX: Location constraint “hydrophobic” was mapped to “hydrophobic” (displacement = 3.79 Å). Location constraint "HBD (smaller sphere)" mapped to "HBD (smaller sphere)" (displacement = 1.41 Å). Location constraint "HBD (bigger sphere)" mapped to "HBD (bigger sphere)" (displacement = 2.37 Å). Location constraint "HBA1 (smaller sphere)" mapped to "HBA (smaller sphere)" (displacement = 3.10 Å). Location constraint "HBA1 (bigger sphere)" mapped to "HBA (bigger sphere)" (displacement = 3.07Å). RMS displacement = 2.86 Å. **Group V and X:** Location constraint "ring aromatic (centroid)" mapped to "ring aromatic (centroid)" (displacement = 1.80 Å). Location constraint "ring aromatic (outer sphere)" mapped to "ring aromatic (outer sphere)" (displacement = 3.03 Å). Location constraint "HBD (smaller sphere)" mapped to "HBD (smaller sphere)" (displacement = 0.96 Å). Location constraint "HBD (bigger sphere)" mapped to "HBD (bigger sphere)" (displacement = 4.85Å). Location constraint "HBA (smaller sphere)" mapped to "HBA (smaller sphere)" (displacement = 4.03 Å). Location constraint "HBA (bigger sphere)" mapped to "HBA (bigger sphere)" (displacement = 4.83 Å). RMS displacement: 3.57 Å

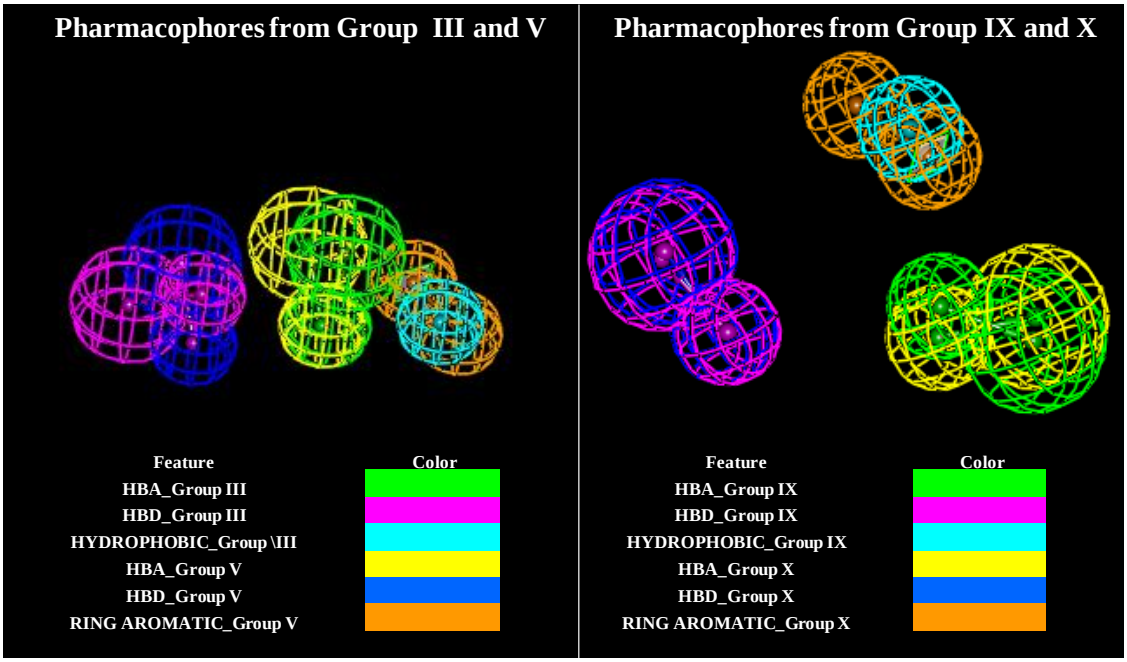

Figure 26. Comparison of UGT1A9 Pharmacophore of Group III with Group V and Group IX with Group X.

Group III and V: Location constraint "HBD (smaller sphere)" mapped to "HBD (smaller sphere)" (displacement = 1.94 Å). Location constraint "HBD (bigger sphere)" mapped to "HBD (bigger sphere)" (displacement = 2.55 Å). Location constraint "HBA (smaller sphere)" mapped to "HBA (smaller sphere)" (displacement = 0.68 Å). Location constraint "HBA (bigger sphere)" mapped to "HBA (bigger sphere)" (displacement = 3.07Å). RMS displacement = 1.81 Å. **Group IX and X:** Location constraint "HBD (smaller sphere)" mapped to "HBD (smaller sphere)" (displacement = 0.22 Å). Location constraint "HBD (bigger sphere)" mapped to "HBD (bigger sphere)" (displacement = 0.26 Å). Location constraint "HBA (smaller sphere)" mapped to "HBA (smaller sphere)" (displacement = 0.94 Å). Location constraint "HBA (bigger sphere)" mapped to "HBA (bigger sphere)" (displacement = 0.72 Å). RMS displacement: 0.61 Å. Hydrophobic feature in pharmacophore of group III and IX were not mapped to ring aromatic feature in pharmacophore of group V and X, respectively.

Table 7 Root-mean-square displacement between each pair of 5 UGT1A9 pharmacophores

Pharmacophore 1	Pharmacophore 2	Root-mean-square (RMS) displacement (Å)
II	III	1.75
II	V	0.13
II	IX	0.56
II	X	0.06
III	V	1.81
III	IX	2.86
III	X	1.77
V	IX	2.79
V	X	3.57
IX	X	0.61

Root-mean square (RMS) displacement provides a comparison between two pharmacophores with regards to distance between key feature centers, with low RMS values indicating better overlapping of features. Figures 23-26 describes the displacement values of individual features for selected pair of pharmacophores. Table 7 showed the RMS displacement values of each pair of pharmacophores compared. When pharmacophore II (with four features) was compared with pharmacophores from other groups (with only three features), we observed that pharmacophores from all group mapped well with group II pharmacophore, except group III (Figures 23 and 24). Group X pharmacophore (0.06 Å) (Figure 24) showed the lowest (RMS) displacement from group II pharmacophore, followed by group V (0.13 Å) (Figure 23) and group IX (0.56 Å) (Figure 24) pharmacophore (Table 7). It is to be noted that the lowest RMS in case of group II compared with group X, was based on overlapping of two features (HBA and HBD) only. However, if three features pharmacophores were compared to each other (Figures 25 and 26, each pair presented high RMS displacement, except group IX and X pharmacophores (0.61 Å) (Table 7).

This suggested that in general, group II pharmacophore with four features (two hydrogen bond acceptors, one hydrogen bond donor and one hydrophobic center) can be considered as the best representative pharmacophore for the selected group of compounds. Also, we observed that most compounds showed good fitting with pharmacophore from group II and one or more other group pharmacophore. In summary, we were able to develop five

distinct semi-quantitative 3-D QSMR pharmacophores, which together can correctly predict the selected compounds as high versus low metabolizing compounds with more than 75% accuracy.

6.4.5. 2-D/3-D QSMR models

Same 10 randomized group training and test sets as in pharmacophore modeling were used to build 2-D and/or 3-D QSMR models using PLS regression. 10 and 15 principle components were used to build UGT1A8 and UGT1A9 PLS models, respectively. Each compound was mapped against the 5 pharmacophores of UGT1A9 and error of estimated Cl_{int} values from the experimental Cl_{int} values was calculated. Similarly, each compound was mapped against the 4 pharmacophores of UGT1A8 which passed the criteria of >60% predictive ability for training set and error was calculated. The confirmation of compound which gave the least error with any of the selected pharmacophores was assumed as the most probable confirmation of compound in the enzyme active site. These confirmations of compound were selected for calculating descriptors. It is to be noted that same compound could show different best confirmation for UGT1A8 and UGT1A9 modeling. Also, for UGT1A9, two confirmations of 3H4'MF was used as both gave almost similar error values with different pharmacophores. To account for the standard deviation in the Cl_{int} values, each compound was entered in the spreadsheet three times with three distinct experimentally derived activity values, such that total

number of compounds for UGT1A9 were 111 (37 x 3) and for UGT1A9 were 96 (32 x 3) or 99 (where 3H4'MF was part of the training set).

PLS models which gave r^2 value of equal to or more than 0.6 and average squared error of less than 50 with the training sets were selected for validation by test sets. We observed than none of the randomized group training sets were able to generate models with $r^2 \geq 0.6$ with 2-D and 3-D descriptors alone. Only when 2-D and 3-D descriptors were used in combination, PLS models with $r^2 \geq 0.6$ were generated. In UGT1A8 randomized groups, three groups III, IV and VII could not generate PLS models with $r^2 \geq 0.6$. Similarly, in UGT1A9 randomized groups three groups V, VII and IX could not generate PLS models with $r^2 \geq 0.6$. However, out of 7 PLS models of UGT1A9 with $r^2 \geq 0.6$, only group IV model gave a reasonable squared error (15.5) and was tested further for validation with test set compounds (Table 8). Similarly, out of 7 PLS models of UGT1A8 with $r^2 \geq 0.6$, only model of 5 groups (I, II, VIII, IX and X) gave lower average squared error values and tested further for validation with respective test set compounds (Table 8).

To further improve the model, we tried to optimize the number of descriptors and principle components in order to improve the correlation and lower the average squared error. We multiplied the minimum and maximum value of descriptors of all compounds with the coefficients of descriptors obtained with various models.

Table 8 Correlation coefficient (r^2) of the linear regression between experimental and estimated Cl_{int} values and average of squared error of the estimated Cl_{int} values of UGT1A8 and UGT1A9

Training sets					
UGT1A8			UGT1A9		
Group	r^2	Average squared error	Group	r^2	Average squared error
I	0.62	0.56	I	0.61	4906.47
II	0.67	0.58	II	0.61	658.85
III	0.54	5.51	III	0.61	3554.98
IV	0.52	1.12	IV	0.72	15.48
V	0.64	395.57	V	0.58	662.49
VI	0.68	1197.55	VI	0.73	98.14
VII	0.5	2.73	VII	0.58	263.77
VIII	0.7	1.68	VIII	0.64	1794.06
IX	0.6	4.51	IX	0.53	4125.94
X	0.72	47.05	X	0.67	256.82
Test sets					
UGT1A8			UGT1A9		
Group	r^2	Average squared error	Group	r^2	Average squared error
I	0.86	48225.63	IV	0.3	335.1
II	0.35	1907820			
VIII	0.33	7.59			
IX	0.03	4195			
X	0.65	1.45			

For UGT1A8, all descriptors (total 60) with product value more than 10^4 were selected from all the randomized groups, whereas for UGT1A9, all descriptors (total 65) with product value more than 10^5 were selected from all the randomized groups. These descriptors were used to rebuild the PLS models. Result showed that there was either no improvement in the r^2 values or the r^2 decreases for most groups in both UGT1A8 and UGT1A9 with the used of lower number of descriptors. So, finally 135 2-D and 3-D descriptors were used to building final models. We also tried to reduce the number of components. But for most groups of UGT1A8 and UGT1A8, selection of less than 10 and 15 principle components to build model resulted in r^2 values of less than 0.6.

When the selected PLS models were tested for prediction of test set, all models failed on one or both of the criteria of $r^2 \geq 0.6$ and average squared error < 50, except UGT1A8 group X PLS model (Table 8). It is to be noted that group VIII model gave very less average squared error but the r^2 of the experimental and estimated values was lower than desired (0.33). But this model had the potential for further improvement by using various combinatorial *in silico* techniques and probably increasing the number of compounds.

The selected models also did not estimate all activity values in training set as positive. Group I model estimated Cl_{int} of one compound (4'H6MF) as negative value. Group II model estimated Cl_{int} of two compounds (3H5MF and 4'H6MF) as negative value. Group VIII and IX estimated negative value Cl_{int} for 7 and 5 compounds, respectively. Group X model also estimated Cl_{int} of two compounds (5,7DM3HF and 4'H6MF) as negative

value. Group I, II, VIII and IX model estimated their respective test set compound Cl_{int} as positive value whereas group X model estimated Cl_{int} of 50% of the test compounds as negative values. This difference could be mainly due to the fact that the constant in the PLS regression equation of these models had a positive sign, whereas the constant in PLS regression equation of group X model had a negative sign (-1.13×10^7). Hence, we deduced that none of the above models could be successfully used for prediction purpose.

6.5. Discussion

We concluded that semi-quantitative pharmacophore-based 3-D SMR prediction models could be developed for UGT1A9 with the predictive ability of more than 75%. This conclusion is supported by the fact that we developed and validated four three-featured and one four-featured pharmacophores for UGT1A9 using 5 randomly divided training and test set (Figure 20-22) with predictive ability of > 60%. All pharmacophores could correctly predict at least 60% training and test compounds as lowly (with $Cl_{int} < 3 \times 10^5$ ml per min per mg of protein) or highly metabolizing (with $Cl_{int} \geq 3 \times 10^5$) compounds, and one three-featured pharmacophore showed >75% predictive ability.

We also showed that all the five pharmacophores could be defined using three or four of the five features (two hydrogen bond acceptors (HBA), one hydrogen bond donor (HBD), one hydrophobic center and one aromatic ring) in different 3-D spatial arrangements (Figure 20-22). The two three-featured pharmacophores had one HBA, one HBD and one hydrophobic center, however the HBA in both pharmacophores were placed at different 3-D space (Figure 21). Similarly, other two three-featured pharmacophores had one HBA, one HBD and one aromatic ring, with HBA in both pharmacophores again placed at different space (Figure 22). The four-featured pharmacophore had two HBA, one HBD and one hydrophobic center (Figure 20). The two HBAs in four-featured pharmacophore overlapped with the two different HBAs in the three-featured pharmacophores (Figures 23-24).

Upon comparison of all the pharmacophores with each other we found that the four-featured pharmacophore showed very low root-mean-square (RMS) displacement values from all the three-featured pharmacophores except group III (Figures 23-24, Table 7). This strongly indicates that the four-feature pharmacophore could be used as representative 3-D arrangements of important chemical features in the structure of flavonoids responsible for the glucuronidation by UGT1A9. This was also supported by the fact that except for the pharmacophores of group IX and X, all the other pairs of pharmacophores on comparison showed very high RMS displacement values (Figures 25-26, Table 7).

This also suggests that using these five pharmacophores, one single four-featured pharmacophore with location constraints ± standard deviation can be generated, which might successfully map and semi-quantitatively predict all the training and test compounds. The location constrain ± standard deviation of this resulting pharmacophore can be derived from the displacement values of individual features of all the three-featured pharmacophores from the four-featured pharmacophore. It is to be noted that since the cut-off value of low versus high metabolizing compounds were arbitrarily set, changing the cut-off value might or might not significantly impact the choice of the best pharmacophore with different location constraints for a randomized group.

We were not able to develop any pharmacophore for UGT1A8 which could successfully predict both training and test set with >60% predictive ability. Most pharmacophores

developed for UGT1A8 were over estimating the Cl_{int} values. Even though, certain pharmacophores could successfully differentiate between the low versus high metabolizing compounds of training set (> 80% predictive ability), no pharmacophore could rightly predict the low metabolizing test set compounds in the right category. The main reason for this failure could be that the chemical space of the compound randomized as test set in these cases were not well represented in the training set.

We also observed that there was no correlation what-so-ever between the pharmacophore estimated versus experimental Cl_{int} values, suggesting that these pharmacophore-based 3-D models could not be used for any kind of quantitative prediction. This suggests that probably the closely related rigid planar structure of flavonoids with not-so diverse Cl_{int} activities might be a limiting factor in generation of quantitative prediction model using pharmacophore modeling. However, these pharmacophores could be successfully used as the starting point for other modeling techniques such as CoMFA (comparative molecular field analysis) to generate QSMR models. We successfully used the pharmacophores in this study to derive the best conformation to give the least deviation from the experimental Cl_{int} values and used that to generate 2-D/3-D QSAR models. This significantly helps to improve the prediction and reducing the average squared error than using all the possible conformation of a compound to build the models.

We observed that PLS models developed using 2-D and 3-D descriptors in combination gave better correlation r^2 between estimated versus experimental Cl_{int} values than the PLS

models developed using either 2-D or 3-D descriptors alone. This suggests that certain 2-D and 3-D descriptors are important to define the quantitative structure-glucuronidation relationship between flavonoids and UGTs. But even using 2-D/3-D descriptors in combination, we could not develop a desired QSMR prediction model ($r^2 > 0.6$ and error < 50). However, better models could be developed for UGT1A8 data than UGT1A9 data in terms of much lower average squared error and has the potentially for further improvement (Table 8).

We tried to improve the model using lower number of descriptors, 60-65 versus 135 descriptors, but it made the models worse with lower r^2 values. This suggested that the technique of choosing more important descriptors based on the values of product of coefficient of descriptors obtained by PLS model and the respective range of descriptor values of selected compounds was not the right one.

We believe that addition of more compounds with varied structure and activity covering the whole chemical space and activity range could help to improve both pharmacophores and 2-D/3-D QSMR models. Ideally activity range should be minimum 3-4 log value apart and should show equal distribution. In contrast, current data set though showed 3-4 log difference in activity values but distribution of activity was not equal, with most Cl_{int} values derived in the range of 10^5-10^4. Also, adding excluded volumes for methoxyl groups in the model might also help to further improve the predictive ability of pharmacophore models.

The experimental data used in this study was the experimentally derived approximate Cl_{int} values, based on assumption that all selected flavonoids follow MM enzyme kinetics for glucuronidation by UGTs. Since it is known from the recent published[87] and unpublished data from our lab that all the compounds do not follow MM enzyme kinetics with all the isoforms, there might be a need to derive the actual K_m and V_{max} to get the more accurate Cl_{int} data for these compounds, though we are not yet sure how much this approach would improve the models.

From the perspective of predicting flavonoid glucuronidation that directly impacts bioavailability, it would be desirable to predict their overall glucuronidation by UGT isoforms irrespective of the position of glucuronidation. Hence, we used the overall Cl_{int} values irrespective of the position of glucuronidation, which were derived from summation of Cl_{int} values for multiple mono-glucuronides of a flavonoid. However, this approach might not be the best one from the modeling perspective. We assume that use of position-specific Cl_{int} values might be more useful in the development of better prediction models, although that remains to be validated.

This study was our first attempt to understand the use of our experimental values to derive predictive models using various techniques. It is clear that semi-quantitative pharmacophore-based 3-D SMR prediction models could be developed for UGT isoforms with good predictability. Our overall efforts indicate that we might require more diverse experimental data, and better interaction between experimentally derived SMR and *in*

silico derived SMR to increase the chances of successfully developing the semi-quantitative and quantitative prediction models for glucuronidation of flavonoids.

CHANGES IN FLAVONOID BACKBONE AFFECT EXCRETION OF FLAVONOID SULFATES MORE THAN THE EXCRETION OF FLAVONOID GLUCURONIDES IN CACO-2 CELL MONOLAYERS

7.1. Abstract

The objective of this study was to determine how changes in flavonoid backbone structure affect the disposition of flavonoids in the Caco-2 cell culture model. Five flavonoids were used, one from each subclass of flavone (apigenin), isoflavone (genistein), flavonol (kaempferol), flavanone (naringenin) or chalcone (phloretin), but all having the same numbers of hydroxyl groups at the same corresponding position. The rates of excretion of glucuronides and sulfates were determined at both apical and basolateral (BL) side during their AP to BL basolateral transport at 10μM. The rates of excretion of glucuronides of all flavonoids in Caco-2 cell monolayer were comparable and rapid except for genistein which excreted slowly, due to the position in phenyl ring at C-3 as opposed to C-2 in other flavonoids ($p<0.05$). However, rates of excretion of sulfates of apigenin were the highest in Caco-2 cell monolayers, followed by kaempferol, naringenin, phloretin and genistein ($p<0.05$), most probably due to difference in their rates of sulfation by SULT 1A3 in Caco-2 cells. The rates of formation of glucuronide(s) of apigenin, genistein and phloretin in Caco-2 cell lysate were significantly higher than their corresponding rates of excretion, indicating that rates of excretion was limited by the efflux transporters. Whereas, rates of formation and excretion of glucuronide(s) of

naringenin and kaempferol did not show significant differences ($p<0.05$), indicating that rates of excretion of these glucuronides were not limited by the efflux transporters. In conclusion, change in backbone structures impact the excretion of flavonoid sulfates more significantly than the excretion of their glucuronides in Caco-2 cells, and excretion of glucuronides were limited either by the formation or efflux transporters depending on their structures.

7.2. Introduction

Flavonoids have shown various health benefits such as antioxidants and prevention against cancer and cardiovascular diseases[1-5]. Structurally, flavonoids are benzo-pyrone derivatives consisting of phenolic and pyrane rings (Figure 1, pg 5) and are classified according to the degree of oxidation or substitution pattern of their central pyran ring. In and among different sub-classes of flavonoid, compounds usually differ in number and position of hydroxy, methoxy and methyl groups. Based on their chemical structures backbone, flavonoids can be categorized into seven major sub-classes found in foods, namely, flavones (2-phenylchromen-4-one backbone); isoflavones (3-phenylchromen-4-one backbone); flavonols (3-hydroxy-2-phenylchromen-4-one backbone); flavanones (2,3-dihydro-2-phenylchromen-4-one backbone); flavanols (2-phenyl-3,4-dihydro-2H-chromen-3-ol backbone); chalcone (Phenyl styryl ketone backbone) and anthocyanidins (flavylium (2-phenylchromenylium) ion backbone)[14, 19, 22] (Figure 1, pg 5).

Despite the above-mentioned beneficial properties, it is challenging to develop them as viable chemopreventive agents due to poor *in vivo* bioavailability (< 5%) of flavonoids.[6-8] The main reason for poor bioavailability of flavonoids have been attributed to extensive *in vivo* phase-II metabolism by uridine-5'-diphospho-glucuronyltransferase enzymes (UGTs) and sulfotransferases (SULTs).[9-11, 69] UGTs and SULTs are fairly well-expressed in intestinal epithelial cells and hepatocytes which are the first-pass organ for metabolism of drugs in oral drug delivery.

Flavonoids from different sub-classes either can occur exclusively in certain plant products or can over-lapping distribution. For example, soy products are abundant in isoflavones such as genistein and diadzein, where as anthocyandinis such are EGCG are found in berries. Isoflavones (genistein) are the structural analogs of flavones (apigenin) with the phenyl side chain at position C-2 than C-3 in flavones and other sub-classes (Figure 1, pg 5). Due to this position of side chain, isoflavones are usually less glucuronidated than other sub-classes.[179] Flavonones (naringenin) are different from flavones by having the double bond at C2-C3 saturated bond, while flavonols (kaempferol) have an additional hydroxy group at C-3 (Figure 1, pg 5). Saturation of double bond at C2-C3 has been shown to be favorable feature for glucuronidation by UGT1A10.[86]

Similarly, Wong *et al.* (2009) showed that increasing the number of hydroxyl groups on A- or B-ring would enhance the glucuronidation activity of flavones, whereas adding a 3-OH on C-ring might not.[95] Hence, we decided to study how change in the backbone in the flavonoid with the similar number and position of hydroxyl group will affect the intestinal disposition of flavonoids.

The Caco-2 cell culture model is an FDA (Food and Drug Administration) recognized model for determining the absorption of drugs. *In silico* prediction models developed using the data of drug transport and permeability in Caco-2 cell, which can successfully predict the fate of drug absorption in human intestine, have been extensively published

and used in pharmaceutical industry.[180-183] But there are only occasional reports published for describing the structure-metabolism relationship (SMR) or predicting the fate of drug metabolism and excretion in human intestine using Caco-2 cell model.[8, 133, 184]

The objective of present study was to systematically determine the effect of changes in backbone on the disposition of flavonoids in the Caco-2 cells. We used five flavonoids, one from each sub-class flavones (apigenin), isoflavones (genistein), flavonols (kaempferol), flavanones (naringenin) and chalcone (phloretin), which were analogous in number and position of hydroxyl groups on their different backbones (Figure 1), to systematically study how the small change in the structural features in the backbone without changing the position and number of hydroxyl groups in the structure will affects the excretion of conjugates in the Caco-2 cells. We did not select the analog compounds from flavanol (epicatechin) and anthocyanidins (pelargonidine chloride) sub-class, as epicatechin was unstable and very poorly glucuronidated and pelargonidine chloride was an ionic compound and did not have a good UV absorbance for method development.

7.3. Materials and Methods

7.3.1. Materials

Cloned Caco-2 cells, TC-7, were a kind gift from Dr. Moniqué Rousset of INSERM U178 (Villejuit, France). Apignenin, genistein, naringenin, phloretin and kaempferol were purchased from Indofine Chemicals (Somerville, NJ). Recombinant human UGT isoforms (commercially known as "Supersomes™") were purchased from BD Biosciences (Woburn, MA). Uridine diphosphoglucuronic acid (UDPGA), β-Glucuronidase, alamethicin, D-saccharic-1,4-lactone monohydrate, magnesium chloride, and Hanks' balanced salt solution (powder form) were purchased from Sigma-Aldrich (St Louis, MO). All other materials (typically analytical grade or better) were used as received.

7.3.2. Solubility and stability of the tested flavonoids

Solubility and stability (with or without 0.1% vitamin C) of the tested flavonoids were established at the experimental conditions as per the method explained in section 3.1 (Chapter 3).

7.3.3. Cell culture

The culture conditions for growing Caco-2 cells have been described previously.[11, 185, 186] The seeding density (100,000 cells/cm^2), growth media (DMEM supplemented with 10%

fetal bovine serum), and quality control criteria were all implemented in the present study as they were described previously.[11, 185, 186] Caco-2 TC-7 cells fed every other day, and the monolayers were ready for experiments from 19-22 days post-seeding.

7.3.4. Transport experiments in the Caco-2 cell culture model

Experiments in triplicate were performed in pH 7.4 Hank's balanced salt solution (or HBSS).[185, 186] The protocol for performing cell culture experiments was from those described previously.[10, 11] Briefly, the cell monolayers (4.2 cm^2) were washed three times with 37°C pH 7.4 HBSS. The transepithelial electrical resistance values were measured, and those with transepithelial electrical resistance values less than 420 ohms x cm^2 were discarded. The monolayers were incubated with the buffer for 1 hour and the incubation medium was then aspirated. Afterwards, the solution containing the compound of interest was loaded on to the AP side and amounts of transepithelial transport were followed as a function of time. Four donor samples (400 µl) and four receiver samples (400 µl) were taken every 30 or 60 min, followed by the addition of 400 µl of donor solution to the donor side or 400 µl of fresh buffer to the receiver side. A 100 µl of acetonitrile: acetic acid (94:6) containing 50 µM of formononetin for apigenin or 50µM testosterone for other compounds was added to each sample as internal standard and preservative. Afterwards, the mixture centrifuged at 13,000 rpm for 15 minutes, and the supernatant was analyzed by UPLC (see below).

7.3.5. Preparation of Caco-2 cell lysate for glucuronidation studies

Cell lysates were prepared using fresh monolayers for measuring rates of glucuronides formation in Caco-2 cells. For preparing cell lysate, each membrane was cut into pieces and added to 400 µl of 100mM of ice cold pH 7.4 potassium phosphate buffer in a centrifuge tube. The tubes were first sonicated using Aquasonic 150D sonicator (VWR Scientific, Bristol, CT) for 30 min at the maximum power (135 average watts) in an ice-cold water bath and then centrifuged at 13000 rpm for 8 minutes. The cell lysate resulting from fresh monolayers was then harvested, pooled. It was used fresh or frozen at -80ºC until use, for measuring the rates of formation of glucuronides.

7.3.6. Preparation of Caco-2 cell lysate for measuring microsomal protein concentrations and the cellular concentrations of flavonols and their conjugates in monolayers

Cell lysates were prepared using monolayers used in the transport experiment. After the last sample, the solution from donor and receiver side was aspirated and 2.5 ml of pH 7.4 HBSS buffer was added on both sides. Cells were incubated at 37°C to wash of any compound and the respective conjugates sticking on to the surface of the cell and the solution was aspirated after 10 minutes. The cell lysate was prepared the same way as explained in section 7.3.5 above. The resulting cell lysate were used to measure the

microsomal protein concentration and the cellular concentration of compounds and its conjugates accumulated inside the cells during the course of transport study.

7.3.7. Measurement of cell lysate protein concentration

Protein concentration of cell lysate prepared for doing glucuronidation studies and cell lysates prepared from the monolayers used in each transport studies was determined using the BCA protein assay, using the bovine serum albumin as the standard.

7.3.8. Glucuronidation activities of cell lysate

The incubation procedures for measuring glucuronidation activities were essentially the same as published before.[51, 52] Briefly, incubation procedures using cell lysate were as follows: (1) cell lysate (final concentration ≈ 0.1 mg of protein per mL), magnesium chloride (0.88 mM), saccharolactone (4.4 mM), alamethicin (0.022 mg/mL), 10 μM concentrations of substrates in a 50 mM potassium phosphate buffer (pH 7.4), and UDPGA (3.5 mM, add last) were mixed; (2) the mixture (final volume = 200 μL) was incubated at 37°C for a predetermined period of time (30 or 60 min); and (3) the reaction was stopped by the addition of 50μL of 94% acetonitrile/6% glacial acetic acid containing 50 μM formononetin for apigenin or testosterone for other compounds as the internal standard.

7.3.9. UPLC analysis of flavonoids and their conjugates

We analyzed five flavonoids and their respective conjugates by using the following common method: system, Waters Acquity UPLC with photodiode array detector and Empower software; column, BEH C_{18}, 1.7 μm, 2.1 × 50 mm; and injection volume, 10μL. Details of mobile phase A, mobile phase B, gradients and flow rate for each compound are given in table 9. Genistein, kaempferol and their respective conjugates were analyzed at 254 nm, whereas naringenin, phloretin and their respective conjugates were analyzed at 286 nm. Apigenin and its conjugates were analyzed at 340 nm. Linearity was established in the range of 0.781-50 μM (total 8 concentrations) for all compounds. The LLOQ for all compounds was 0.39 μM for all compounds. Analytical methods for each compound were validated for inter-day and intra-day variation using 6 samples at three concentrations (20, 5 and 1.56 μM). Precision and accuracy for all compounds were in acceptable range of 85% to 115%.

7.3.10. Quantification of glucuronides and sulfates of flavonoids

The quantification of glucuronides and sulfates was done using the standard curve of the parent compound with a correction factor for difference in extinction coefficient of the compound and its metabolites. The correction factor was measured using the method as explained in section 3.5 and 3.6 (Chapter 3).

Table 9 UPLC conditions for analyzing flavonoids and their respective conjugates.

Compounds	Mobile phase A	Mobile phase B	Gradient Condition
Apigenin	100% aqueous buffer (2.5mM NH_4Ac, pH 4.5)	100% Acetonitrile	Condition 1
Genistein	100% aqueous buffer (2.5mM NH_4Ac, pH 7.4)	100% Acetonitrile	Condition 1
Phloretin	Aqueous buffer (0.06%$C_6H_{15}N$ and 0.045% CH_2O_2, pH 3.0): Acetonitrile (90:10)	Acetonitrile : H_2O (90:10)	Condition 2
Naringenin	Aqueous buffer (0.06%$C_6H_{15}N$ and 0.045% CH_2O_2, pH 3.0): Acetonitrile (90:10)	Acetonitrile : H_2O (90:10)	Condition 2
Kaempferol	0.2% Formic acid	100% Methanol	Condition 3

Condition 1: 0 to 2min, 10-20% B, 2 to 3 min, 20–70%B, 3 to 3.5 min, 70%B, 3.5 to 4.0 min, 70-90% B, 4.0 to 4.5 min, 90-10% B, and 4.5 to 5.0 min, 10% B; flow rate = 0.45 ml/min.

Condition 2: 0 to 0.3 min, 0% B, flow rate = 1ml/min, 0.3 to 1.80, 0-50% B, flow rate = 0.925 ml/min, 1.80 to 2.10, 50-100% B, flow rate = 0.925ml/min, 2.10 to 2.40, 100% B, flow rate = 0.925, 2.40 to 2.50, 100%-0% B, flow rate = 1ml/min.

Condition 3: 0 to 2min, 10-20% B, 2 to 3 min, 20–40%B, 3 to 3.5 min, 40–50%B, 3.5 to 4.0 min, 50-70% B, 4.0 to 5.0 min, 70-90% B, 5.0 to 5.5 min, 90-10% B, and 5.5 to 6.0 min, 10% B, flow rate = 0.45 ml/min.

We have observed that for a particular compound and its glucuronides at various positions, correction factor for each glucuronide was dependent on the extent of shift in the UV spectrum of the glucuronide from the UV spectrum of aglycone at a given wavelength. It was also observed that conjugation of aglycone with glucuronic acid and sulfate at the same position might or might not produce a similar λ_{max} shift. The spectra of glucuronide and sulfate in most cases were almost overlapping (Figure 27). Based on this observation, we assumed that the correction factor for a glucuronide and sulfate conjugated at the same position should be similar within experimental error. Hence, correction factor of glucuronide at a particular position was used for calculation of concentration of sulfate at the same position.

7.3.11. Confirmation of flavonoids conjugates structure by LC-MS/MS

Five flavonoids and their respective glucuronides and sulfates were separated by the same UPLC system but using slightly different chromatographic conditions because of mass spectrometer requirements. Here, mobile phase A was ammonium acetate buffer (pH 7.5) and mobile phase B was 100% acetonitrile with the gradient as follows: 0-2.0 min, 10–35% B, 2.0-3.0 min, 35–70% B, 3.2-3.5 min, 70–10% B, 3.5-3.7 min, 10% B. The flow rate was 0.5 mL/min. The effluent was introduced into an API 3200 Qtrap triple-quadrupole mass spectrometer (Applied Biosystem/MDS SCIEX, Foster City, CA) equipped with a TurboIonSpray^{TM} source.

Table 10 UPLC/MS/MS optimized ion source/compound parameters for precursor ion scan

Parameters	**Flavonoids**				
	Apigenin	**Genistein**	**Naringenin**	**Kaempferol**	**Phloretin**
Ion Mode	Negative	Negative	Negative	Negative	Negative
DP	-55	-55	-40	-85	-40
EP	-5	-2	-7.5	-3	-6.5
CEP	-20	-24	-18	-18	-18

The mass spectrometer was operated in negative ion mode to perform the analysis of five flavonoids and their conjugates. The main working parameters for the mass spectrometers were set as follows: ion source temperature, 600°C; nebulizer gas (gas1), nitrogen, 40 psi; turbo gas (gas2), nitrogen, 40 psi; curtain gas, nitrogen, 20 psi; CE, -30V; CXP, -3V and IS -4.5KV. Minor adjustments in DP, EP and CEP were then made for each flavonoid. The working parameters for the mass spectrometers and compound-specific MS conditions are given in table 10. The mass of each individual peak of separated glucuronides was measured using QSMS mode. In MS2 scan, precursor ion mode was used to confirm the identity of each peak as glucuronide, in which Q3 was held to measure the occurrence of the aglycone fragment ion and Q1 is scanned for the glucuronide(s) ions that result in the corresponding aglycone ion.[158, 159]

The donor and receiver media in Caco-2 transport study at end of the experiments were pooled. These conjugates were extracted by solid phase extraction from these samples and re-constituted in small amount of 30% acetonitrile in water. The concentrated samples were then used to identify the glucuronides and sulfates in UPLC/MS/MS.

7.3.12. Identification of position of glucuronidation and sulfation in the structure of apigenin and kaempferol by UV shift method

The sites of glucuronic acid substitutions in flavones and flavonols were established based on the online UV spectral shift method, optimized and validated in our lab based

on the published literature.[171, 172] Briefly, substitution of a single hydroxyl group by glucuronic acid in the structure of flavones or flavonols at a specific position would result in diagnostic shifts or no shift in λ_{max} of Band I (300-380 nm) and/or Band II (240-280 nm) in the UV spectrum of the resulting glucuronide as compared to the UV spectrum of parent compound. Based on these differentiating diagnostic shifts for each position of glucuronidation, structure of a glucuronide can be estimated. The details of the method and its validation can be found in Singh *et al.* (2010).[173]

We observed that the glucuronidation and sulfation at same position might or might not produce the similar shit in λ_{max}. Therefore, in order to identify the position of sulfation, first the rule of elimination was used, for example C-3 position was not favored for sulfation based on published reports. Second, comparison of sulfate spectrum with the available glucuronide(s) spectra of the same flavonoid helped to estimate the position of sulfation. Hence, the position of sulfation was identified based on which glucuronide spectra the sulfation spectrum matched best. UV peak of apigenin, kaempferol and their corresponding mono-*O*-glucuronides and mono-*O*-sulfate found in Caco-2 cell lysate and transport experiments were compared to study the peak shift and determining the position of glucuronidation and sulfation.

7.3.13. Data analysis

Rate of conjugate excretion of selected flavonoids was determined as the slope of first two detectable points in the linear region of amounts excreted versus time plots.

7.3.14. Statistical analysis

One-way ANOVA or an unpaired Student's t-test (GraphPad Prism®, GraphPad software Inc., CA) with or without Tukey-Kramer multiple comparison (posthoc) tests was used to analyze the statistical significance among various data. The prior level of significance was set at 5%, or $p<0.05$.

7.4. Results

7.4.1. Confirmation of flavonoid conjugate structure by LC-MS/MS

We conducted simple LC-MS/MS studies of the metabolites to show that all glucuronides and sulfates formed during the transport study were mono-*O*-glucuronides and mono-*O*-sulfates (Figures A1-A3, Appendix A). Genistein and naringenin formed only one quantifiable mono-*O*-glucuronide (Figures A1b and A1d, Appendix A), while apigenin formed two quantifiable mono-*O*-glucuronides (Figures A2a-A2b, Appendix A). Phloretin and (Figures A3b-A3c, Appendix A) kaempferol (Figures A4a-A4c, Appendix A) formed three quantifiable mono-*O*-glucuronides each. Due to the closely eluting peaks of the three glucuronides of phloretin, we were only able to clearly identify two of the glucuronides (Figures A3b-A3c, Appendix A). We believe the peak of third mono-*O*-glucuronide had got merged with one of the other two mono-*O*-glucuronides, making it undetectable, as MS could not differentiate between two overlapping mono-*O*-glucuronides. Also, the second mono-*O*-glucuronides of genistein and naringenin were detectable in concentrated samples in UPLC/MS/MS.

We did not find any di-*O*-glucuronide and di-*O*-sulfates of flavonoids in this study. One mono-*O*-sulfate conjugate was detected for each genistein (Figure A1a, Appendix A), apigenin (Figure A2c, Appendix A), naringenin (Figure A1c, Appendix A), phloretin (Figure A3a, Appendix A), and kaempferol (Figure A4d, Appendix A). Sulfate of genistein and second glucuronides of genistein, naringenin were recognized in the

concentrated samples in the UPLC/MS/MS but were below the limit of detection or quantification of UPLC, when experimental samples were analyzed.

7.4.2. Position of conjugates in the structure of apigenin and kaempferol by UV shift method

We determined the position of glucuronidation of apigenin and kaempferol based on the diagnostic shift in λ_{max} of Band I and Band II of UV spectra of glucuronides (Figure 27). Position of sulfation of flavonols was determined by the rule of elimination and comparing the spectra of sulfates with the glucuronides. Table B1 (Appendix B) showed the λ_{max} of Band I and II of flavonols and their conjugates and shift in λ_{max} of Band I and Band II of the conjugates as compared to their corresponding aglycone.

The position of conjugation of first glucuronide, second glucuronide and sulfate of apigenin were 7-*O*-G, 4'-*O*-G, and 7-*O*-S, respectively (Figure 27). Whereas, in case of kaempferol, the position of conjugation of first, second and third glucuronides and sulfate of kaempferol were 7-*O*-G, 4'-*O*-G, 3-*O*-G and 7-*O*-S, respectively (Figure 27).

7.4.3. Determination of correction factor of conjugates of flavonoids

Amounts of conjugates formed were determined using the corrections factors for individual glucuronides of flavonols as described in the method section.

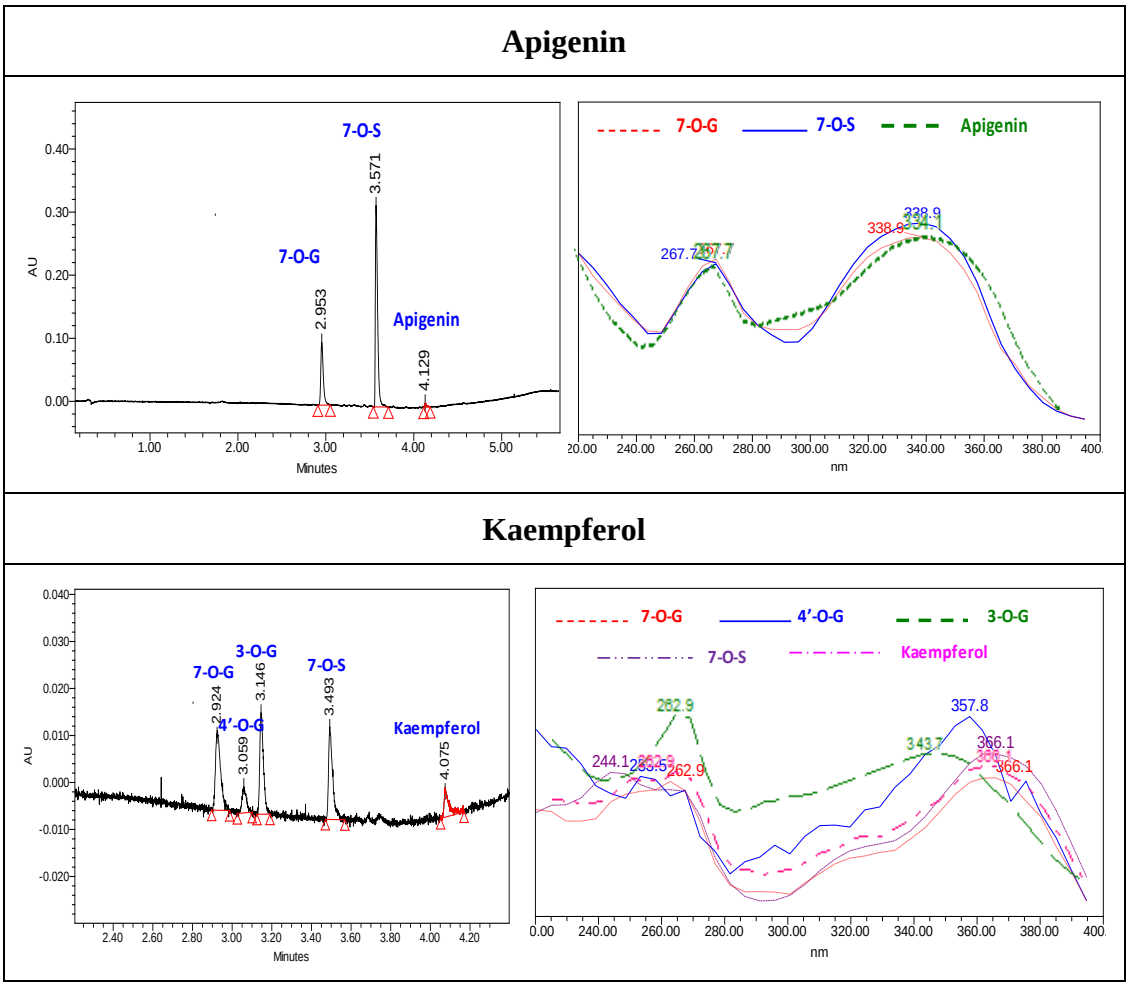

Figure 27. UPLC chromatograms and UV spectra of apigenin, kaempferol and their respective glucuronides and sulfates in Caco-2 cell transport study samples

UGT isoforms and wavelength used in generation of correction factor and the correction factor for each glucuronides are detailed in Table C1 (Appendix C). The correction factors were in the range of 0.87 (for 7-*O*-G of kaempferol) to 1.67 (for Glu2 of phloretin). Correction factors of sulfates of flavonols were not determined experimentally. Based on the comparative UV spectra of sulfate and glucuronide of a flavonol conjugated at the same position, correction factors of sulfates conjugated at a particular position was assumed to be similar to the corresponding glucuronide. Although this assumption was confirmed in the case of genistein (not shown), it may need to be validated with appropriate experiments in the future.

7.4.4. Formation rates of glucuronides of flavonoids in Caco-2 cell lysate

We incubated 10µM of each flavonoid with Caco2 Cell lysate (final protein concentration ~0.1 mg/ml) for 2 hours and measured the concentration of glucuronide(s) generated. Formation rate of each glucuronide was calculated as concentration of glucuronide formed per unit time. The rate of formation of total glucuronides of a flavonoid was calculated as the sum of rates of formation of all glucuronides of that flavonoid. The rates of formation of total glucuronides of flavonoids followed the following rank order: phloretin (22.72 ± 0.77) > apigenin (19.16 ± 0.92) > kaempferol (13.74 ± 0.25) ~ naringenin (12.13 ± 0.27) > genistein (5.47 ± 0.18 nmol/hr/mg of protein) (Figure 28).

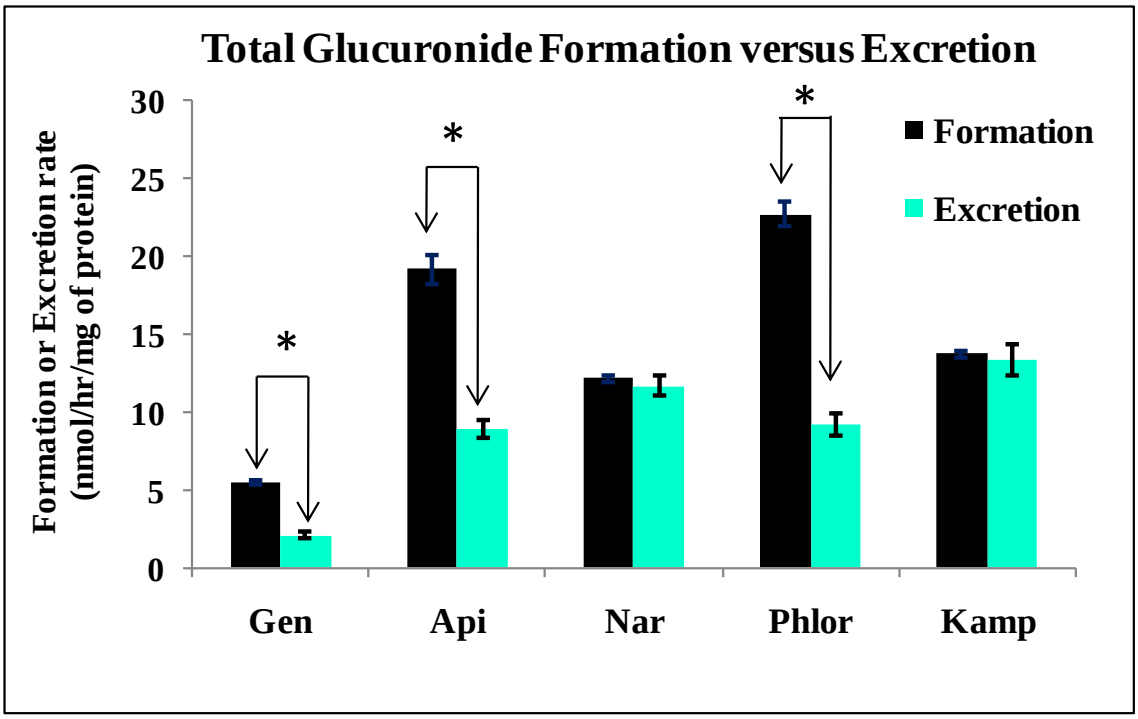

Figure 28. Formation and excretion of glucuronides of five flavonoids in Caco-2 cells.

Formation rates of glucuronides of flavonoids, apigenin (Api), genistein (Gen), naringenin (Nar), phloretin (Phlor) and kaempferol (Kamp) were measured using Caco-2 cell lysate (protein concentration ~0.1 mg/ml) at 10 µM substrate concentration incubated for 2 hrs at 37ºC. Rates of excretion of total glucuronides on AP and BL side during AP (pH =7.4) to BL (pH =7.4) transport of flavonoids (at 10 µM concentration) in the Caco-2 cell monolayer at 37ºC (B) were calculated as the slope of amount of glucuronides excreted vs time profile in Figures F1a-F1b and F2a-F2c (Appendix F), using only the first two data points of each profile, i.e., 0.5 and 1 hr for kaempferol; 1 and 1.5 hrs for apigenin; and 1 and 2 hr for other flavonoids. Rates of excretion for each flavonoid were normalized to the corresponding protein concentration of experimental monolayer of each flavonoid. Each bar is the average of three determinations, and the error bars are the standard deviations of the mean (n=3). * on the top of each bar represents that the excretion rates of total (AP+BL) glucuronides compound was significantly different from the formation rates of their glucuronides ($p<0.05$).

The formation rates of total glucuronides of naringenin and kaempferol were not significantly different from each other ($p < 0.05$ Figure 28). Apart from this, all other flavonoid showed significant difference among their rates of formation of glucuronides ($p<0.05$, Figure 28). Phloretin which is a chalcone with open ring (Figure 1, pg 5) showed the maximum glucuronidation whereas genistein, an isoflavones with phenyl side chain at position C-3 (Figure 1, pg 5) showed the minimum glucuronidation in Caco-2 cells. Addition of a free hydroxyl group at C-3 as in flavonols (kaempferol) or saturation of double bond C2-C3 as in flavonones (naringenin) seemed to similarly reduce the glucuronidation as compared to flavones (apigenin) by UGTs present in Caco-2 cells.

7.4.5. Excretion of total glucuronides of flavonoids in intact Caco-2 cell monolayer

We loaded 10 μM of the five selected flavonoids solution in pH 7.4 HBSS buffer on the apical side of the Caco-2 cell monolayer. During the course of transport of the flavonoids from AP to BL side, glucuronides were excreted to both sides of the cell monolayer, and the amounts of glucuronides of a flavonoid excreted were measured. The amounts of total glucuronides (i.e. sum of amounts of all glucuronides of a flavonoid) excreted increased linearly as a function of time up to 1 hour for kaempferol; 1.5 hours for apigenin and up to 2 hour for genistein, naringenin and phloretin (Figures F1a-F1b, Appendix F).

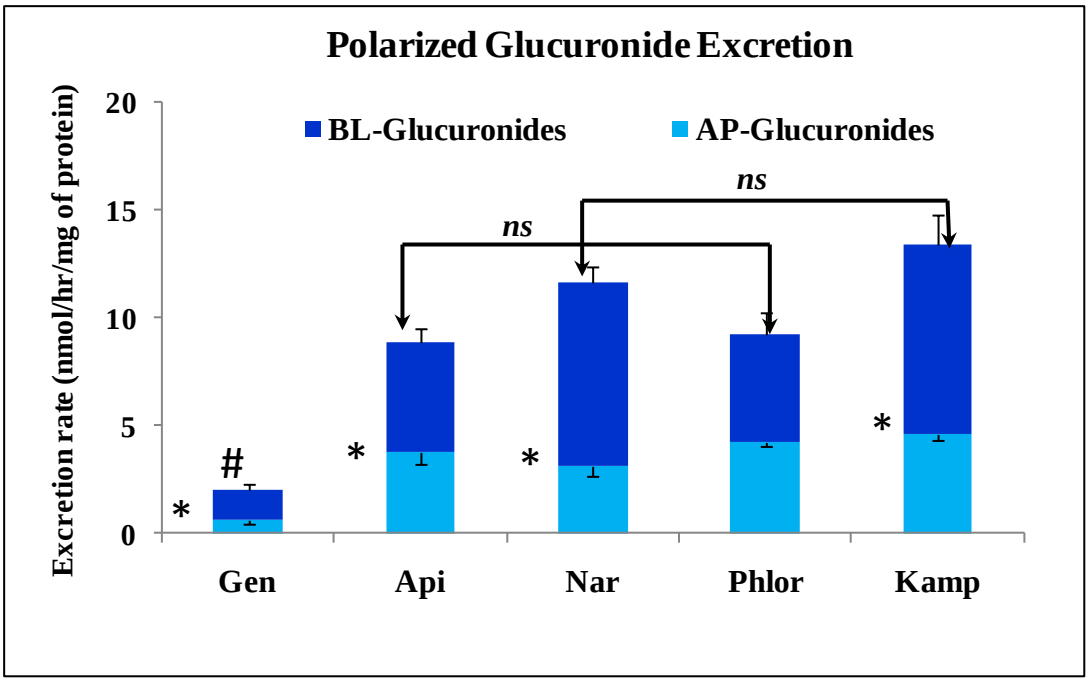

Figure 29. Excretion of total glucuronides in Caco-2 cell monolayer.
Rates of excretion of total glucuronides on AP and BL side during AP (pH =7.4) to BL (pH =7.4) transport of flavonoids (at 10 µM concentration) in the Caco-2 cell monolayer at 37ºC were calculated as the slope of amount of glucuronides excreted vs time profile in Figures F1a-F1b and F2a-F2c (Appendix F), using only the first two data points of each profile, i.e., 0.5 and 1 hr for kaempferol; 1 and 1.5 hrs for apigenin; and 1 and 2 hr for other flavonoids. Each bar is the average of three determinations, and the error bars are the standard deviations of the mean (n=3). * on the side of each bar represents the significant difference between, AP and BL excretion of total glucuronides of each flavonoid ($p<0.05$). # on the top of each bar represents that the excretion rates of total (AP+BL) glucuronides of the compound was significantly different from the excretion rates of total glucuronides of all other compounds, respectively ($p<0.05$). Since most bars showed significant difference to the other bars, ones with no significant difference (not significant, *ns*) were shown on the top ($p<0.05$) to make graphs easily readable.

The rates of excretion of total glucuronides of flavonoids to AP and BL sides were calculated as the slope of amount of glucuronides excreted vs time profile, using only the first two data points of each profile, i.e., 0.5 and 1 for kaempferol; 1 and 1.5 for apigenin; and 1 and 2 hrs for genistein, naringenin and phloretin. We choose only the first two data points, as in most cases, they fell in the linear portion of the curve (Figures F1a-F1b and F2a-F2c, Appendix F). The rates of excretion of all glucuronides of a flavonoid were normalized against the corresponding protein concentration of the Caco-2 cells monolayers used in its transport and rates of excretion were reported as nmol/hr/mg of protein.

The rates of formation of glucuronides of genistein, apigenin and phloretin were significantly different from their corresponding total (AP+BL) rates of excretion of glucuronides ($p<0.05$) (Figure 28). Whereas, there was no significant difference between the rates of formation of glucuronides of naringenin and kaempferol and their corresponding total (AP+BL) rates of excretion of glucuronides ($p<0.05$) (Figure 28).

The rates of excretion of total glucuronides of flavonoids followed the following rank order: kaempferol (13.35 ± 1.06) > naringenin (11.67 ± 0.61) > phloretin (9.20 ± 0.74) > apigenin (8.87 ± 0.55) > genistein (2.03 ± 0.22) nmol/hr/mg of protein (Figure 29), which indicated that across different sub-class of flavonoids, the glucuronides of compound with a free hydroxyl group at C-3 position was excreted fastest, whereas the glucuronides

of compound with a phenyl side chain at C-3 position was excreted slowest in the Caco-2 cell monolayer ($p<0.05$) (Figure 29).

Rates of excretion of glucuronides of most flavonoids were comparable, except for the glucuronides of genistein which excreted about 4-6 times slower than the total glucuronides of other flavonoids ($p <0.05$) (Figure 29). The rates of excretion of total glucuronides of apigenin and phloretin; and naringenin and kaempferol were not significantly different from each other ($p <0.05$) (Figure 29). Apart from these two pairs, the excretion rates of total glucuronides of all flavonoids showed significant difference among each other ($p <0.05$) (Figure 29).

Total glucuronides of all flavonoids showed preferential BL excretion, except for phloretin which showed similar excretion on both sides ($p<0.05$) (Figure 29). Since, BL to AP ratios of excretion for genistein, apigenin, naringenin, phloretin and kaempferol ranged from 2.21, 1.38, 2.68, 1.17 and 1.89, it was concluded that the efflux transporter(s) responsible for excretion of flavonoid glucuronides were expressed more on BL than on AP membrane of Caco-2 cells (Figure 29).

7.4.6. Correlation of formation and excretion rates of glucuronides of flavonoids

We tried to correlate formation rates of total glucuronides of flavonoids to their corresponding total (AP+BL) excretion rates (Figure 28), but we found very poor correlation ($r^2 = 0.22$) (plots not shown here).

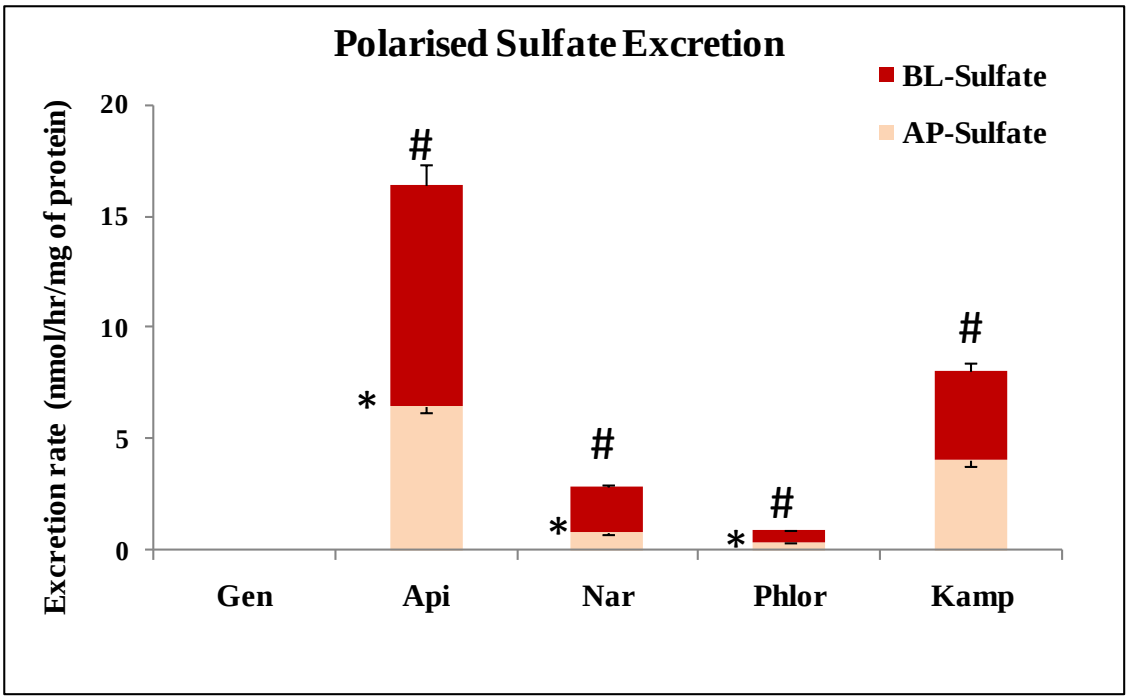

Figure 30. Excretion of sulfates in Caco-2 cell monolayer.
Rates of excretion of sulfates on AP and BL side during AP (pH =7.4) to BL (pH =7.4) transport of flavonoids (at 10 µM concentration) in the Caco-2 cell monolayer at 37ºC were calculated as the slope of amount of sulfate excreted vs time profile in Figures F1c-F1d (Appendix F), using only the first two data points of each profile, i.e., 0.5 and 1 hr for kaempferol; 1 and 1.5 hrs for apigenin; and 1 and 2 hr for other flavonoids. Each bar is the average of three determinations, and the error bars are the standard deviations of the mean (n=3). * on the side of each bar represents the significant difference between, AP and BL excretion of sulfate of each flavonoid ($p<0.05$). # on the top of each bar represents that the excretion rates of total (AP+BL) sulfate of the compound was significantly different from the excretion rates of sulfate of all other compounds, respectively ($p<0.05$). Since most bars showed significant difference to the other bars, ones with no significant difference (not significant, *ns*) were shown on the top ($p<0.05$) to make graphs easily readable.

There was no correlation what-so-ever between the rates of formation and rates of excretion of glucuronides of flavonoids.

7.4.7. Excretion of sulfates of flavonoids in intact Caco-2 cell monolayer

We also measured the amount of sulfates of a flavonoid excreted on both AP and BL sides during AP to BL transport of flavonoid (at 10 μM substrate concentration) in Caco-2 cell monolayer (Figure 30). The amounts of sulfate excreted increased linearly as a function of time up to 1 hour for kaempferol; 1.5 hours for apigenin and up to 2 hour for genistein, naringenin and phloretin (Figures F1c-F1d, Appendix F).

The rates of excretion of flavonoids sulfate to AP and BL sides were calculated as the slope of amount of sulfate excreted vs time profile, using only the first two data points of each profile, i.e., 0.5 and 1 for kaempferol; 1 and 1.5 for apigenin; and 1 and 2 hrs for genistein, naringenin and phloretin (Figures F1c-F1d, Appendix F). We chose only the first two data points due to same reasoning as explained in section 6.4.5 for glucuronides. The rates of excretion of sulfate of a flavonoid were normalized against the corresponding protein concentration of the Caco-2 cells monolayers used in its transport and rates of excretion were reported as nmol/hr/mg of protein.

The rates of excretion of sulfates of flavonoids followed the following rank order: apigenin (16.43 ± 0.45) > kaempferol (8.03 ± 0.25) > naringenin (2.87 ± 0.12) > phloretin (0.87 ± 0.04) nmol/hr/mg of protein. Genistein did not form quantifiable amount of

sulfate during the Caco-2 transport study. The excretion rates of sulfates of all flavonoids were significantly different from each other ($p < 0.05$) (Figure 30).

Addition of a free hydroxyl group at C-3 position (kaempferol) in the structure of flavone (apigenin) (Figure 1, pg 5) reduced the rates of sulfate excretion about two-folds ($p<0.05$) (Figure 30). On the other hand, saturation of the double bond between C-2 and C-3 (naringenin) in the structure of flavone (Figure 1, pg 5), reduced the rates of sulfate excretion about five-folds ($p<0.05$). Also, genistein with a phenyl side chain at C-3 position and phloretin with an open ring structure (Figure 1, pg 5) showed the very poor excretion of sulfate in the Caco-2 cell monolayer ($p<0.05$) (Figure 30).

This indicated that across different sub-class of flavonoids, in contrast to glucuronidation, the sulfation of compound was significantly affected by the change in back-bone. However, whether this is due to the difference in the rate of formation or the rates of excretion of sulfates of flavonoids needs to be investigated. Sulfates of all flavonoids showed preferential BL excretion at 10µM substrate concentration, except for kaempferol which showed similar excretion on both sides ($p<0.05$) (Figure 30).

7.4.8. Excretion of total conjugates of flavonoids in intact Caco-2 cell monolayer

All flavonoids showed higher total glucuronides than sulfate excretion, except apigenin ($p<0.05$) (Figure 31).

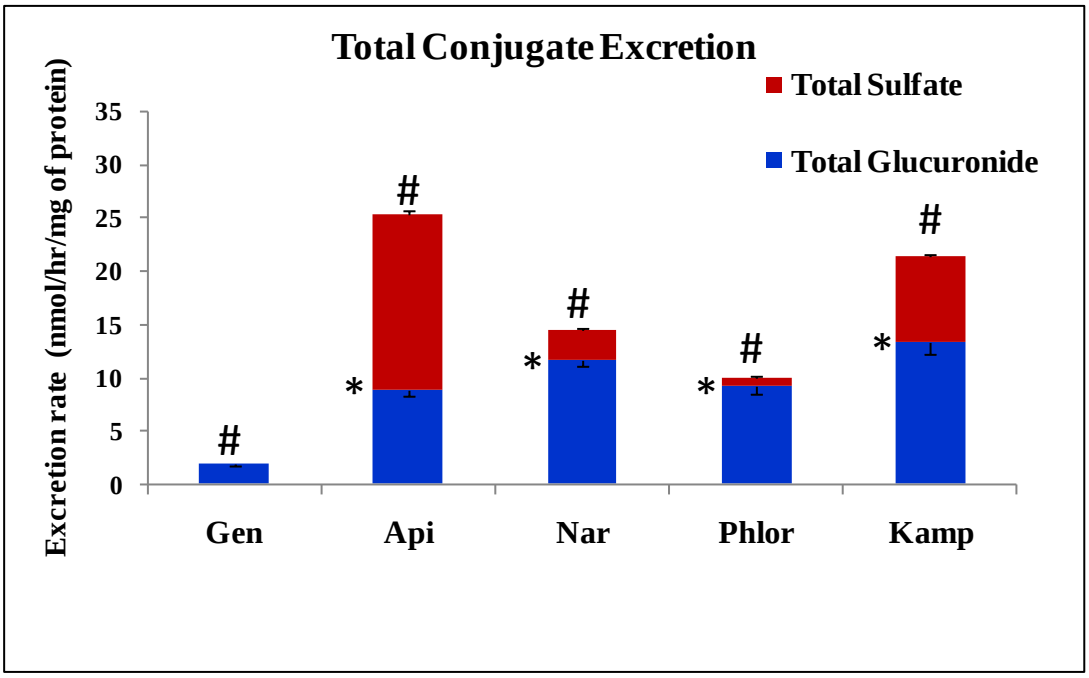

Figure 31. Excretion of total conjugates of flavonoids in Caco-2 cell monolayer. Rates of excretion of total (AP+BL) glucuronides and total (AP+BL) sulfates during AP (pH =7.4) to BL (pH =7.4) transport of flavonoids (at 10 µM concentration) in the Caco-2 cell monolayer at 37ºC were calculated as the slope of amount of total glucuronide and sulfate excreted vs time profile in Figures F1a-F1d (Appendix F) respectively, using only the first two data points of each profile, i.e., 0.5 and 1 hr for kaempferol; 1 and 1.5 hrs for apigenin; and 1 and 2 hr for other flavonoids. Each bar is the average of three determinations, and the error bars are the standard deviations of the mean (n=3). * on the side of each bar represents the significant difference between the excretion of glucuronides and sulfate of each flavonoid ($p<0.05$). # on the top of each bar represents that the excretion rates of total (glucuronide + sulfate) conjugate of the compound was significantly different from the excretion rates of total (glucuronide + sulfate) conjugate of all other compounds, respectively ($p<0.05$).

In the disposition of apigenin and kaempferol in Caco-2 cells, sulfation was equally important as glucuronidation, whereas sulfation played comparatively minor role in the disposition of naringenin, phloretin and genistein in Caco-2 cells. The ratio of glucuronidation to sulfation ranged from 10.62 (for phloretin) to 0.54 (for apigenin).

The rank order of rates of total conjugates excretion was apigenin (25.30 ± 0.50) > kaempferol (21.38 ± 0.77) > naringenin (14.53 ± 0.44) > phloretin (10.07 ± 0.52) > genistein (2.03 ± 0.22) nmol/mg/mg of protein. All flavonoids showed significant difference among their total (glucuronides plus sulfates) conjugates excretion rates ($p<0.05$) (Figure 31). This suggested that difference in sulfation rather than glucuronidation might be responsible for the difference in overall metabolism and in turn bioavailability of compounds from different sub-classes.

7.5. Discussion

We concluded that the excretion of flavonoids glucuronides in Caco-2 cells was usually independent of changes in back-bone among flavonoid sub-classes except for isoflavones, whereas the excretion of flavonoids sulfates changed drastically with the change in flavonoid back-bone. This is supported by the fact that the rates of excretion of flavonoids glucuronides in Caco-2 cell monolayer were comparable (ranging from 8.87 ± 0.55 to 13.35 ± 1.06 nmol/hr/mg of protein) (Figure 29) for the compounds from four sub-classes (except isoflavone). On the other hand, there were about ~20 fold difference in rates of excretion rates with respect to their sulfates (ranging from 0.87 ± 0.04 to 16.35 ± 0.45 nmol/hr/mg of protein) (Figure 30).

The isoflavones sub-class differs from other four sub-classes in that the position of phenyl side (ring) chain is at C-3 position instead of at C-2 position (Figure 1, pg 5). This strongly suggests that the position of phenyl side chain at C-2 favors the glucuronidation of flavonoids versus position of phenyl side chain at C-3. This is also supported by the published report of Murota *et al.* (2002) which compared the cellular metabolism of isoflavones (genistein), flavones (luteolin, apigenin) and flavonols (quercetin, kaempferol) during apical to basolateral transport in Caco-2 cells and showed that only genistein aglycone was transported intact to the basolateral solution.[179] Whereas, the comparison of flavones and flavonol with same number and position of hydroxyl groups

in their chemical structure, i.e. kaempferol and apigenin, and quercetin and luteolin, showed that there were no significant difference in the metabolism and transport of aglycones from those two different sub-classes.[179]

The rates of formation and excretion of glucuronides in Caco-2 cells were poorly correlated ($r^2 \sim 0.2$). The rates of formation of glucuronides of genistein, apigenin, and phloretin were significantly higher than their corresponding rate of excretion in Caco-2 cells, whereas naringenin and kaempferol showed similar rates of formation and excretion of glucuronides ($p < 0.05$) (Figure 28). This indicated that for certain sub-classes of flavonoids (flavonone and flavonol), the rates of excretion of glucuronides might be rate-limited by their formation rates, whereas for other sub-classes (flavones, isoflavones and chalcone), the rates of excretion of glucuronides might be rate-limited by the excretion of glucuronides by efflux transporters.

The difference in rates of sulfate excretion could be supported by the published literature on the Caco-2 expression of SULT isoforms and the rate of sulfation of various flavonoids.[129, 187, 188] According to published reports, expression levels of SULT 1A3 in Caco-2/TC-7 cells was highest, followed by 2A1 (430). SULT1A1, 1A2 and 1E1 had poor but similar expression levels.[129] Also, Harris *et al.* (2004) showed that at substrate concentration of 10μM, rates of sulfation of genistein, apigenin, naringenin and kaempferol by platelet cytosolic SULT (SULT1A1:SULT1A3, 1:2) were 2.8 ± 0.16, 52.4

± 0.02, 28.8 ± 0.65 and 30.9 ± 0.25 pmol/min/mg protein, respectively. Phloretin sulfation rates were not published in that study.[187]

The rank order of reported rates of sulfation completely matched with the rank order of sulfate excretion shown in our study. Though the rates of sulfation of kaempferol and naringenin were similar,[187] we observed about 3-folds difference in the rates of sulfate excretion (kaempferol > naringenin) (Figure 30), which might be due to the fact that flavonol sulfate was a better substrate of efflux transporters than flavanones sulfate.

The fact that isoflavones are less conjugated as compared to other flavonoids (Figure 31) leads to suggestion that their aglycone forms might be more bioavailable as compared to other flavonoids. This could also be supported by the published reports on the bioavailability of aglycones from different sub-classes of flavonoids. The bioavailability of genistein aglycone was reported low after a single dose of 50 mg of genistein, 3.7 ± 1.1% in the first 2 h and 1.6 ± 0.1% once steady state had been established.[40] Gugler *et al.* (1975) showed that no unchanged quercetin (a flavonol) was found when 4 gm and 100 mg doses were administered oral and intravenously respectively in human.[189] The bioavailability of chrysin (a flavone) aglycone in human was reported as 0.003–0.02% at an oral dose of 400 mg.[190] However, reported bioavailability of flavanones aglycones, naringenin (~3%) and hesperetin (~5%) in human subjects[191] were similar to genistein.

All flavonoids glucuronides except phloretin was preferably excreted on basolateral side (Figure 29), which is also supported by the published literature on the preferable basolateral excretion of glucuronides of genistein,[90] apigenin,[10] and kaempferol[192]. Apigenin[10] and kaempferol[192] sulfates have been reported to prefer apical excretion. However, in our study we found that sulfates of apigenin and other flavonoids were excreted preferably on basolateral side and kaempferol did not show any apical or basolateral preference (Figure 30). We think that this discrepancy in the polarized excretion of apigenin and kaempferol sulfate is most probably due to the lower substrate concentration used in our study, which did not produce enough sulfates to saturate the high affinity transporters of sulfates on basolateral side.

In conclusion, the excretion of flavonoids glucuronides in Caco-2 cells is limited by efflux transporters or UGT activities, depending on their structures. Change in flavonoid backbone structures affects the excretion of their sulfates more than the excretion of their glucuronides, which were usually much less sensitive although isoflavone glucuronide excretion was drastically reduced.

EXCRETION OF FLAVONOL GLUCURONIDES IN CACO-2 CELLS IS MAINLY DRIVEN BY THE FORMATION RATES RATHER THAN LIMITED BY THE EFFLUX TRANSPORTERS

8.1. Abstract

The objective of this study was to determine the disposition of flavonols in Caco-2 cell culture model via glucuronidation, using six congeneric flavonols with different numbers and positions of hydroxyl groups. The excretion rates of glucuronides were measured at both apical and basolateral (BL) sides using selected flavonols at 10µM concentration. We showed that the rates of formation of regiospecific glucuronides of the selected flavonols in Caco-2 cell lysate correlated very well (slope = 0.89, r^2 ~ 0.9) with the corresponding rates of total (AP+BL) excretion of these glucuronides in the intact Caco-2 cell monolayer. Hence, the formation rates of glucuronides in Caco-2 cell lysate could reasonably be used for predicting the major position(s) of glucuronidation and rates of regiospecific glucuronidation of a new flavonol. The total glucuronides as well as most regiospecific glucuronides for all the selected flavonols were excreted more to the BL side than to the apical side, with 3-O-G showing more BL preference than glucuronide(s) at other -OH position of same compound. In conclusion, the excretion of flavonol glucuronides in Caco-2 cells is generally driven by formation rates, and not rate-limited by efflux transporters, which can be mainly attributed to the favorable basolateral efflux of flavonol glucuronides, especially 3-O-G.

8.2. Introduction

Flavonoids are polyphenolic compounds occurring naturally in plant products such as fruits, vegetables and soybeans. They have been shown to posses various health promoting benefits such as anti-aging, cancer chemoprevention and protection against cardiovascular diseases. Flavonoids are benzo-pyrone derivatives consisting of phenolic and pyrane rings (Figure 1, pg 5), and are classified according to the degree of oxidation or substitution pattern of their central pyran ring. In and among different sub-classes of flavonoids, compounds usually differ in number and position of hydroxy, methoxy and methyl groups. Over 4000 natural flavonoid compounds have been purified and structurally identified.[161]

Based on their backbone structures, flavonoids can be categorized into seven major sub-classes found in foods, namely, flavones, isoflavones, flavonols, flavanones, flavanols, chalcone and anthocyanidins (Figure 1, pg 5).[14, 19, 22] Flavonols constitutes the major percentage of the estimated dietary intake of flavonoids in United States population.[193] Good sources of flavonols in the diet are onion, kale, broccoli, lettuce, tomato, apple, grape, berries, tea, and red wine. The major dietary flavonols are fistein, quercetin, kaempferol, myricetin and isorhamnetin.[194] Figure 1 (pg 5) shows the basic structure of flavonol sub-class where a hydroxyl (~OH) group is present at C-3 position on the flavonoid scaffold.[14, 19, 22]

Despite the above-mentioned beneficial properties, it is challenging to develop flavonoids as viable chemopreventive agents due to their poor bioavailability *in vivo* (< 5%).[6-8] The main reason for the poor biaovailabilities of has been attributed to extensive *in vivo* metabolism by uridine-5'-diphospho-glucuronyltransferase enzymes (UGTs) and sulfotransferases (SULTs).[10, 11, 69] UGTs are fairly well-expressed in intestinal epithelial cells and hepatocytes which are the first-pass organs for metabolism by the oral drug delivery. Hence, it is important to study the disposition of flavonoids that might help to identify the candidates with low potential for UGT metabolism in intestinal cells, which could benefit their development of flavonoids into chemopreventive agents.

Research published from various laboratories including ours has shown that metabolism and disposition of various flavonoids in the intestine is affected by the structure of the compounds. Chen *et al.* (2005) showed that the total uptake of isoflavones and polarized as well as total excretion of their metabolites were dependent on structure of isoflavones. They also showed that the glucuronidation was favored for isoflavones with hydroxyl group at position C-7.[90] Wang *et al.* (2006) also supported this observation, and showed that prunetin, an isoflavone with a methoxy group at C-7, had the slowest metabolism and disposition in rat intestinal perfusion model as compared to other analogs with 7-OH group.[13]

Wen and Walle (2006) using Caco-2 cell culture model showed that the unmethylated polyphenols such as apigenin and chrysin showed 5-8 times lower absorption than

corresponding methylated phenols. The study suggested that the structure determine the metabolic stability and hence the intestinal absorption of flavones.[162] But the compounds used in that study were either unmethylated or fully methylated, so it did not provide any information about if the methylation of one hydroxyl group position was more useful in increasing the metabolic stability than others.

The Caco-2 cell culture model is an FDA (Food and Drug Administration) recognized model for determining the absorption of drugs. *In silico* prediction models (developed using the data of drug transport and permeability in Caco-2 cell) that can successfully predict the fate of drug absorption in human intestine, have been extensively published and used in pharmaceutical industry.[180-183] But there are only occasional reports published for describing the structure-metabolism relationship (SMR) or predicting the fate of drug metabolism and excretion in human intestine using Caco-2 cell model.[8, 133, 184]

The objective of present study was to systematically determine the effect of structural changes on the disposition of flavonols in the Caco-2 cells via glucuronidation. Another objective of the study was to determine if there exists a correlation between the formation and excretion rates of flavonoids glucuronides in Caco-2 cells. We also planned to investigate any correlation that might exist and may be used to predict the metabolic outcome of drugs in Caco-2 cells, which might further be used to predict the disposition of drugs in human intestine.

We studied the effect of structural changes on the excretion of conjugates of selected compounds during apical to basolateral transport of compounds in Caco-2 cell monolayers. We used six congeneric compounds of flavonol subclass, 3-hydroxyflavone (3HF), 3,4'-dihydroxyflavone (3,4'DHF), 3,7-dihydroxyflavone (3,7DHF), 3,7,4'-trihydroxyflavone (3,7,4'THF), 3,5,7-trihydroxyflavone (3,5,7THF) and 3,5,7,4'-tetrahydroxyflavone (3,5,7,4'QHF) (Figure 4, pg 65), to systematically study how the addition of one or more –OH group at different positions in the structure affects the region-specific conjugation of flavonols, rates of metabolism of flavonols and excretion of their conjugates in the Caco-2 cells.

8.3. Materials and Methods

8.3.1. Materials

Cloned Caco-2 cells, TC-7, were a kind gift from Dr. Moniqué Rousset of INSERM U178 (Villejuit, France). 3HF, 3,4'DHF, 3,7DHF, 3,7,4'THF (or resokaempferol), 3,5,7THF (or galangin), and 3,5,7,4'QHF (or kaempferol) were purchased from Indofine Chemicals (Somerville, NJ). Recombinant human UGT isoforms (commercially known as "supersomes") were purchased from Biosciences (Woburn, MA). Uridine diphosphoglucuronic acid (UDPGA), β-Glucuronidase, alamethicin, D-saccharic-1,4-lactone monohydrate, magnesium chloride, and Hanks' balanced salt solution (powder form) were purchased from Sigma-Aldrich (St Louis, MO). All other materials (typically analytical grade or better) were used as received.

8.3.2. Solubility and stability of the tested flavonoids

Solubility and stability (with or without 0.1% vitamin C) of the tested flavonoids were established at the experimental conditions as per the method explained in section 3.1 (Chapter 3).

8.3.3. Transport experiments in the Caco-2 cell culture model

The culture conditions for growing Caco-2 cells and transport experiment protocols were same as described in sections 7.3.3 and 7.3.4, respectively (Chapter 7). A 100 µl of

acetonitrile: acetic acid (94:6) containing 50 μM of testosterone (for 3,4'DHF, 3,7,4'THF, and 3,5,7,4'QHF) or formononetin (for 3HF and 3,5,7THF) or 5HF (for 3,7DHF) was added to each sample as internal standard and preservative.

8.3.4. Preparation of Caco-2 cell lysate for glucuronidation studies and measuring microsomal protein concentrations and the cellular concentrations of flavonols and their conjugates in monolayers

Cell lysates preparations were same as described in sections 7.3.5 and 7.3.6, respectively (Chapter 7).

8.3.5. Measurement of protein concentration and glucuronidation activities of cell lysate

Protein concentrations and glucuronidation activities of cell lysates were measured as per the method described in sections 7.3.7 and 7.3.8, respectively (Chapter 7). The glucuronidation reaction was stopped by the addition of 50μL of 94% acetonitrile/6% glacial acetic acid containing 50 μM testosterone (for 3,4'DHF, 3,7,4'THF, and 3,5,7,4'QHF) or formononetin (for 3HF and 3,5,7THF) or 5HF (for 3,7DHF) as the internal standard.

Table 11 UPLC condition for analyzing flavonols and their respective conjugates.

Compounds	Mobile phase A	Mobile phase B	Gradient Condition
3HF	100% aqueous buffer (2.5mM NH_4Ac, pH 7.4)	100% Methanol	Condition 1
3,4'DHF	100% aqueous buffer (2.5mM NH_4Ac, pH 4.5)	100% Acetonitrile	Condition 2
3,7DHF	100% aqueous buffer (2.5mM NH_4Ac, pH 3)	100% Acetonitrile	Condition 2
3,7,4'THF	100% aqueous buffer (2.5mM NH_4Ac, pH 4.5)	100% Acetonitrile	Condition 2
3,5,7THF	100% aqueous buffer (2.5mM NH_4Ac, pH 4.5)	100% Acetonitrile	Condition 2
3,5,7,4'QHF	0.2% Formic acid	100% Acetonitrile	Condition 1

Condition 1: 0 to 2min, 10-20% B, 2 to 3 min, 20–40%B, 3 to 3.5 min, 40–50%B, 3.5 to 4.0 min, 50-70% B, 4.0 to 5.0 min, 70-90% B, 5.0 to 5.5 min, 90-10% B, and 5.5 to 6.0 min, 10% B.

Condition 2: 0 to 2min, 10-20% B, 2 to 3 min, 20–70%B, 3 to 3.5 min, 70%B, 3.5 to 4.0 min, 70-90% B, 4.0 to 4.5 min, 90-10% B, and 4.5 to 5.0 min, 10% B.

8.3.6. UPLC analysis of flavonols and their conjugates

We analyzed six flavonols and their respective conjugates by using the following common method: system, Waters Acquity UPLC with photodiode array detector and Empower software; column, BEH C_{18}, 1.7 μm, 2.1 × 50 mm; flow rate 0.45 mL/min and injection volume, 10μL. Details of mobile phase A, mobile phase B and gradients for each compound are given in table 11. 3,4'DHF, 3,7DHF, 3,7,4'THF and their respective conjugates were analyzed at 340 nm. 3,5,7THF and its conjugates were analyzed at 263 nm, whereas 3HF, 3HF-glucuronide, 3,5,7,4'QHF, 3,5,7,4'QHF-conjugates and internal standards was analyzed at 254 nm. Linearity was established in the range of 0.3-20 μM (a total of 7 concentrations) for 3,7DHF and 3,5,7THF and 0.16-20 μM (a total of 8 concentrations) for other compounds. The LLOQ for all compounds was 0.3 μM for 3,7DHF and 3,5,7THF, and 0.16 μM for other compounds. Analytical methods for each compound were validated for inter-day and intra-day variation using 6 samples at three concentrations (20, 5 and 1.56 μM). Precision and accuracy for all compounds were in acceptable range of 85% to 115%.

8.3.7. Quantification of glucuronides and sulfates of flavonols

The quantification of glucuronides and sulfates was done using the standard curve of the parent compound with a correction factor for difference in extinction coefficient of the compound and its metabolites. The correction factor was measured using the method as

explained in section 3.5 and 3.6 (Chapter 3). We have observed that for a particular compound and its glucuronides at various positions, correction factor for each glucuronide was dependent on the extent of shift in the UV spectrum of the glucuronide from the UV spectrum of aglycone at a given wavelength.

It was also observed that conjugation of aglycone with glucuronic acid and sulfate at the same position produced λ_{max} shift and overlapping spectra of glucuronide and sulfate in flavonols (Figure 32). Based on this observation, we assumed that the correction factor for a glucuronide and sulfate conjugated at the same position should be similar within experimental error. Hence, correction factor of glucuronide at a particular position was used for the calculation of concentration of sulfate at the same position.

8.3.8. Confirmation of flavonols conjugates structure by LC-MS/MS

Six flavonols and their respective glucuronides and sulfates were separated by the same UPLC system but using slightly different chromatographic conditions because of mass spectrometer requirements. Here, mobile phase A was ammonium acetate buffer (pH 7.5) and mobile phase B was 100% acetonitrile with the gradient as follows: 0-2.0 min, 10–35% B, 2.0-3.0 min, 35–70% B, 3.2-3.5 min, 70–10% B, 3.5-3.7 min, 10% B. The flow rate was 0.5 mL/min. The effluent was introduced into an API 3200 Qtrap triple-quadrupole mass spectrometer (Applied Biosystem/MDS SCIEX, Foster City, CA) equipped with a TurboIonSpray^{TM} source.

The mass spectrometer was operated in negative ion mode to perform the analysis of six flavonols and their conjugates. The main working parameters for the mass spectrometers were set as follows: ion source temperature, 600°C; nebulizer gas (gas1), nitrogen, 40 psi; turbo gas (gas2), nitrogen, 40 psi; curtain gas, nitrogen, 20 psi; 20 psi; DP, -50 V; EP, -10V; CE, -30V; CXP, -3V and IS -4.5KV. Minor adjustments were then made for each flavonol. Flavonols mono-*O*-glucuronides and mono-*O*-sulfates were identified by MS and MS2 full scan modes.

The donor and receiver media in Caco-2 transport study at end of the experiments were pooled. These conjugates were extracted by solid phase extraction from these samples and re-constituted in small amount of 30% acetonitrile in water. The concentrated samples were then used to identify the glucuronides and sulfates in UPLC/MS/MS.

8.3.9. Identification of position of glucuronidation and sulfation in the structure of flavonols by UV shift method

The identification of position of conjugation of flavonol glucuronides and sulfates was done similar to method described in section 7.3.12. The details of the method and its validation can be found in Singh *et al.* (2010).[173]

8.3.10. Data analysis and statistical analysis

Data and statistical analysis was done the same way as described in sections 7.3.13 and 7.3.14, respectively (Chapter 7). Linear regression plots for correlation with 95% confidence interval bands were generated using Statistica 6 (StatSoft, Inc., OK).

8.4. Results

8.4.1. Confirmation of flavonols conjugates structure by LC-MS/MS

We conducted simple LC-MS/MS studies of the metabolites to show that all glucuronides and sulfates of the selected flavonols formed during the transport study were mono-*O*-glucuronides and mono-*O*-sulfates (Figures A4-A8, Appendix A). We did not find any di-glucuronide and di-sulfates of flavonols in the present study. One mono-*O*-glucuronide of 3HF (Figure A5, Appendix A), two mono-*O*-glucuronides of each 3,4'DHF (Figure A6, Appendix A) and 3,7DHF (Figure A4, Appendix A), and three mono-*O*-glucuronides of each 3,7,4'THF (Figure A7, Appendix A), 3,5,7THF (Figure A8, Appendix A) and 3,5,7,4'QHF (Figure A4, Appendix A) were detected in the Caco-2 transport study samples. Also, mono-*O*-glucuronides of each flavonol formed during glucuronidation reaction in cell lysate were same as found in the transport study. The similar results for 3,7,4'THF and 3,5,7,4'QHF has been reported by Barrington *et al.* (2009), however they reported a sulfo-glucuronide of kaempferol (3,5,7,4'QHF) also which we did not find in our study.[192]

One mono-*O*-sulfate was detected for both 3,7DHF (Figure A5, Appendix A) and 3,5,7,4'QHF (Figure A4, Appendix A). Two mono-*O*-sulfates were detected for 3,4'DHF (Figure A6, Appendix A), 3,7,4'THF (Figure A7, Appendix A), 3,5,7THF (Figure A8, Appendix A), while no sulfate was detected for 3HF (Figure A5, Appendix A). One of the mono-*O*-sulfate of 3,4'DHF, 3,7,4'THF, 3,5,7THF were recognized in the

concentrated samples (10X) in the UPLC/MS/MS only but they were either below the limit of detection or quantification of UPLC or quantifiable only in the experimental samples taken at the last time point of the studies. Hence, they were not quantified and reported here.

8.4.2. Position of conjugates in the structure of flavonols by UV shift method

We determined the position of glucuronidation based on the diagnostic shift in λ_{max} of Band I and Band II of UV spectra of glucuronides (Figure 32). Position of sulfation of flavonols was determined by the rule of elimination and comparing the spectra of sulfates with the glucuronides. Table B2 (Appendix B) showed the λ_{max} of Band I and II of flavonols and their conjugates and shift in λ_{max} of Band I and Band II of the conjugates as compared to their corresponding aglycone.

For 3,4'DHF, the first glucuronide was 4'-*O*-G while the second glucuronide was 3-*O*-G. Sulfation in 3,4'DHF happened at position 4, whereas for 3,7 DHF, the first glucuronide was 3-*O*-G, while the second glucuronide and sulfate was conjugated at position C-7 (Figure 32). In case of 3,5,7THF, the position of conjugation of first, second and third glucuronides and sulfate were 3-*O*-G, 7-*O*-G, 5-*O*-G and 7-*O*-S, respectively, whereas, in case of 3,7,4'THF, the position of conjugation of first, second and third glucuronides and sulfate of 3,7,4'THF were 7-*O*-G, 4'-*O*-G, 3-*O*-G and 7-*O*-S, respectively (Figure 32).

3-Hydroxyflavone (3HF)

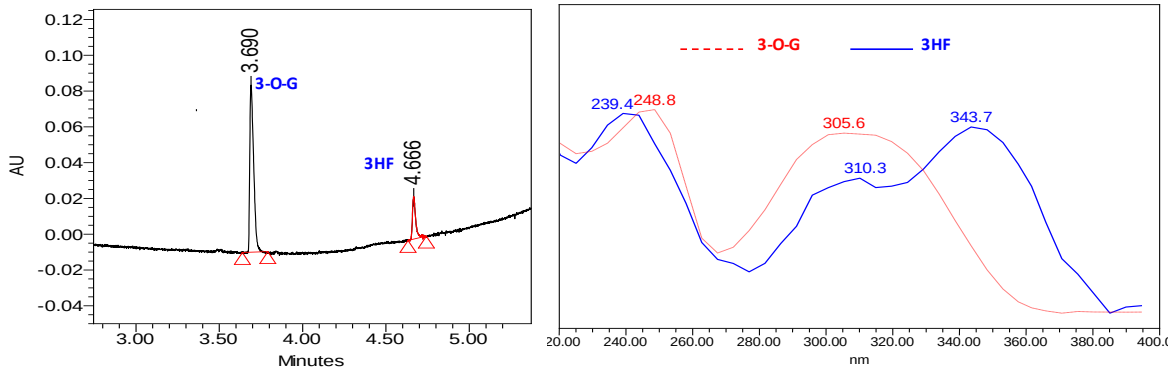

3,4'-Dihydroxyflavone (3,4'DHF)

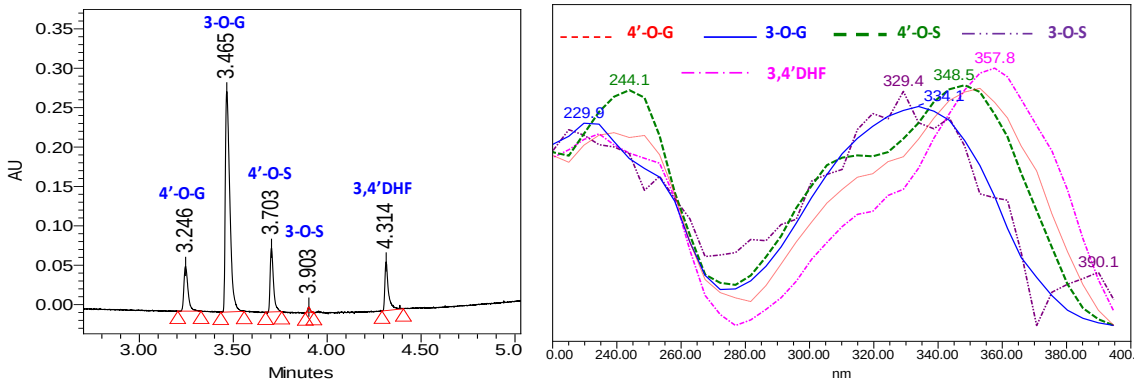

3,7-Dihydroxyflavone (3,7DHF)

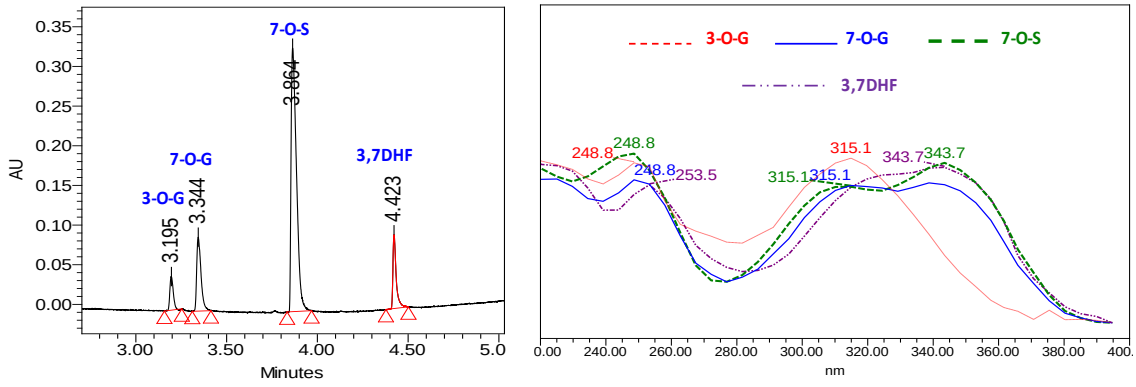

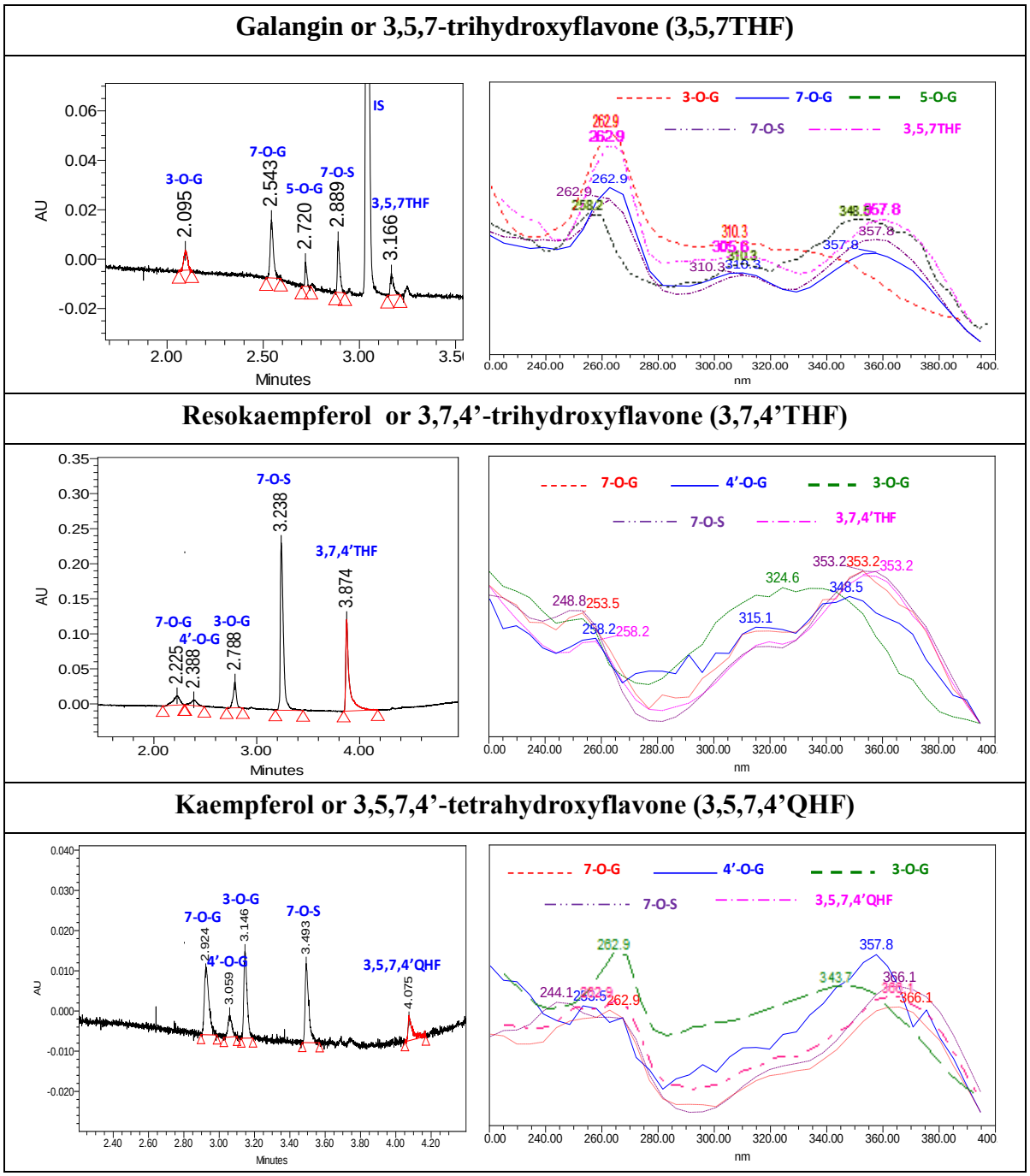

Figure 32. UPLC chromatograms and UV spectra of flavonols and their respective glucuronides and sulfates in Caco-2 cell transport study samples

Similarly, for 3,5,7,4'QHF, the position of conjugation of first, second and third glucuronides and sulfate of 3,5,7,4'QHF were 7-*O*-G, 4'-*O*-G, 3-*O*-G and 7-*O*-S, respectively (Figure 32).

8.4.3. Determination of correction factors for conjugates of flavonols

Amounts of conjugates formed were determined using the corrections factors for individual glucuronides of flavonols as described in the method section. UGT isoforms and wavelength used in generation of correction factor and the correction factor for each glucuronides are detailed in Table C2 (Appendix C). The correction factors were in the range of 0.5 (for 3-*O*-G of 3HF) to 2.5 (for 3-*O*-G for 3,7DHF). Correction factors of sulfates of flavonols were not determined experimentally. Based on the comparative UV spectra of sulfate and glucuronide of a flavonol conjugated at the same position, correction factors of sulfates conjugated at a particular position was assumed to be similar to the corresponding glucuronide. Although this assumption was confirmed in the case of genistein (not shown), it may need to be validated with appropriate experiments in the future.

All compounds except 3HF formed both sulfate and glucuronides during the transport study though the amount of glucuronides in all cases was higher than sulfates (Figure 33). Out of the total phase-II metabolism, percentage of glucuronidation of 3HF, 3,4'DHF, 3,7DHF, 3,7,4'THF, 3,5,7THF, 3,5,7,4'QHF was 100, 93, 60, 51, 68, and 62 (Figure 33).

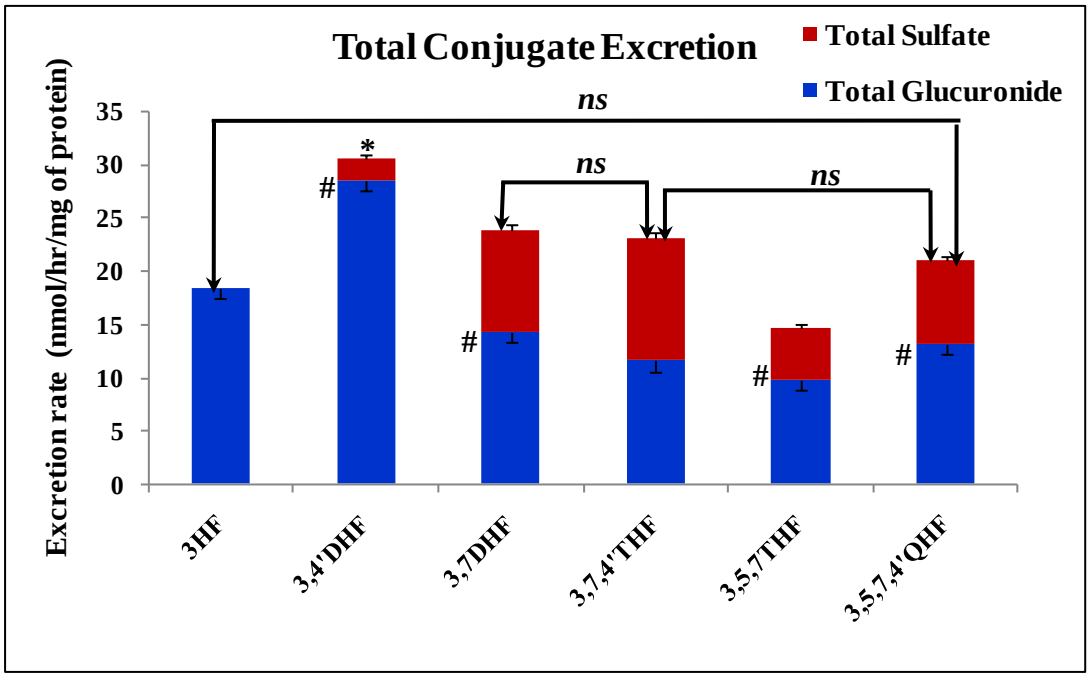

Figure 33. Excretion of total conjugates of flavonols in Caco-2 cell monolayer. Rates of excretion of total (AP+BL) glucuronides and total (AP+BL) sulfates during AP (pH =7.4) to BL (pH =7.4) transport of flavonols (at 10 µM concentration) in the Caco-2 cell monolayer at 37ºC were calculated as the slope of amount of total glucuronide and sulfate excreted vs time profile in Figures F3a-F3-D (Appendix F) respectively, using only the first two data points of each profile, i.e., 1 and 2 hrs for 3,7,4'THF and 0.5 and 1 hr for all other flavonols. Each bar is the average of three determinations, and the error bars are the standard deviations of the mean (n=3). Rates of excretion of total glucuronides and sulfate for each flavonol were normalized to the corresponding protein concentration of experimental monolayer of each flavonol. # on the side of each bar represents the significant difference between the rates of total glucuronides and total sulfate for each flavonol ($p<0.05$). * on the top of each bar represents that the excretion rates of total conjugates (glucuronides and sulfate together) of the compound was significantly different from the excretion rates of total conjugates of all other compounds, respectively ($p<0.05$). Since most bars showed significant difference to the other bars (B), ones with no significant difference (not significant, *ns*) were shown on the top ($p<0.05$) to make graphs easily readable.

This showed that for flavonols though sulfation is important, in most cases glucuronidation was the major metabolic pathway. Also, all sulfates were formed at 7-*O* position, except for flavonols where 7-OH is not present (for 3HF, no sulfate was formed and for 3,4'DHF, sulfation occurred at 4'-*O*). Therefore, the compound chosen is not particularly suited to study sulfate formation and excretion. Based on above-mentioned reasons, this chapter is focused on the glucuronidation of flavonols in detail.

8.4.4. Formation rates of glucuronides of flavonols in Caco-2 cell lysate

The rates of formation of total glucuronides of flavonols (10 μM) followed the following rank order: 3,4'DHF (26.9 ± 0.3) ~3,5,7THF (26.4 ± 1.2) >3HF (15.8 ± 0.2) > 3,5,7,4'QHF (13.7 ± 0.43) > 3,7DHF (5.1 ±0.5) ~ 3,7,4'THF (4.9 ± 0.2) nmol/hr/mg of protein (Figure 34). The formation rates of total glucuronides of 3,4'DHF and 3,5,7THF; and 3,7DHF and 3,7,4'THF were not significantly different. Apart from these two pairs, all other flavonols showed significant difference among their rates of formation of glucuronides ($p<0.05$) (Figure 34). There seemed to be no obvious relation between the structure of flavonol and the rates of glucuronidation in Caco-2 cell lysate. The lowest glucuronidated flavonols (3,7,4'THF and 3,7DHF) were 5 times less rapidly metabolized than the highest glucuronidated flavonols (3,5,7THF and 3,4'DHF) ($p<0.05$) (Figure 34).

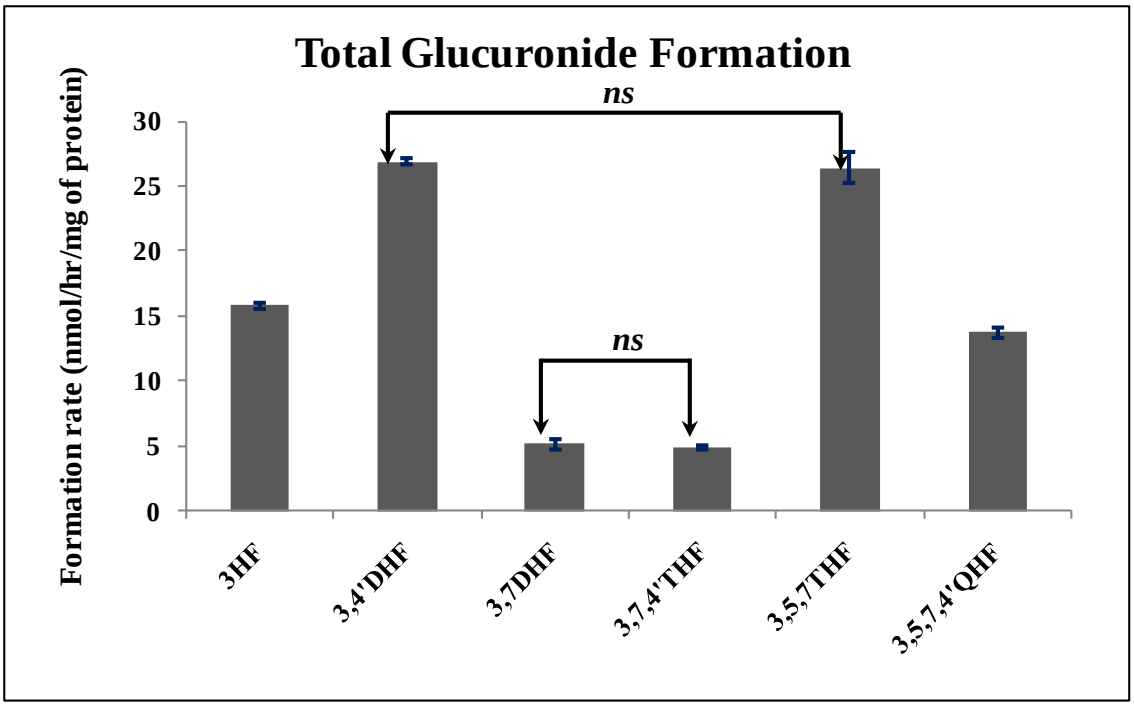

Figure 34. Formation of glucuronides of flavonols in Caco-2 cells.
Formation rates of glucuronides of flavonols were measured using Caco-2 cell lysate (protein concentration ~0.1mg/ml) at 10 µM substrate concentration incubated for 2 hrs at 37ºC. Each bar is the average of three determinations, and the error bars are the standard deviations of the mean (n=3). Since most bars showed significant difference to the other bars, ones with no significant difference (not significant, *ns*) were shown on the top ($p<0.05$) to make graphs easily readable.

8.4.5. Excretion of total glucuronides of flavonols in intact Caco-2 cell monolayer

The amounts of total glucuronides (i.e. sum of amounts of all glucuronides of a flavonol) excreted increased linearly as a function of time up to for 2 hours for 3,7,4'THF and up to 1 hour for all other flavones (Figures F3a-F3b Appendix F). The rates of excretion of flavonols total glucuronides to AP and BL sides were calculated as the slope of amount of conjugate excreted vs time profile, using only the first two data points of each profile, i.e., 1 and 2 hrs for 3,7,4'THF and 0.5 and 1 hr for all other flavonols. We choose only the first two data points, as in most cases, they fell in the linear portion of the curve (Figures F3a-F3b, Appendix F).

The rates of excretion of all glucuronides of a flavonol were normalized against the corresponding protein concentration of the Caco-2 cells monolayers used in its transport and rates of excretion were reported as nmol/hr/mg of protein. The total (AP+BL) rates of excretion of glucuronides all flavonols were significantly different from the other compounds, except the following pairs, 3,7DHF and 3,5,7,4'QHF; 3,4,7'THF and 3,5,7,4'QHF; and 3,4,7'THF and 3,5,7THF, ($p < 0.05$) (Figure 35).

The rates of excretion of total glucuronides followed the following rank order: 3,4'DHF (28.55 ± 2.37) > 3HF (18.45 ± 1.13) ~ 3,7DHF (14.33 ± 0.63) > 3,5,7,4'QHF (13.21 ± 1.05) ~ 3,7,4'THF (11.65 ± 0.25) ~ 3,5,7THF (9.89 ± 0.53) > nmol/hr/mg of protein (Figure 35).

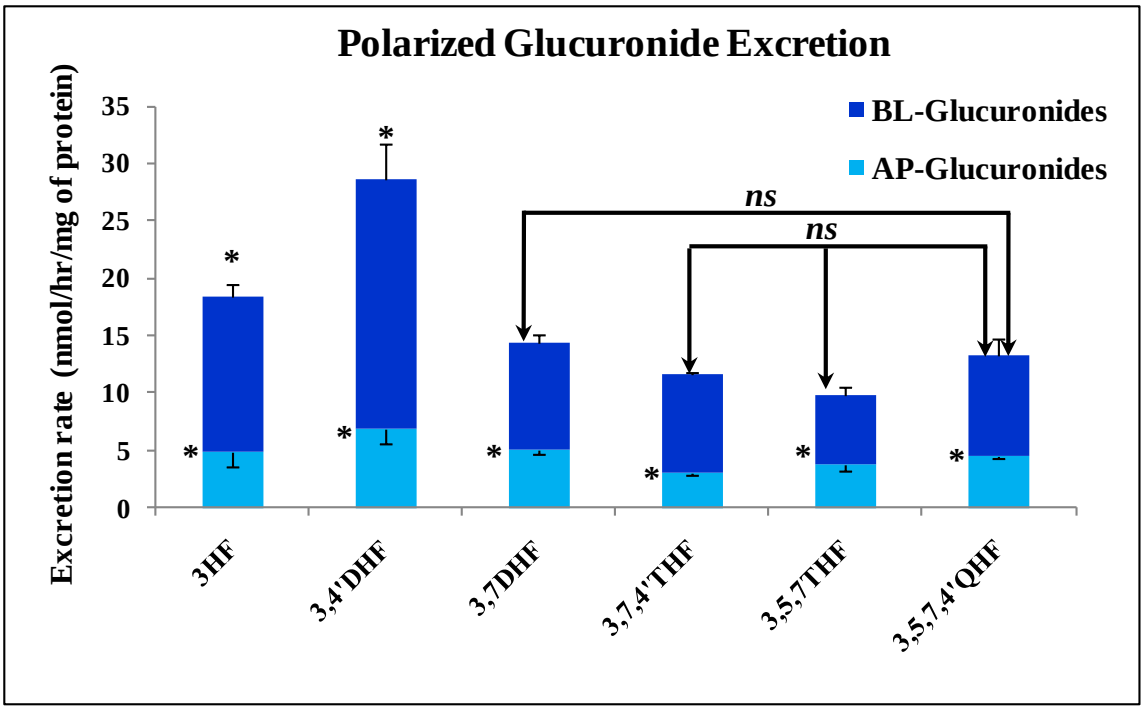

Figure 35. Excretion of total glucuronides in Caco-2 cell monolayer.
Rates of excretion of total glucuronides on AP and BL side during AP (pH =7.4) to BL (pH =7.4) transport of flavonols (at 10 µM concentration) in the Caco-2 cell monolayer at 37ºC were calculated as the slope of amount of glucuronides excreted vs time profile in Figures F3a-F3b (Appendix F), using only the first two data points of each profile, i.e., 1 and 2 hrs for 3,7,4'THF and 0.5 and 1 hr for all other flavonols. Rates of excretion for each flavonol were normalized to the corresponding protein concentration of experimental monolayer of each flavonol. Each bar is the average of three determinations, and the error bars are the standard deviations of the mean (n=3). # on the side of each bar represents the significant difference between, AP and BL excretion of total glucuronides of each flavonol ($p<0.05$). * on the top of each bar represents that the excretion rates of total (AP+BL) glucuronides of the compound was significantly different from the excretion rates of total glucuronides of all other compounds, respectively ($p<0.05$). Since most bars showed significant difference to the other bars, ones with no significant difference (not significant, *ns*) were shown on the top ($p<0.05$) to make graphs easily readable.

This indicated that for compounds with more than two hydroxyl group, structure of the flavonol did not significantly affect the rates of glucuronide excretion in Caco-2 cell monolayer ($p<0.05$). Also, overall glucuronidation of flavonols with more than two hydroxyl groups in intact Caco-2 cells was significantly less than the overall glucuronidation of flavonols with one or two hydroxyl group in their structure ($p<0.05$) (Figure 35).

8.4.6. Correlation of formation and excretion rates of glucuronides of flavonols

We correlated formation rates of total glucuronides of flavones to their corresponding AP, BL and total (AP+BL) excretion rates (Figures 34-35), but we found very poor correlation for AP ($r^2 = 0.2$), BL ($r^2 = 0.18$) as well as total excretion ($r^2 = 0.17$). 3,5,7THF was found to be an outlier in this series without which the correlation for AP ($r^2 = 0.69$), BL ($r^2 = 0.83$) and total ($r^2 = 0.8$) excretion improved (plots not shown here).

8.4.7. Formation of regiospecific glucuronides of flavonols in Caco-2 cell lysate

The rates of formation of the two glucuronides of each 3,4'DHF and 3,7DHF in Caco-2 cell lysate were significantly different ($p<0.05$). Similarly, rates of formation of the three glucuronides of each 3,7,4'THF and 3,5,7,4'QHF were also significantly different ($p<0.05$) (Figure 36A).

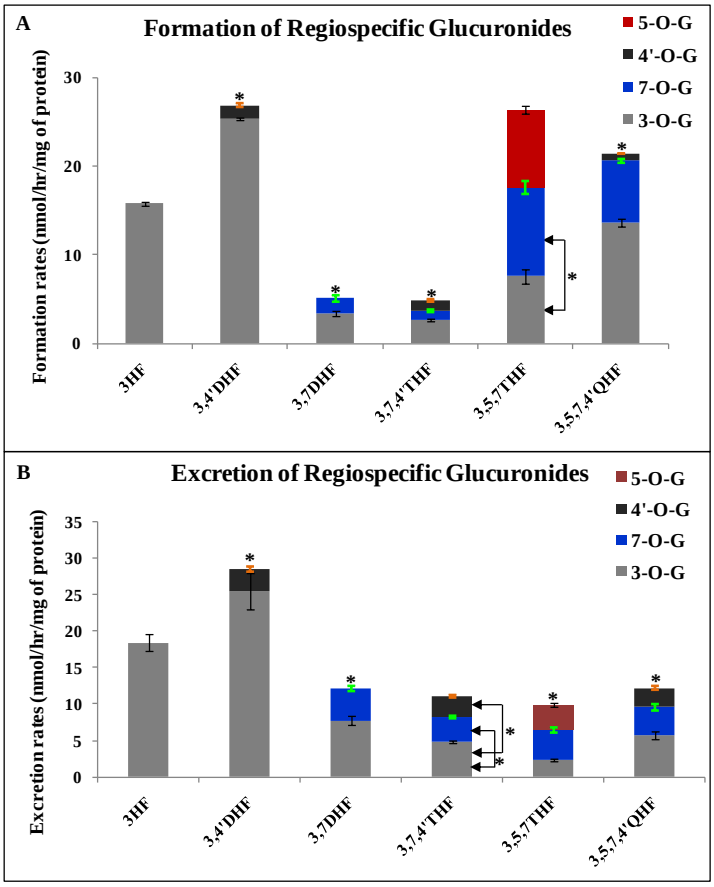

Figure 36. Regiospecific glucuronides formation (A) and excretion (B) of flavonols in Caco-2 cells.

Formation rates of glucuronides of flavonols were measured using Caco-2 cell lysate (protein concentration ~0.1mg/ml) at 10 µM substrate concentration incubated for 2 hrs at 37ºC. Rates of total (AP and BL) excretion of glucuronides of flavonols in AP to BL transport in Caco-2 cell monolayer were calculated as the slope of amount of individual glucuronide excreted on both AP and BL side vs time profile in Figures F3a-F3b and Figures F4a-F4e (Appendix F), using only the first two data points of each profile. Rates of excretion of glucuronide(s) for each flavonol were normalized to the corresponding protein concentration of experimental monolayer of each flavonol. Each bar is the average of three determinations, and the error bars are the standard deviations of the mean (n=3). * on the top of each bar represents that the formation/ excretion rates of all glucuronides are significantly different from each other, whereas # on the side of each bar represents that only individual pairs showed significant difference ($p<0.05$).

However, only the rate of formation of 3-*O*-G of 3,5,7THF was significantly different from the rate of formation of its 7-*O*-G but there was no significant difference between rates of formation of 3-*O*-G and 5-*O*-G, and 7-*O*-G and 5-*O*-G of 3,5,7THF ($p<0.05$) (Figure 36A). 3-*O*-G of 3,4'DHF (25.39 ± 0.17) was formed ~17 times faster than its 4'-*O*-G (1.51 ± 0.22 nmol/hr/mg of protein), while 3-*O*-G of 3,7DHF (3.42 ± 0.32) was formed only twice faster than its 7-*O*-G (1.70 ± 0.33 nmol/hr/mg of protein) ($p<0.05$), suggesting that for di-hydroxyflavones, 3-*O* was the most favored position for glucuronidation, followed by 7-*O* and 4'-*O* (Figure 36A).

For 3,7,4'THF, 3-*O*-G (2.71 ± 0.16) was formed ~2.3 and 2.7 times faster than 4'-*O*-G (1.18 ± 0.12) and 7-*O*-G (1.00 ± 0.10 nmol/hr/mg of protein) ($p<0.05$), respectively, whereas for 3,5,7THF, 7-*O*-G (10.02 ± 0.77) was formed 1.3 times faster than 3-*O*-G (7.62 ± 0.08) and 1.1 times faster than 5-*O*-G (8.76 ± 0.44 nmol/hr/mg of protein) ($p<0.05$). 3,5,7,4'QHF, 3-*O*-G (10.64 ± 0.42) was formed ~4.5 and 13.5 times faster than 7-*O*-G (2.31 ± 0.09) and 4'-*O*-G (0.78 ± 0.01 nmol/hr/monolayer), respectively ($p<0.05$) (Figure 36A). This showed that for flavonols 3-*O* was be the main position of glucuronidation followed by 7-*O*, except for 3,5,7THF where excretion of 7-*O*-G was faster than 3-*O*-G. Also, 4'-*O* and 5-*O* were equally important to 7-*O* position in cases of 3,7,4'THF and 3,5,7THF, respectively, but not favored at all in case of 3,5,7,4'THF.

8.4.8. Excretion of regiospecific conjugates of flavonols in intact Caco-2 cell monolayer

The amounts of each regiospecific glucuronides of flavonol excreted increased linearly as a function of time up to for 2 hours for 3,7,4'THF and up to 1 hour for all other flavones (Figures F4a-F4e, Appendix F). The rates of excretion of the two glucuronides of 3,4'DHF and 3,7DHF and three glucuronides of 3,5,7THF and 3,5,7,4'QHF in the intact Caco-2 cell monolayer were significantly different from each other ($p<0.05$) (Figure 36B). However for 3,7,4'THF, there was no significant difference between rates of excretion of 7-*O*-G and 4'-*O*-G, but the rates of excretion of the 3-*O*-G was significantly different from both 7-*O*-G and 4'-*O*-G ($p<0.05$) (Figure 36B).

3-*O*-G of 3,4'DHF (25.48 ± 2.42) was excreted about 8 times faster than the 4'-*O*-G (3.06 ± 0.33 nmol/hr/mg of protein), while 3-*O*-G of 3,7DHF (7.73 ± 0.59) was excreted only 1.7 faster than the 7-*O*-G (4.45 ± 0.31 nmol/hr/ mg of protein) ($p<0.05$) (Figure 36B). This suggested that for glucuronidation of di-hydroxyflavones in intact Caco-2 cells, 3-*O* was the most favored position followed by 7-*O* and 4'-*O*, similar to Caco-2 cell lysate (Figure 36B).

For 3,7,4'THF, 3-*O*-G (4.88 ± 0.22) was excreted ~1.5 and 1.7 times faster than 7-*O*-G (3.35 ± 0.14) and 4'-*O*-G (2.81 ± 0.20 nmol/hr/ mg of protein), respectively ($p<0.05$) (Figure 36B).

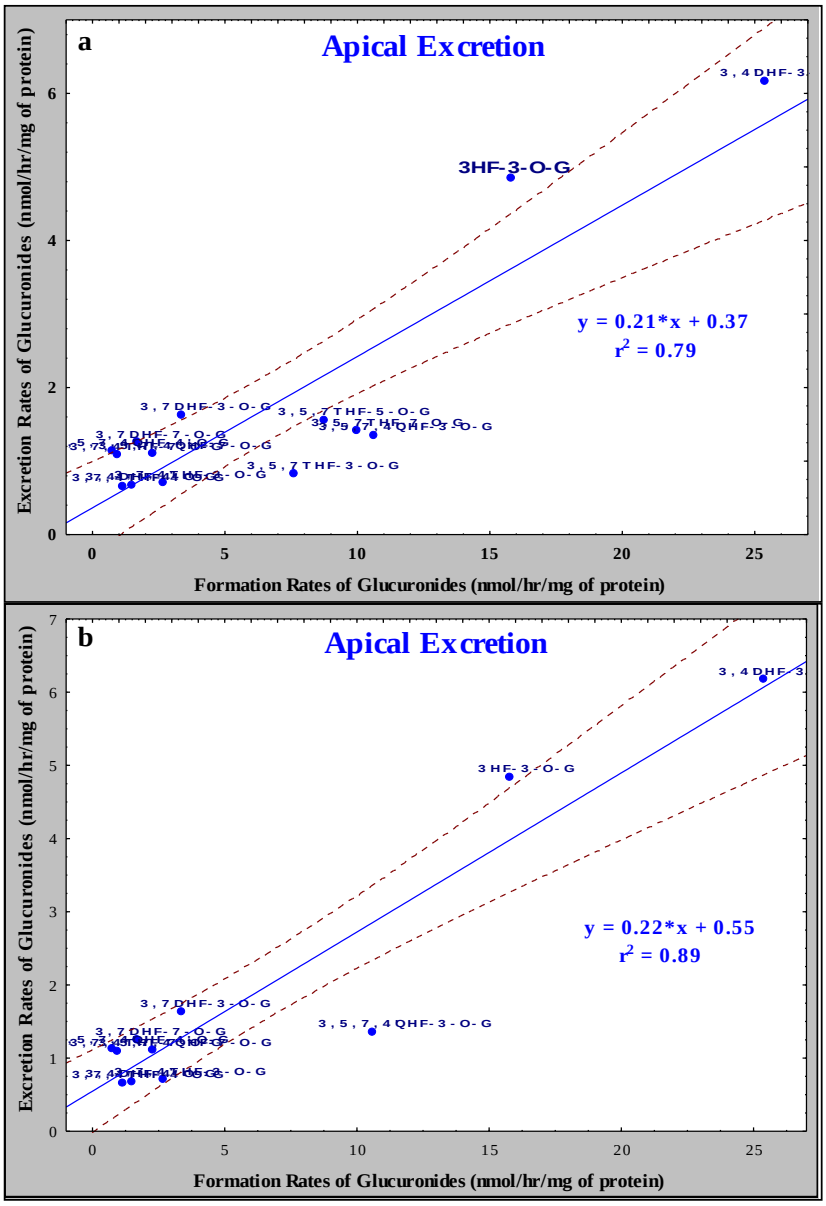

Figure 37. Correlation between formation and apical excretion of regiospecific glucuronides of flavonols in Caco-2 cells.

The apical rates of excretion with (a) and without (b) 3,5,7THF of all regiospecific glucuronides of flavones excreted in intact Caco-2 cell monolayer were plotted against their corresponding rates of formation in Caco-2 cell lysate. Solid blue line is line of best fit and dotted brown lines are the 95% confidence interval lines. Each data point is the average of three determinations.

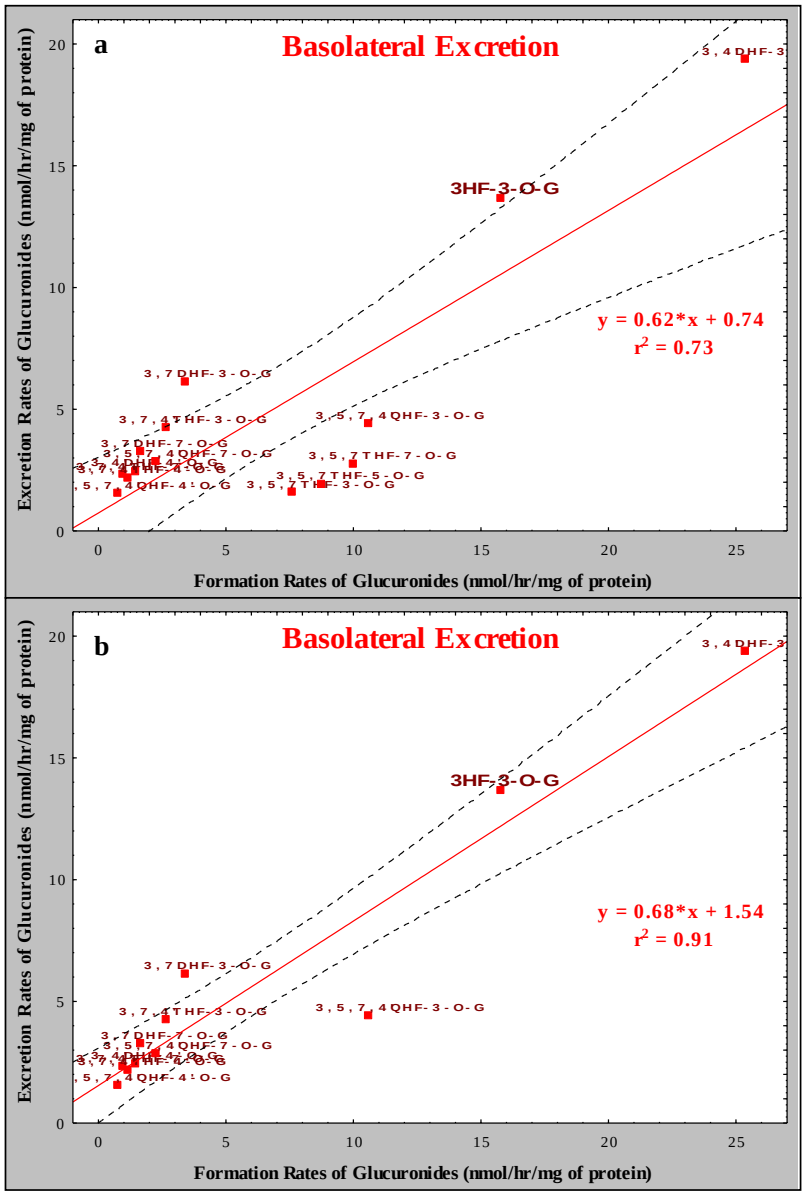

Figure 38. Correlation between formation and basolateral excretion of regiospecific glucuronides of flavonols in Caco-2 cells.

The basolateral rates of excretion with (a) and without (b) 3,5,7THF of all regiospecific glucuronides of flavones excreted in intact Caco-2 cell monolayer were plotted against their corresponding rates of formation in Caco-2 cell lysate. Solid red line is line of best fit and dotted black lines are the 95% confidence interval lines. Each data point is the average of three determinations.

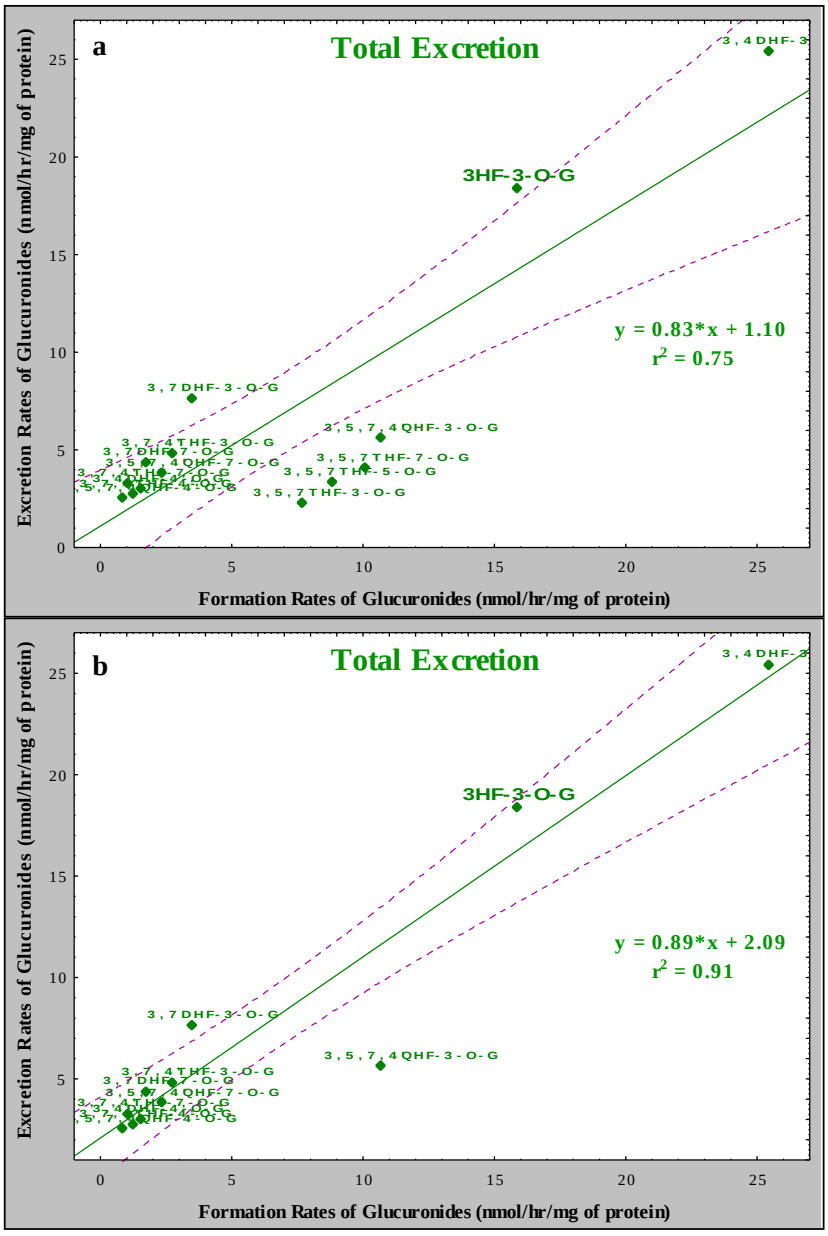

Figure 39. Correlation between formation and total excretion of regiospecific glucuronides of flavonols in Caco-2 cells.

The total (AP+BL) rates of excretion with (a) and without (b) 3,5,7THF of all regiospecific glucuronides of flavones excreted in intact Caco-2 cell monolayer were plotted against their corresponding rates of formation in Caco-2 cell lysate. Solid green line is line of best fit and dotted purple lines are the 95% confidence interval lines. Each data point is the average of three determinations.

3,5,7,4'QHF, 3-*O*-G (5.70 ± 0.54) was excreted ~1.5 and 1.8 times faster than 7-*O*-G (3.88 ± 0.41) and 4'-*O*-G (2.61 ± 0.24 nmol/hr/mg of protein), respectively ($p<0.05$). Whereas for 3,5,7THF, 7-*O*-G (4.13 ± 0.35) was excreted 1.8 times faster than 3-*O*-G (2.34 ± 0.18) and 1.2 times faster than 5-*O*-G (3.43 ± 0.23 nmol/hr/ mg of protein) ($p<0.05$) (Figure 36B). This showed that in general, for flavones with three or more hydroxyl groups, the rank order of glucuronides excretion in intact Caco-2 cells were similar to the rank order of glucuronides formation in Caco-2 cell lysate, though the ratios might be somewhat different.

8.4.9. Correlation of formation and excretion rates of regiospecific glucuronides of flavonols

We correlated the formation rates of regiospecific glucuronides of the six flavonols to their corresponding AP, BL and total (AP+BL) excretion rates (Figures 37-39) and it showed good correlation. The correlation coefficient (r^2) for AP, BL and total (AP+BL) excretion were 0.82 (Figure 37a), 0.73 (Figure 38a) and 0.77 (Figure 39a), respectively. Based on 95% confidence interval lines, three regiospecific glucuronides of 3,5,7THF and 3-*O*-G of 3,7DHF and 3,5,7,4'QHF were found as the outlier in the series. This indicated that the actual excretion rates of all the glucuronides of 3,5,7THF and 3-*O*-G of 3,7DHF and 3,5,7,4'QHF in Caco-2 cell monolayer were much lower than the predicted

excretion rates, derived based on the formation rates of these glucuronides in Caco-2 cell lysate.

Since all the three regiospecific glucuronides of 3,5,7THF were outliers, so we re-plotted the formation rates of regiospecific glucuronides of five flavones (leaving out the glucuronides of 3,5,7THF) to their corresponding AP (Figure 37b), BL (Figure 38b) and total (AP+BL) (Figure 39b) excretion rates. We found that the correlations improved further. The correlation coefficient (r^2) for AP, BL and total (AP+BL) excretion now were 0.89, 0.91 and 0.91, respectively. For this series also, 3-*O*-glucuronides of 3,7DHF and 3,5,7,4'QHF were still found as outliers. The slope of the lines of best fit for AP, BL and total excretion were 0.22, 0.68 and 0.89, respectively.

Upon further removal of under-excreted 3-*O*-G of 3,5,7,4'QHF, both the correlation and slopes improved (plots not shown here). The correlation coefficient (r^2) for AP, BL and total (AP+BL) excretion now were 0.97, 0.98 and 0.98, respectively. The slope of the lines of best fit for AP, BL and total excretion were 0.23, 0.71 and 0.94.

8.4.10. Polarized excretion of glucuronides in Caco-2 cell monolayer

Most flavonols showed preferential BL excretion ($p<0.05$), except for 3,5,7THF which showed similar excretion on both sides (Figure 35). The latter can be attributed to the difference in the rates of polarized excretion of regiospecific glucuronides of 3,5,7THF (Figure 40), as discussed below.

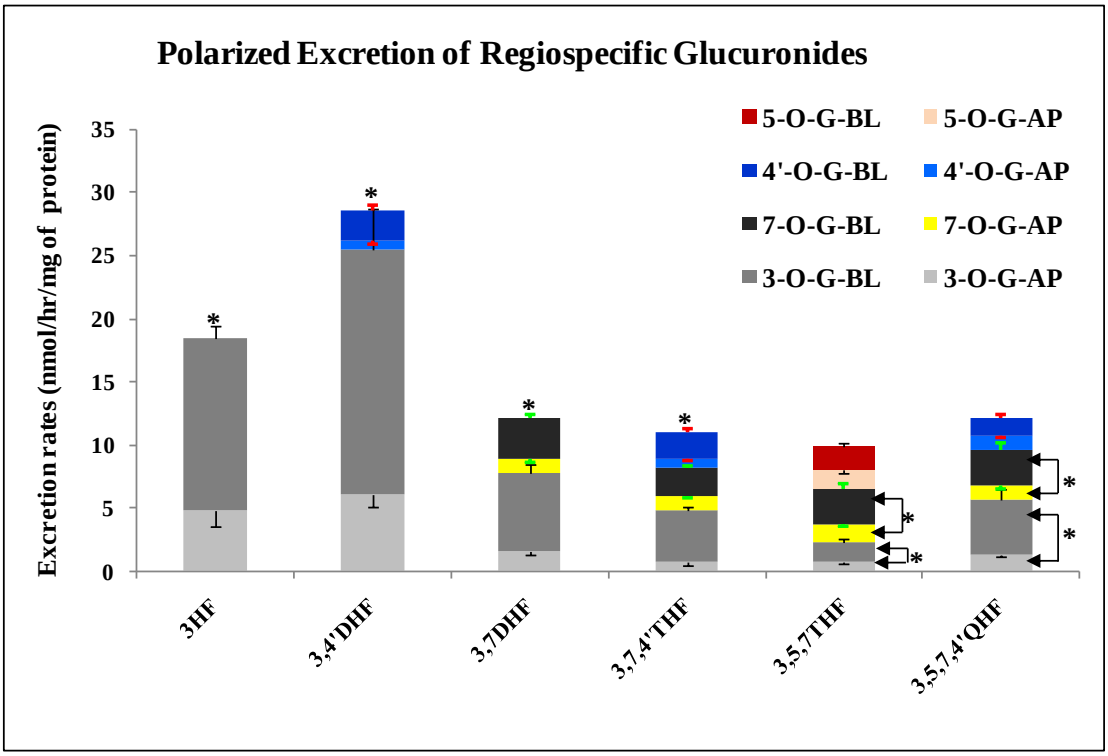

Figure 40. Polarized excretion of regiospecific glucuronide(s) of flavonols in Caco-2 cell monolayer.

Apical (AP) and basolateral (BL) excretion rates of 3-*O*, 4'-*O*, 5-*O* and 7-*O* -glucuronides during apical to basolateral transport of flavonols at 10 µM concentration in Caco-2 Cell Monolayer were calculated as the slope of amount of conjugate excreted vs time profile in Figures F3a-F3b for 3HF and Figures F4a-F4e for other compounds (Appendix F), using only the first two data points of each profile, i.e., 1 and 2 hrs for 3,7,4'THF and 0.5 and 1 hr for all other flavonols. Rates of excretion of glucuronide(s) for each flavonol were normalized to the corresponding protein concentration of experimental monolayer of each flavonol. Each bar is the average of three determinations, and the error bars are the standard deviations of the mean (n=3). * on the top of each bar represents that the AP excretion rates of each glucuronide of flavonol was significantly different from their respective BL excretion rates ($p<0.05$). # on the side of each bar in next to a specific glucuronide represents that the AP excretion rate of that glucuronide of flavonol was significantly different from its respective BL excretion rate ($p<0.05$).

Since, BL to AP ratios of excretion ranged from 1.6 (for 3,5,7THF) to 3.28 (for 3HF), it was concluded that the efflux transporter(s) responsible for excretion of flavonol glucuronides were expressed more on BL than on AP membrane of Caco-2 cells. 7-*O* and 3-*O* glucuronides of all flavonols were excreted preferably to the BL side than to the AP side, BL/AP ratio ranged from 1.95 to 2.6 for 7-*O*-glucuronides and from 1.91 to 6.06 for 3-*O*-glucuronides ($p<0.05$) (Figure 40). Similarly, 4'-*O* glucuronides of 3,4'DHF (BL/AP ratio = 3.67) and 3,7,4'THF (BL/AP ratio = 2.33) were excreted preferably to the BL side than to the AP side, but 4'-*O*-glucuronide of 3,5,7,4'QHF (BL/AP ratio = 0.89) did not show any significant difference in AP and BL excretion ($p<0.05$). There was only one 5-*O*-G formed in the whole series and it showed no preference in excretion to BL or AP membrane (BL/AP ratio = 1.23) ($p<0.05$) (Figure 40).

The fact that 5-*O*-G of 3,5,7THF did not show any preference in excretion to the BL side than to the AP side, could explain the observation that the rates of excretion of total glucuronides of 3,5,7THF on AP and BL side were very comparable (low BL/AP ratio = 1.6) (Figure 35).

8.5. Discussion

In this first systematic study of flavonol disposition in Caco-2 cells, we concluded that the excretion of flavonol glucuronides in Caco-2 cells was generally shown to be not rate-limited by the efflux transporters. This conclusion can be supported by the fact that the rate of formation of glucuronides (Figures 34 and 36A) of the selected flavonols (Figure 4, pg 65) in Caco-2 cell lysate correlated very well ($r^2 \sim 0.9$) with the corresponding rates of total (AP+BL) excretion (Figures 35 and 36B) of these glucuronides in intact Caco-2 cell monolayer, except for 3,5,7THF. The slope of the linear relationship (Excretion rate = 0.89* Formation rate + 2.09) which described the line of best fit of total excretion of regiospecific glucuronides was close to 1 (Figure 39b). This indicates that the rates of excretion of regiospecific flavonol glucuronides at the 10µM can be reasonably predicted by their corresponding rates of formation in Caco-2 cells.

We also showed that the slope of the best fit line for BL excretion (0.68) (Figure 38b) was about three times more than the slope for the AP excretion (0.22) (Figure 37b), indicating the preferred BL excretion of glucuronides, which was also obvious in other related results that displayed preferred BL excretion of total as well as most regiospecific glucuronides (Figures 35 and Figure 40). When we added the two slopes, the result was again close to 1, indicating that we can use the linear relationship of line of best fit for AP and BL excretion (Figures 37b and 38b) to successfully predict the AP as well BL excretion of regiospecific glucuronides in Caco-2 cells. The preferential and uninhibited

BL excretion of high amounts of flavonol glucuronides at 10µM, most probably by the high expressing MRP3 transporter in Caco-2 cells, seems to be the reason for the good correlation between formation and excretion rate of glucuronides.

Our finding are also supported by the recently published report on the Caco-2 transport of kaempferol (3,5,7,4'QHF) by Barrington *et al.* (2009), which showed that neither transporter nor enzyme saturation was evident at the concentrations of kaempferol applied (5 to 100 µM). The efflux of 3-*O* and 7-*O* glucuronides of kaempferol was not limited at the transport or enzyme level. However, the cellular production and cellular efflux of kaempferol-4'-O-glucuronide appeared to be saturated in the study.[192] The study also showed that glucuronides exhibited favorable BL excretion over AP excretion.

The fact that efflux transporters are not playing a rate-limiting step for the glucuronides of flavonol subclass is consistent with the published reports on isoflavone sub-class. Chen *et al.* (2005) showed that at substrate concentration of 10 µM (5 µM for prunetin), the formation served as the rate-limiting step for all isoflavone conjugates (glucuronides and sulfates) except for genistein glucuronide, which had comparable excretion and formation similar to flavonols.[90] On the other hand, for apigenin, a compound of flavone sub-class, excretion by efflux transporters was shown to be the rate-limiting step.[10] Formation rate of apigenin glucuronide at 10µM was 3 times faster than its excretion rate.[10, 163] Therefore, the observed correlation is probably specific to the flavonol subclass of flavonoids.

The preferential BL excretion of flavonol glucuronides, especially 3-*O*-G, might be responsible for efflux transporters not playing a rate-limiting role in disposition of flavonols in Caco-2 cells. BL/AP ratio of regiospecific glucuronides showed that except for 3,5,7THF, 3-*O*-glucuronide was more preferential for BL excretion than other glucuronide(s) of a flavonol (Figure 40). For example, BL/AP ratio of 3-*O*-G, 7-*O*-G and 4'-*O*-G of 3,7,4'THF were 6.06, 2.11 and 3.29, respectively. Similarly, 3-*O*-G and 7-*O*-G of 3,7DHF showed BL/AP ratio of 3.78 and 2.6, respectively (Figure 40). Reported study on quercetin glucuronides showed that 7-*O*-G was better substrate of MRP2 (apical transporter) than 3-*O*-G[195] strongly supporting that there could be differences in the AP and BL preferences among the regiospecific glucuronides of the same flavonol.

Based on the discussion above, we can speculate that during intestinal absorption of flavonols, higher amount of glucuronides will be secreted in mesenteric vein than in the gut lumen, which means that for flavonols, there will certainly be less enteric and possibly even less enterohepatic recycling, since conjugates are not well taken up by the hepatocytes. This could result in higher amount of a regiospecific glucuronide in the systemic circulation. This becomes more important in cases where glucuronides are either biologically active or acted upon by β-glucuronidase in different tissues to convert the glucuronides back to bioactive aglycone.[80, 81]

The correlation between excretion rates and formation rates was better when regiospecific glucuronides of 3,5,7THF were not plotted (r^2 ~ 0.9) (Figures 37b, 38b,

39b) than when they were plotted (r^2 ~ 0.75) (Figures 37a, 38a, 39a). Also, when 3-O-G of 3,5,7,4'QHF was removed, correlation improved further (r^2 ~ 0.98) (plots not shown). This indicates that for some reason, rates of excretion of 3,5,7THF glucuronides were much lower than what was predicted based on rates of formation. Somehow, the structure of 3,5,7THF was not supported by the efflux transporters, indicating that may be this particular structural feature in 3-D is either not favored by or inhibits the efflux transporters involved in the excretion of these glucuronides such as BCRP, MRP2 and MRP3, which are expressed in the Caco-2 cells.[106]

In conclusion, the excretion of flavonol glucuronides in Caco-2 cells is generally not rate-limited by efflux transporters, which can be mainly attributed to the favorable basolateral efflux of flavonol glucuronides, especially 3-*O*-G. More studies in future are required in this area to understand the structure and regiospecific excretion preferences of various efflux transporters involved in excretion of flavonol conjugates, which will help to understand the other transport component of overall disposition process of flavonoids.

7-HYDROXY GROUP IN FLAVONES IS THE MOST FAVORED POSITION FOR GLUCURONIDATION AND SULFATION IN CACO-2 CELLS

9.1. Abstract

The objective of this study was to determine the role of efflux transporters in the disposition of flavones in Caco-2 cell culture model. We used seven congeneric compounds of flavone sub-class with different number and position of hydroxyl group in their structure. We measured the rate of excretion of glucuronides and sulfates at both apical (AP) and basolateral (BL) side during AP to BL basolateral transport of selected flavones (at 10µM substrate concentration, 5µM for 5-hydroxyflavone) in Caco-2 cell monolayer. We showed that the most favored position for glucuronidation and sulfation was 7-hydroxy group in the structure of flavones. We also showed that the rates of formation of total (sum of all) glucuronides of the selected flavones in Caco-2 cell lysate had a very good ($r^2 \sim 0.9$) linear correlation with the corresponding rates of AP, BL and total (AP+BL) excretion of the glucuronides in the intact Caco-2 cell monolayer, but with a slope of much less than 1 (~0.3). When the formation versus excretion rates correlation profiles of 4'-*O*-G and 7-*O*-G of flavonols and flavones plotted together, were compared with the correlation profiles of 3-O-G of flavonols, the slopes of line of best fit were 0.7, 0.44, and 0.95 for 4'-*O*-G, 7-*O*-G and 3-*O*-G, respectively. This indicated that the excretion of 3-*O*-G was not, whereas the excretion of 4'-*O*-G and 7-*O*-G glucuronides was limited by the efflux transporters. In conclusion, flavones are preferentially

glucuronidated and sulfated at 7-*O* position and the excretion of flavone glucuronides is rate-limited by the efflux transporters.

9.2. Introduction

Flavonoids are polyphenolic compounds occurring naturally in plant products such as fruits, vegetables and soy products. The flavonoids have shown various disease preventive health benefits such as anti-aging, cancer chemoprevention and protection against cardiovascular diseases.[161] Based on their backbone structures, flavonoids can be categorized into seven major sub-classes found in foods, namely, flavones, isoflavones, flavones, flavanones, flavanols, chalcone and anthocyanidins. Figure 1 (pg 5) shows the basic structure of flavone sub-class.

Flavones are found in a variety of plants, vegetables, fruits, and herbs as well as their extracts, which are commonly marketed as diet and herbal supplements. Apigenin, chrysin, luteolin and bicalein are some of the important and common flavones and have demonstrated anticancer activities and other beneficial effects.[1, 162, 177, 196, 197] Recently, various flavonoids including flavones has been shown to have the potential to prevent prostate cancer via cell cycle regulation, apoptosis, inhibition of androgen synthesis, or inhibition of oncogenic protein kinases.[196-201] However, apigenin and chrysin, like many other flavones that are part of popular herbal supplements, is poorly bioavailable.[1, 177, 190]

Most flavones are mainly conjugated in the human body to their sulfate and glucuronide conjugates, by the sulfotransferases (SULTs) and uridine diphosphoglucuronosyl transferase (UGT) enzyme superfamilies, respectively, which limits the bioavailability of

intact aglycone.[13, 121, 163, 190] Though, glucuronides have been shown to be the major components of circulating flavones in a number of studies in humans and animals, sulfation also played an important role in determining the oral bioavailability of flavones in humans.[10, 163, 202, 203]

UGTs[61] and SULTs[76] are fairly well-expressed in intestinal epithelial cells and hepatocytes which are the first-pass organ for metabolism by the oral drug delivery. First pass intestinal metabolism by phase II enzymes have shown to play an important role in the disposition of flavones after oral administration.[13, 53, 100, 132] Hence, it is important to study the disposition of flavonoids that might help to identify the structural features of flavones with low potential for phase-II metabolism in intestinal cells, which could benefit their development into chemopreventive agents.

Research published from various lab including ours have shown that metabolism and disposition various flavonoids in the intestine had been affected by the structure of the compounds. Chen *et al.* (2005) showed that the total uptake of isoflavones and polarized as well as total excretion of their metabolites were dependent on structure of isoflavones. They also showed that the glucuronidation was favored for isoflavones with hydroxyl group at position C-7.[90] Wang *et al.* (2006) work also supported this observation, and showed that prunetin, an isoflavone with a methoxy group at C-7, had the slowest metabolism and disposition in rat intestinal perfusion model as compared to other analogs with 7-OH group.[13]

Wen and Walle (2006) using Caco-2 cell culture model showed that the unmethylated polyphenols such as apigenin and chrysin showed 5-8 times lower absorption than corresponding methylated phenols. The study suggested that the structure determine the metabolic stability and hence the intestinal absorption of flavones.[162] But the compounds used in that study were either unmethylated or fully methylated, so it did not provide any information about if the methylation of one hydroxyl group position was more useful in increasing the metabolic stability than others.

Recent review articles explained various chemical structural properties of flavonoids which have shown to impact the metabolism of flavonoids by UGTs.[77, 94, 100] We found one report which studied the sulfation of 37 flavonoids in platelets and liver cytosol which gives some idea of the effect of structure on sulfation of flavonoids.[187] Ung and Nagar (2007) also studied the isoform specific sulfation of certain flavonoids.[204] But such reports are few and there is a need of further detailed studies in this field to obtain better information on the SMR of flavonoids metabolism by UGTs and SULTs.

The Caco-2 cell culture model is an FDA (Food and Drug Administration) recognized model for determining the absorption of drugs. *In silico* prediction models developed using the data of drug transport and permeability in Caco-2 cell, which can successfully predict the fate of drug absorption in human intestine, have been extensively published and used in pharmaceutical industry.[128, 180, 181, 183] But there are only occasional reports published for describing the structure-metabolism relationship (SMR) or predicting the

fate of drug metabolism and excretion in human intestine using Caco-2 cell model.[133, 135, 205]

The objective of present study was to systematically determine the role of efflux transporters in the excretion of regiospecific glucuronides of flavones in the Caco-2 cells. Another objective of the study was to study the effect of structural changes on the position of conjugation in flavones. These objectives might further be useful to enhance our knowledge about the SMR of flavonoids glucuronidation and sulfation in intestinal cells.

We studied the effect of structural changes on the conjugation of selected flavones during apical to basolateral transport of compounds in Caco-2 cell monolayers. We used seven congeneric flavones, three mono-hydroxyflavones, 4'-hydroxyflavone (4'HF), 5-hydroxyflavone (5HF), 7-hydroxyflavone (7HF); three di-hydroxyflavones, 5,4'-dihydroxyflavone (5,4'DHF), 5,7-dihydroxyflavone (5,7DHF, chrysin), 7,4'-dihydroxyflavone (7,4'DHF); and 5,7,4'-trihydroxyflavone (5,7,4'THF, apigenin) (Figure 4, pg 65), to systematically study how the addition of one or more –OH group at different position in the structure of flavones affects the position of conjugation in their structure, rates of metabolism of flavones and the excretion of their conjugates in the Caco-2 cells.

9.3. Materials and Methods

8.3.1. Materials

Cloned Caco-2 cells, TC-7, were a kind gift from Dr. Moniqué Rousset of INSERM U178 (Villejuit, France). 4'HF, 5HF, 7HF 5,4'DHF, 5,7DHF (or chrysin), 7,4'DHF, and 5,7,4'THF (or apigenin) were purchased from Indofine Chemicals (Somerville, NJ). Recombinant human UGT isoforms (commercially known as "supersomes") were purchased from Biosciences (Woburn, MA). Uridine diphosphoglucuronic acid (UDPGA), β-Glucuronidase, alamethicin, D-saccharic-1,4-lactone monohydrate, magnesium chloride, and Hanks' balanced salt solution (powder form) were purchased from Sigma-Aldrich (St Louis, MO). All other materials (typically analytical grade or better) were used as received.

9.3.2. Solubility and stability of the tested flavonoids

Solubility and stability (with or without 0.1% vitamin C) of the tested flavonoids were established at the experimental conditions as per the method explained in section 3.1 (Chapter 3).

9.3.3. Transport experiments in the Caco-2 cell culture model

The culture conditions for growing Caco-2 cells and transport experiment protocols were same as described in sections 7.3.3 and 7.3.4, respectively (Chapter 7). A 100µL of 94%

acetonitrile/6% glacial acetic acid containing 50 μM of testosterone (for 5HF, 7HF, 7,4'DHF) or formononetin (for 4'HF, 5,4'DHF, 5,7DHF and 5,7,4'THF) as the internal standard and preservative.

9.3.4. Preparation of Caco-2 cell lysate for glucuronidation studies and measuring microsomal protein concentrations and the cellular concentrations of flavonols and their conjugates in monolayers

Cell lysates preparations were same as described in sections 7.3.5 and 7.3.6, respectively (Chapter 7).

9.3.5. Measurement of protein concentration and glucuronidation activities of cell lysate

Protein concentrations and glucuronidation activities of cell lysates were measured as per the method described in sections 7.3.7 and 7.3.8, respectively (Chapter 7). The glucuronidation reaction was stopped by the addition of 50μL of 94% acetonitrile/6% glacial acetic acid containing 50 μM of testosterone (for 5HF, 7HF, 7,4'DHF) or formononetin (for 4'HF, 5,4'DHF, 5,7DHF and 5,7,4'THF) as the internal standard.

9.3.6. UPLC analysis of flavones and their conjugates

We analyzed seven flavones and their respective conjugates by using the following common method: system, Waters Acquity UPLC with photodiode array detector and

Empower software; column, BEH C_{18}, 1.7 μm, 2.1 × 50 mm; flow rate 0.45 mL/min and injection volume, 10μL. Two different set of mobile phase A, mobile phase B and gradients conditions were used to analyze the compounds are. For 4'HF, 7HF and 5,7,4'THF, mobile phase A, 100% aqueous buffer (2.5mM NH_4Ac, pH 4.5); mobile phase B, 100% acetonitrile; and gradient, 0 to 2min, 10-20% B, 2 to 3 min, 20–70%B, 3 to 3.5 min, 70%B, 3.5 to 4.0 min, 70-90% B, 4.0 to 4.5 min, 90-10% B, and 4.5 to 5.0 min, 10% B. For 5HF, 5,4'DHF, 5,7DHF and 7,4'DHF, mobile phase A, 100% aqueous buffer (2.5mM NH_4Ac, pH 7.4); mobile phase B, 100% methanol; and gradient 0 to 2min, 10-20% B, 2 to 3 min, 20–40%B, 3 to 3.5 min, 40–50%B, 3.5 to 4.0 min, 50-70% B, 4.0 to 5.0 min, 70-90% B, 5.0 to 5.5 min, 90-10% B, and 5.5 to 6.0 min, 10% B.

4HF, 7HF and their respective conjugates were analyzed at 320 nm and 310 nm, respectively. 5HF, 5,7DHF and their respective conjugates were analyzed at 268 nm, whereas 5,4'DHF, 7,4'DHF, 5,7,4'THF and their respective conjugates were analyzed at 340 nm. Testosterone and formononetin were analyzed at 254 and 268 nm, respectively. Linearity was established in the range of 0.6-20 μM (total 6 concentrations) for 5HF and 0.3-20 μM (total 7 concentrations) for other compounds. The LLOQ was 0.3 μM for 5HF and 0.16 μM for all the other compounds. Analytical methods for each compound were validated for inter-day and intra-day variation using 6 samples at three concentrations (20, 5 and 1.56 μM). Precision and accuracy for all compounds were in acceptable range of 85% to 115%.

9.3.7. Quantification of glucuronides and sulfates of flavones

The quantification of glucuronides and sulfates was done using the standard curve of the parent compound with a correction factor for difference in extinction coefficient of the compound and its metabolites. The correction factor was measured using the method as explained in section 3.5 and 3.6 (Chapter 3). The spectra of glucuronide and sulfate in most cases were almost overlapping (Figure 40). Based on this observation, the correction factor of glucuronide at a particular position was used for calculation of concentration of sulfate at the same position.

9.3.8. Confirmation of flavones conjugates structure by LC-MS/MS

Confirmation of flavone conjugate structure in LS-MS/MS was done as described in section 8.3.8 (Chapter 8)

9.3.9. Identification of position of glucuronidation and sulfation in the structure of flavonols by UV shift method

The identification of position of conjugation of flavonol glucuronides and sulfates was done similar to method described in section 7.3.12 (Chapter 7). The details of the method and its validation can be found in Singh *et al.* (2010).[173]

9.3.10. Data analysis and statistical analysis

Data and statistical analysis was done the same way as described in sections 7.3.13 and 7.3.14, respectively (Chapter 7). Linear regression plots for correlation with 95% confidence interval bands were generated using Statistica 6 (StatSoft, Inc., OK). Hyperbolic correlation curves were plotted using GraphPad Prism® (GraphPad software Inc., CA).

9.4. Results

9.4.1. Confirmation of flavones conjugates structure by LC-MS/MS

We conducted simple LC-MS/MS studies of the metabolites to show that all glucuronides and sulfates of the selected flavones formed during the transport study were mono-*O*-glucuronides and mono-*O*-sulfates (Figure A2, A9-A13, Appendix A). We did not find any di-glucuronide and di-sulfates of flavones in the present study. One mono-*O*-glucuronide and one mono-*O*-sulfate were detected for 4'HF (Figure A9, Appendix A), 5HF (Figure A9, Appendix A) and 7HF (Figure A10, Appendix A) in UPLC/MS/MS, whereas two mono-*O*-glucuronides and one mono-*O*-sulfate was detected for each 5,4'DHF (Figure A11, Appendix A), 5,7DHF (Figure A12, Appendix A), 7,4'DHF (Figure A13, Appendix A) and 5,7,4'THF (Figure A2, Appendix A) in the Caco-2 transport study samples. Also, mono-*O*-glucuronides of each flavone formed during glucuronidation reaction in cell lysate were same as found in the transport study, except 4'-*O*-G of 5,7,4'THF, which was very low in quantity and only detectable in concentrated samples in UPLC/MS/MS but not quantifiable in UPLC.

Similarly, mono-*O*-sulfates of 4'HF (Figure A9, Appendix A) and 5,4'DHF (Figure A11, Appendix A) from transport study samples though detected in UPLC/MS/MS but they were either below the limit of detection or quantification of UPLC or quantifiable only in the experimental samples taken at the last time point of the studies. Hence, they were not quantified and reported here.

9.4.2. Position of conjugates in the structure of flavones by UV shift method

We determined the position of glucuronidation based on the diagnostic shift in λ_{max} of Band I and Band II of UV spectra of glucuronides (Figure 41). Position of sulfation of flavones was determined by the rule of elimination and comparing the spectra of sulfates with the glucuronides. Table B3 (Appendix B) showed the λ_{max} of Band I and II of flavones and their conjugates and shift in λ_{max} of Band I and Band II of the conjugates as compared to their corresponding aglycone.

Glucuronidation in 5,4'DHF happened at position C-4', whereas sulfation happened at position C-5. For 5,7DHF, the first glucuronide was 5-*O*-Glu, while the second glucuronide and sulfate was conjugated at position C-7 (Figure 41). In case of 7,4'DHF, the position of conjugation of first and second glucuronides and sulfate were 7-*O*-G, 4'-*O*-G and 7-*O*-S, respectively, whereas, in case of 5,7,4'THF, the position of conjugation of first and second glucuronides and sulfate were 4'-*O*-G, 7-*O*-G and 7-*O*-S, respectively (Figure 41).

9.4.3. Determination of correction factor of conjugates of flavones

Amounts of conjugates formed were determined using the corrections factors for individual glucuronides of flavones as described in the method section. UGT isoforms and wavelength used in generation of correction factor and the correction factor for each glucuronides are detailed in Table C3 (Appendix C).

4’-Hydroxyflavone (4’HF)

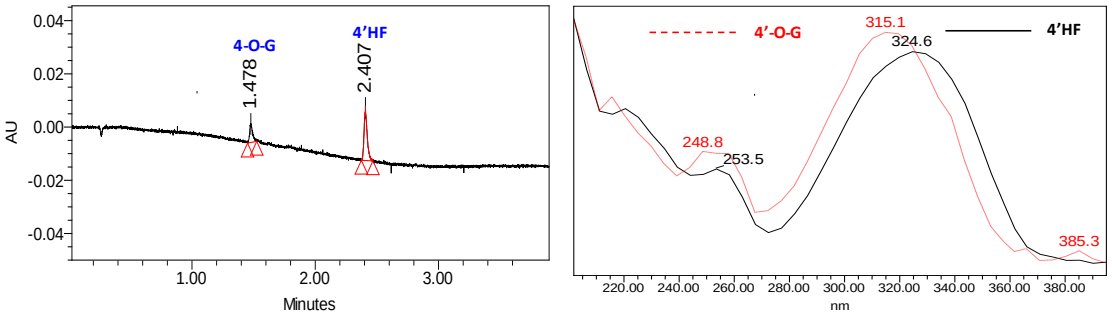

5-Hydroxyflavone (5HF)

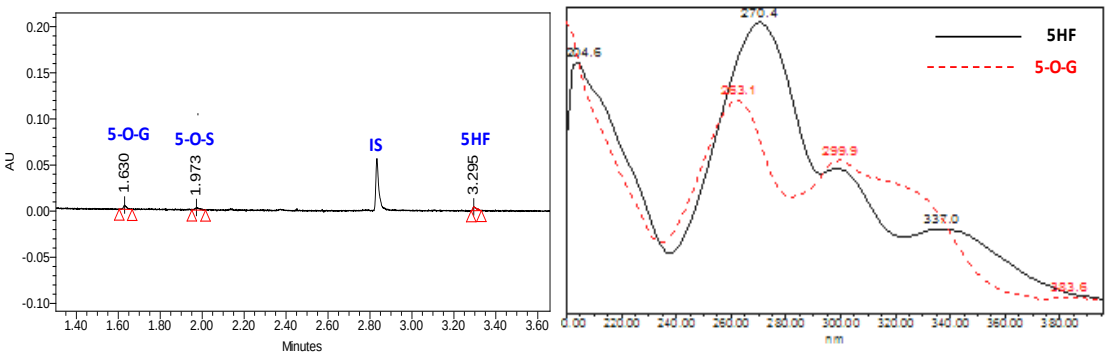

7-Hydroxyflavone (7HF)

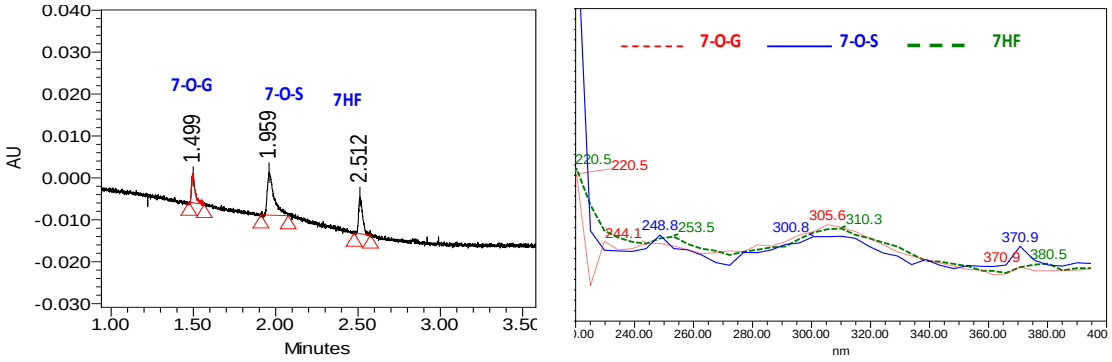

5,4’-dihydroxyflavone (5,4’DHF)

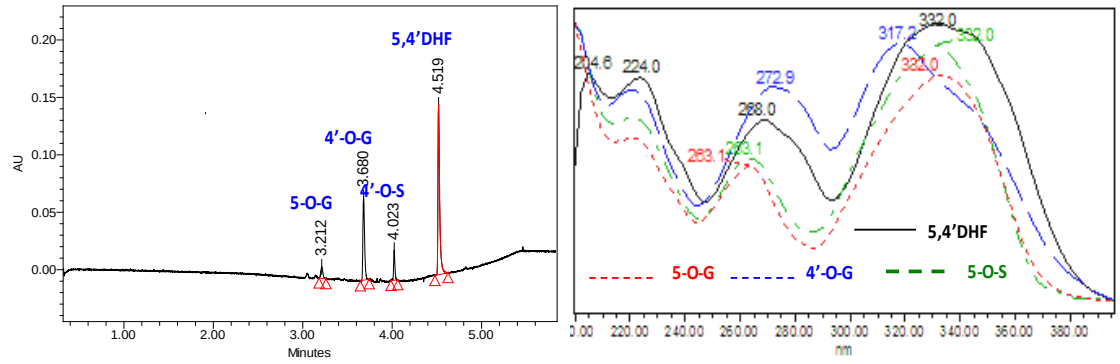

5,7-dihydroxyflavone (5,7DHF)

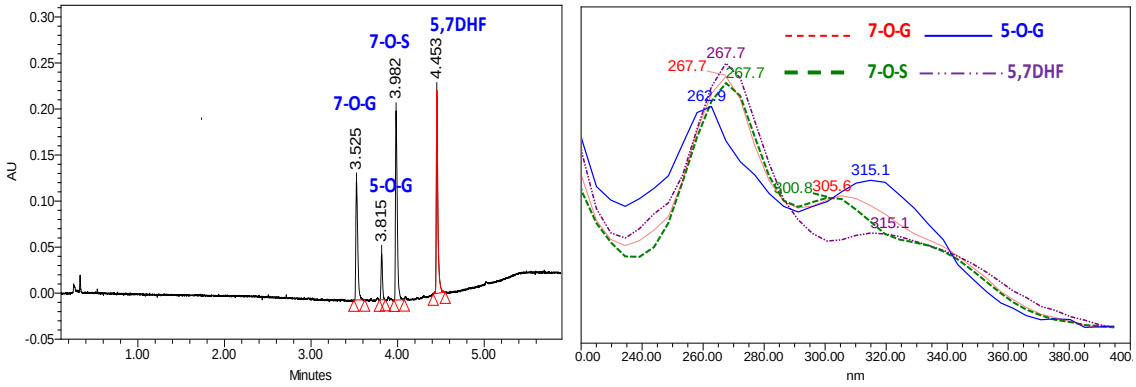

7,4’-dihydroxyflavone (7,4’DHF)

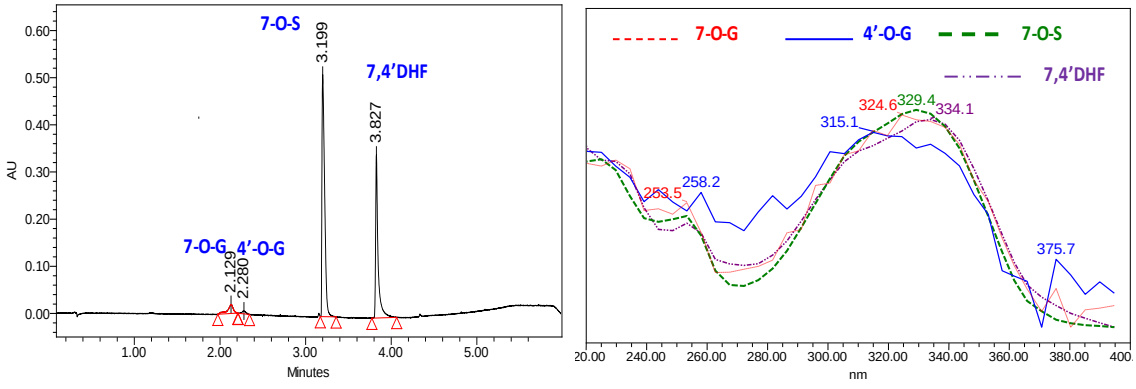

Apigenin or 5,7,4'-trihydroxyflavone (5,7,4'THF)

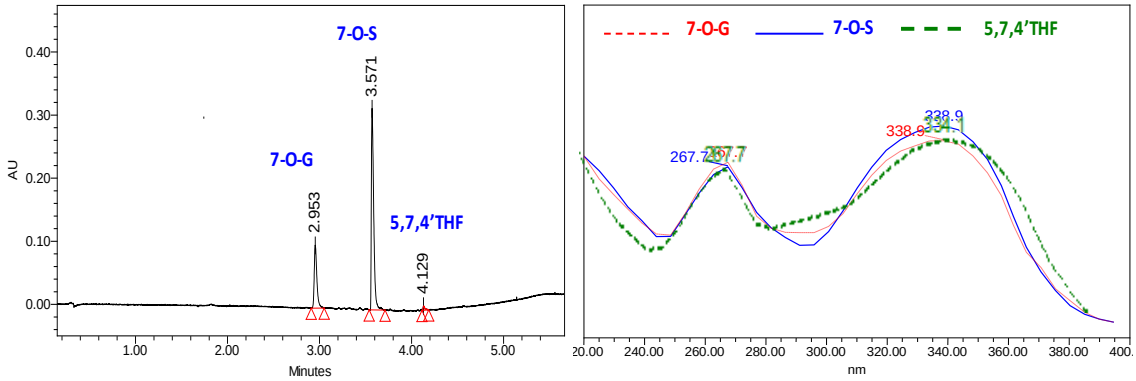

Figure 41. UPLC chromatograms and UV spectra of flavones and their respective glucuronides and sulfates in Caco-2 cell transport study samples

The correction factors were in the range of 0.72 (for 7-*O*-G of 5,7DHF) to 1.38 (for 5-*O*-G for 5,4'DHF). Correction factors of sulfates of flavones were not determined experimentally. Based on the comparative UV spectra of sulfate and glucuronide of a flavone conjugated at the same position, correction factors of sulfates conjugated at a particular position was assumed to be similar to the corresponding glucuronide. Although this assumption was confirmed in the case of genistein (not shown), it may need to be validated with appropriate experiments in the future.

9.4.4. Excretion rates of conjugates of flavones in Caco-2 cell lysate

All flavones excreted both glucuronides and sulfates except 4'HF and 5,4'DHF (Figure 42), which excreted only small amount of sulfates on the apical side in the 4 hour samples of transport of aglycone across Caco-2 cell monolayer. In most cases, metabolism through glucuronidation pathway was more important than sulfation, except for 7,4'DHF and 5,7,4'THF, which more sulfate was excreted than glucuronides during Caco-2 cell transport. The rates of excretion of total conjugates (glucuronides plus sulfates) of flavones followed the following rank order: 5,7,4'THF (24.23 ± 0.29) > 5,7DHF (15.30 ± 0.34) > 7,4'DHF (12.42 ±0.12) > 7HF (10.37 ± 0.41) > 5HF (4.91 ± 0.49) ~ 4'HF (4.57 ± 0.13) ~ 5,4'DHF (4.17 ± 0.12) nmol/hr/mg of protein. There was no significant difference between the excretion rates of total conjugates 4'HF, 5HF and 5,4'DHF ($p<0.05$) (Figure 42).

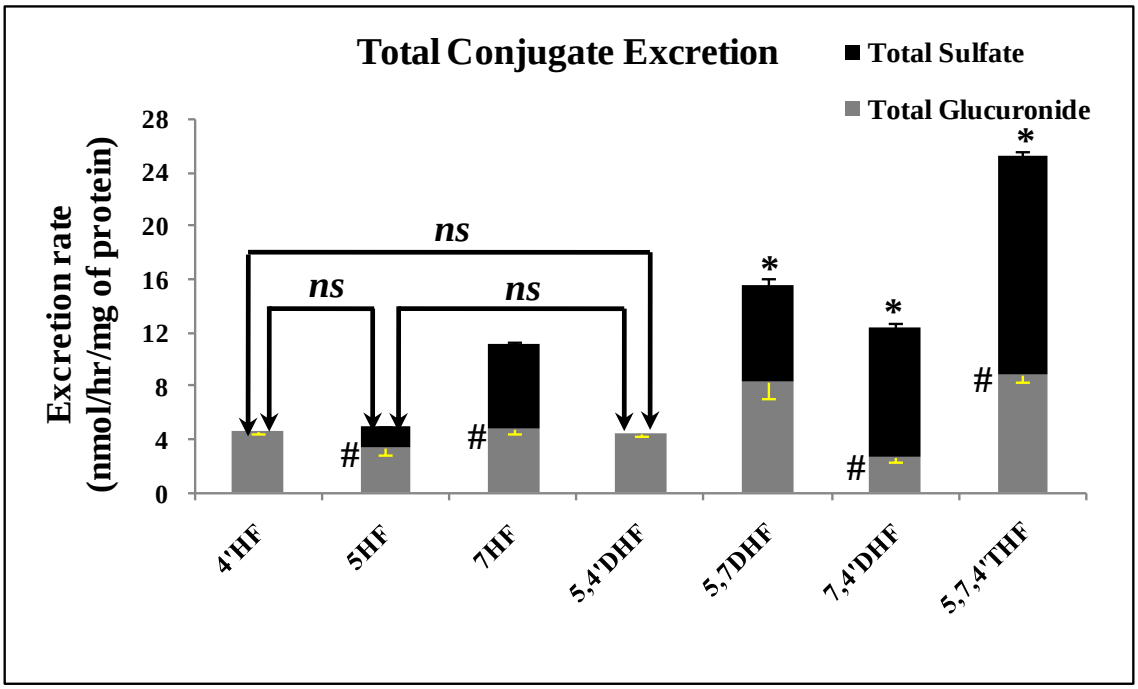

Figure 42. Excretion of conjugates in Caco-2 cell monolayer.
Rates of excretion of conjugates on AP and BL side during AP (pH =7.4) to BL (pH =7.4) transport of flavones (at 10 µM concentration, 5µM for 5HF) in the Caco-2 cell monolayer at 37ºC were calculated as the slope of amount of conjugates excreted vs time profile in Figures F5a-F5d (Appendix F), using only the first two data points of each profile, i.e., 1 and 1.5 hrs for 5,7DHF and 5,7,4'THF and 1 and 2 hr for all other flavones. Rates of excretion for each flavone were normalized to the corresponding protein concentration of experimental monolayer of each flavone. Each bar is the average of three determinations, and the error bars are the standard deviations of the mean (n=3). # on the side of each bar represents the significant difference between, AP and BL excretion of conjugates of each flavones ($p<0.05$). * on the top of each bar represents that the excretion rates of total (AP+BL) conjugates of the compound was significantly different from the excretion rates of conjugates of all other compounds, respectively ($p<0.05$). Since most bars showed significant difference to the other bars, one with no significant difference (not significant, *ns*) was shown on the top ($p<0.05$) to make graphs easily readable.

Apart from these three pairs, all excretion rates of total conjugates of all flavones were significantly different from each other ($p<0.05$) (Figure 42).

9.4.5. Regiospecific glucuronidation of flavones in Caco-2 cells

We studied the formation (Figure 43A) and excretion (Figure 43B) of regiospecific glucuronides of flavones in Caco-2 cells. Flavones with free hydroxyl group at C-7 (5,7DHF, 7,4'DHF and 5,7,4'THF) were glucuronidated more significantly at C-7 than other positions ($p<0.05$) (Figures 43A). Also, 7-*O*-Glucuronides of 5,7DHF, 7,4'DHF and 5,7,4'THF always excreted faster than their other respective glucuronides ($p<0.05$) (Figures 43B). In cases of 5,4'DHF (di-hydroxyflavone without a free hydroxy group at C-7), the rates of glucuronide formation and excretion in Caco-2 cells favors the position C-4' more than C-5 ($p<0.05$) (Figures 43A-43B). There was no detectable amount of 5-*O*-G formed or excreted for 5,4'DHF. This showed that C-7 was the most favored position of glucuronidation in di- and tri- hydroxyflavones with a free hydroxy group at C-7.

9.4.6. Regiospecific sulfation of flavones in Caco-2 cells

We also studied the excretion of regiospecific sulfates of flavones in Caco-2 cells (Figure 44). All flavones excreted quantifiable amount of sulfates in Caco-2 cells except 4'HF and 5,4'DHF (Figure 44).

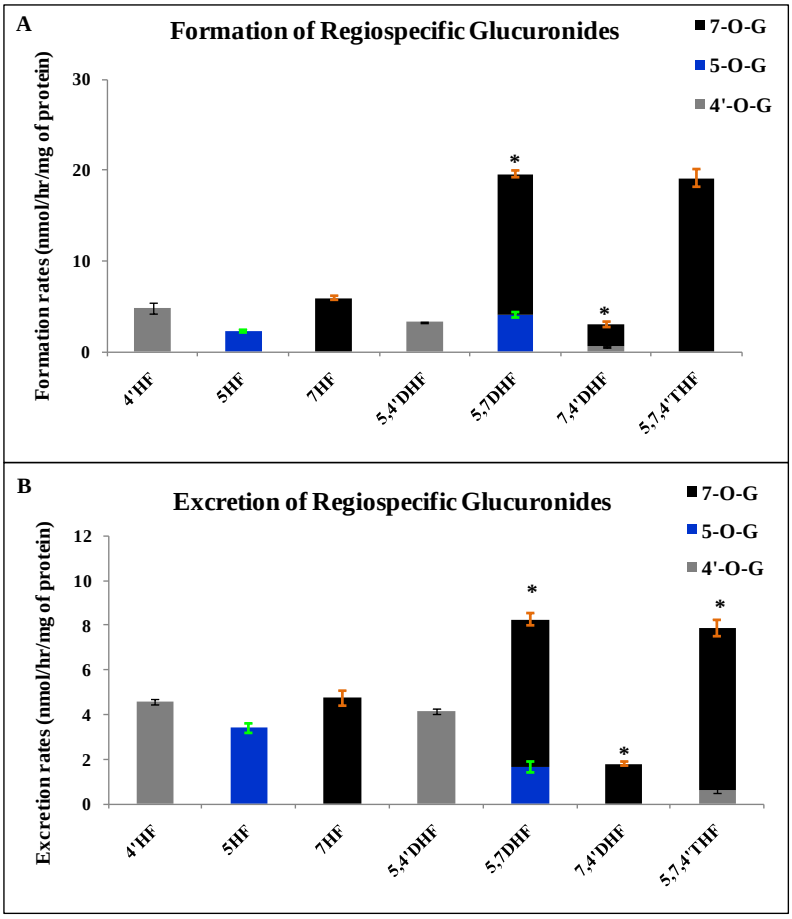

Figure 43. Regiospecific glucuronides formation (A) and excretion (B) of flavones in Caco-2 cells.

Formation rates of glucuronides of flavones were measured using Caco-2 cell lysate (protein concentration ~0.1mg/ml) at 10 µM substrate concentration incubated for 2 hrs at 37ºC. Rates of total (AP and BL) excretion of glucuronides of flavones in AP to BL transport in Caco-2 cell monolayer were calculated as the slope of amount of individual glucuronide excreted on both AP and BL side vs time profile in Figures F5a-F5b and Figures F6a-F6c (Appendix F), using only the first two data points of each profile. Rates of excretion of glucuronide(s) for each flavone were normalized to the corresponding protein concentration of experimental monolayer of each flavone. Each bar is the average of three determinations, and the error bars are the standard deviations of the mean (n=3). * on the top of each bar represents that the formation/ excretion rates of all glucuronides are significantly different from each other ($p<0.05$).

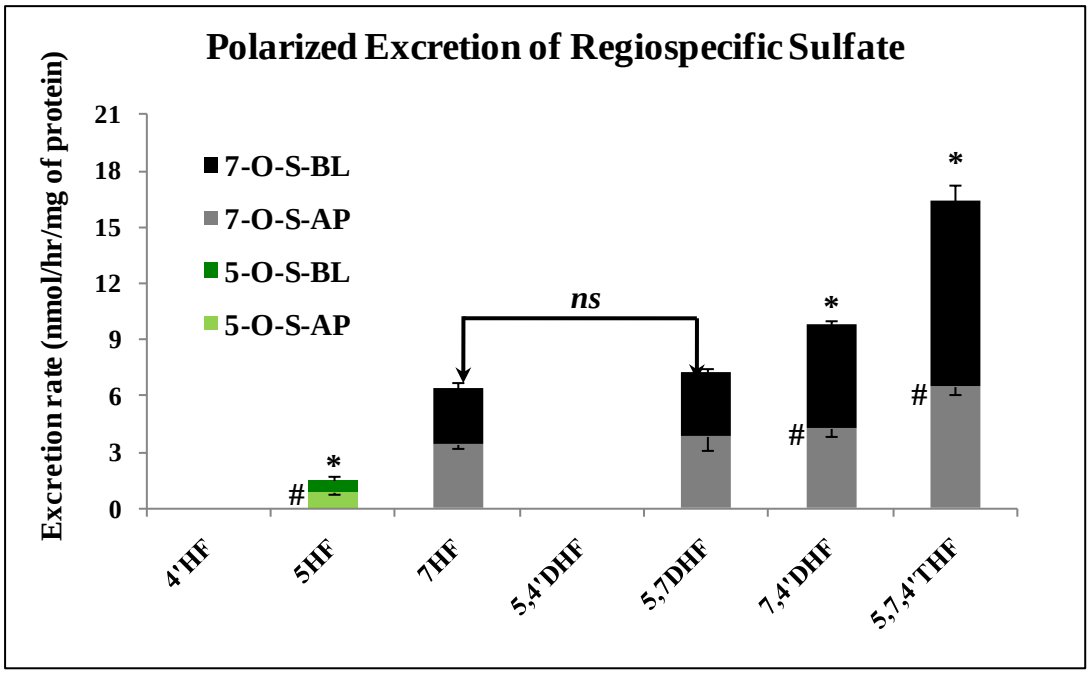

Figure 44. Polarized excretion of regiospecific sulfates in Caco-2 cell monolayer. Rates of excretion of sulfates on AP and BL side during AP (pH =7.4) to BL (pH =7.4) transport of flavones (at 10 µM concentration, 5µM for 5HF) in the Caco-2 cell monolayer at 37ºC were calculated as the slope of amount of sulfates excreted vs time profile in Figures F5c-F5d (Appendix F), using only the first two data points of each profile, i.e., 1 and 1.5 hrs for 5,7DHF and 5,7,4'THF and 1 and 2 hr for all other flavones. Rates of excretion for each flavone were normalized to the corresponding protein concentration of experimental monolayer of each flavone. Each bar is the average of three determinations, and the error bars are the standard deviations of the mean (n=3). # on the side of each bar represents the significant difference between, AP and BL excretion of sulfates of each flavones ($p<0.05$). * on the top of each bar represents that the excretion rates of total (AP+BL) sulfates of the compound was significantly different from the excretion rates of sulfates of all other compounds, respectively ($p<0.05$). Since most bars showed significant difference to the other bars, one with no significant difference (not significant, *ns*) was shown on the top ($p<0.05$) to make graphs easily readable.

Sulfates of 4'HF (Figure A9b, Appendix A) and 5,4'DHF (Figure A11c, Appendix A) were detected in the concentrated (10X) transport samples in UPLC/MS/MS. All flavones with a free hydroxyl group at position C-7 formed one mono-*O*-sulfate i.e. 7-*O*-S ($p<0.05$) (Figures 44). 4'HF, 5HF, and 5,4'DHF, the flavones with no free hydroxyl group at position C-7, formed 4'-*O*-S, 5-*O*-S and 5-*O*-S, respectively.

9.4.7. Formation rates of glucuronides of flavones in Caco-2 cell lysate

We incubated 10µM (5µM for 5HF) of each flavone with Caco2 Cell lysate (final protein concentration ~0.1 mg/ml) for 2 hours and measured the concentration of glucuronide(s) generated. Formation rate of each glucuronide was calculated as concentration of glucuronide formed per unit time. The rate of formation of total glucuronides of a flavone was calculated as the sum of rates of formation of all glucuronides of that flavone. The rates of formation of total glucuronides of flavones followed the following rank order: 5,7DHF (19.55 ± 0.36) ~ 5,7,4'THF (19.16 ± 0.92) > 7HF (5.89 ± 0.24) ~ 4'HF (4.71 ± 0.55) > 5,4'DHF (3.29 ±0.09) ~ 7,4'DHF (2.98 ±0.20) ~ 5HF (2.28 ± 0.12) nmol/hr/mg of protein (Figure 45).

The formation rates of total glucuronides of flavones 4'HF and 7HF; 5,4'DHF and 7,4'DHF; and 5,7DHF and 5,7,4'THF were not significantly different ($p<0.05$) (Figure 45). Also, formation rate of glucuronide of 5HF was not significantly different from the formation rates of total glucuronides of 5,4'DHF and 7,4'DHF ($p<0.05$) (Figure 45).

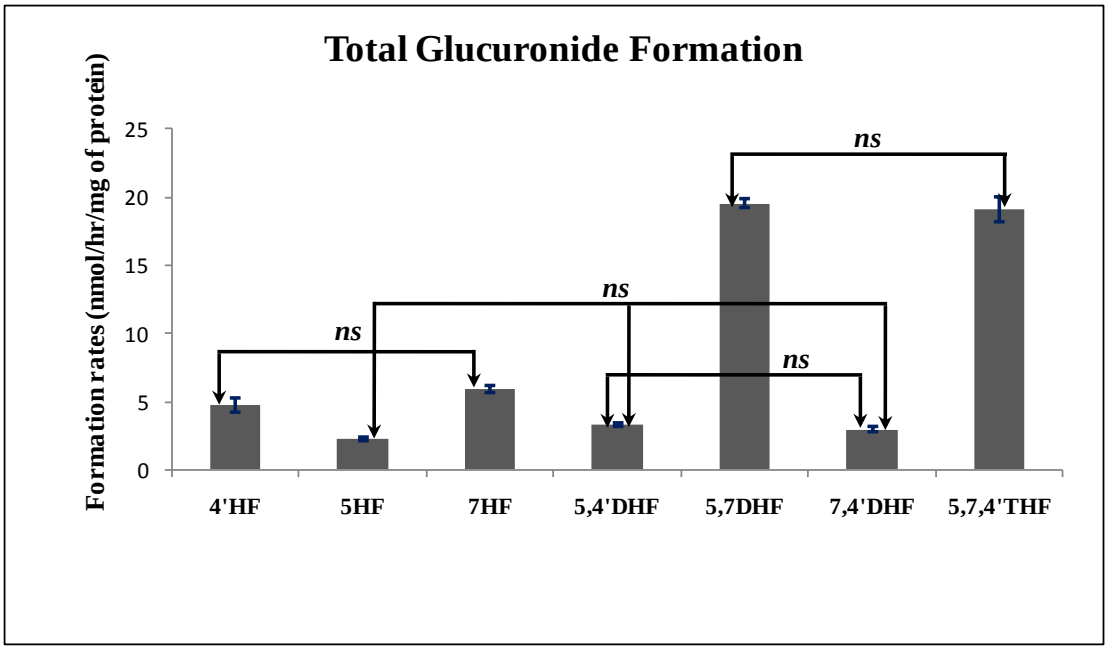

Figure 45. Formation of total glucuronides of flavones in Caco-2 cells.
Formation rates of glucuronides of flavones were measured using Caco-2 cell lysate (protein concentration ~0.1mg/ml) at 10 µM substrate concentration (5 µM for 5HF) incubated for 2 hrs at 37ºC. Each bar is the average of three determinations, and the error bars are the standard deviations of the mean (n=3). Since most bars showed significant difference to the other bars, ones with no significant difference (not significant, *ns*) were shown on the top ($p<0.05$) to make graphs easily readable.

Apart from the above-mentioned pairs, all other flavones showed significant difference among the rates of formation of total glucuronides ($p<0.05$) (Figure 45). The lowest glucuronidated flavones (5HF, 5,4'DHF and 7,4'DHF) were about 6 times less rapidly metabolized than the highest glucuronidated flavones (5,7DHF and 5,7,4'THF) ($p<0.05$) (Figure 45). This indicated that hydroxyl groups at C-5 and C-7 together in the structure of the flavone significantly favors the rates of glucuronidation in Caco-2 cells.

Among the regiospecific glucuronides, 5-*O*-G and 4'-*O*-G of 5,7DHF and 7,4'DHF respectively were formed about ~ 4 times slower than their respective 7-*O*-G ($p<0.05$) (Figure 43A). Whereas for 5,7,4'THF, no other glucuronide except 7-*O*-G was detected in the glucuronidation experiment with Caco-2 cell lysate (Figure 43A). This again indicated that 7-*O*-G was more favored position for glucuronidation in flavones.

9.4.8. Excretion rates of glucuronides of flavones in Caco-2 cell monolayer

We loaded 10 µM (5 µM for 5HF) of the seven selected flavones solution in pH 7.4 HBSS buffer on the apical side of the Caco-2 cell monolayer. During the course of transport of the flavonoids from AP to BL side, glucuronides were excreted to both sides of the cell monolayer, and the amounts of glucuronides of a flavone excreted were measured. The amounts of total glucuronides (i.e. sum of amounts of all glucuronides of a flavone) excreted increased linearly as a function of time up to for 1.5 hour for 5,7DHF and 5,7,4'THF and up to 2 hours for all other flavones (Figures F5a-F5b, Appendix F).

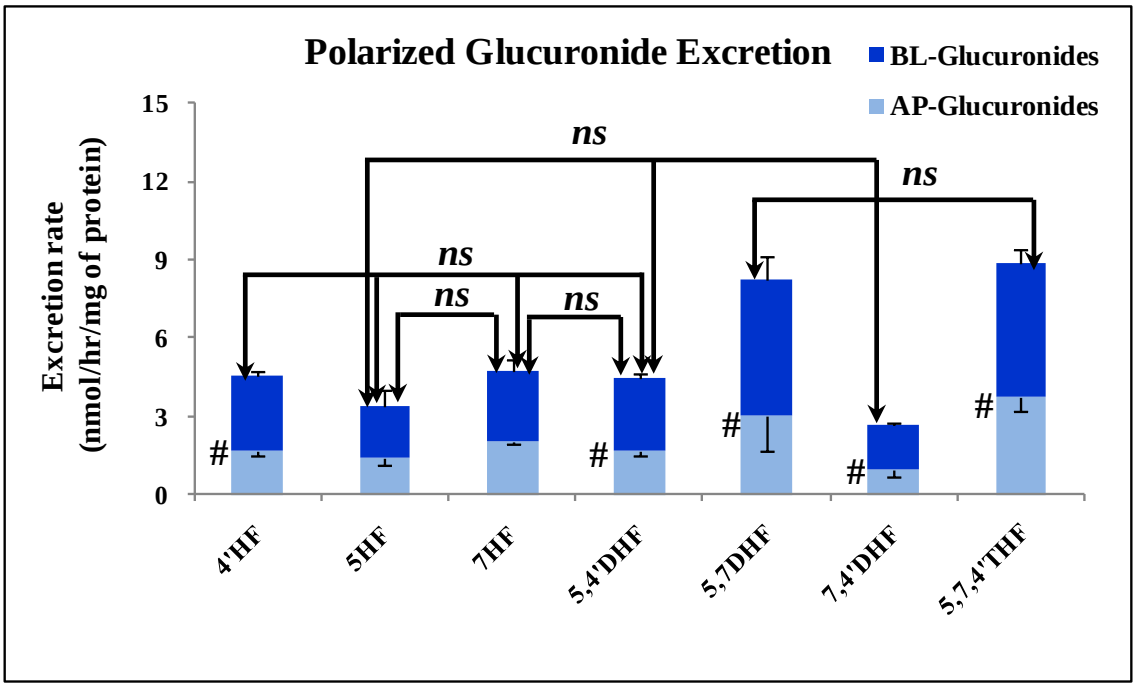

Figure 46. Polarized excretion of total glucuronides in Caco-2 cell monolayer.
Rates of excretion of total glucuronides on AP and BL side during AP (pH =7.4) to BL (pH =7.4) transport of flavones (at 10 µM concentration, 5µM for 5HF) in the Caco-2 cell monolayer at 37ºC were calculated as the slope of amount of glucuronides excreted vs time profile in Figures F5a-F5b (Appendix F), using only the first two data points of each profile, i.e., 1 and 1.5 hrs for 5,7DHF and 5,7,4'THF and 1 and 2 hr for all other flavones. Rates of excretion for each flavone were normalized to the corresponding protein concentration of experimental monolayer of each flavone. Each bar is the average of three determinations, and the error bars are the standard deviations of the mean (n=3). # on the side of each bar represents the significant difference between, AP and BL excretion of total glucuronides (A) and sulfate (B) of each flavone ($p<0.05$). Since most bars showed significant difference to the other bars, ones with no significant difference (not significant, *ns*) were shown on the top ($p<0.05$) to make graphs easily readable.

The rates of excretion of flavones total glucuronides to AP and BL sides were calculated as the slope of amount of conjugate excreted versus time profile, using only the first two data points of each profile, i.e., 1 and 1.5 hrs for 5,7DHF and 5,7,4'THF and 1 and 2 hrs for all other flavones. We choose only the first two data points, as in most cases, they fell in the linear portion of the curve (Figures F5a-F5b, Appendix F). The rates of excretion of all glucuronides and sulfates of a flavone were normalized against the corresponding protein concentration of the Caco-2 cells monolayers used in its transport and rates of excretion were reported as nmol/hr/mg of protein.

The rates of excretion of total glucuronides of flavones followed the following rank order: 5,7,4'THF (8.83 ± 0.55) ~ 5,7DHF (8.27 ± 1.10) > 7HF (4.75 ± 0.32) ~ 5,4'DHF (4.49 ± 0.14) ~ 4'HF (4.57 ± 0.13) > 5HF (3.39 ± 0.47) > 7,4'DHF (2.65 ± 0.22) nmol/hr/mg of protein (Figure 46), which indicated that hydroxyl groups at C-5 and C-7 together in the structure of the flavone significantly favors the rates of glucuronide excretion in Caco-2 cell monolayer. This was similar to rates of formation in Caco-2 cell lysate (Figure 45), though the magnitude of difference was more in case of formation rates (6 folds) than in excretion rates (2-3 folds) ($p<0.05$).

Rates of excretion of glucuronides of most flavonol were comparable, except for the total glucuronides of 5,7DHF and 5,7,4'THF which excreted about 2-3 times faster than the total glucuronides of other flavones ($p <0.05$) (Figure 46). The rates of excretion of

glucuronides of 5,7DHF and 5,7,4'THF; and 7HF and 7,4'DHF were not significantly different from each other ($p < 0.05$) (Figure 46). The excretion rate of 4'HF-glucuronide did not show any significant difference from the excretion rates of glucuronides of 5HF, 7HF and 5,4'DHF ($p < 0.05$) (Figure 46). Additionally, the excretion rate of 5HF-glucuronide was not different from the excretion rates of glucuronides of 7HF, 5,4'DHF and 7,4'DHF ($p < 0.05$) (Figure 46).

Among the regiospecific glucuronides, 4'-*O*-G of 5,7,4'THF was excreted ~12 folds slower than their respective 7-*O*-G ($p<0.05$) (Figure 43B). This was different from rates of formation as no 4'-*O*-G was detected during glucuronidation of 5,7,4'THF in Caco-2 cell lysate (Figure 43A). In case of 5,7DHF, 5-*O*-G was excreted about ~4 folds slower than 7-*O*-G, which was similar to the difference in their rates of formation ($p<0.05$) (Figures 43A-43B). For 7,4'DHF, 4'-*O*-G was excreted only about ~2 folds slower than 7-*O*-G, whereas 4'-*O*-G was formed about ~4 folds slower than 7-*O*-G in Caco-2 cells ($p<0.05$) (Figures 43A-43B).

9.4.9. Excretion of sulfates of flavones in Caco-2 cells monolayer

The rates of excretion of sulfate showed the following rank order: 5,7,4'THF (16.36 ± 0.65) > 7,4'DHF (9.77 ±0.33) > 5,7DHF (7.22 ± 0.58) > 7HF (5.62 ± 0.26) > 5HF (1.52 ± 0.14) nmol/hr/mg of protein. The excretion rates of 7-*O*-sulfates of 7HF and 5,7DHF were not significantly different from each other ($p<0.05$) (Figure 44).

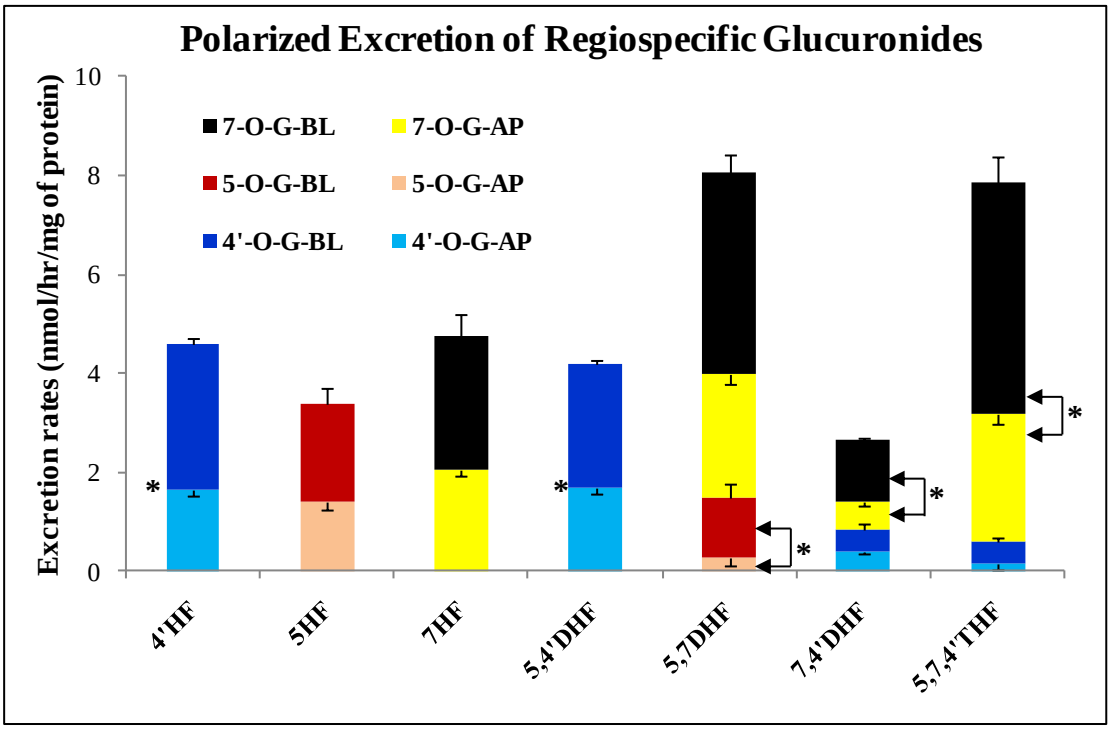

Figure 47. Polarized excretion of regiospecific glucuronides of flavones in Caco-2 cell monolayer.

Rates of total (AP and BL) excretion of regiospecific glucuronides of flavones in AP to BL transport in Caco-2 cell monolayer were calculated as the slope of amount of individual glucuronide excreted on both AP and BL side vs time profile in Figures F5a-F5b and Figures F6a-F6c (Appendix F), using only the first two data points of each profile, i.e., 1 and 1.5 hrs for 5,7DHF and 5,7,4'THF and 1 and 2 hr for all other flavones. Rates of excretion of glucuronide(s) for each flavone were normalized to the corresponding protein concentration of experimental monolayer of each flavone. Each bar is the average of three determinations, and the error bars are the standard deviations of the mean (n=3). * on the side of each bar represents the significant difference between, AP and BL excretion of the particular regiospecific glucuronide of each flavone ($p<0.05$).

Except this one pair, the excretion rates of sulfates of all flavones were significantly different from each other ($p<0.05$) (Figure 44).

9.4.10. Polarized excretion of glucuronides and sulfates of flavones in Caco-2 cell monolayer

Glucuronides of all flavonols showed preferable basolateral excretion, except 5HF and 7HF, which did not show any significant difference between AP and BL excretion of their glucuronides ($p <0.05$) (Figure 46). BL/AP ratio for flavonols glucuronides excretion ranged from 1.31 (for 7HF) to 1.8 (for 7,4'DHF) (Figure 46). Among the regiospecific glucuronides, 5-*O*-G (BL/AP = 2.6), 7-*O*-G (BL/AP = 2.24) and 7-*O*-G (BL/AP = 1.8) of 5,7DHF, 7,4'DHF and 5,7,4'THF, respectively, showed preferable basolateral excretion, whereas 7-*O*-G, 4'-*O*-G and 4'-*O*-G of 5,7DHF, 7,4'DHF and 5,7,4'THF, respectively, did not show any significant difference between their AP and BL excretion ($p <0.05$) (Figure 47). This showed that preference of excretion on AP or BL side was dependent not only on the site of glucuronidation but also on the structure of the flavones.

On the other hand, sulfates of all flavonols showed varied excretion behavior. 7-*O*-sulfates of 5,7DHF and 5,7,4'THF showed preferable basolateral excretion. Whereas 7-*O*-sulfates of 7HF and 7,4'DHF did not show any significant difference between AP and BL excretion of their sulfates (Figure 44). 5-*O*-S of 5HF showed excreted preferably to

the apical side. BL/AP ratio for flavonols sulfates excretion ranged from 0.75 (for 5HF sulfate) to 1.5 (for 5,7,4'THF sulfate) (Figure 44).

9.4.11. Correlation of formation and excretion rates of glucuronides of flavones

We plotted the formation rates of total glucuronides of flavones against their corresponding AP, BL and total (AP+BL) excretion rates (Figures 45-46), and found very good correlation for AP (r^2 = 0.88) (Figure 48a), BL (r^2 = 0.94) (Figure 48b) as well as total excretion (r^2 = 0.94) (Figure 48c). When the formation rates of regiospecific glucuronides of flavones were plotted against their corresponding AP, BL and total (AP+BL) excretion rates (Figures 43A and 47), we again found decent correlation for AP (r^2 = 0.65) (Figure 49a), BL (r^2 = 0.81) (Figure 49b) as well as total excretion (r^2 = 0.76) (Figure 49c), though the correlations in case of regiospecific glucuronides excretion (Figure 49) were not as good as in the case of total glucuronides excretion (Figure 48).

9.4.12. Correlation of glucuronides of flavones and flavonols based on position of glucuronidation

To understand if there was any relation between the regiospecific glucuronidation and good correlation between the excretion and formation rates, we studied the correlation based on position of glucuronidation. Formation rates of 4'-*O*-glucuronides of flavonoids from both flavonol and flavone sub-classes were against their corresponding AP, BL and total excretion rates (Figure 50).

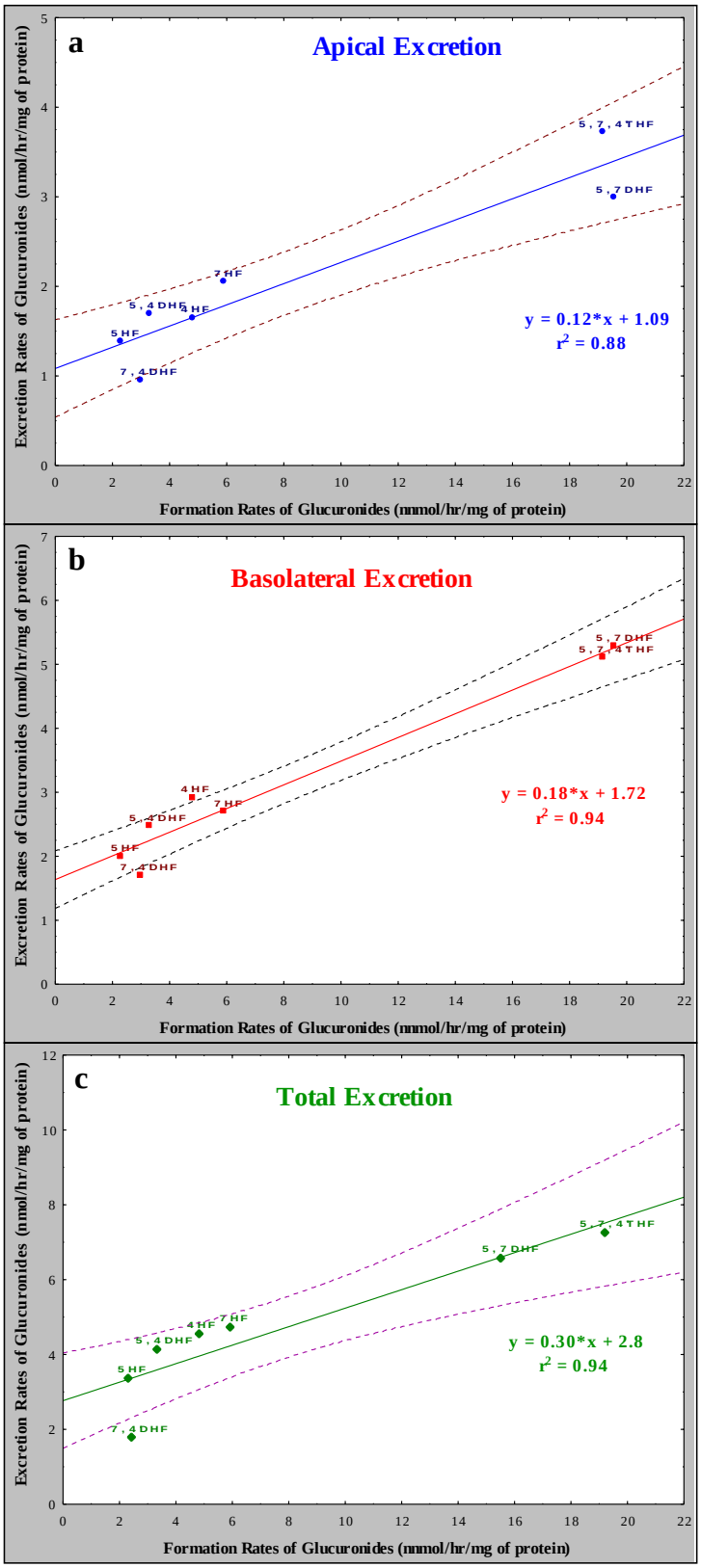

Figure 48. Correlation between rates of formation and excretion of total glucuronides (sum of all glucuronides of a flavone) of flavones in Caco-2 cells. The apical (a), basolateral (b) and total (apical plus basolateral) (c) rates of excretion of glucuronides of flavones excreted in intact Caco-2 cell monolayer were plotted against their corresponding rates of formation in Caco-2 cell lysate. Each data point represents the average of three determinations.

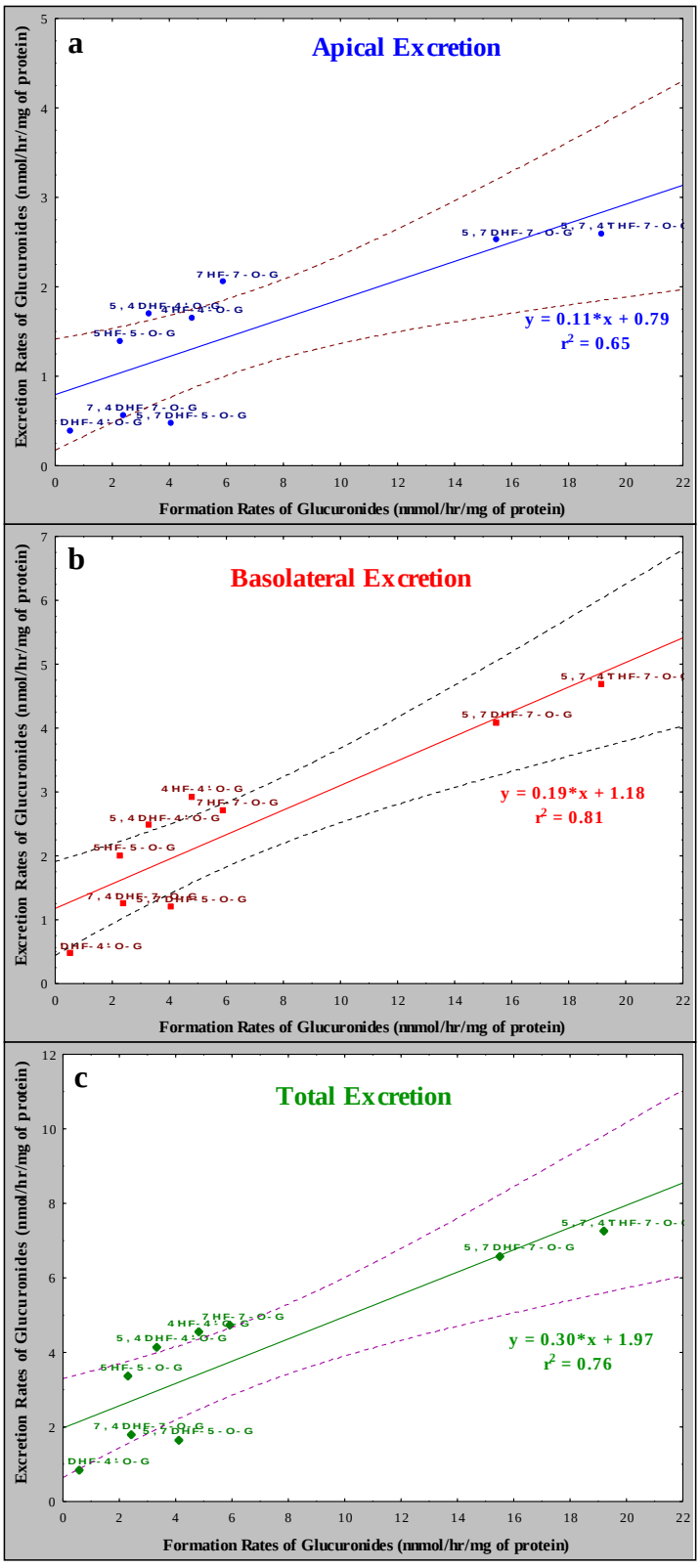

Figure 49. Correlation between rates of formation and excretion of regiospecific glucuronides of flavones in Caco-2 cells.

The apical (a), basolateral (b) and total (apical plus basolateral) (c) rates of excretion of all regiospecific glucuronides of flavones excreted in intact Caco-2 cell monolayer were plotted against their corresponding rates of formation in Caco-2 cell lysate. Each data point represents the average of three determinations.

Similar plots were made for the 3-*O*-glucuronides of flavonols (Figure 51) as well as the 7-*O*-glucuronides of flavonols and flavones (Figure 52). The formation rates of 4'-*O*-glucuronides of flavones (Figure 43A) and flavonols (Figure 36A, Chapter 8) were plotted against their corresponding AP, BL and total (AP+BL) excretion rates (Figures 43B and 47, and Figures 36B and 40 of Chapter 8).

We found decent correlation for AP (r^2 = 0.71) (Figure 50a), BL (r^2 = 0.62) (Figure 50b) as well as total excretion (r^2 = 0.76) (Figure 50c) for 4'-*O*-G. The slopes of the lines of best fit for AP, BL and total excretion of 4'-*O*-glucuronides of flavones and flavonols were 0.28, 0.44 and 0.71, respectively. The slope of line of best fit for total excretion was not close to 1. This indicated that the excretion rates were less than with the rates of formation of 4'-*O*-glucuronides, such that the excretion of 4'-*O*-glucuronides of flavones and flavonols by the efflux transporters was the rate limiting step in the disposition of 4'-*O*-glucuronides in the Caco-2 cell monolayers.

When the formation rates of only 3-*O*-glucuronides of flavonols (Figure 36A, Chapter 8) were plotted against their corresponding AP, BL and total (AP+BL) excretion rates (Figures 36B and 40, Chapter 8), a good correlation for AP (r^2 = 0.84) (Figure 51a), BL (r^2 = 0.78) (Figure 51b) as well as total excretion (r^2 = 0.80) (Figure 51c) was observed. The slopes of the lines of best fit for AP, BL and total excretion of 3-*O*-glucuronides of flavonols were 0.25, 0.7 and 0.95, respectively.

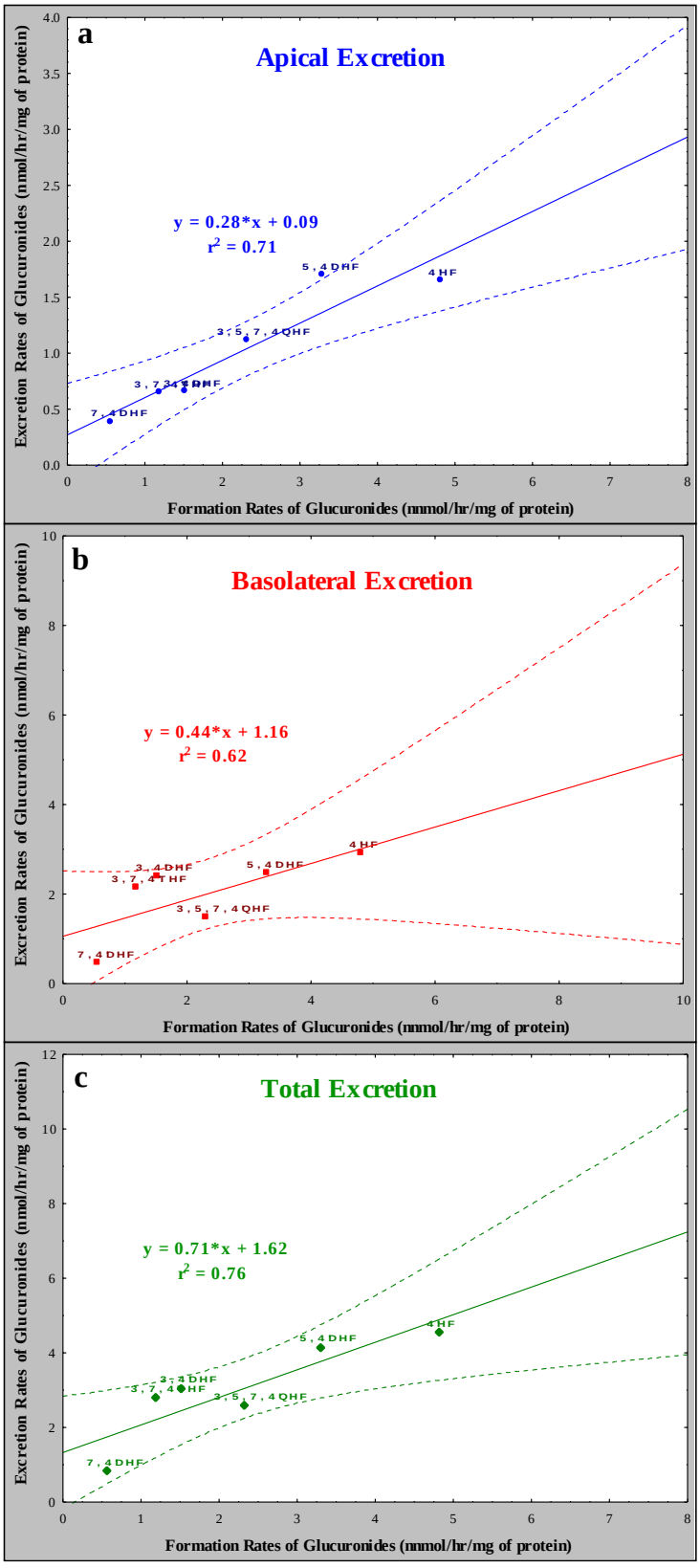

Figure 50. Linear correlation between rates of formation and excretion of 4'-*O*-glucuronides of flavones and flavonols in Caco-2 cells.
The apical (a), basolateral (b) and total (apical plus basolateral) (c) rates of excretion of 4'-*O*-glucuronides of flavones and flavonols excreted in intact Caco-2 cell monolayer were plotted against their corresponding rates of formation in Caco-2 cell lysate. The data for 4'-*O*-glucuronides of flavonols has been re-plotted here from Figures 36A-36B and 40, Chapter 8. Each data point represents the average of three determinations.

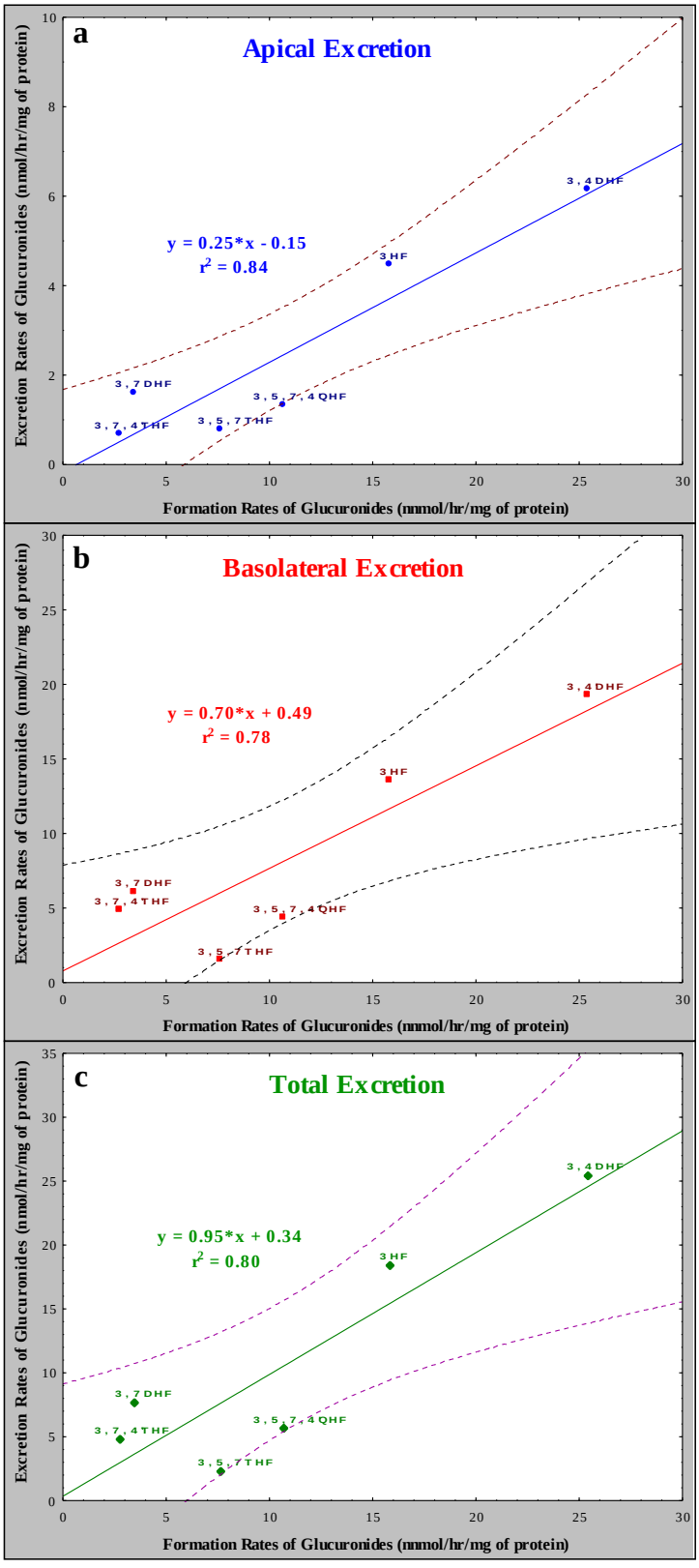

Figure 51. Linear correlation between rates of formation and excretion of 3-*O*-glucuronides of flavonols in Caco-2 cells.

The apical (a), basolateral (b) and total (apical plus basolateral) (c) rates of excretion of 3-*O*-glucuronides of flavonols excreted in intact Caco-2 cell monolayer were plotted against their corresponding rates of formation in Caco-2 cell lysate. The data for 3-*O*-glucuronides of flavonols has been re-plotted here from Figures 36A-36B and 40, Chapter 8. Each data point represents the average of three determinations.

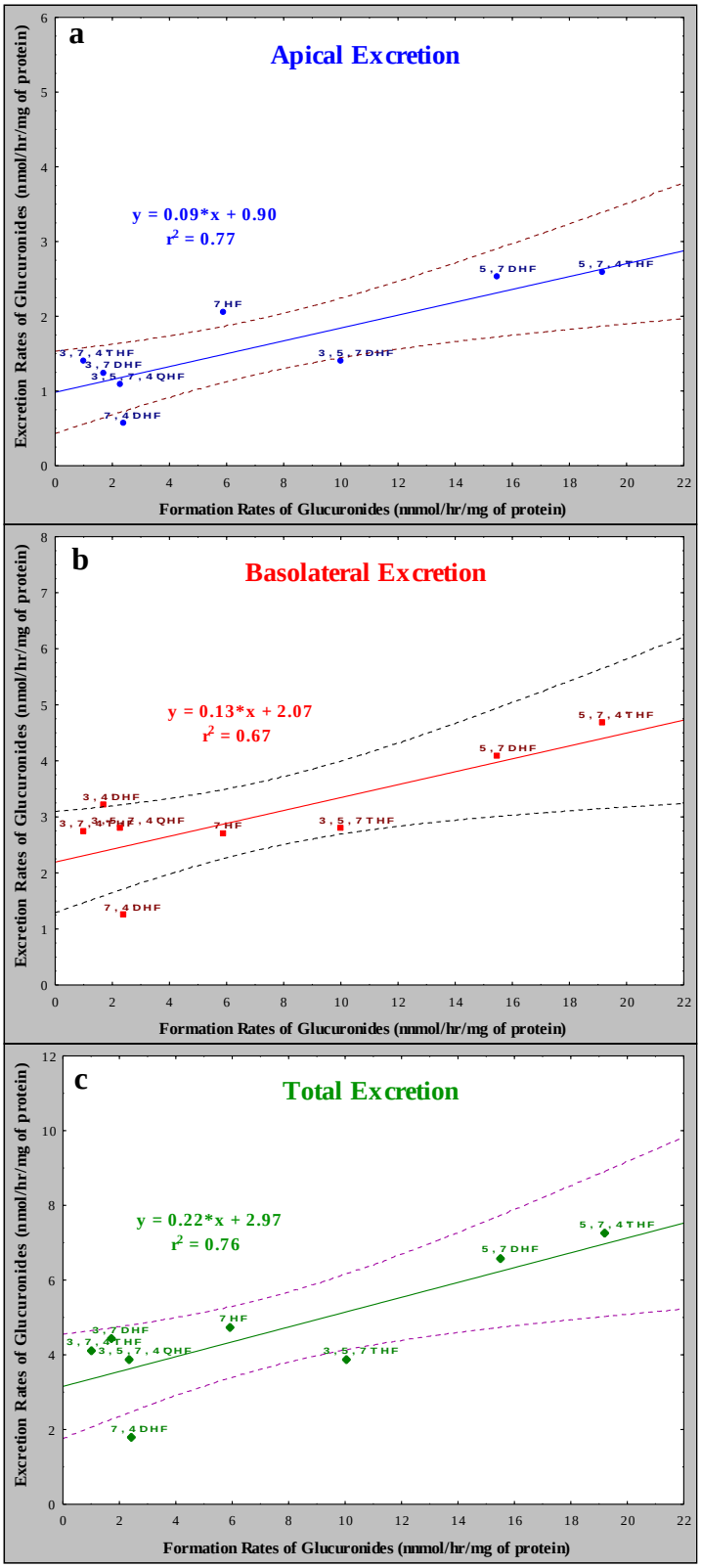

Figure 52. Linear correlation between rates of formation and excretion of 7-*O*-glucuronides of flavones and flavonols in Caco-2 cells. The apical (a), basolateral (b) and total (apical plus basolateral) (c) rates of excretion of 7-*O*-glucuronides of flavones and flavonols excreted in intact Caco-2 cell monolayer were plotted against their corresponding rates of formation in Caco-2 cell lysate. The data for 7-*O*-glucuronides of flavonols has been re-plotted here from Figures 36A-36B and 40, Chapter 8. Each data point represents the average of three determinations.

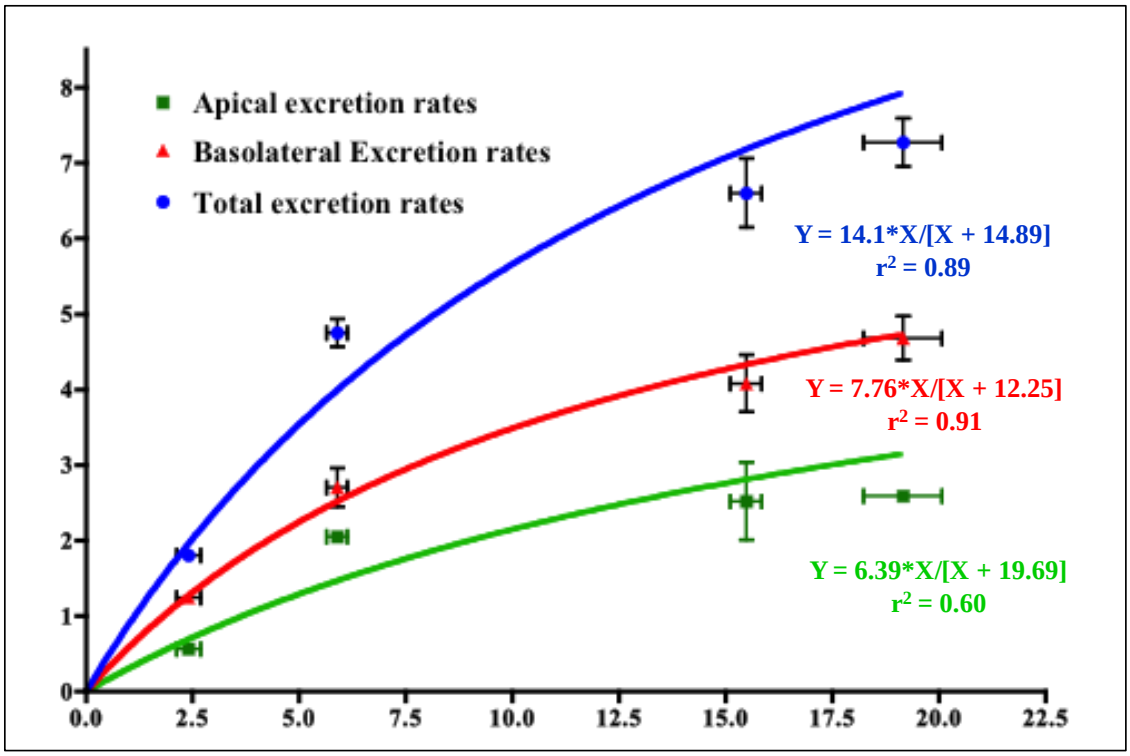

Figure 53. Hyperbolic correlations between rates of formation and the apical (green), basolateral (red) and total (blue) excretion of 7-*O*-glucuronides of flavones in Caco-2 cells.

The apical, basolateral and total (apical plus basolateral) rates of excretion of 7-*O*-glucuronides of flavones excreted in intact Caco-2 cell monolayer were plotted against their corresponding rates of formation in Caco-2 cell lysate. The equation of line of best fit was $Y=Y_{max}X/(X + X_c)$, where Y_{max} was the maximum rate of excretion that can be achieved by the efflux transporters in Caco-2 cell monolayers and X_c was the rate of formation by the UGTs at which half the Y_{max} can be achieved in Caco-2 cells. Each bar is the average of three determinations, and the error bars are the standard deviations of the mean (n=3).

The slope of line of best fit for total excretion was close to 1. This indicated that the excretion rates were comparable with the rates of formation of 3-*O*-glucuronides, hence disposition of 3-*O*-glucuronides of flavonols in the Caco-2 cell monolayers was not limited by the excretion of 3-*O*-glucuronides by efflux transporters.

Similarly, when the formation rates of 7-*O*-glucuronides of flavones (Figure 43A) and flavonols (Figure 36A, Chapter 8) were plotted against their corresponding AP, BL and total (AP+BL) excretion rates (Figures 43B and 47, and Figures 36A and 40 of Chapter 8), a decent correlation for AP (r^2 = 0.77) (Figure 52a), BL (r^2 = 0.67) (Figure 52b) as well as total excretion (r^2 = 0.76) (Figure 52c) was observed. However, the slopes of the lines of best fit for AP, BL and total excretion of 7-*O*-glucuronides of flavones and flavonols were 0.09, 0.13 and 0.22, respectively.

The slope of line of best fit for total excretion was nowhere close to 1. This strongly indicated that the excretion rates were much less than with the rates of formation of 7-*O*-glucuronides, most probably because the excretion of 7-*O*-glucuronides of flavones and flavonols by the efflux transporters was not favored and hence acted as the rate limiting step in the disposition of 7-*O*-glucuronides in the Caco-2 cell monolayers.

The fact that excretion of 7-*O*-glucuronides of high metabolizing flavones was not favored by the efflux transporters was also evident by the good hyperbolic correlation (r^2 ~ 0.9) that was observed between the formation and excretion rates of 7-*O*-glucuronides

of flavones (Figure 53). The equation of line of best fit was $Y=Y_{max}X/(X + X_c)$, where Y_{max} was the maximum rate of excretion that can be achieved by the efflux transporters in Caco-2 cell monolayers and X_c was the rate of formation by the UGTs at which half the Y_{max} can be achieved in Caco-2 cells. The parameters Y_{max} and X_c for the lines of best fit along with r^2 for AP, BL and total excretion of 7-*O*-glucuronides of flavones were shown in table 12.

The result showed that the basolateral and total excretion of 7-*O*-glucuronides of flavonols followed saturation kinetics (Figure 53), such that only a maximum rate of excretion could be achieved with the efflux transporters, even if the formation rates of 7-*O*-glucuronides of certain flavonols were higher. This again indicated that disposition of flavones in the Caco-2 cell via glucuronidation at position C-7 was rate limited by the excretion of 7-*O*-glucuronides by the efflux transporters. The standard error of the parameters obtained from the line of best fit for the apical excretion was very high indicating that apical excretion was not following the hyperbolic correlation very well (Table 12).

However, there was no hyperbolic correlation observed if the 7-*O*-glucuronides of flavones and flavonols were plotted together (correlation plots not shown here). This showed that the excretion of 7-*O*-glucuronides of flavonoids in Caco-2 cells was dependent on the sub-class of flavonoids.

Table 12 Parameters for the hyperbolic correlation between the formation rates and the corresponding apical, basolateral and total excretion rates of 7-*O*-glucuronides of flavones

Parameters of hyperbolic correlation	Excretion (best fit value ± std. error)		
	Apical	Basolateral	Total (AP+BL)
Y_{max}	6.39 ± 3.09	7.76 ± 1.14	14.10 ± 2.82
X_c	19.69 ± 12.44	12.25 ± 2.52	14.89 ± 4.07
r^2	0.60	0.91	0.89

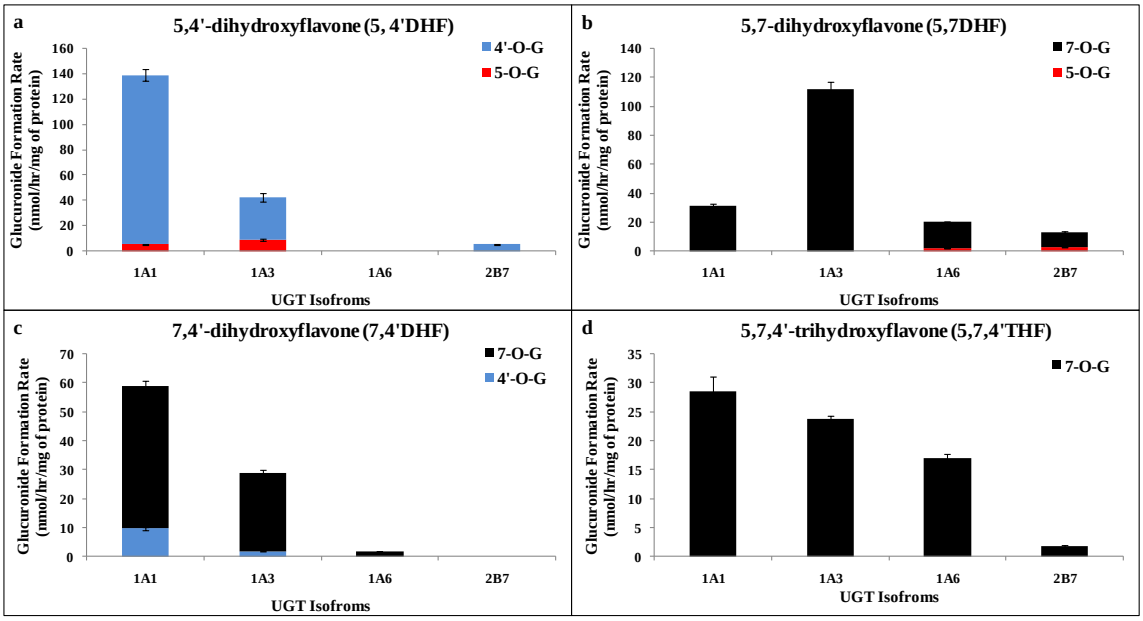

Figure 54. Glucuronidation of flavones by recombinant human UGT 1A1, 1A3, 1A6 and 2B7.

5,4'DHF (a), 5,7DHF (b), 7,4'DHF (c), and 5,7,4'THF (d) at 10 µM concentration were incubated at 37 ºC for 1 (or 0.5) hr with each UGT isoform (using optimum final protein concentration ~ 0.25, 0.5 or 1 mg/ml). The amounts of mono-*O*-glucuronide(s) formed were measured using UPLC. Rates of glucuronide(s) formation were calculated as nmol/hr/mg of protein. Each bar is the average of three determinations, and the error bars are the standard deviations of the mean (n=3). (This data has been re-plotted from here from Figure 5, Chapter 4).

9.5. Discussion

We concluded that 7-*O* is the most favored position of glucuronidation and sulfation in flavone subclass in Caco-2 cells and excretion of flavone glucuronides is limited by efflux transporters. This can be supported by the fact that in the present study, we found that during AP to BL transport of flavones in Caco-2 cells monolayers, flavones with a C-7 hydroxyl group were primarily metabolized into 7-*O*-glucuronides (Figure 43B) or 7-*O*-sulfates (Figure 44). On the other hand, strong linear correlations between formation rates (x-axis) and excretion rates with slopes significantly less than 1 indicate that efflux transporters are limiting the efflux of glucuronides of flavone subclass.

Evidence supporting the favored position of conjugation at 7-*O* position included the higher rates of formation and excretion of 7-*O*-glucuronides and 7-*O*-sulfates as compared to other regiospecific glucuronides and sulfates. 7-*O*-glucuronides of 5,7DHF and 5,7,4'THF was formed about 4-6 folds faster than the 4'-*O*-G of 4'HF and 5,4'DHF, while 8 folds faster than the 5-*O*-G of 5HF in Caco-2 cells (Figure 43A). Similarly, 7-*O*-glucuronides of 5,7DHF and 5,7,4'THF was excreted about 2 folds faster than the 4'-*O*-G of 4'HF and 5,4'DHF, and 2.5 folds faster than the 5-*O*-G of 5HF in Caco-2 cell monolayers (Figure 43B). On the other hand, 7-*O*-sulaftes of flavones were excreted about 4-10 times faster than the 5-*O*-S of 5HF, whereas 4'HF and 5,4'DHF did not excrete any quantifiable sulfates in Caco-2 cell monolayers (Figure 44).

In Caco-2/TC-7 cells, UGT1A1, 1A3, 1A4, 1A6 were highly expressed whereas UGT1A8 and UGT1A9 were poorly expressed and UGT1A7 and 1A10 are probably not expressed [116]. Another report showed higher expression levels of UGT2B7 and 2B17.[134] Since, UGT1A4 and 2B17 did not glucuronidate most flavones, we re-plotted the regiospecific glucuronidation of these flavones by UGT isoforms 1A1, 1A3, 1A6 and 2B7 at 10 µM substrate concentration (Figure 54) and results strongly indicated that all UGT isoforms richly expressed in the Caco-2 cells primarily glucuronidated flavone at the 7-*O* position.

We believe that the formation of 7-*O*-sulfate in Caco-2/TC-7 cells is due to the action of SULT1A3. This is because, SULT1A3 is highly expressed in Caco-2/TC-7[129] and metabolize apigenin very fast (Figure G1, Appendix G). Another highly expressed SULT isoform, SULT2A1[129] slowly metabolized apigenin (50 folds lower than SULT1A3) (Figure G1, Appendix G). On the other hand, SULT1A1, which has shown high activity against chrysin (5,7DHF)[204] and apigenin (5,7,4'THF)[204] (Figure G1, Appendix G) was expressed 30 fold less than SULT1A3 in Caco-2/TC-7[129]. Therefore, SULT1A3 is the most important isoform responsible for sulfation of flavones at 7-*O* position.

This conclusion is consistent with the results of Harris *et al.* (2004) who showed that at substrate concentration of 10µM, 7HF (61.7 ± 2.56), 5,7DHF (47.4 ± 0.30) and 5,7,4'THF (52.4 ± 0.02) were sulfated about ~150-200 times faster than 5-HF (0.3±0.25 pmol/min/mg protein) in platelet cytosol (SULT1A1:SULT1A3, 1:2).[187] It is also

consistent with Walle *et al.* (2001) who showed that chrysin (5,7DHF) in human volunteers formed only one mono-*O*-sulfate[190] and Williamson *et al.* (2005) who reported that chrysin-7-*O*-S was found *in vivo*.[79]

Our study showed that excretion of flavones' glucuronides and sulfates in Caco-2 cells is rate limited by the efflux transporters, such as MRP2[10, 114, 163, 169, 195, 206, 207] and BCRP[114, 163, 169, 208] at the apical side and an OAT[10], MRP1[169], and MRP3[163] on the basolateral side. This is supported by the fact that the formation rates of total as well as regiospecific glucuronides of highly glucuronidated flavones such 5,7DHF and 5,7,4'THF were about 2-3 times faster than their corresponding excretion rates in Caco-2 cells (Figures 43A-43B and 45-47) , which is also reflected by the slopes that were generally much less than 1 (~0.3). Also, the correlation coefficients of linear relationships of AP, BL and total (AP+BL) excretions rates of total (sum of all) glucuronides were better than the correlation coefficient of regiospecific glucuronides (Figures 48a-48c and 49a-49c). This showed that excretion rates of certain regiospecific glucuronides were not well correlated with their formation rates, such as 4'-*O*-G of 5,4'DHF and 5-*O*-G of 5,7DHF were outliers in all the cases (Figures 49a-49c).

We also found decent linear correlations between formation and excretion rates of regiospecific glucuronides of flavonols and flavones (Figures 50-52). However, the slopes of line of best fit of total excretion of 4'-*O*-G were less than 1 (Figure 50c) and the slope of 7-*O*-G was much lower than 1 (Figure 52c). On the other hand, slope of line of

best fit for the total excretion for 3-*O*-G of flavonols was about 1 (Figure 51c). This suggested that the excretion of 3-*O*-G of flavonols was not, but excretion of 4'-*O*-G and 7-*O*-G of flavones and flavonols was rate limited by the efflux transporters.

It should be noted that 7-*O*-G of flavones alone showed good hyperbolic correlation between the formation and excretion rates (Figure 53, table 12), but not when plotted with 7-*O*-G of flavonols (correlation plots not shown). This suggested that excretion of metabolites of different sub-classes, even though glucuronidated at the same position might still not follow the same profiles. Excretion of flavones sulfates also supposedly was rate-limited by the efflux transporters[10], however additional studies are required to prove this.

In conclusion, flavones are preferentially glucuronidated and sulfated at 7-*O* position and the excretion of flavone glucuronides is rate-limited by the efflux transporters.

SUMMARY

The purpose of these studies was to establish structure-metabolism relation between UGT and flavonoids for predicting glucuronidation of flavonoids. We first determined the most important isoforms responsible for the *in vivo* glucuronidation of flavonoids in and across different sub-classes. Using recombinant human UGT isoform glucuronidation model, we found that out of 12 commercially available UGT isoforms, in most cases, UGT1A9 was the fastest glucuronidating isoform for the 13 tested flavonoids (apigenin, genistein, phloretin, naringenin, kaempferol, 3-hydroxyflavone, 3,4'-dihydroxyflavone, 3,7--dihydroxyflavone, 5,4'-dihydroxyflavone, 5,7-dihydroxyflavone, 7,4'-dihydroxyflavone, 3,5,7-trihydroxyflavone, and 3,7,4'-trihydroxyflavone) at all the three substrate concentrations (2.5, 10, 35µM), except for phloretin, for which UGT1A8 was the fastest glucuronidating isoform at all the three substrate concentrations. We also found that UGT1A1 usually showed faster glucuronidation than UGT1A8 at lower substrate concentration (2.5µM), whereas UGT1A8 usually showed faster glucuronidation at higher substrate concentration (35µM). Glucuronidation of flavonoids by UGT 1A3, 1A6, 1A7, 1A10 and 2B7 was also dependent on the structure and concentration of the flavonoids. These data suggest that UGT1A9, UGT1A8 and UGT1A1 will play most important role in glucuronidating flavonoids at different concentrations. Based on published literature (Ohno and Nakajin, 2009), among liver and intestine, the two major first pass metabolism organs, UGT1A9 is exclusively expressed in liver, UGT1A8 in

intestine and UGT1A9 in both liver and intestine. This also gave us the rationale of choosing UGT isoforms for further studies on isoform-specific substrate-selectivity, regiospecificity and developing isoform-specific prediction models later.

We then studied the substrate-selectivity and regiospecificity of eight important UGT isoforms (1A1, 1A3, 1A6, 1A7, 1A8, 1A9, 1A10 and 2B7). For the purpose of understanding, we randomly categorized the degree of regiospecificity into dominant (i.e. one position is favored to the other(s) by 9:1 or larger ratio), preferred (i.e. one position is favored to the other(s) by at least 3:1 ratio, but less than 9:1 ratio), weak (i.e. one position is favored to the other(s) by at least 2:1 ratio but less than 3:1 ratio) and no preference (i.e. no position is favored to the other(s) by less than 2:1 ratio). We found that in general, UGT1A1, 1A6 and 1A10 showed no regiospecificity for any particular position of glucuronidation. UGT1A3 showed dominant regiospecificity for glucuronidating 7-*O* position, whereas, UGT1A7 showed dominant regiospecificity for glucuronidating 3-*O* position. UGT1A8 and UGT1A9 showed dominant, preferred or weak regiospecificity for 3-*O* or 7-*O* position, depending on the structure of the flavonoid. We showed that the rates of glucuronidation of 3-*O* and 7-*O* positions in flavones and flavonols were affected by the addition of multiple hydroxyl groups at different positions as well as by the substrate concentrations (2.5, 10 and 35μM).

We also found that the rates of glucuronidation of 3-*O* and 7-*O* positions in flavones and flavonols were affected by the addition of multiple hydroxyl groups at different positions

as well as by the substrate concentrations. In substrate-selectivity studies of flavones and flavonols, we found that the addition of hydroxyl group at C-4' reduced, whereas the addition of hydroxyl group at C-5 and/or C-7 improved the rates of glucuronidation of flavonoids by UGT1A8 and 1A9. However, the rates of glucuronidation by UGT1A1 always reduced as number of hydroxyl group in the structure increased. These studies suggested that regiospecificity and substrate-selectivity were dependent on UGT isoform, substrate structure and concentration.

Since UGT1A8 and UGT1A9 were one of the most important isoform glucuronidating flavonoids and exclusively expressed in the intestine and liver, respectively, we sought to develop isoform-specific semi-quantitative and quantitative structure-metabolism prediction (SMR) models using isoform-specific approximate intrinsic clearance (Cl_{int}) values of flavonoids as metabolic activity of UGT1A8 and UGT1A9. Semi-quantitative SMR models were developed using Pharmacophore-based 3-D QSAR modeling, whereas quantitative SMR models were developed using 2-D/3-D QSAR modeling techniques. We were successfully able to develop semi-quantitative SMR prediction models for UGT1A9 with a predictive ability of >75%, which could differentiate between the compounds into two different categories of metabolism (low versus high) based on arbitrary cut-off Cl_{int} value of 3×10^5 ml/min/mg of protein. We could not develop any successful semi-quantitative SMR prediction model for UGT1A8. The pharmacophore generated in the semi-quantitative SMR models help to decide the best confirmation of

compounds to be used in the quantitative SMR prediction models. But, we could not develop any successful quantitative SMR prediction model for UGT1A8 and UGT1A9 using 2-D and 3-D descriptors. But we believe that better use of experimental data information such as position-specific glucuronidation activity of flavonoids and combinatorial *in silico* modeling techniques might further improve these prediction models.

We then investigated the how the change in backbone of flavonoids across different sub-classes affect the excretion of conjugates of flavonoids in Caco-2 cells. We found that the rates of excretion of glucuronides of all flavonoids in Caco-2 cell monolayer were comparable and rapid except for genistein which excreted slowly, due to the position in phenyl ring at C-3 as opposed to C-2 in other flavonoids. However, rates of excretion of sulfates of apigenin were the highest in Caco-2 cell monolayers, followed by kaempferol, naringenin, phloretin and genistein. The rates of formation of glucuronide(s) of apigenin, genistein and phloretin in Caco-2 cell lysate were significantly higher than their corresponding rates of excretion, indicating that rates of excretion was limited by the efflux transporters. Whereas, rates of formation and excretion of glucuronide(s) of naringenin and kaempferol did not show significant differences ($p<0.05$), indicating that rates of excretion of these glucuronides were not limited by the efflux transporters. These studies suggested that change in backbone structures impact the excretion of flavonoid sulfates more significantly than the excretion of their glucuronides in Caco-2 cells, and

excretion of glucuronides were limited either by the formation or efflux transporters depending on their structures.

We then studied the role of efflux transporter in the excretion of flavonol glucuronides in Caco-2 cells. We found that the rates of formation of regiospecific glucuronides of the selected flavonols in Caco-2 cell lysate correlated very well (slope = 0.89, $r^2 \sim 0.9$) with the corresponding rates of total (AP+BL) excretion of these glucuronides in the intact Caco-2 cell monolayer. This suggested that the formation rates of glucuronides in Caco-2 cell lysate could reasonably be used for predicting the major position(s) of glucuronidation and rates of regiospecific glucuronidation of a new flavonol. The total glucuronides as well as most regiospecific glucuronides for all the selected flavonols were excreted more to the BL side than to the apical side, with 3-*O*-G showing more BL preference than glucuronide(s) at other -OH position of same compound. These studies suggested that the excretion of flavonol glucuronides in Caco-2 cells is generally driven by formation rates, and not rate-limited by efflux transporters, which can be mainly attributed to the favorable basolateral efflux of flavonol glucuronides, especially 3-*O*-G.

We then investigated the regiospecific conjugation of flavone glucuronides in Caco-2 cells. We found that the most favored position for glucuronidation and sulfation was 7-hydroxy group in the structure of flavones. The rates of formation of total (sum of all) glucuronides of the selected flavones in Caco-2 cell lysate had a very good ($r^2 \sim 0.9$) linear correlation with the corresponding rates of AP, BL and total (AP+BL) excretion of

the glucuronides in the intact Caco-2 cell monolayer, but with a slope of much less than 1 (~0.3). When the formation versus excretion rates correlation profiles of 4'-*O*-G and 7-*O*-G of flavonols and flavones plotted together, were compared with the correlation profiles of 3-*O*-G of flavonols, the slopes of line of best fit were 0.7, 0.44, and 0.95 for 4'-*O*-G, 7-*O*-G and 3-*O*-G, respectively. This indicated that the excretion of 3-*O*-G was not, whereas the excretion of 4'-*O*-G and 7-*O*-G glucuronides was limited by the efflux transporters. Based on the published expression levels of UGT isoform in Caco-2 cells (Siissalo *et al.,* 2009) the important intestinal isoforms responsible for glucuronidation of flavonoids in intestinal cells (UGT1A8 and UGT1A10) are poorly expressed in Caco-2 cells. Therefore, though the Caco-2 cells are a good model for studying the mechanism of flavonoids' disposition, its role in the actual prediction of *in vivo* disposition of flavonoids in intestinal cells is limited.

Taken together, we have demonstrated that flavonoids show UGT isoform-specific structure-glucuronidation relationship. Rates of glucuronidation by recombinant human UGT isoforms could be very helpful in understanding this relationship in terms of the most important UGT isoforms contributing to the metabolism of flavonoids, as well as differences in the substrate selectively and regiospecificity difference among various isoforms. This relationship however, could not give quantitative prediction of isoform-specific metabolic fate of compound. The study indicated that ligand-based *in silico* modeling could be a more viable approach for generating semi-quantitative and

quantitative SMR models to predict isoform-specific metabolism. Additionally, study of the flavonoid glucuronidation in Caco-2 cells delineated the role of efflux transporters in the excretion of position-specific glucuronides of flavonoids and gave more insight to the possible structure-disposition relationship of flavonoids in intestinal cell. However, future studies are required to develop the prediction models for the excretion of glucuronides by various efflux transporters.

REFERENCE

(1) Birt, D. F.; Hendrich, S.; Wang, W. *Pharmacol Ther* 2001, *90*.

(2) Jacobsen, B. K.; Knutsen, S. F.; Fraser, G. E. *Cancer Causes Control* 1998, *9*, 553-557.

(3) Kurzer, M. S.; Xu, X. *Annu Rev Nutr* 1997, *17*, 353-381.

(4) Lamartiniere, C. A. *Am J Clin Nutr* 2000, *71*, 1705S-1707S; discussion 1708S-1709S.

(5) Tham, D. M.; Gardner, C. D.; Haskell, W. L. *J Clin Endocrinol Metab* 1998, *83*, 2223-2235.

(6) Busby, M. G.; Jeffcoat, A. R.; Bloedon, L. T.; Koch, M. A.; Black, T.; Dix, K. J.; Heizer, W. D.; Thomas, B. F.; Hill, J. M.; Crowell, J. A.; Zeisel, S. H. *Am J Clin Nutr* 2002, *75*, 126-136.

(7) Kelly, G. E.; Joannou, G. E.; Reeder, A. Y.; Nelson, C.; Waring, M. A. *Proc Soc Exp Biol Med* 1995, *208*, 40-43.

(8) Nettleton, J. A.; Greany, K. A.; Thomas, W.; Wangen, K. E.; Adlercreutz, H.; Kurzer, M. S. *J Nutr* 2004, *134*, 1998-2003.

(9) Chen, J.; Lin, H.; Hu, M. *J Pharmacol Exp Ther* 2003, *304*, 1228-1235.

(10) Hu, M.; Chen, J.; Lin, H. *J Pharmacol Exp Ther* 2003, *307*, 314-321.

(11) Liu, Y.; Hu, M. *Drug Metab Dispos* 2002, *30*, 370-377.

(12) Chen, J.; Wang, S.; Jia, X.; Bajimaya, S.; Lin, H.; Tam, V. H.; Hu, M. *Drug Metab Dispos* 2005, *33*, 1777-1784.

(13) Wang, S. W.; Chen, J.; Jia, X.; Tam, V. H.; Hu, M. *Drug Metab Dispos* 2006, *34*, 1837-1848.

(14) Nijveldt, R. J.; van Nood, E.; van Hoorn, D. E.; Boelens, P. G.; van Norren, K.; van Leeuwen, P. A. *Am J Clin Nutr* 2001, *74*, 418-425.

(15) Formica, J. V.; Regelson, W. *Food Chem Toxicol* 1995, *33*, 1061-1080.

(16) de Groot, H.; Dehmlow, C.; Raven, U. *Methods Find Exp Clin Pharmacol* 1996, *18 Suppl B*, 23-25.

(17) Ren, W.; Qiao, Z.; Wang, H.; Zhu, L.; Zhang, L. *Med Res Rev* 2003, *23*, 519-534.

(18) Geleijnse, J. M.; Hollman, P. *Am J Clin Nutr* 2008, *88*, 12-13.

(19) Ullah, M. F.; Khan, M. W. *Asian Pac J Cancer Prev* 2008, *9*, 187-195.

(20) Dewick, P. M. *Nat Prod Rep* 1995, *12*, 579-607.

(21) Middleton, E. *Trends Pharmacol Sci* 1984, *5*, 335-338.

(22) Prasain, J. K.; Wang, C. C.; Barnes, S. *Free Radic Biol Med* 2004, *37*, 1324-1350.

(23) Kuti, J. O.; Konuru, H. B. *J Agric Food Chem* 2004, *52*, 117-121.

(24) Chu, Y. F.; Sun, J.; Wu, X.; Liu, R. H. *J Agric Food Chem* 2002, *50*, 6910-6916.

(25) Lotito, S. B.; Frei, B. *Free Radic Biol Med* 2004, *36*, 201-211.

(26) Vinson, J. A.; Su, X.; Zubik, L.; Bose, P. *J Agric Food Chem* 2001, *49*, 5315-5321.

(27) Aaby, K.; Skrede, G.; Wrolstad, R. E. *J Agric Food Chem* 2005, *53*, 4032-4040.

(28) Moyer, R. A.; Hummer, K. E.; Finn, C. E.; Frei, B.; Wrolstad, R. E. *J Agric Food Chem* 2002, *50*, 519-525.

(29) Astill, C.; Birch, M. R.; Dacombe, C.; Humphrey, P. G.; Martin, P. T. *J Agric Food Chem* 2001, *49*, 5340-5347.

(30) Actis-Goretta, L.; Mackenzie, G. G.; Oteiza, P. I.; Fraga, C. G. *Ann N Y Acad Sci* 2002, *957*, 279-283.

(31) Scalbert, A.; Manach, C.; Morand, C.; Remesy, C.; Jimenez, L. *Crit Rev Food Sci Nutr* 2005, *45*, 287-306.

(32) Scalbert, A.; Williamson, G. *J Nutr* 2000, *130*, 2073S-2085S.

(33) Franke, A. A.; Hankin, J. H.; Yu, M. C.; Maskarinec, G.; Low, S. H.; Custer, L. J. *J Agric Food Chem* 1999, *47*, 977-986.

(34) Reinli, K.; Block, G. *Nutr Cancer* 1996, *26*, 123-148.

(35) Wang, L. Q. *J Chromatogr B Analyt Technol Biomed Life Sci* 2002, *777*, 289-309.

(36) Krenn, L.; Unterrieder, I.; Ruprechter, R. *J Chromatogr B Analyt Technol Biomed Life Sci* 2002, *777*, 123-128.

(37) Barnes, S. *J Nutr* 2004, *134*, 1225S-1228S.

(38) Prasain, J. K.; Jones, K.; Kirk, M.; Wilson, L.; Smith-Johnson, M.; Weaver, C.; Barnes, S. *J Agric Food Chem* 2003, *51*, 4213-4218.

(39) Setchell, K. D. *Am J Clin Nutr* 1998, *68*, 1333S-1346S.

(40) Setchell, K. D.; Brown, N. M.; Desai, P.; Zimmer-Nechemias, L.; Wolfe, B. E.; Brashear, W. T.; Kirschner, A. S.; Cassidy, A.; Heubi, J. E. *J Nutr* 2001, *131*, 1362S-1375S.

(41) Yang, C. S.; Landau, J. M.; Huang, M. T.; Newmark, H. L. *Annu Rev Nutr* 2001, *21*, 381-406.

(42) Krishna, D. R.; Klotz, U. *Clin Pharmacokinet* 1994, *26*, 144-160.

(43) Nowell, S. A.; Massengill, J. S.; Williams, S.; Radominska-Pandya, A.; Tephly, T. R.; Cheng, Z.; Strassburg, C. P.; Tukey, R. H.; MacLeod, S. L.; Lang, N. P.; Kadlubar, F. F. *Carcinogenesis* 1999, *20*, 1107-1114.

(44) Strassburg, C. P.; Nguyen, N.; Manns, M. P.; Tukey, R. H. *Gastroenterology* 1999, *116*, 149-160.

(45) Tukey, R. H.; Strassburg, C. P. *Annu Rev Pharmacol Toxicol* 2000, *40*, 581-616.

(46) Cappiello, M.; Giuliani, L.; Pacifici, G. M. *Eur J Clin Pharmacol* 1991, *41*, 345-350.

(47) Cappiello, M.; Giuliani, L.; Rane, A.; Pacifici, G. M. *Dev Pharmacol Ther* 1991, *16*, 83-88.

(48) Fisher, M. B.; Paine, M. F.; Strelevitz, T. J.; Wrighton, S. A. *Drug Metab Rev* 2001, *33*, 273-297.

(49) Nagar, S.; Remmel, R. P. *Oncogene* 2006, *25*, 1659-1672.

(50) Kiang, T. K.; Ensom, M. H.; Chang, T. K. *Pharmacol Ther* 2005, *106*, 97-132.

(51) Joseph, T. B.; Wang, S. W.; Liu, X.; Kulkarni, K. H.; Wang, J.; Xu, H.; Hu, M. *Mol Pharm* 2007, *4*, 883-894.

(52) Liu, X.; Tam, V. H.; Hu, M. *Mol Pharm* 2007, *4*, 873-882.

(53) Liu, Z.; Hu, M. *Expert Opin Drug Metab Toxicol* 2007, *3*, 389-406.

(54) Suzuki, H.; Sugiyama, Y. *Eur J Pharm Sci* 2000, *12*, 3-12.

(55) Mackenzie, P. I.; Bock, K. W.; Burchell, B.; Guillemette, C.; Ikushiro, S.; Iyanagi, T.; Miners, J. O.; Owens, I. S.; Nebert, D. W. *Pharmacogenet Genomics* 2005, *15*, 677-685.

(56) Mackenzie, P. I.; Gregory, P. A.; Gardner-Stephen, D. A.; Lewinsky, R. H.; Jorgensen, B. R.; Nishiyama, T.; Xie, W.; Radominska-Pandya, A. *Curr Drug Metab* 2003, *4*, 249-257.

(57) Mackenzie, P. I.; Rogers, A.; Treloar, J.; Jorgensen, B. R.; Miners, J. O.; Meech, R. *J Biol Chem* 2008, *283*, 36205-36210.

(58) Court, M. H.; Hazarika, S.; Krishnaswamy, S.; Finel, M.; Williams, J. A. *Mol Pharmacol* 2008, *74*, 744-754.

(59) Bosio, A.; Binczek, E.; Le Beau, M. M.; Fernald, A. A.; Stoffel, W. *Genomics* 1996, *34*, 69-75.

(60) Sorich, M. J.; Miners, J. O.; McKinnon, R. A.; Smith, P. A. *Mol Pharmacol* 2004, *65*, 301-308.

(61) Ohno, S.; Nakajin, S. *Drug Metab Dispos* 2009, *37*, 32-40.

(62) Fisher, M. B.; Vandenbranden, M.; Findlay, K.; Burchell, B.; Thummel, K. E.; Hall, S. D.; Wrighton, S. A. *Pharmacogenetics* 2000, *10*, 727-739.

(63) Strassburg, C. P.; Manns, M. P.; Tukey, R. H. *J Biol Chem* 1998, *273*, 8719-8726.

(64) Falany, C. N. *Faseb J* 1997, *11*, 206-216.

(65) Falany, C. N. *Faseb J* 1997, *11*, 1-2.

(66) Negishi, M.; Pedersen, L. G.; Petrotchenko, E.; Shevtsov, S.; Gorokhov, A.; Kakuta, Y.; Pedersen, L. C. *Arch Biochem Biophys* 2001, *390*, 149-157.

(67) Petrotchenko, E. V.; Pedersen, L. C.; Borchers, C. H.; Tomer, K. B.; Negishi, M. *FEBS Lett* 2001, *490*, 39-43.

(68) Yoshinari, K.; Petrotchenko, E. V.; Pedersen, L. C.; Negishi, M. *J Biochem Mol Toxicol* 2001, *15*, 67-75.

(69) Chen, G.; Zhang, D.; Jing, N.; Yin, S.; Falany, C. N.; Radominska-Pandya, A. *Toxicol Appl Pharmacol* 2003, *187*, 186-197.

(70) Gamage, N.; Barnett, A.; Hempel, N.; Duggleby, R. G.; Windmill, K. F.; Martin, J. L.; McManus, M. E. *Toxicol Sci* 2006, *90*, 5-22.

(71) Hildebrandt, M. A.; Carrington, D. P.; Thomae, B. A.; Eckloff, B. W.; Schaid, D. J.; Yee, V. C.; Weinshilboum, R. M.; Wieben, E. D. *Pharmacogenomics J* 2007, *7*, 133-143.

(72) Teubner, W.; Meinl, W.; Florian, S.; Kretzschmar, M.; Glatt, H. *Biochem J* 2007, *404*, 207-215.

(73) Ozawa, S.; Tang, Y. M.; Yamazoe, Y.; Kato, R.; Lang, N. P.; Kadlubar, F. F. *Chem Biol Interact* 1998, *109*, 237-248.

(74) Tabrett, C. A.; Coughtrie, M. W. *Biochem Pharmacol* 2003, *66*, 2089-2097.

(75) Honma, W.; Shimada, M.; Sasano, H.; Ozawa, S.; Miyata, M.; Nagata, K.; Ikeda, T.; Yamazoe, Y. *Drug Metab Dispos* 2002, *30*, 944-949.

(76) Riches, Z.; Stanley, E. L.; Bloomer, J. C.; Coughtrie, M. W. *Drug Metab Dispos* 2009, *37*, 2255-2261.

(77) Wong, Y. C.; Zhang, L.; Lin, G.; Zuo, Z. *Expert Opin Drug Metab Toxicol* 2009, *5*, 1399-1419.

(78) Lambert, J. D.; Sang, S.; Yang, C. S. *Mol Pharm* 2007, *4*, 819-825.

(79) Williamson, G.; Barron, D.; Shimoi, K.; Terao, J. *Free Radic Res* 2005, *39*, 457-469.

(80) Janisch, K. M.; Williamson, G.; Needs, P.; Plumb, G. W. *Free Radic Res* 2004, *38*, 877-884.

(81) van Zanden, J. J.; van der Woude, H.; Vaessen, J.; Usta, M.; Wortelboer, H. M.; Cnubben, N. H.; Rietjens, I. M. *Biochem Pharmacol* 2007, *74*, 345-351.

(82) Ishizawa, K.; Izawa-Ishizawa, Y.; Ohnishi, S.; Motobayashi, Y.; Kawazoe, K.; Hamano, S.; Tsuchiya, K.; Tomita, S.; Minakuchi, K.; Tamaki, T. *J Pharmacol Sci* 2009, *109*, 257-264.

(83) Steffen, Y.; Gruber, C.; Schewe, T.; Sies, H. *Arch Biochem Biophys* 2008, *469*, 209-219.

(84) O'Leary, K. A.; Day, A. J.; Needs, P. W.; Sly, W. S.; O'Brien, N. M.; Williamson, G. *FEBS Lett* 2001, *503*, 103-106.

(85) Basu, N. K.; Ciotti, M.; Hwang, M. S.; Kole, L.; Mitra, P. S.; Cho, J. W.; Owens, I. S. *J Biol Chem* 2004, *279*, 1429-1441.

(86) Lewinsky, R. H.; Smith, P. A.; Mackenzie, P. I. *Xenobiotica* 2005, *35*, 117-129.

(87) Tang, L.; Singh, R.; Liu, Z.; Hu, M. *Mol Pharm* 2009, *6*, 1466-1482.

(88) Day, A. J.; Bao, Y.; Morgan, M. R.; Williamson, G. *Free Radic Biol Med* 2000, *29*, 1234-1243.

(89) Boersma, M. G.; van der Woude, H.; Bogaards, J.; Boeren, S.; Vervoort, J.; Cnubben, N. H.; van Iersel, M. L.; van Bladeren, P. J.; Rietjens, I. M. *Chem Res Toxicol* 2002, *15*, 662-670.

(90) Chen, J.; Lin, H.; Hu, M. *Cancer Chemother Pharmacol* 2005, *55*, 159-169.

(91) Doerge, D. R.; Chang, H. C.; Churchwell, M. I.; Holder, C. L. *Drug Metab Dispos* 2000, *28*, 298-307.

(92) Sorich, M. J.; Smith, P. A.; McKinnon, R. A.; Miners, J. O. *Pharmacogenetics* 2002, *12*, 635-645.

(93) Yin, H.; Bennett, G.; Jones, J. P. *Chem Biol Interact* 1994, *90*, 47-58.

(94) Sorich, M. J.; McKinnon, R. A.; Miners, J. O.; Smith, P. A. *J Chem Inf Model* 2006, *46*, 2692-2697.

(95) Wong, Y. C.; Zhang, L.; Lin, G.; Zuo, Z. *Int J Pharm* 2009, *366*, 14-20.

(96) Zhang, L.; Lin, G.; Zuo, Z. *Life Sci* 2006, *78*, 2772-2780.

(97) Endres, C. J.; Hsiao, P.; Chung, F. S.; Unadkat, J. D. *Eur J Pharm Sci* 2006, *27*, 501-517.

(98) Kim, R. B. *Toxicology* 2002, *181-182*, 291-297.

(99) Lin, J. H. *Expert Opin Drug Metab Toxicol* 2007, *3*, 81-92.

(100) Zhang, L.; Zuo, Z.; Lin, G. *Mol Pharm* 2007, *4*, 833-845.

(101) Gutmann, H.; Hruz, P.; Zimmermann, C.; Beglinger, C.; Drewe, J. *Biochem Pharmacol* 2005, *70*, 695-699.

(102) Schinkel, A. H.; Jonker, J. W. *Adv Drug Deliv Rev* 2003, *55*, 3-29.

(103) Taipalensuu, J.; Tornblom, H.; Lindberg, G.; Einarsson, C.; Sjoqvist, F.; Melhus, A.; Garberg, P.; Sjostrom, B.; Lundgren, B.; Artursson, P. *The Journal of Phramacology and Experimental Therapeutics* 2001, *299*, 164–170.

(104) Takano, M.; Yumoto, R.; Murakami, T. *Pharmacol Ther* 2006, *109*, 137-161.

(105) Zimmermann, C.; Gutmann, H.; Hruz, P.; Gutzwiller, J. P.; Beglinger, C.; Drewe, J. *Drug Metab Dispos* 2005, *33*, 219-224.

(106) Englund, G.; Rorsman, F.; Ronnblom, A.; Karlbom, U.; Lazorova, L.; Grasjo, J.; Kindmark, A.; Artursson, P. *Eur J Pharm Sci* 2006, *29*, 269-277.

(107) Maubon, N.; Le Vee, M.; Fossati, L.; Audry, M.; Le Ferrec, E.; Bolze, S.; Fardel, O. *Fundam Clin Pharmacol* 2007, *21*, 659-663.

(108) Huang, S. M.; Lesko, L. J. *J Clin Pharmacol* 2004, *44*, 559-569.

(109) Lin, J. H. *Adv Drug Deliv Rev* 2003, *55*, 53-81.

(110) Jager, W.; Gehring, E.; Hagenauer, B.; Aust, S.; Senderowicz, A.; Thalhammer, T. *Life Sci* 2003, *73*, 2841-2854.

(111) O'Leary, K. A.; Day, A. J.; Needs, P. W.; Mellon, F. A.; O'Brien, N. M.; Williamson, G. *Biochem Pharmacol* 2003, *65*, 479-491.

(112) van de Wetering, K.; Burkon, A.; Feddema, W.; Bot, A.; de Jonge, H.; Somoza, V.; Borst, P. *Mol Pharmacol* 2009, *75*, 876-885.

(113) van de Wetering, K.; Feddema, W.; Helms, J. B.; Brouwers, J. F.; Borst, P. *Gastroenterology* 2009, *137*, 1725-1735.

(114) Xu, H.; Kulkarni, K. H.; Singh, R.; Yang, Z.; Wang, S. W.; Tam, V. H.; Hu, M. *Mol Pharm* 2009, *6*, 1703-1715.

(115) Benet, L. Z.; Cummins, C. L.; Wu, C. Y. *Int J Pharm* 2004, *277*, 3-9.

(116) Jeong, E. J.; Jia, X.; Hu, M. *Mol Pharm* 2005, *2*, 319-328.

(117) Jia, X.; Chen, J.; Lin, H.; Hu, M. *J Pharmacol Exp Ther* 2004, *310*, 1103-1113.

(118) Doherty, M. M.; Charman, W. N. *Clin Pharmacokinet* 2002, *41*, 235-253.

(119) Knight, B.; Troutman, M.; Thakker, D. R. *Curr Opin Pharmacol* 2006, *6*, 528-532.

(120) Lau, Y. Y.; Wu, C. Y.; Okochi, H.; Benet, L. Z. *J Pharmacol Exp Ther* 2004, *308*, 1040-1045.

(121) Wang, S. W.; Kulkarni, K. H.; Tang, L.; Wang, J. R.; Yin, T.; Daidoji, T.; Yokota, H.; Hu, M. *J Pharmacol Exp Ther* 2009, *329*, 1023-1031.

(122) Harper, T. W.; Brassil, P. J. *AAPS J* 2008, *10*, 200-207.

(123) Lu, A. Y.; Wang, R. W.; Lin, J. H. *Drug Metab Dispos* 2003, *31*, 345-350.

(124) Bauman, J. N.; Goosen, T. C.; Tugnait, M.; Peterkin, V.; Hurst, S. I.; Menning, L. C.; Milad, M.; Court, M. H.; Williams, J. A. *Drug Metab Dispos* 2005, *33*, 1349-1354.

(125) Picard, N.; Ratanasavanh, D.; Premaud, A.; Le Meur, Y.; Marquet, P. *Drug Metab Dispos* 2005, *33*, 139-146.

(126) Balimane, P. V.; Han, Y.; Chong, S. *The AAPS Journal* 2006, *8*, Article 1 (http://www.aapsj.org).

(127) Meunier, V.; Bourrié, M.; Berger, Y.; Fabre, G. *Cell Biol Toxicol.* 1995, *11*, 187-194.

(128) Hidalgo, I. J.; Raub, T. J.; Borchardt, R. T. *Gastroenterology* 1989, *96*, 736–749.

(129) Meinl, W.; Ebert, B.; Glatt, H.; Lampen, A. *Drug Metabolism and Disposition* 2008, *36*, 276–283.

(130) Sabolovic, N.; Magdalou, J.; Netter, P.; Abid, A. *Life Sciences* 2000, *67*, 185-196.

(131) Jeong, E. J.; Liu, X.; Jia, X.; Chen, J.; Hu, M. *Curr Drug Metab* 2005, *6*, 455-468.

(132) Zhang, Y.; Benet, L. Z. *Clin Pharmacokinet* 2001, *40*, 159-168.

(133) Siissalo, S., University of Helsinki, Finland, 2009.

(134) Siissalo, S.; Zhang, H.; Stilgenbauer, E.; Kaukonen, A. M.; Hirvonen, J.; Finel, M. *Drug Metabolism and Disposition* 2008, *36*, 2331–2336.

(135) Hu, M.; Ling, J.; Lin, H.; Chen, J. In *Optimization in Drug Discovery: In Vitro Methods*; Yan, Z., Caldwell, G. W., Eds.; Humana Press Inc., : Totowa, NJ, 2004, pp 19-35

(136) Sambuy, Y.; De Angelis, I.; Ranaldi, G.; Scarino, M. L.; Stammati, A.; Zucco, F. *Cell Biol Toxicol.* 2005, *21*, 1-26.

(137) Borlak, J.; Zwadlo, C. *Xenobiotica* 2003, *33* 927-943.

(138) Jeong, E. J.; Liu, Y.; Lin, H.; Hu, M. *Drug Metab Dispos* 2005, *33*, 785-794.

(139) Kapetanovic, I. M. *Chem Biol Interact* 2008, *171*, 165-176.

(140) Penzotti, J. E.; Landrum, G. A.; Putta, S. *Curr Opin Drug Discov Devel* 2004, *7*, 49-61.

(141) Miners, J. O.; Smith, P. A.; Sorich, M. J.; McKinnon, R. A.; Mackenzie, P. I. *Annu Rev Pharmacol Toxicol* 2004, *44*, 1-25.

(142) Norinder, U. *SAR QSAR Environ Res* 2005, *16*, 1-11.

(143) O'Brien, S. E.; de Groot, M. J. *J Med Chem* 2005, *48*, 1287-1291.

(144) van de Waterbeemd, H.; Gifford, E. *Nat Rev Drug Discov* 2003, *2*, 192-204.

(145) Wilson, A. G.; White, A. C.; Mueller, R. A. *Curr Opin Drug Discov Devel* 2003, *6*, 123-128.

(146) Ekins, S.; Stresser, D. M.; Williams, J. A. *Trends Pharmacol Sci* 2003, *24*, 161-166.

(147) Smith, P. A.; Sorich, M. J.; McKinnon, R. A.; Miners, J. O. *Clin Exp Pharmacol Physiol* 2003, *30*, 836-840.

(148) Ekins, S.; Bravi, G.; Binkley, S.; Gillespie, J. S.; Ring, B. J.; Wikel, J. H.; Wrighton, S. A. *Drug Metab Dispos* 2000, *28*, 994-1002.

(149) Ekins, S.; Bravi, G.; Ring, B. J.; Gillespie, T. A.; Gillespie, J. S.; Vandenbranden, M.; Wrighton, S. A.; Wikel, J. H. *J Pharmacol Exp Ther* 1999, *288*, 21-29.

(150) Ekins, S.; de Groot, M. J.; Jones, J. P. *Drug Metab Dispos* 2001, *29*, 936-944.

(151) Smith, P. A.; Sorich, M. J.; McKinnon, R. A.; Miners, J. O. *J Med Chem* 2003, *46*, 1617-1626.

(152) Sorich, M. J.; McKinnon, R. A.; Miners, J. O.; Winkler, D. A.; Smith, P. A. *J Med Chem* 2004, *47*, 5311-5317.

(153) Senafi, S. B.; Clarke, D. J.; Burchell, B. *Biochem J* 1994, *303 (Pt 1)*, 233-240.

(154) Smith, P. A.; Sorich, M. J.; Low, L. S.; McKinnon, R. A.; Miners, J. O. *J Mol Graph Model* 2004, *22*, 507-517.

(155) Ethell, B. T.; Ekins, S.; Wang, J.; Burchell, B. *Drug Metab Dispos* 2002, *30*, 734-738.

(156) Smith, P. A.; Sorich, M. J.; McKinnon, R. A.; Miners, J. O. *J Med Chem* 2003, *46*, 1617-1626.

(157) Tang, L.; Ye, L.; Singh, R.; Wu, B.; Zhao, J.; Lv, C.; Liu, Z.; Hu, M. *Molecular Pharmaceutics* 2010, *DOI: 10.1021/mp900223c*.

(158) Clarke, N. J.; Rindgen, D.; Korfmacher, W. A.; Cox, K. A. *Anal Chem* 2001, *73*, 430A-439A.

(159) King, R.; Fernandez-Metzler, C. *Curr Drug Metab* 2006, *7*, 541-545.

(160) Otake, Y.; Hsieh, F.; Walle, T. *Drug Metab Dispos* 2002, *30*, 576-581.

(161) Cook, N. C.; Samman, S. *Journal of Nutritional Biochemistry* 1996, *7*, 66-76

(162) Wen, X.; Walle, T. *Drug Metab Dispos* 2006, *34*, 1786-1792.

(163) Zhang, L.; Lin, G.; Kovacs, B.; Jani, M.; Krajcsi, P.; Zuo, Z. *Eur J Pharm Sci* 2007, *31*, 221-231.

(164) Izukawa, T.; Nakajima, M.; Fujiwara, R.; Yamanaka, H.; Fukami, T.; Takamiya, M.; Aoki, Y.; Ikushiro, S.; Sakaki, T.; Yokoi, T. *Drug Metab Dispos* 2009, *37*, 1759-1768.

(165) Mizuma, T. *Int J Pharm* 2009, *378*, 140-141.

(166) Lewis, B. C.; Mackenzie, P. I.; Elliot, D. J.; Burchell, B.; Bhasker, C. R.; Miners, J. O. *Biochem Pharmacol* 2007, *73*, 1463-1473.

(167) Radominska-Pandya, A.; Czernik, P. J.; Little, J. M.; Battaglia, E.; Mackenzie, P. I. *Drug Metab Rev* 1999, *31*, 817-899.

(168) Cermak, R. *Expert Opin Drug Metab Toxicol* 2008, *4*, 17-35.

(169) Morris, M. E.; Zhang, S. *Life Sci* 2006, *78*, 2116-2130.

(170) Fang, J. L.; Beland, F. A.; Doerge, D. R.; Wiener, D.; Guillemette, C.; Marques, M. M.; Lazarus, P. *Cancer Res* 2002, *62*, 1978-1986.

(171) Mabry, T. J.; Markham, K. R.; Thomas, M. B. *The systematic identification of flavonoids*; Springer-Verlag: New York,, 1970.

(172) Markham, K. R. *Techniques of flavonoid identification*; Academic Press: London ; New York, 1982.

(173) Singh, R.; Wu, B.; Tang, L.; Liu, Z.; Hu, M. *J Agric Food Chem* 2010.

(174) Chen, Y. K.; Chen, S. Q.; Li, X.; Zeng, S. *Xenobiotica* 2005, *35*, 943-954.

(175) Davis, B. D.; Brodbelt, J. S. *J Am Soc Mass Spectrom* 2008, *19*, 246-256.

(176) Messina, M. J. *Am J Clin Nutr* 1999, *70*, 439S-450S.

(177) Ross, J. A.; Kasum, C. M. *Annu Rev Nutr* 2002, *22*, 19-34.

(178) Setchell, K. D.; Cassidy, A. *J Nutr.* 1999, *129*, 758S-767S.

(179) Murota, K.; Shimizu, S.; Miyamoto, S.; Izumi, T.; Obata, A.; Kikuchi, M.; Terao, J. *J Nutr* 2002, *132*, 1956-1961.

(180) Shah, P.; Jogani, V.; Bagchi, T.; Misra, A. *Biotechnol Prog* 2006, *22*, 186-198.

(181) Hubatsch, I.; Ragnarsson, E. G.; Artursson, P. *Nat Protoc* 2007, *2*, 2111-2119.

(182) Hidalgo, I. J. *Curr Top Med Chem* 2001, *1*, 385-401.

(183) Artursson, P.; Palm, K.; Luthman, K. *Adv Drug Deliv Rev* 2001, *46*, 27-43.

(184) Li, C.; Liu, T.; Cui, X.; Uss, A. S.; Cheng, K. C. *J Biomol Screen* 2007, *12*, 1084-1091.

(185) Hu, M.; Chen, J.; Tran, D.; Zhu, Y.; Leonardo, G. *J Drug Target* 1994, *2*, 79-89.

(186) Hu, M.; Chen, J.; Zhu, Y.; Dantzig, A. H.; Stratford, R. E., Jr.; Kuhfeld, M. T. *Pharm Res* 1994, *11*, 1405-1413.

(187) Harris, R. M.; Wood, D. M.; Bottomley, L.; Blagg, S.; Owen, K.; Hughes, P. J.; Waring, R. H.; Kirk, C. J. *J Clin Endocrinol Metab* 2004, *89*, 1779-1787.

(188) Pai, T. G.; Suiko, M.; Sakakibara, Y.; Liu, M. C. *Biochem Biophys Res Commun* 2001, *285*, 1175-1179.

(189) Gugler, R.; Leschik, M.; Dengler, H. J. *Eur. J. Clin. Pharmacol* 1975, *9*, 229–234.

(190) Walle, T.; Otake, Y.; Brubaker, J. A.; Walle, U. K.; Halushka, P. V. *Br J Clin Pharmacol* 2001, *51*, 143-146.

(191) Kanaze, F. I.; Bounartzi, M. I.; Georgarakis, M.; Niopas, I. *Eur J Clin Nutr* 2007, *61*, 472-477.

(192) Barrington, R.; Williamson, G.; Bennett, R. N.; Davis, B. D.; Brodbelt, J. S.; Kroon, P. A. *J Funct Foods* 2009, *1*, 74-87.

(193) Graf, B. A.; Milbury, P. E.; Blumberg, J. B. *J Med Food* 2005, *8*, 281-290.

(194) Manach, C.; Scalbert, A.; Morand, C.; Rémésy, C.; Jiménez, L. *Am J Clin Nutr* 2004, *79*, 727-747.

(195) Williamson, G.; Aeberli, I.; Miguet, L.; Zhang, Z.; Sanchez, M. B.; Crespy, V.; Barron, D.; Needs, P.; Kroon, P. A.; Glavinas, H.; Krajcsi, P.; Grigorov, M. *Drug Metab Dispos* 2007, *35*, 1262-1268.

(196) Gupta, S.; Afaq, F.; Mukhtar, H. *Biochem Biophys Res Commun* 2001, *287*, 914-920.

(197) Wang, W.; Heideman, L.; Chung, C. S.; Pelling, J. C.; Koehler, K. J.; Birt, D. F. *Mol Carcinog* 2000, *28*, 102-110.

(198) Knowles, L. M.; Zigrossi, D. A.; Tauber, R. A.; Hightower, C.; Milner, J. A. *Nutr Cancer* 2000, *38*, 116-122.

(199) Kobayashi, T.; Nakata, T.; Kuzumaki, T. *Cancer Lett* 2002, *176*, 17-23.

(200) Lee, S. C.; Kuan, C. Y.; Yang, C. C.; Yang, S. D. *Anticancer Res* 1998, *18*, 1117-1121.

(201) Makela, S.; Poutanen, M.; Kostian, M. L.; Lehtimaki, N.; Strauss, L.; Santti, R.; Vihko, R. *Proc Soc Exp Biol Med* 1998, *217*, 310-316.

(202) Galijatovic, A.; Otake, Y.; Walle, U. K.; Walle, T. *Xenobiotica* 1999, *29*, 1241-1256.

(203) Piskula, M. K. *Biofactors* 2000, *12*, 175-180.

(204) Ung, D.; Nagar, S. *Drug Metab Dispos* 2007, *35*, 740-746.

(205) Li, J.; Hidalgo, I. J. In *The Process of New Drug Discovery and Development*, Second ed.; Smith, C. G., O' Donnell, J. T., Eds.; Informa Health Care: London, UK, 2006, pp 162-179.

(206) Walle, U. K.; French, K. L.; Walgren, R. A.; Walle, T. *Res Commun Mol Pathol Pharmacol* 1999, *103*, 45-56.

(207) Walle, U. K.; Galijatovic, A.; Walle, T. *Biochem Pharmacol* 1999, *58*, 431-438.

(208) Sesink, A. L.; Arts, I. C.; de Boer, V. C.; Breedveld, P.; Schellens, J. H.; Hollman, P. C.; Russel, F. G. *Mol Pharmacol* 2005, *67*, 1999-2006.

Appendix A. MS2 sacns of glucuronides and sulfates of flavonoids in Caco-2 Cells transport or supersomes glucuronidation studies samples.

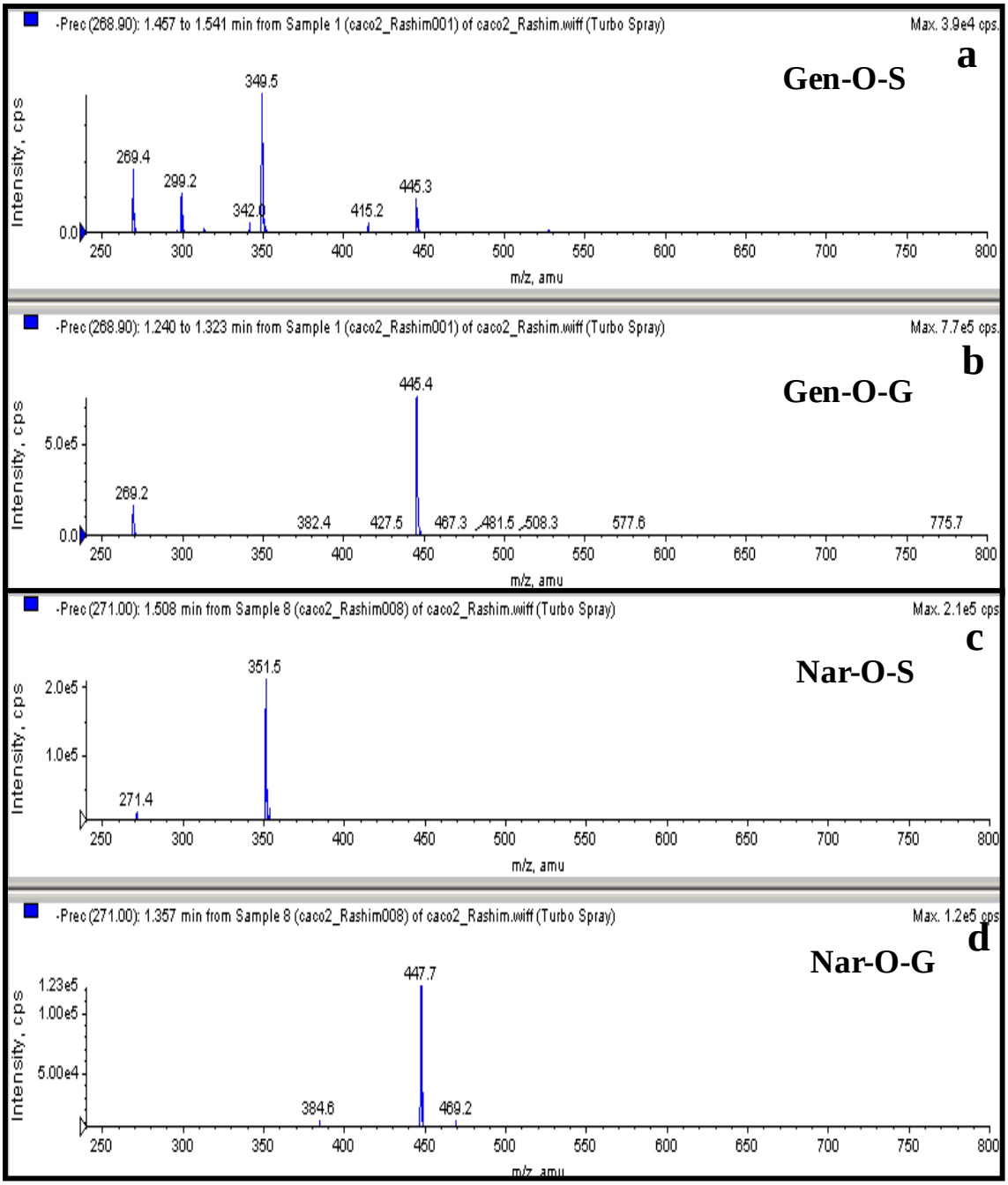

Figure A1. MS2 (precursor ion scan) of genistein (Gen) sulfate (a), genistein glucuronide (b), naringenin (Nar) sulfate (c), and naringenin *O*-glucuronide (d) in Caco-2 Cells transport or supersomes glucuronidation studies samples.

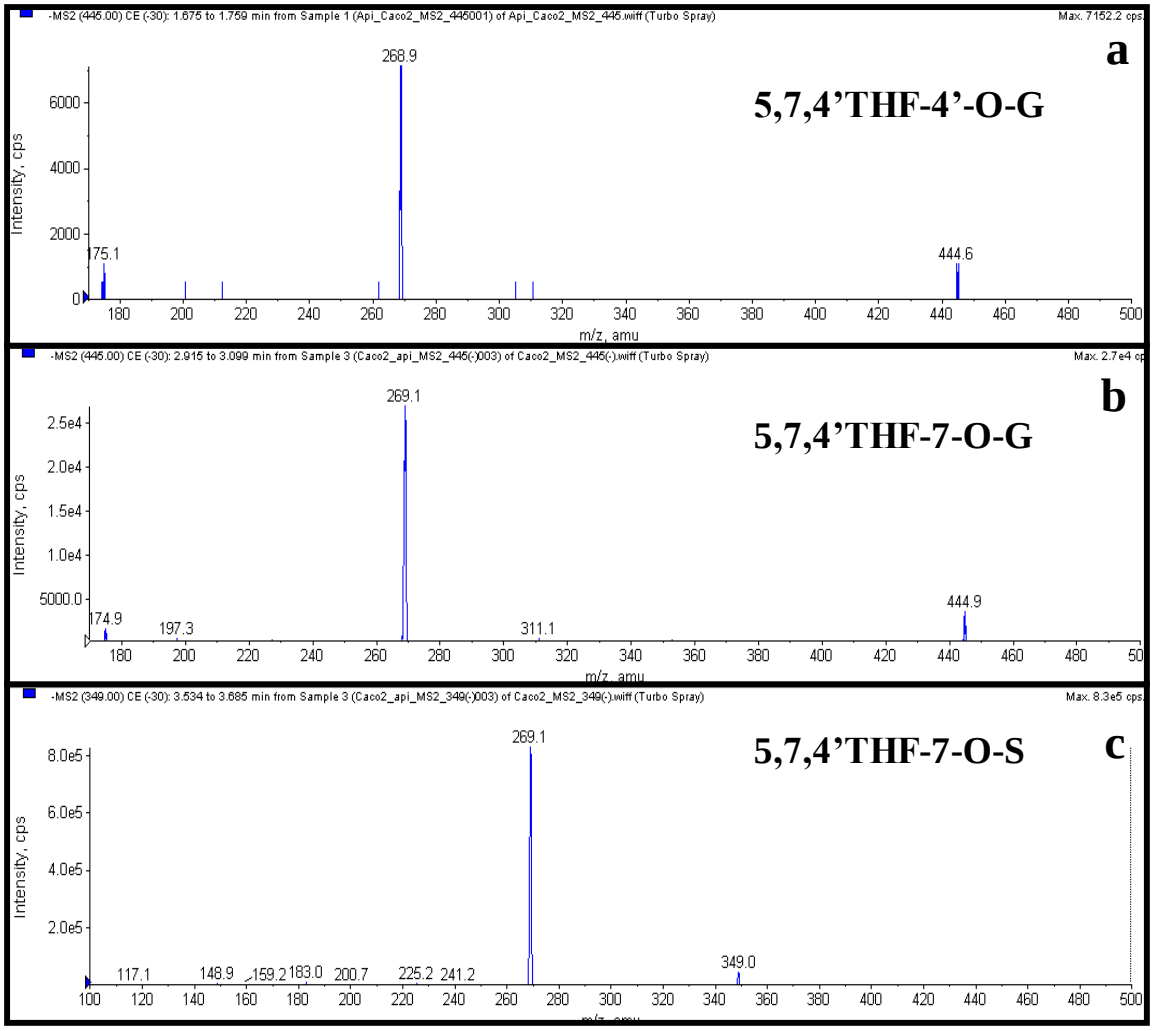

Figure A2. MS2 of 5,7,4'THF (5,7,4'-trihydroxyflavone, apigenin) 4'-*O*-glucuronide (a), 5,7,4'THF 7-*O*-glucuronide (b), and 5,7,4'THF 7-*O*-sulfate (c) in Caco-2 Cells transport or supersomes glucuronidation studies samples.

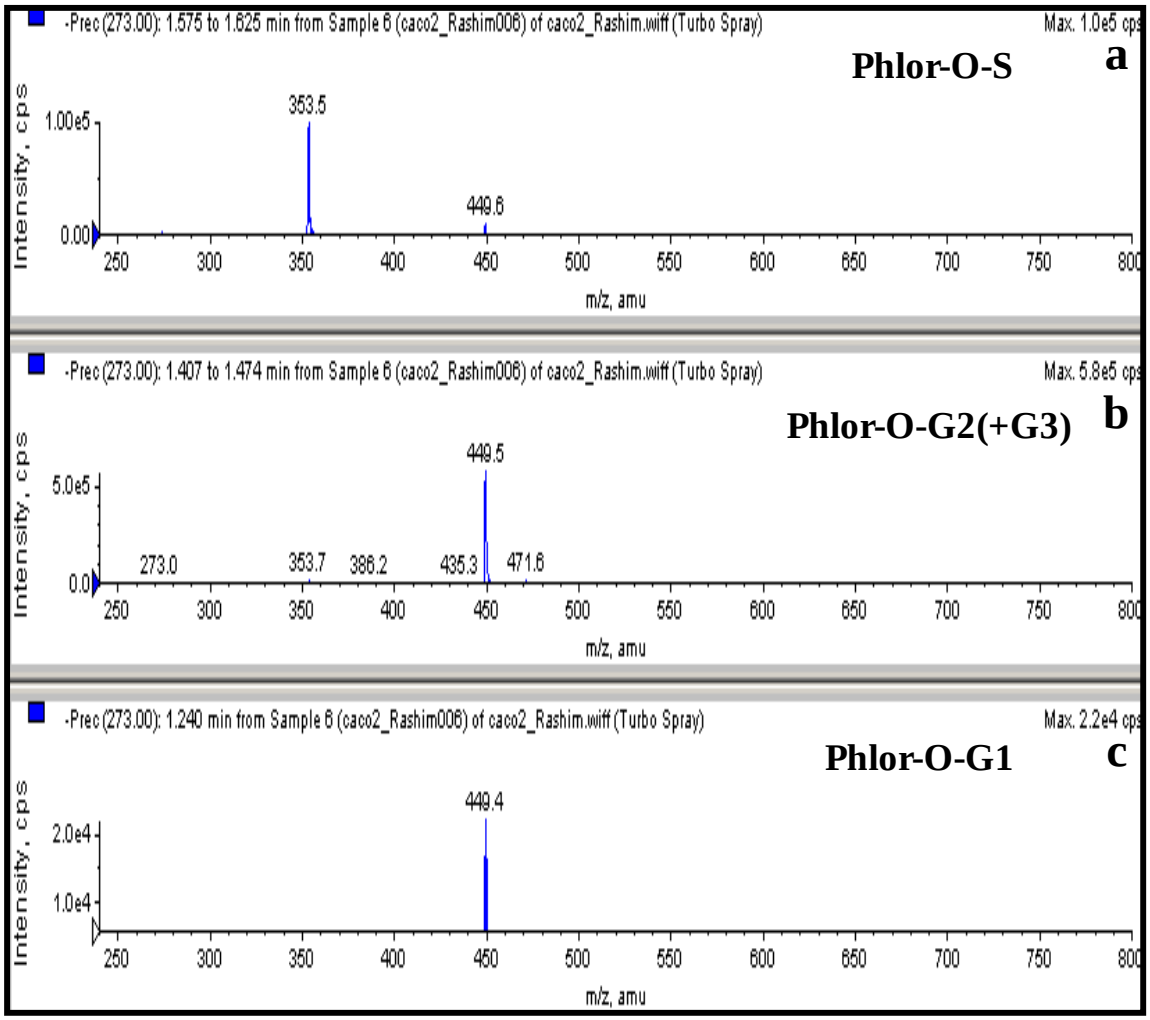

Figure A3. MS2 (precursor ion scan) of phloretin *O*-sulfate (Phlor), (a) phloretin *O*-glucuronides 2 and 3 overlapped (b), and phloretin *O*-glucuronide 1 (c) in Caco-2 Cells transport or supersomes glucuronidation studies samples.

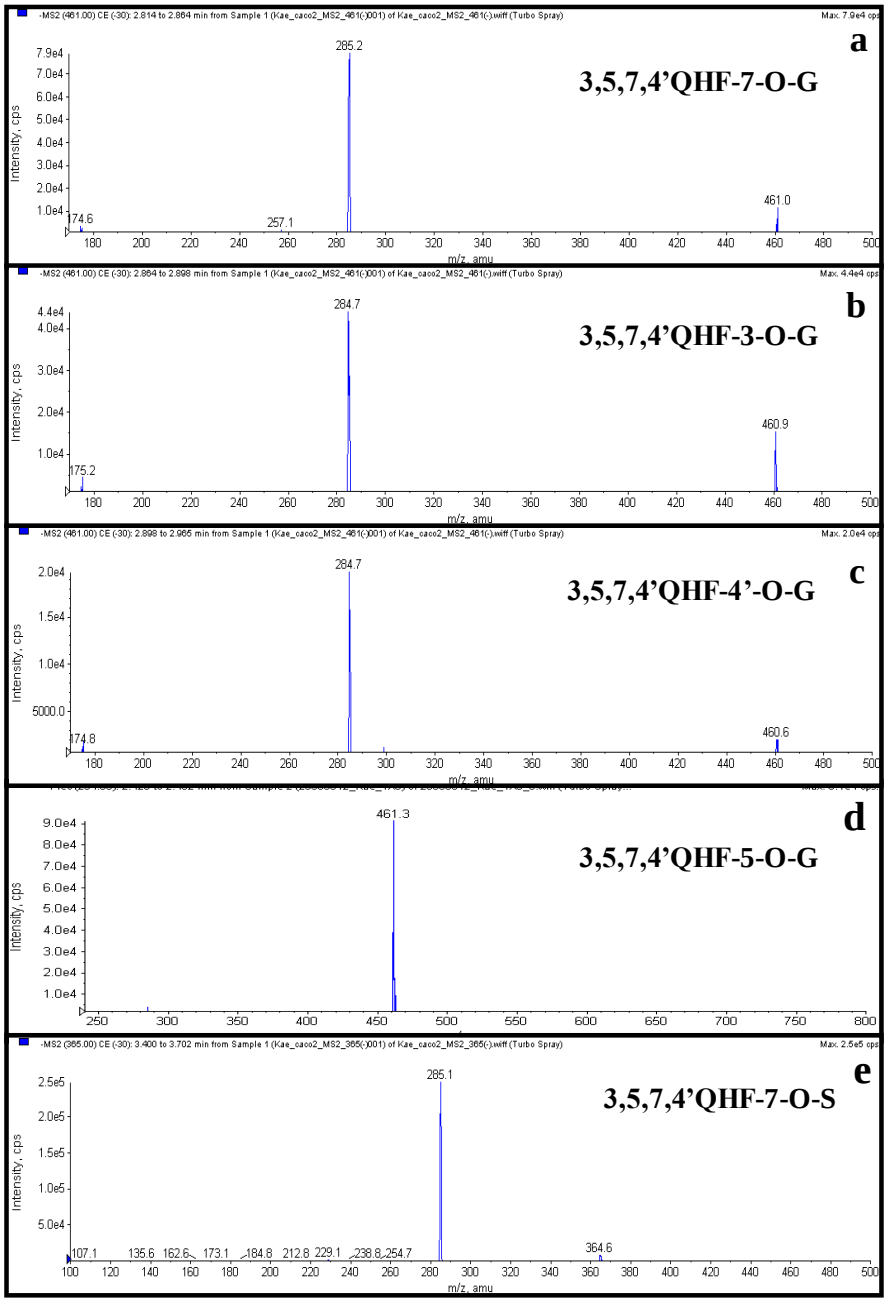

Figure A4. MS2 of 3,5,7,4'QHF(3,5,7,4'-tetrahydroxyflavone, kaempferol) 7-*O*-glucuronide (a), 3,5,7,4'QHF 3-*O*-glucuronide (b), 3,5,7,4'QHF 4'-*O*-glucuronide (c), 3,5,7,4'QHF 5-*O*-glucuronide (precursor ion scan) (d), and 3,5,7,4'QHF 7-*O*-sulfate (e) in Caco-2 Cells transport or supersomes glucuronidation studies samples.

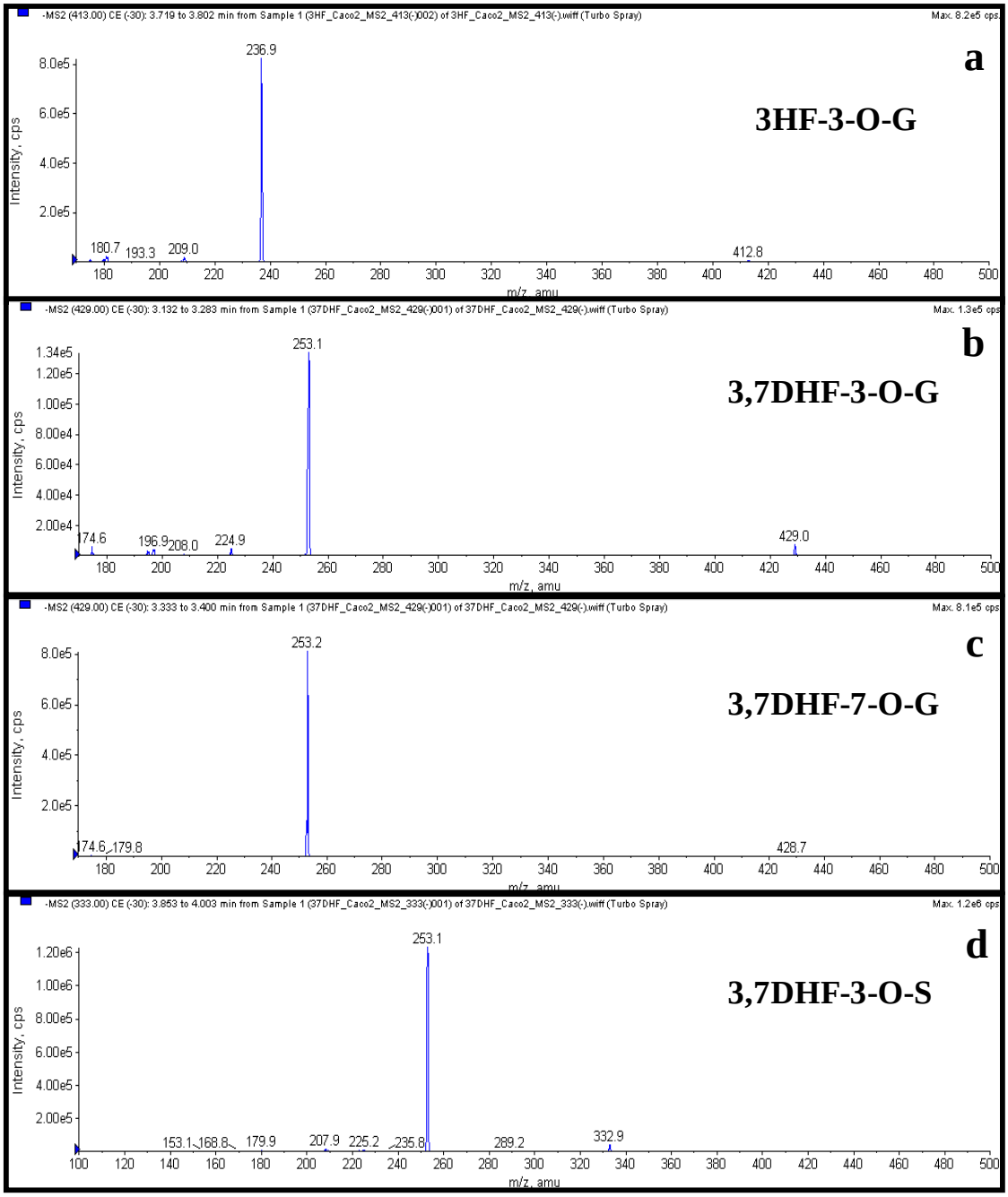

Figure A5. MS2 of 3HF (3-hydroxyflavone) 3-*O*-glucuronide (a), 3,7DHF (3,7-dihydroxyflavone) 3-*O*-glucuronide (b), 3,7DHF 7-*O*-glucuronide (c), and 3,7DHF 7-*O*-sulfate (d) in Caco-2 Cells transport or supersomes glucuronidation studies samples.

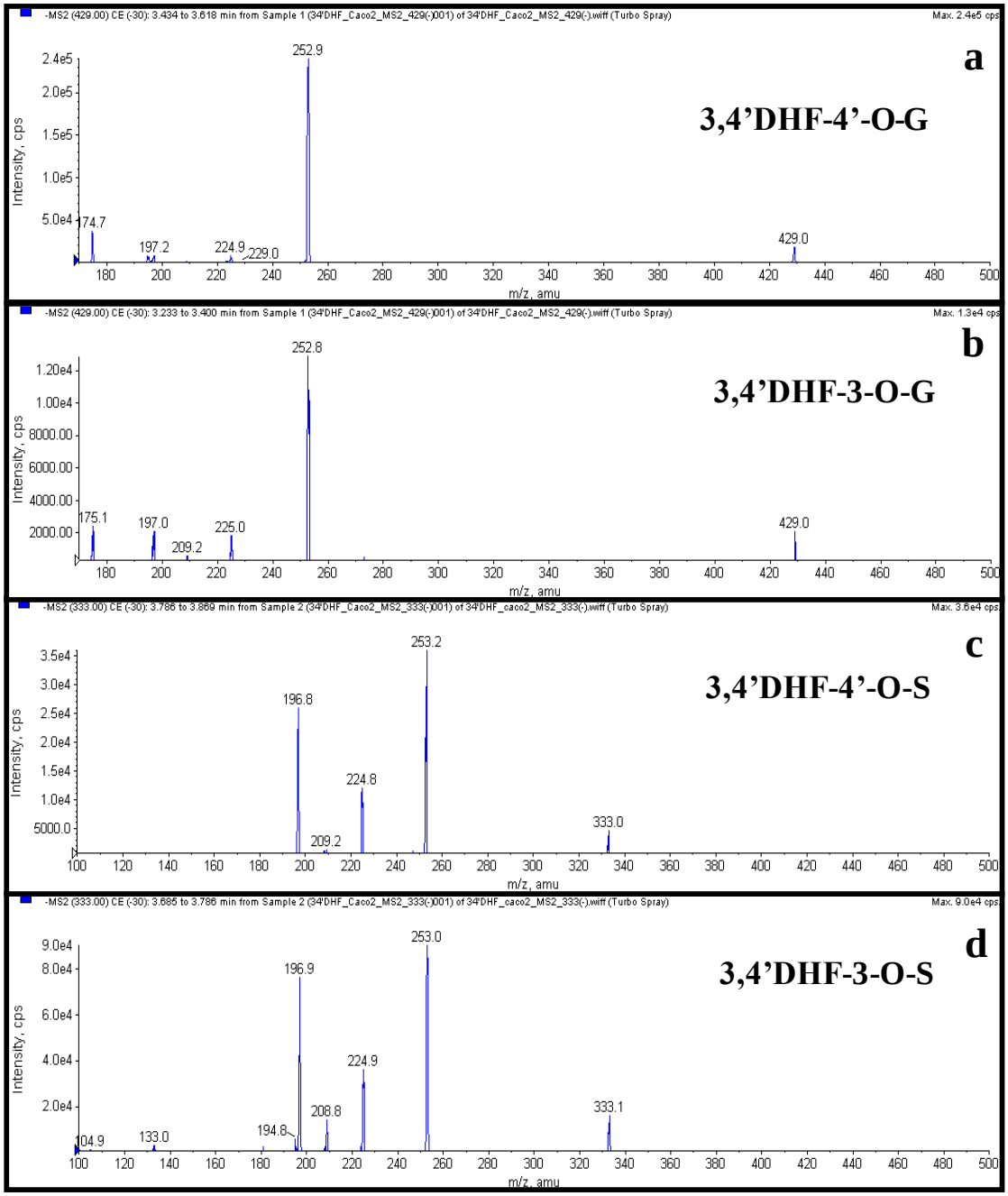

Figure A6. MS2 of 3,4'DHF (3,4'-dihydroxyflavone) 4'-*O*-glucuronide (a), 3,4'DHF 3-*O*-glucuronide (b), 3,7DHF 4'-*O*-sulfate (c), and 3,7DHF 3-*O*-sulfate (d) in Caco-2 Cells transport or supersomes glucuronidation studies samples.

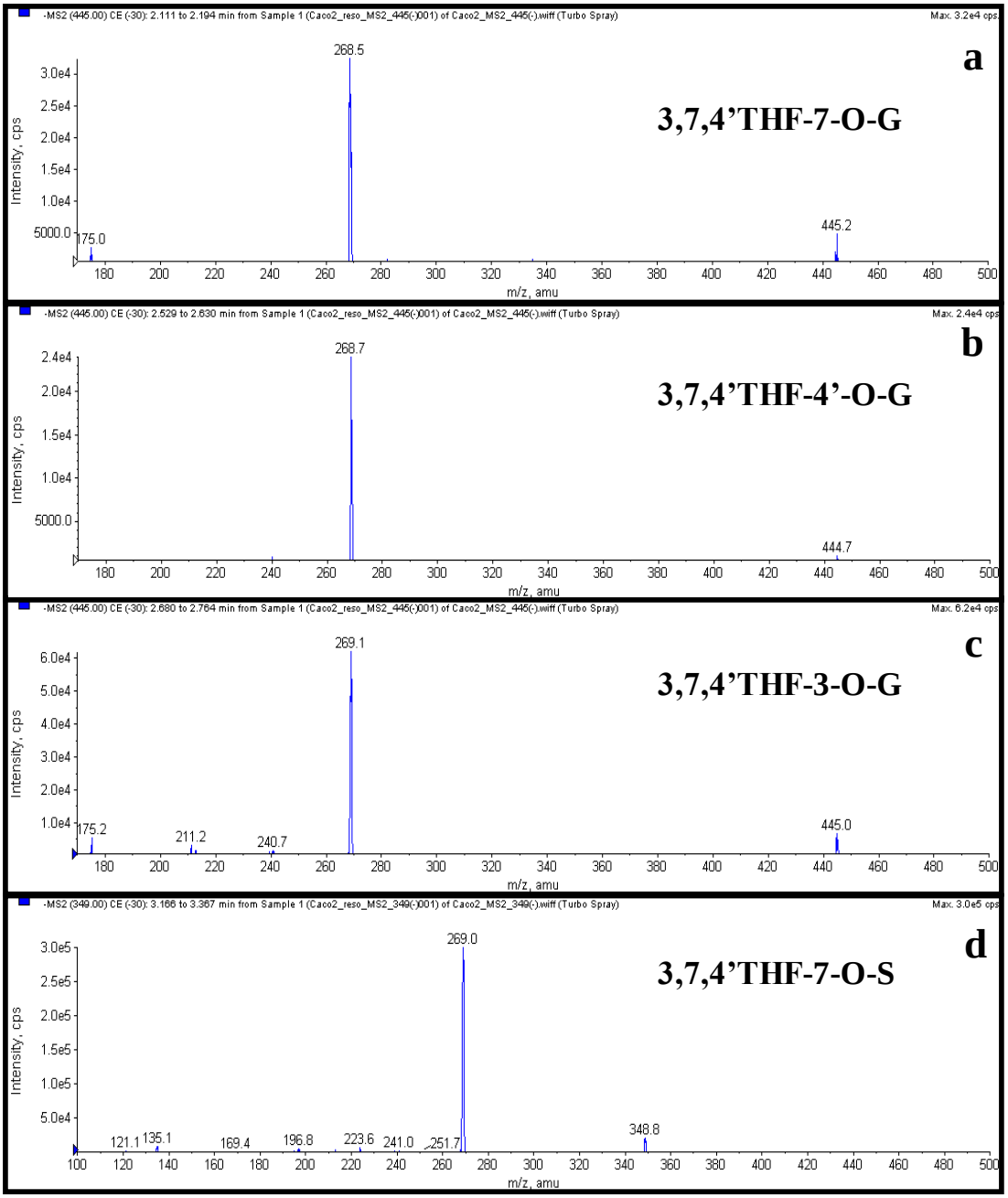

Figure A7. MS2 of 3,7,4'THF (3,7,4'-trihydroxyflavone) 7-*O*-glucuronide (a), 3,7,4'THF 4'-*O*-glucuronide (b), 3,7,4'THF 3-*O*-glucuronide (c), and 3,7,4'THF 7-*O*-sulfate (d) in Caco-2 Cells transport or supersomes glucuronidation studies samples.

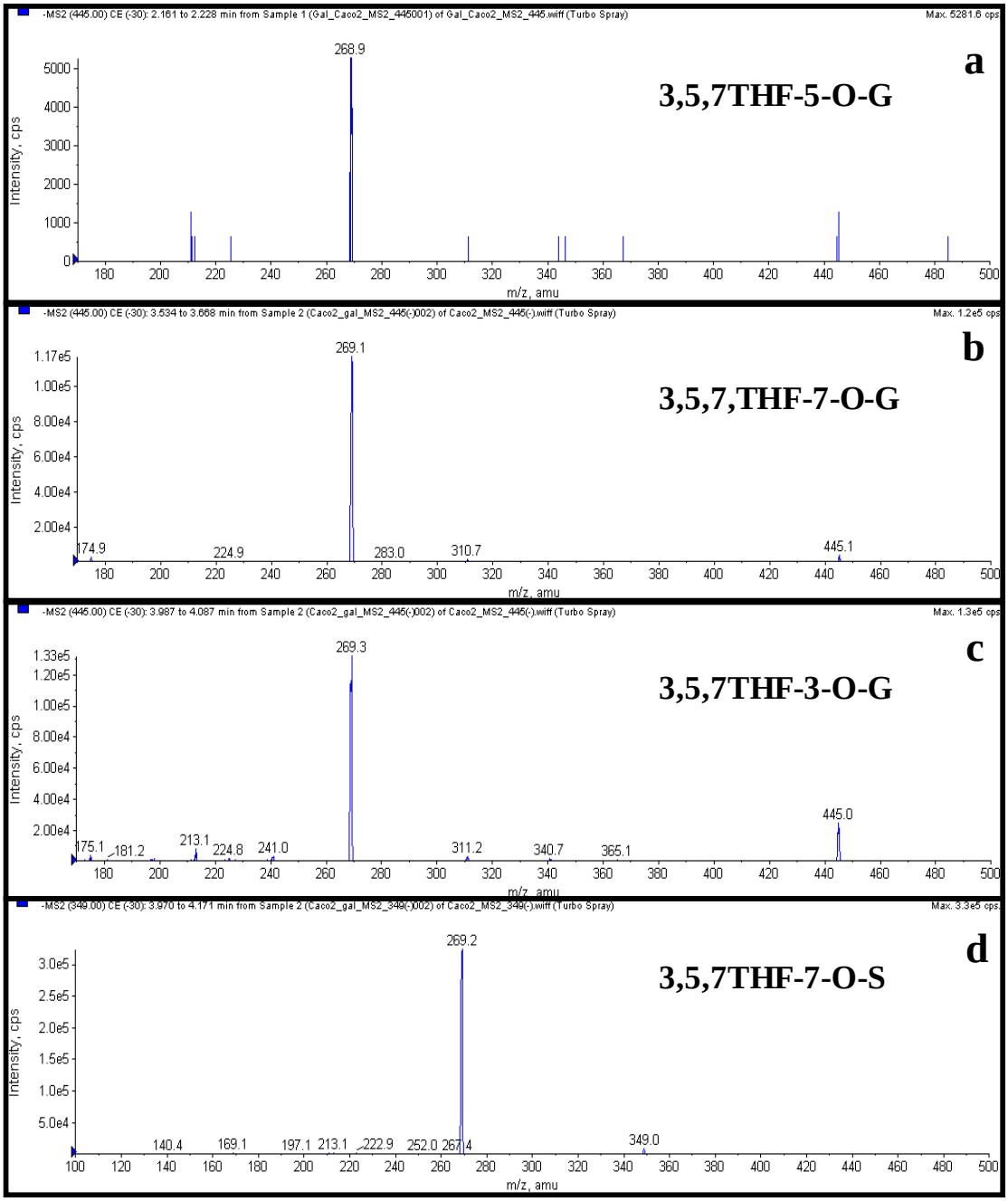

Figure A8. MS2 of 3,5,7THF (3,5,7-trihydroxyflavone) 5-*O*-glucuronide (a), 3,5,7THF 7-*O*-glucuronide (b), 3,5,7THF 3-*O*-glucuronide (c), and 3,5,7THF 7-*O*-sulfate (d) in Caco-2 Cells transport or supersomes glucuronidation studies samples.

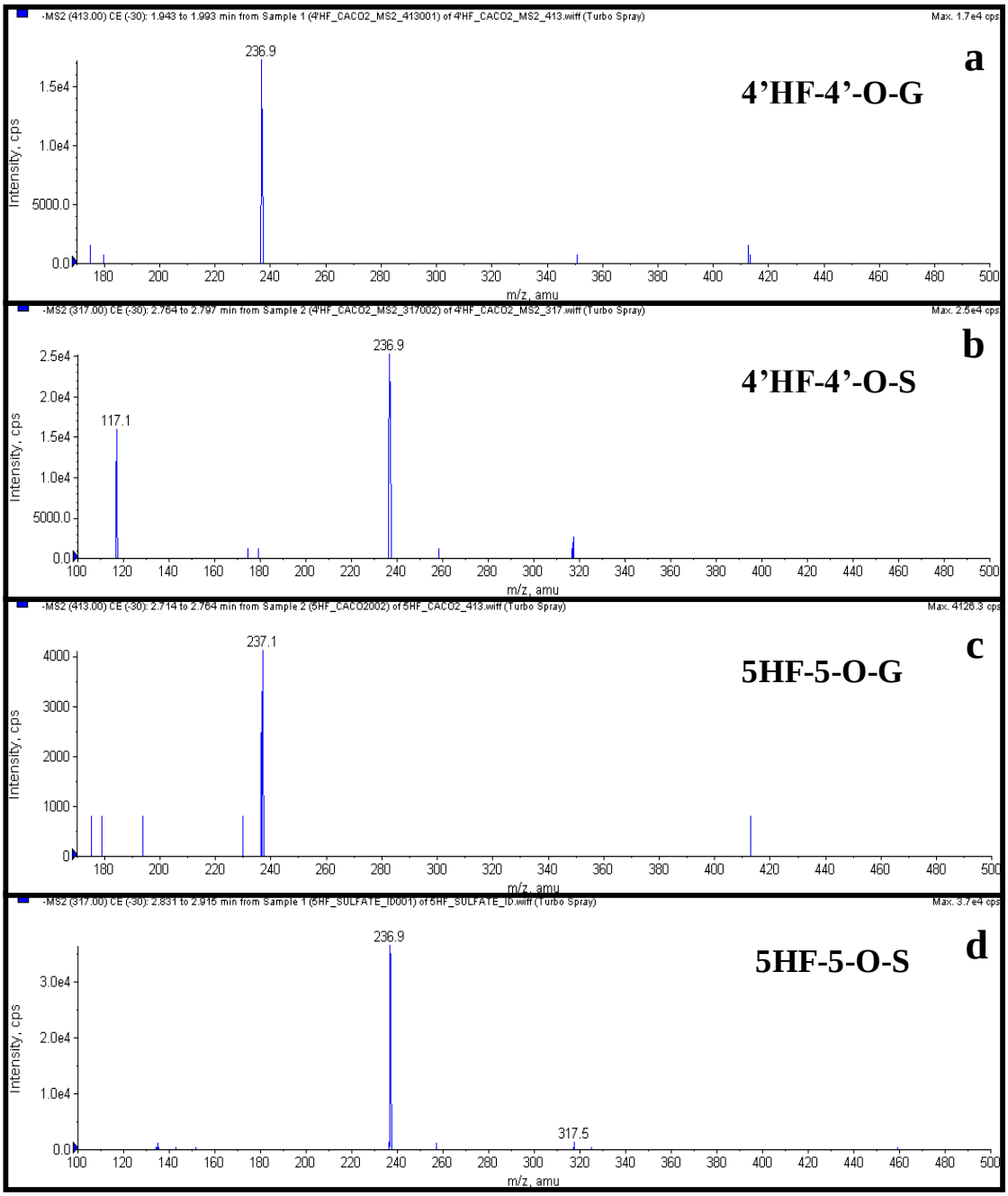

Figure A9. MS2 of 4'HF (4'-hydroxyflavone) 4'-*O*-glucuronide (a), 4'HF 4'-*O*-sulfate (b), 5HF (4'-hydroxyflavone) 5-*O*-glucuronide (c), and 5HF 5-*O*-sulfate (d) in Caco-2 Cells transport or supersomes glucuronidation studies samples.

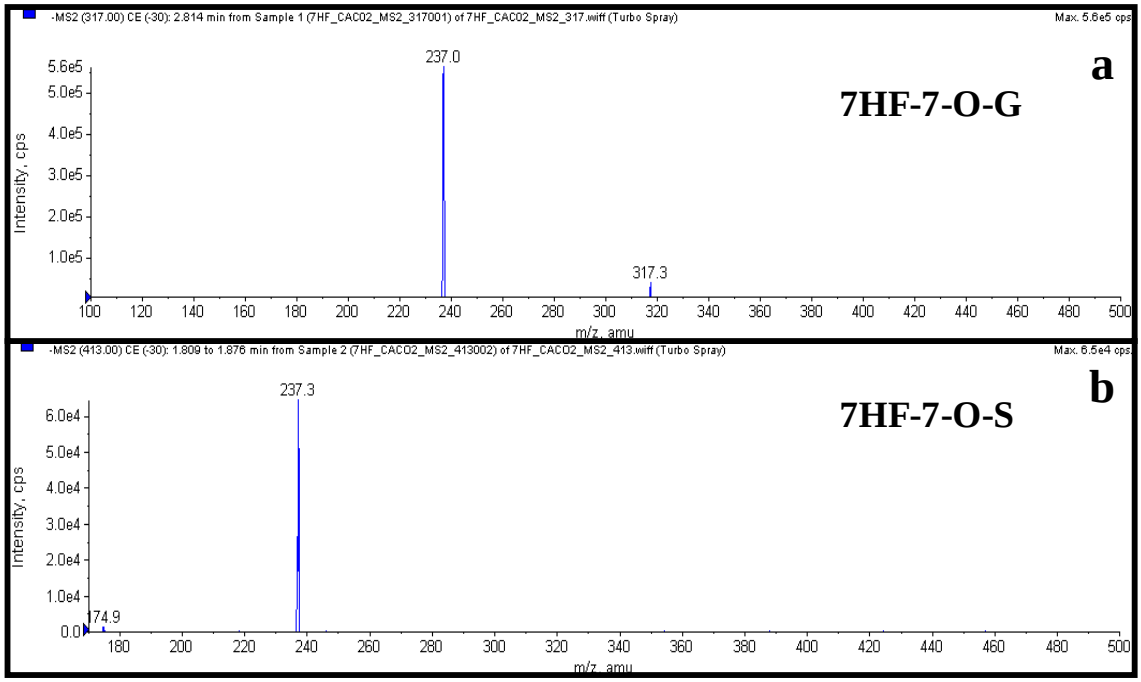

Figure A10. MS2 of 7HF (7-hydroxyflavone) 7-*O*-glucuronide (a), and 7HF 7-*O*-sulfate (b) in Caco-2 Cells transport or supersomes glucuronidation studies samples.

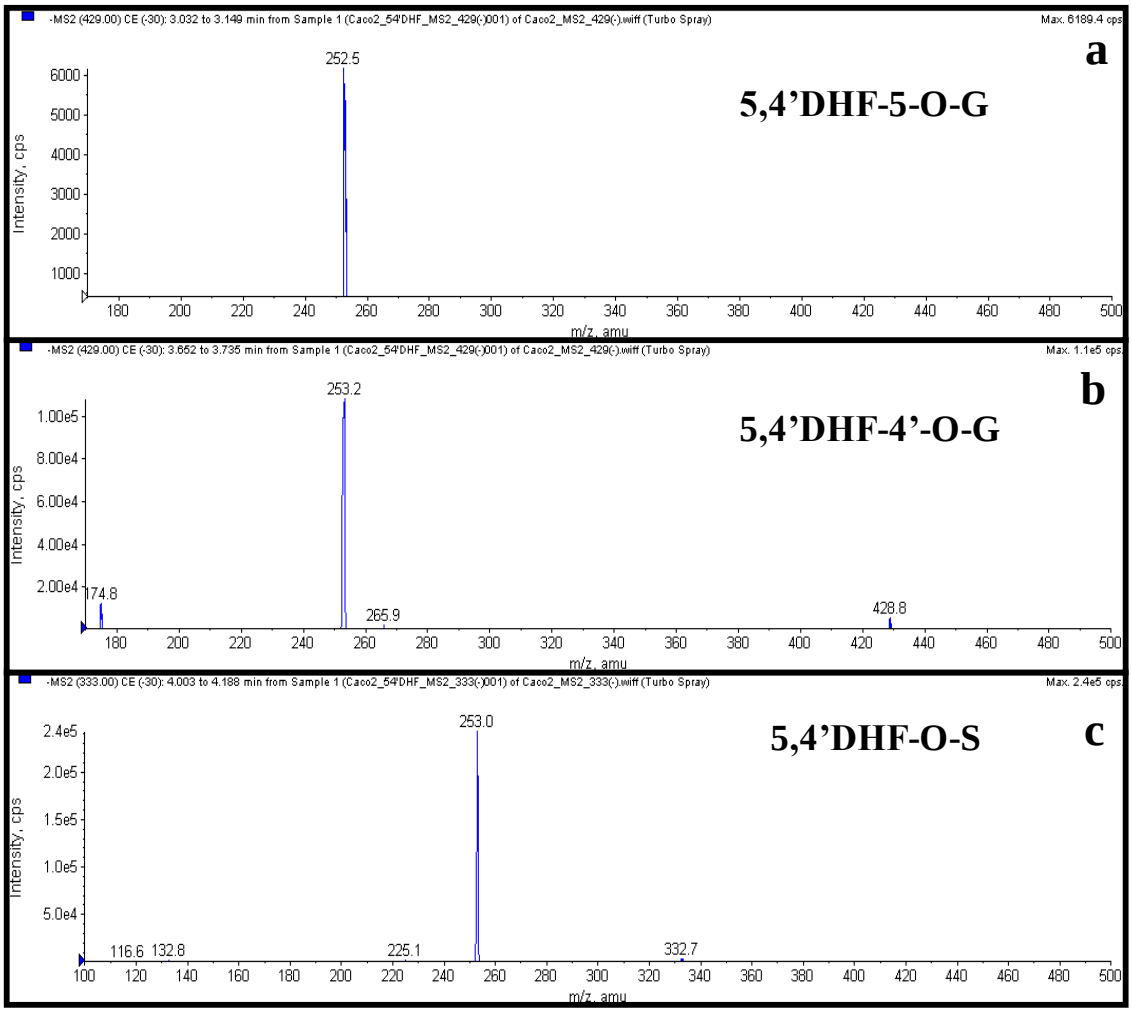

Figure A11. MS2 of 5,4'DHF (5,4'-dihydroxyflavone) 5-*O*-glucuronide (a), 5,4'DHF 4'-*O*-glucuronide (b), and 5,4'DHF *O*-sulfate (c) in Caco-2 Cells transport or supersomes glucuronidation studies samples.

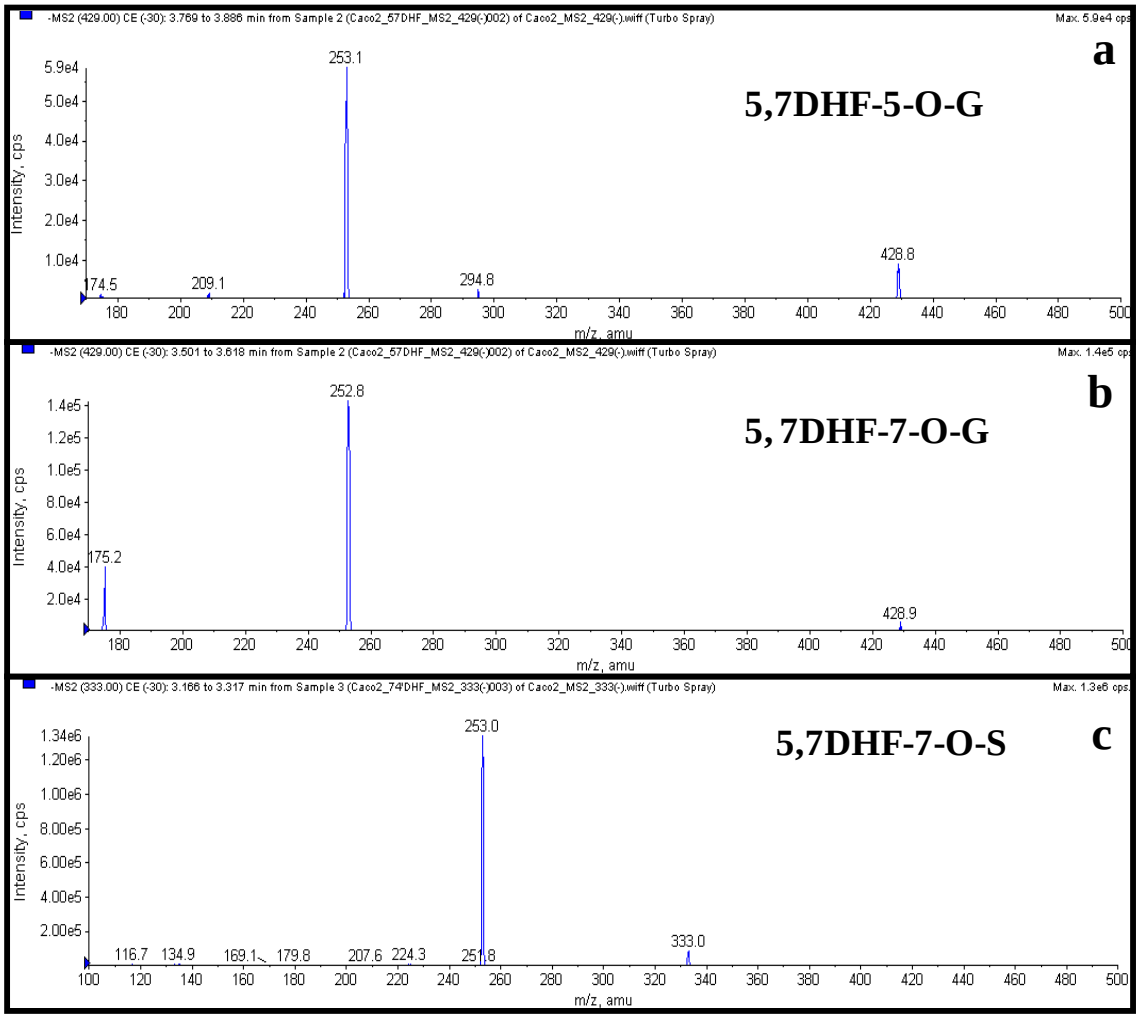

Figure A12. MS2 of 5,7DHF (5,7-dihydroxyflavone) 5-*O*-glucuronide (a), 5,7DHF 7-*O*-glucuronide (b), and 5,7DHF 7-*O*-sulfate (c) in Caco-2 Cells transport or supersomes glucuronidation studies samples.

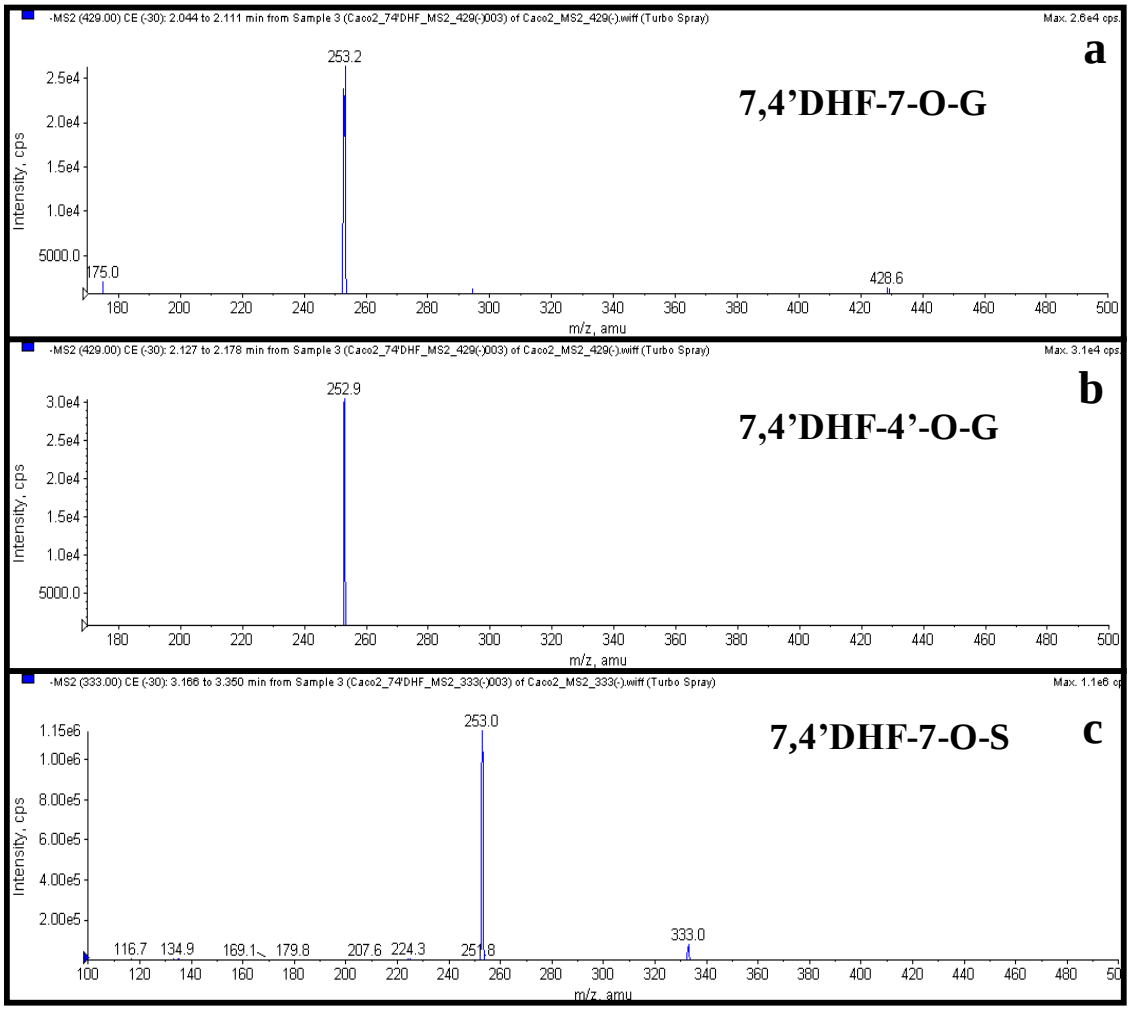

Figure A13. MS2 of 7,4'DHF (7,4'-dihydroxyflavone) 7-*O*-glucuronide (a), 7,4'DHF 4'-*O*-glucuronide (b), and 7,4'DHF 7-*O*-sulfate (c) in Caco-2 Cells transport or supersomes glucuronidation studies samples.

Appendix B. UV λ_{max} shift in Band I and Band II of the UV spectra of the flavonoids and their respective glucuronide(s) and sulfates

Table B1 UV λ_{max} shift in Band I and Band II of the UV spectra of the apigenin, kaempferol and their respective *O*-glucuronide(s) and *O*-sulfates

Flavonols/ Glucuronides/ Sulfates	UV λ_{max} (nm)				Position of Conjugation based on λ_{max} Shift
	Band I	λ_{max} Shift	Band II	λ_{max} Shift	
Apigenin (Api)	334.8		267.7		
Api-*O*-G1	-		-		4'-O-G*
Api-*O*-G2	338.9	+ 4.1	267.7	No Change	7-O-G
Api-*O*-S	338.9	+ 4.1	267.7	No Change	7-O-S
Kaempferol (Kamp)	366.1		262.9		
Kamp-*O*-G1	366.1	No change	262.9	No change	7-O-G
Kamp -*O*-G2	357.8	- 8.3	253.8	No change	4'-O-G
Kamp -*O*-G3	343.7	- 22.4	262.9	No change	3-O-G
Kamp -*O*-S	366.1	No change	262.9	No change	7-O-S

** Position was guessed based on high reactivity of 4'-O position as compared to 5-O as we could not get a good UV spectrum due to low concentration of glucuronide.

Table B2 UV λ_{max} shift in Band I and Band II of the UV spectra of the flavonols and their respective glucuronide(s) and sulfates

Flavonols/ Glucuronides/ Sulfates	UV λ_{max} (nm)				Position of Conjugation based on λ_{max} Shift
	Band I	λ_{max} Shift	Band II	λ_{max} Shift	
3HF	343.7		239.4		
3HF-3-*O*-G	-	Band I Disappeared	248.8	+ 9.4	3-O-G
3,4'DHF	357.3		ND		
3,4'DHF-*O*-G1	348.5	- 8.8	ND		4'-O-G
3,4'DHF-*O*-G2	334.1	- 23.2	229.9		3-O-G
3,4'DHF-*O*-S	352.5	- 4.8	244.1		4'-O-S
3,7DHF	343.7		253.5		
3,7DHF-*O*-G1	315.1	- 28.6	248.8	- 4.5	3-O-G
3,7DHF-*O*-G2	343.7	No change	248.8	- 4.5	7-O-G
3,7DHF-*O*-S	343.7	No change	248.8	- 4.5	7-O-S
3,5,7THF	357.8		269.3		
3,5,7THF-*O*-G1	-	Band I Disappeared	269.3	No change	3-O-G

Flavonols/ Glucuronides/ Sulfates	UV λ_{max} (nm)				Position of Conjugation based on λ_{max} Shift
	Band I	λ_{max} Shift	Band II	λ_{max} Shift	
3,5,7THF-*O*-G2	357.8	No change	269.3	No change	7-O-G
3,5,7THF-*O*-G3	348.5	- 9.3	258.2	- 4.7	5-O-S
3,5,7THF-*O*-S	357.8	No change	269.3	No change	7-O-S
3,7,4'THF	353.2		258.2		
3,7,4'THF-*O*-G1	353.2	No Change	253.5	- 4.7	7-O-G
3,7,4'THF-*O*-G2	348.5	- 4.7	258.2	No change	4'-O-G
3,7,4'THF-*O*-G3	324.6	- 28.6	253.5	- 4.7	3-O-G
3,7,4'THF-*O*-S	353.2	No Change	248.8	- 9.4	7-O-S
3,5,7,4'QHF	366.1		262.9		
3,5,7,4'QHF-*O*-G1	366.1	No change	262.9	No change	7-O-G
3,5,7,4'QHF-*O*-G2	357.8	- 8.3	253.8	No change	4'-O-G
3,5,7,4'QHF-*O*-G3	343.7	- 22.4	262.9	No change	3-O-G
3,5,7,4'QHF-*O*-S	366.1	No change	262.9	No change	7-O-S

* ND means not detected by the Empower software in the spectra

Table B3 UV λ_{max} shift in Band I and Band II of the UV spectra of the flavones and their respective glucuronide(s) and sulfates

Flavones/ Glucuronides/ Sulfates	UV λ_{max} (nm)				Position of Conjugation based on λ_{max} Shift
	Band I	λ_{max} Shift	Band II	λ_{max} Shift	
4'HF	324.1		253.5		
4'HF-4'-*O*-G	315.6	- 8.5	248.8	- 5.0	4'-O-G
5HF	ND		270.4		
5HF-5-*O*-G	ND		263.1	- 7.3	5-O-G
5HF-5-*O*-S	-		-		5-O-S**
7HF	310.3		253.5		
7HF-7-*O*-G	305.6	-4.7#	ND	-	7-O-G
7HF-7-*O*-S	300.8	-9.5#	248.8		7-O-S
5,4'DHF	332.0		268.0		
5,4'DHF-*O*-G1	332.0	No change	263.1	- 4.9	5-O-G
5,4'DHF-*O*-G2	317.2	-14.8#	272.9	+ 4.9	4'-O-G
5,4'DHF-*O*-S	332.0	No change	263.1	- 4.9	5-O-S
5,7DHF	315.1		267.7		
5,7DHF-*O*-G1	305.6	- 9.5	267.7	No change	7-O-G
5,7DHF-*O*-G2	315.1	No Change	262.9	- 4.8	5-O-G

Flavones/ Glucuronides/ Sulfates	UV λ_{max} (nm)				Position of Conjugation based on λ_{max} Shift
	Band I	λ_{max} Shift	Band II	λ_{max} Shift	
5,7DHF-*O*-S	300.8	- 14.3	267.7	No change	7-O-S
7,4'DHF	334.1		258.2		
7,4'DHF-*O*-G1	329.4	- 4.6[#]	258.2	No Change	7-O-G
7,4'DHF-*O*-G1	315.1	-19.0[#]	258.2	No Change	4'-O-G
7,4'DHF-*O*-S	324.6	- 9.5[#]	258.2	No Change	7-O-S
5,7,4'THF	334.8		267.7		
5,7,4'THF-*O*-G1	-		-		4'-O-G
5,7,4'THF-*O*-G1	338.9	+ 4.1	267.7	No Change	7-O-G
5,7,4'THF-*O*-S	338.9	+ 4.1	267.7	No Change	7-O-S

* ND means not detected by the Empower software in the spectra

** Due to low concentration of sulfate of 5HF, we could not get a good UV spectrum.

[#] Show deviation from diagnostic no change in λmax, probably as the concentration of these sulfates and glucuronides was too small in sample and we could not get a good UV spectrum. Positions of glucuronidation and sulfation were determined by the known reactivity of site of conjugation and rule of elimination.

Appendix C. UGT isoforms used to generate the glucuronides and the correction factors (K) determined for the adjustment when quantifying glucuronides and sulfates using the standard curve of their corresponding flavonoids in Caco-2 cell transport and UGT "fingerprinting" studies.

Table C1 UGT isoforms used to generate the glucuronides and the correction factors (K) determined for the adjustment when quantifying glucuronides and sulfates using the standard curve of their corresponding flavonoids in Caco-2 cell transport and UGT "fingerprinting" studies.

Glucuronides/ Sulfates	UGT Isoforms used for generating glucuronide	Correction Factor (K)	Wavelength (nm) used
Genistein-*O*-G	1A9	1	254
Naringenin-*O*-G	1A9	0.95	286
Naringenin-*O*-S	--	1[#]	286
Phlor-*O*-G1	1A1,1A8	1.37	286
Phlor-*O*-G2	1A6	1.67	286
Phlor-*O*-G3	1A1,1A8	1.1	286
Phlor-*O*-S	--	1[#]	286
Kamp-7-*O*-G	1A6, 1A7, 1A8, 1A9, 1A10	0.87	254
Kamp-4'-*O*-G	1A8, 1A10	1.55	254
Kamp-3-*O*-G	1A6, 1A7, 1A8, 1A9, 1A10	1.34	254
Kamp-7-*O*-S	--	0.87*	254
5,7,4'THF-4'-*O*-G	--	1.0**	340
5,7,4'THF-7-*O*-G	1A6	1.2	340
5,7,4'THF-7-*O*-S	--	1.2*	340

Table C2 UGT isoforms used to generate the glucuronides and the correction factors (K) determined for the adjustment when quantifying glucuronides and sulfates using the standard curve of their corresponding flavonols in Caco-2 cell transport study and UGT "fingerprinting" studies.

Glucuronides/ Sulfates	UGT Isoforms used for generating glucuronide	Correction Factor (K)	Wavelength (nm) used
3HF-3-*O*-G	1A7	0.5	254
3,4'DHF-4'-*O*-G	1A1	0.98	340
3,4'DHF-3-*O*-G	1A1, 1A9	0.925	340
3,4'DHF-4'-*O*-S	--	0.98*	340
3,7DHF-3-*O*-G	1A3, 1A7, 1A9	2.5	340
3,7DHF-7-*O*-G	1A3, 1A9	1.18	340
3,7DHF-7-*O*-S	--	1.18*	340
3,5,7THF-3-*O*-G	1A3, 1A7, 1A8, 1A9, 1A10	0.84	263
3,5,7THF-7-*O*-G	1A3, 1A8, 1A9, 1A10	0.67	263
3,5,7THF-5-*O*-G	1A3, 1A7, 1A8, 1A10	0.76	263
3,5,7THF-7-*O*-S	--	0.67*	263
3,7,4'THF-7-*O*-G	1A1, 1A3, 1A8, 1A9, 2B7	1.15	340
3,7,4'THF-4'-*O*-G	1A1, 1A3, 1A8, 2B7	1.36	340
3,7,4'THF-3-*O*-G	1A1, 1A8, 1A9, 2B7	1.15	340
3,7,4'THF-7-*O*-S	--	1.15*	340
3,5,7,4'QHF-7-*O*-G	1A6, 1A7, 1A8, 1A9, 1A10	0.87	254
3,5,7,4'QHF-4'-*O*-G	1A8, 1A10	1.55	254
3,5,7,4'QHF-3-*O*-G	1A6, 1A7, 1A8, 1A9, 1A10	1.34	254
3,5,7,4'QHF-7-*O*-S	--	0.87*	254

* Based on almost overlapping spectra of sulfate and glucuronide of a flavonol which were conjugated at the same positions, same correction factors were used for sulfates as determined for the glucuronides at the corresponding positions.

Table C3 UGT isoforms used to generate the glucuronides and the correction factors (K) determined for the adjustment when quantifying glucuronides and sulfates using the standard curve of their corresponding flavones in Caco-2 cell transport study and UGT "fingerprinting" studies.

Glucuronides/ Sulfates	UGT Isoforms used for generating glucuronide	Correction Factor (K)	Wavelength (nm) used
4'HF-4-*O*-G	1A1	1.17	320
5HF-5-*O*-G	1A1	0.82	268
5HF-5-*O*-S	--	0.82*	268
7HF-7-*O*-G	1A3	0.92	310
7HF-7-*O*-S	--	0.92*	310
5,4'DHF-5-*O*-G	1A1, 1A3, 1A9, 1A10	1.38	340
5,4'DHF-4'-*O*-G	1A1, 1A3, 1A9, 1A10	0.97	340
5,7THF-5-*O*-G	--	1.0**	268
5,7THF-7-*O*-G	1A9, 1A10	0.72	268
5,7THF-7-*O*-S	--	0.72*	268
7,4'DHF-7-*O*-G	1A1, 1A9, 1A10	1.08	340
7,4'DHF-4'-*O*-G	1A1, 1A9, 1A10	1.0	340
7,4'DHF-7-*O*-S	--	1.08*	340
5,7,4'THF-5-*O*-G	--	1.0**	340
5,7,4'THF-7-*O*-G	1A6	1.2	340
5,7,4'THF-7-*O*-S	--	1.2*	340

* Based on almost overlapping spectra of sulfate and glucuronide of a flavone which were conjugated at the same positions, same correction factors were used for sulfates as determined for the glucuronides at the corresponding positions.

** Since the amount of these glucuronides formed using any UGT isoforms was very less, it was very difficult to accurately calculate the correction factor for these glucuronides. Hence, the correction factors for these glucuronides were assigned the default value of 1.

Table C4 Correction factors (K) determined for the adjustment when quantifying glucuronides using the standard curve of their corresponding flavonoids in UGT "fingerprinting" studies.

Glucuronides*	Correction Factor (K)	Wavelength (nm) used
3,5-Dihydroxyflavone-3-*O*-G	0.44	263
3-Hydroxy-4'-methoxyflavone-3-*O*-G	0.51	340
3-Hydroxy-5-methoxyflavone-3-*O*-G	1.05	340
3-Hydroxy-6-methoxyflavone-3-*O*-G	1.06	340
3-Hydroxy-7-methoxyflavone-3-*O*-G	1.14	340
4'-Hydroxy-5-methoxyflavone-4'-*O*-G	1.03	340

*All glucuronides were generated using UGT1A9.

Appendix D. UV Spectrum of aglycone and their respective glucuronide(s) for the flavonoids used in *in silico* modeling but not in the published manuscript.

Naringenin	Phlortein
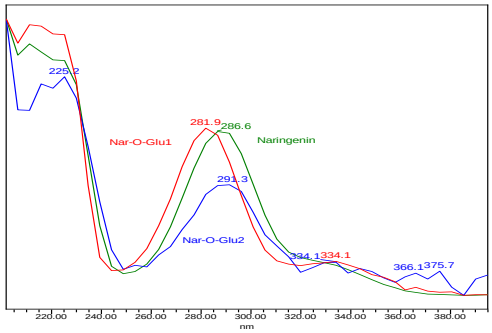	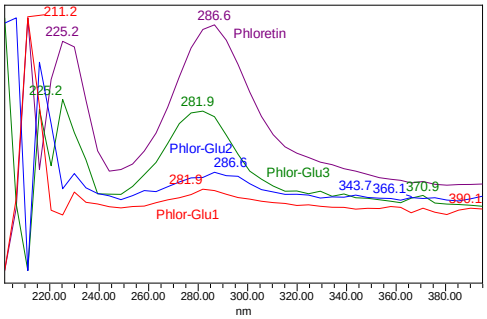
Genistein	**Diadzein**
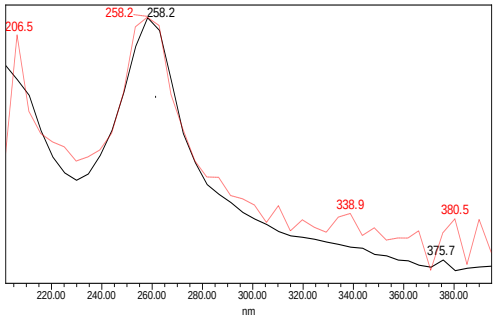	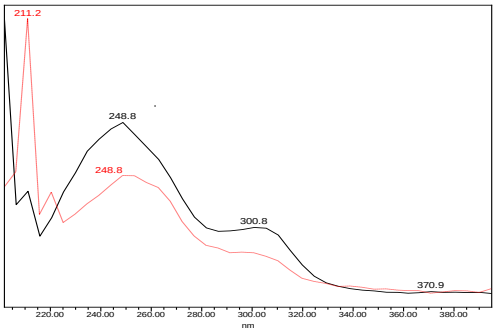
Prunetin	**Glycetin**
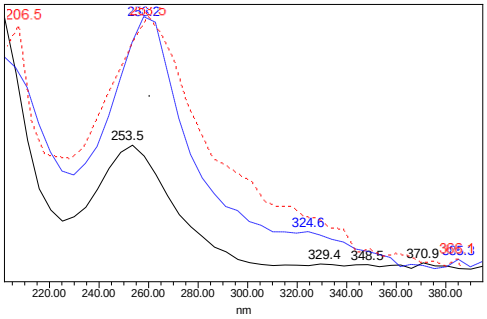	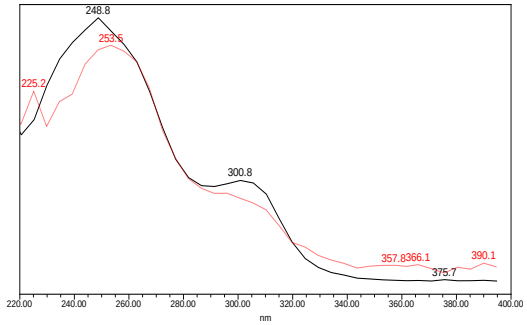

Biochanin A	Formononetin
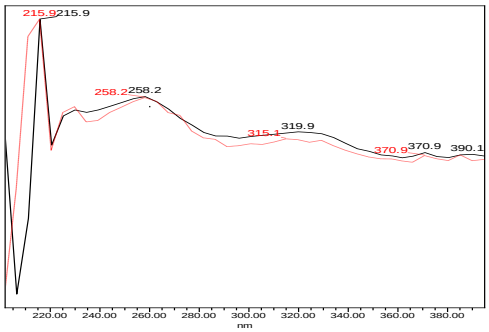	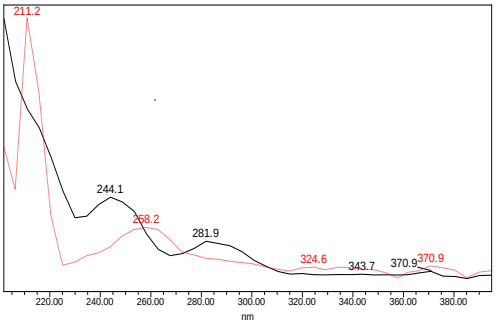
2'-Hydroxyflavone	**3'-Hydroxyflavone**
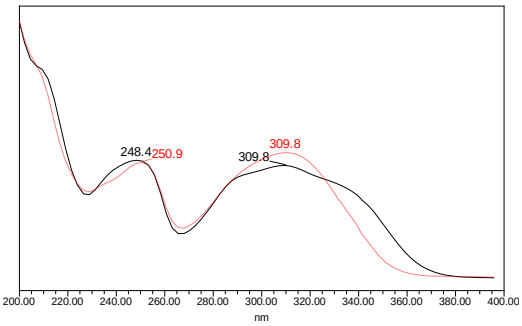	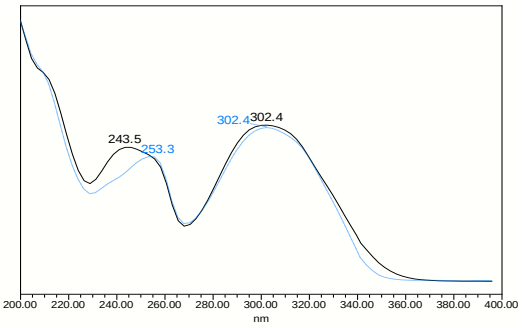
4'-Hydroxy-5-methoxyflavone	**Baicalein**
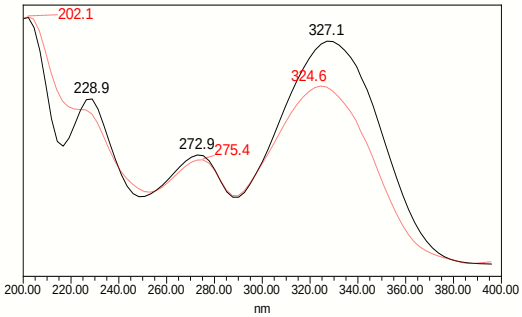	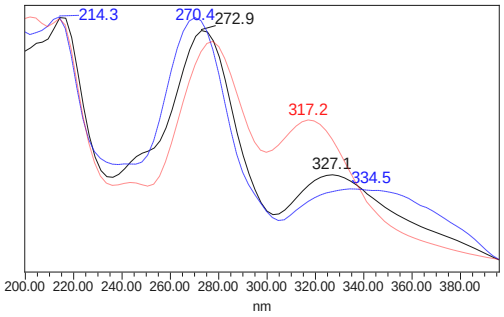

Quercetin	Luteolin
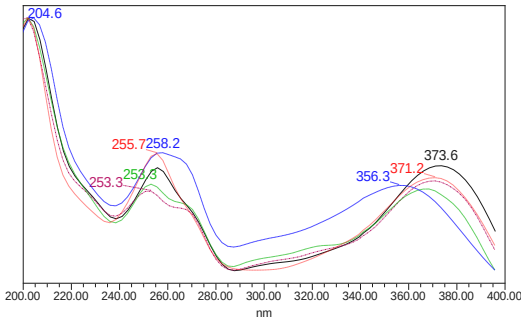	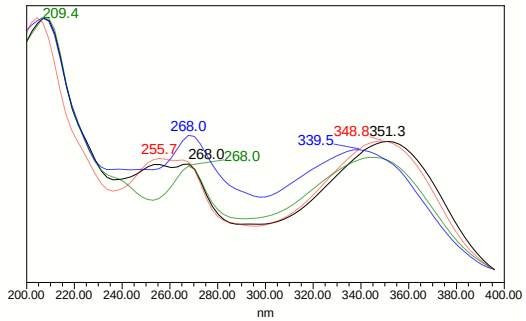
5,4'-Dihydroxyflavone	**5,6-Dihydroxyflavone**
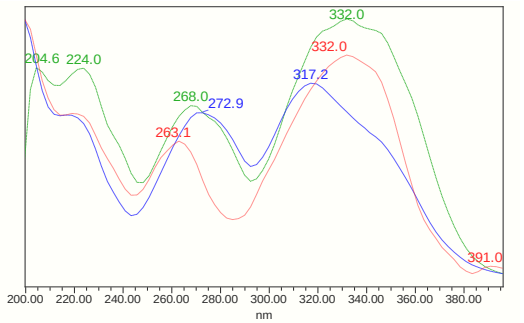	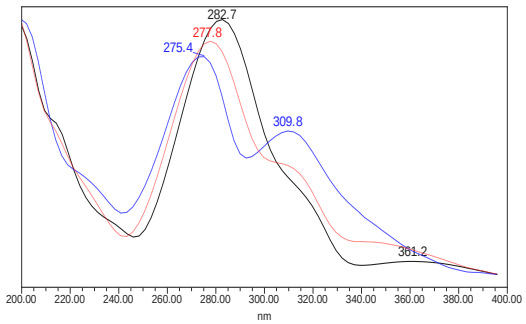
6,4'-Dihydroxyflavone	**6,7-Dihydroxyflavone**
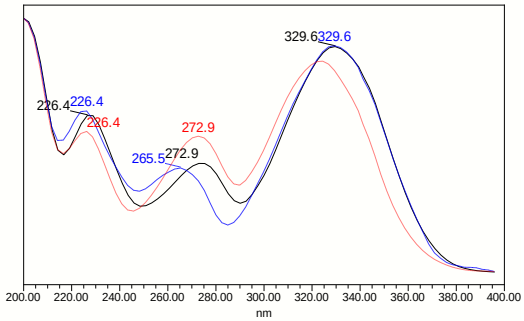	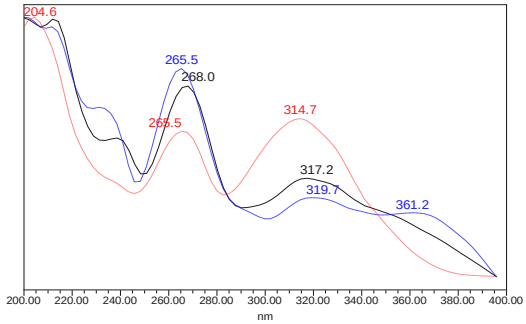

5,4'-Dihydroxy-7-methoxyflavone	5,6-Dihydroxy-7-methoxyflavone
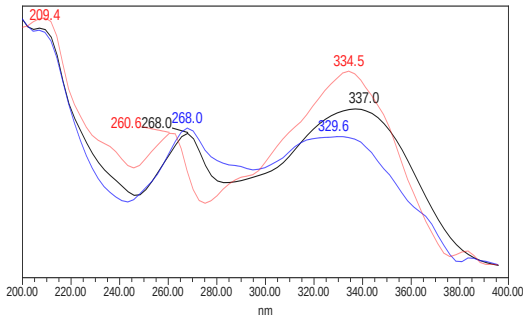	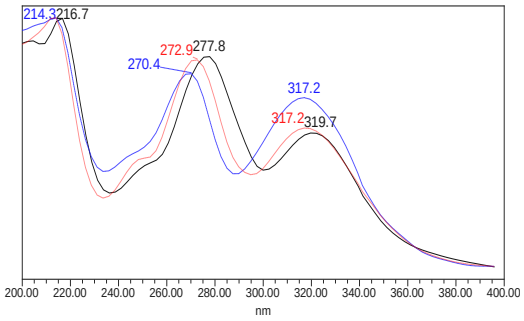

Figure D1. UV Spectrum of flavonoids and their respective glucuronide(s)

Appendix E. *In silico* pharmacophore modeling data for UGT1A8 and UGT1A9

Table E1 Randomized Groups of Training (32 compounds) and Test (8 compounds) Sets of UGT1A8 Substrates

	Randomized Grouping of Substrates into Training and Test Sets for UGT1A8 Modeling									
Compounds	**I**	**II**	**III**	**IV**	**V**	**VI**	**VII**	**VIII**	**IX**	**X**
34'DHF	Training	Test	Training	Training	Training	Training	Training	Training	Training	Test
35DHF	Training	Test	Test	Training	Test	Training	Training	Test	Training	Training
36DHF	Training	Training	Training	Training	Training	Training	Training	Training	Test	Training
37DHF	Training	Training	Training	Training	Training	Training	Training	Training	Training	Training
54'DHF	Training	Training	Training	Training	Training	Test	Training	Training	Training	Training
56DHF	Test	Test	Training	Training	Training	Training	Training	Training	Training	Test
57DHF	Training	Training	Training	Training	Training	Training	Training	Training	Training	Training
64'DHF	Training	Training	Training	Training	Training	Training	Training	Training	Training	Test
67DHF	Training	Training	Training	Test	Training	Training	Test	Test	Training	Training
74'DHF	Test	Training	Training	Training	Training	Training	Training	Training	Training	Training
56DH7MF	Training	Training	Training	Training	Training	Training	Training	Test	Training	Training
57DM3HF	Training	Test	Training	Training	Training	Training	Training	Training	Training	Training
74'DM3HF	Training	Training	Training	Training	Training	Training	Training	Training	Training	Training
Apigenin	Training	Training	Training	Training	Training	Training	Training	Training	Training	Training
Kaempferol	Training	Test	Training	Training	Training	Test	Training	Training	Training	Training
Naringenin	Training	Training	Training	Training	Training	Test	Training	Training	Training	Training
Phloretin	Training	Training	Training	Training	Training	Training	Training	Training	Training	Training
Genistein	Training	Training	Test	Test	Training	Training	Test	Training	Training	Test
Glycetin	Training	Training	Training	Training	Training	Test	Test	Training	Training	Training
Prunetin	Training	Training	Training	Training	Training	Training	Training	Training	Training	Training
3H4'MF	Training	Training	Test	Training	Training	Test	Training	Training	Test	Training

	Randomized Grouping of Substrates into Training and Test Sets for UGT1A8 Modeling									
Compounds	**I**	**II**	**III**	**IV**	**V**	**VI**	**VII**	**VIII**	**IX**	**X**
3H6MF	Training	Test	Training	Training	Training	Training	Training	Training	Training	Training
3H7MF	Training	Training	Training	Training	Test	Training	Training	Training	Training	Training
4'H7MF	Training	Test	Training	Test	Training	Test	Training	Training	Training	Training
6H4'MF	Training	Training	Training	Training	Test	Training	Training	Test	Test	Training
6H7MF	Training	Training	Training	Training	Training	Training	Training	Training	Training	Training
7H4'MF	Training	Training	Training	Training	Training	Test	Training	Training	Training	Test
2'HF	Test	Training	Training	Training	Training	Training	Test	Training	Training	Test
3HF	Training	Training	Test	Training	Test	Training	Training	Test	Training	Training
3'HF	Test	Test	Training	Training	Training	Training	Test	Training	Test	Training
5HF	Test	Training	Training	Training	Test	Training	Training	Training	Test	Training
6HF	Test	Training	Training	Training	Test	Training	Test	Test	Training	Test
7HF	Training	Training	Test	Test	Training	Training	Training	Test	Training	Test
Galangin	Training	Training	Test	Training	Test	Training	Training	Training	Training	Training
3,6,4'THF	Training	Training	Test	Test	Training	Training	Training	Training	Training	Training
3H5MF	Training	Training	Training	Test	Training	Training	Training	Training	Test	Training
Quercetin	Training	Training	Training	Training	Training	Training	Test	Training	Test	Training
Luteolin	Test	Training	Training	Test	Training	Test	Training	Training	Training	Training
Baicalein	Test	Training	Training	Test	Training	Training	Test	Test	Training	Training

Table E2 Randomized Groups of Training (37 compounds) and Test (9 compounds) Sets of UGT1A9 substrates

	Randomized Grouping of Substrates into Training and Test Sets for UGT1A9 Modeling									
Compounds	**I**	**II**	**III**	**IV**	**V**	**VI**	**VII**	**VIII**	**IX**	**X**
34'DHF	Training	Training	Training	Training	Test	Training	Training	Test	Training	Training
35DHF	Training	Test	Training	Training	Training	Training	Test	Test	Training	Training
36DHF	Test	Training	Test	Training	Training	Training	Training	Test	Training	Training
37DHF	Training	Training	Training	Test	Training	Test	Training	Training	Training	Training
54'DHF	Training	Training	Training	Test	Training	Training	Training	Training	Test	Test
56DHF	Training	Training	Training	Training	Test	Training	Test	Training	Training	Training
57DHF	Training	Training	Training	Training	Training	Training	Training	Training	Training	Training
64'DHF	Training	Training	Test	Training	Training	Training	Training	Test	Test	Test
67DHF	Test	Test	Test	Training	Training	Training	Training	Training	Training	Training
74'DHF	Test	Training	Training	Test	Training	Training	Training	Training	Training	Test
54'DH7MF	Test	Training	Training	Training	Training	Training	Training	Training	Training	Training
56DH7MF	Training	Test	Training	Test	Training	Training	Test	Training	Training	Training
57DM3HF	Training	Training	Training	Training	Training	Training	Test	Training	Training	Training
74'DM3HF	Training	Training	Training	Test	Training	Training	Training	Training	Training	Training
Apigenin	Training	Training	Training	Test	Training	Training	Training	Training	Test	Training
kaempferol	Training	Training	Training	Test	Training	Training	Training	Training	Test	Training
naringenin	Training	Training	Training	Training	Training	Training	Training	Training	Training	Test
phloretin	Test	Training	Training	Training	Training	Training	Training	Training	Training	Test
Biochanin A	Training	Training	Training	Training	Training	Training	Training	Training	Training	Training
Diadzein	Training	Training	Training	Training	Training	Training	Training	Training	Training	Training
Genistein	Training	Training	Test	Training	Test	Test	Training	Training	Training	Training

Glycetin	Training	Training	Training	Training	Training	Training	Training	Training	Training	Test
Prunetin	Training	Training	Training	Training	Training	Training	Training	Training	Training	Training
	Randomized Grouping of Substrates into Training and Test Sets for UGT1A9 Modeling									
Compounds	**I**	**II**	**III**	**IV**	**V**	**VI**	**VII**	**VIII**	**IX**	**X**
3H4'MF	Training	Training	Training	Training	Training	Test	Training	Training	Test	Training
3H6MF	Training	Training	Training	Training	Training	Test	Training	Training	Training	Training
3H7MF	Test	Training	Test	Training	Training	Training	Training	Training	Training	Training
4'H6MF	Training	Test	Training	Training	Training	Training	Training	Training	Training	Training
4'H7MF	Training	Training	Training	Training	Test	Training	Test	Test	Training	Training
5H7MF	Training	Training	Training	Training	Training	Test	Test	Test	Training	Training
6H4'MF	Training	Training	Training	Training	Training	Test	Test	Training	Test	Training
6H7MF	Training	Test	Training	Test	Training	Training	Training	Training	Training	Training
7H4'MF	Training	Training	Training	Test	Training	Training	Test	Test	Training	Test
2'HF	Test	Training	Training	Training	Test	Training	Training	Training	Training	Training
3HF	Test	Training	Test	Training	Training	Test	Training	Test	Training	Training
3'HF	Test	Training	Training	Training	Test	Test	Training	Training	Training	Training
4'HF	Training	Training	Test	Training	Training	Training	Training	Training	Training	Training
5HF	Training	Training	Training	Training	Test	Training	Training	Test	Test	Training
6HF	Training	Training	Training	Training	Test	Training	Training	Training	Training	Training
7HF	Training	Test	Training	Training	Test	Training	Training	Training	Test	Training
Resokaempferol	Training	Training	Training	Training	Training	Training	Training	Training	Training	Training
Galangin	Training	Test	Training	Training	Training	Training	Training	Training	Training	Test
3,6,4'THF	Training	Test	Training	Training	Training	Training	Training	Training	Training	Test
3H5MF	Training	Test	Test	Training	Training	Training	Test	Training	Training	Training
Quercetin	Training	Training	Test	Training	Training	Training	Training	Training	Test	Training

Compounds	**I**	**II**	**III**	**IV**	**V**	**VI**	**VII**	**VIII**	**IX**	**X**
Luteolin	Training	Training	Training	Training	Training	Test	Training	Training	Training	Training
Baicalein	Training	Training	Training	Training	Training	Training	Training	Training	Training	Training

Table E3 Prediction of training and test set compounds by pharmacophore of Group II

Compound	Experimental Cl_{int}	Designated Class	Estimated Cl_{int}	Predicted Class	FIT Value
Training Set					
3,7DHF	2.69E+07	I	1.28E+06	I	2.10
Kaempferol	2.95E+06	I	1.27E+06	I	2.09
3,6DHF	2.21E+06	I	3.95E+05	I	1.59
Baicalein	1.99E+06	I	1.26E+06	I	2.09
5,7DHF	1.82E+06	I	1.23E+06	I	2.08
Quercetin	1.49E+06	I	1.24E+06	I	2.08
Luteolin	1.30E+06	I	1.17E+06	I	2.06
3HF	7.30E+05	I	3.96E+05	I	1.59
3H7MF	7.19E+05	I	3.95E+05	I	1.59
Apigenin	6.85E+05	I	1.24E+06	I	2.08
7,4'DM3HF	6.10E+05	I	3.89E+05	I	1.58
3,4'DHF	5.43E+05	I	3.93E+05	I	1.58
Naringenin	4.78E+05	I	1.20E+06	I	2.07
Glycetin	4.59E+05	I	2.22E+05	II	1.34
Resokaempferol	4.20E+05	I	1.27E+06	I	2.09
6,4'DHF	3.13E+05	I	3.95E+05	I	1.59
3H6MF	3.13E+05	I	3.80E+05	I	1.57
Genistein	3.13E+05	I	2.10E+05	II	1.31
3H4'MF	2.93E+05	II	3.88E+05	I	1.58
Diadzein	2.93E+05	II	2.08E+05	II	1.31
5,6DHF	2.88E+05	II	3.85E+05	I	1.58
5,4'DHF	2.19E+05	II	1.15E+05	II	1.05
3'HF	1.90E+05	II	1.17E+05	II	1.06
2'HF	1.74E+05	II	3.95E+05	I	1.59
Phloretin	1.68E+05	II	3.83E+05	I	1.57
7,4'DHF	1.29E+05	II	1.23E+06	I	2.08
5HF	1.16E+05	II	1.16E+05	II	1.05
5,7DM3HF	1.04E+05	II	3.95E+05	I	1.59
4'HF	9.43E+04	II	1.15E+05	II	1.05

Prunetin	8.33E+04	II	2.24E+05	II	1.34
7H4'MF	8.20E+04	II	1.17E+06	I	2.06
Biochanin A	5.95E+04	II	2.35E+05	II	1.36
5,4'DH7MF	4.95E+04	II	3.84E+05	I	1.57
Compound	**Experimental Cl_{int}**	**Designated Class**	**Estimated Cl_{int}**	**Predicted Class**	**FIT Value**
6HF	3.86E+04	II	1.16E+05	II	1.06
5H7MF	2.29E+04	II	3.85E+05	I	1.58
6H4'MF	1.87E+04	II	3.82E+05	I	1.57
4'H7MF	1.73E+04	II	3.80E+05	I	1.57
Predictive ability				**64.86**	
Test Set					
Galangin	1.47E+06	I	1.29E+06	I	2.10
6,7DHF	3.80E+05	I	1.26E+06	I	2.09
3,6,4'THF	5.65E+05	I	6.81E+05	I	1.82
5,6DH7MF	1.96E+05	II	2.81E+05	II	1.44
6H7MF	1.28E+05	II	2.52E+05	II	1.39
4'H6MF	6.62E+03	II	2.24E+05	II	1.34
3H5MF	4.76E+05	I	6.51E+04	II	0.80
3,5DHF	6.10E+05	I	5.98E+04	II	0.77
Predictive ability				**66.67**	

Table E4 Prediction of training and test set compounds by pharmacophore of Group III

Compound	Experimental Cl_{int}	Designated Class	Estimated Cl_{int}	Predicted Class	FIT Value
Training Set					
3,7DHF	2.69E+07	I	1.30E+06	I	3.52
Kaempferol	2.95E+06	I	1.23E+06	I	3.50
Baicalein	1.99E+06	I	1.30E+06	I	3.53
5,7DHF	1.82E+06	I	1.18E+06	I	3.48
Galangin	1.47E+06	I	1.28E+06	I	3.52
Luteolin	1.30E+06	I	1.09E+06	I	3.45
Apigenin	6.85E+05	I	1.27E+06	I	3.51
7,4'DM3HF	6.10E+05	I	1.29E+05	II	2.52
3,5DHF	6.10E+05	I	1.29E+05	II	2.52
3,6,4'THF	5.65E+05	I	3.28E+05	I	2.93
3,4'DHF	5.43E+05	I	2.88E+05	II	2.87
7HF	5.21E+05	I	1.32E+05	II	2.53
Naringenin	4.78E+05	I	1.34E+06	I	3.54
Glycetin	4.59E+05	I	1.25E+05	II	2.51
Resokaempferol	4.20E+05	I	1.21E+06	I	3.49
3H6MF	3.13E+05	I	1.30E+05	II	2.52
3H4'MF	2.93E+05	II	1.30E+05	II	2.52
Diadzein	2.93E+05	II	1.29E+05	II	2.52
5,6DHF	2.88E+05	II	1.30E+05	II	2.52
5,4'DHF	2.19E+05	II	1.07E+05	II	2.44
5,6DH7MF	1.96E+05	II	1.27E+05	II	2.51
3'HF	1.90E+05	II	1.28E+05	II	2.52
2'HF	1.74E+05	II	1.32E+05	II	2.53
Phloretin	1.68E+05	II	1.99E+05	II	2.71
7,4'DHF	1.29E+05	II	1.16E+06	I	3.48
6H7MF	1.28E+05	II	1.29E+05	II	2.52
5HF	1.16E+05	II	1.08E+05	II	2.44
5,7DM3HF	1.04E+05	II	1.30E+05	II	2.53
Prunetin	8.33E+04	II	1.11E+05	II	2.46

7H4'MF	8.20E+04	II	1.04E+06	I	3.43
Biochanin A	5.95E+04	II	1.18E+05	II	2.48
5,4'DH7MF	4.95E+04	II	2.42E+05	II	2.79
6HF	3.86E+04	II	1.22E+05	II	2.50
Compound	**Experimental Cl_{int}**	**Designated Class**	**Estimated Cl_{int}**	**Predicted Class**	**FIT Value**
5H7MF	2.29E+04	II	1.28E+05	II	2.52
6H4'MF	1.87E+04	II	1.23E+05	II	2.50
4'H7MF	1.73E+04	II	2.12E+05	II	2.74
4'H6MF	6.62E+03	II	2.55E+05	II	2.82
Predictive ability				**78.38**	
Test Set					
Quercetin	1.49E+06	I	1.64E+06	I	3.63
Genistein	3.13E+05	I	1.22E+06	I	3.50
6,7DHF	3.80E+05	I	1.20E+06	I	3.49
3,6DHF	2.21E+06	I	3.29E+05	I	2.93
6,4'DHF	3.13E+05	I	3.29E+05	I	2.93
3H7MF	7.19E+05	I	2.10E+05	II	2.73
3HF	7.30E+05	I	1.26E+04	II	1.51
4'HF	9.43E+04	II	6.25E+03	II	1.21
3H5MF	4.76E+05	I	7.55E+02	II	0.29
Predictive ability				**66.67**	

Table E5 Prediction of training and test set compounds by pharmacophore of Group V

Compound	Experimental Cl_{int}	Designated Class	Estimated Cl_{int}	Predicted Class	FIT Value
Training Set					
3,7DHF	2.69E+07	I	1.48E+06	I	2.07
Kaempferol	2.95E+06	I	1.48E+06	I	2.07
3,6DHF	2.21E+06	I	3.02E+05	I	1.38
Baicalein	1.99E+06	I	1.09E+06	I	1.94
5,7DHF	1.82E+06	I	1.19E+06	I	1.98
Quercetin	1.49E+06	I	1.48E+06	I	2.07
Galangin	1.47E+06	I	1.48E+06	I	2.07
Luteolin	1.30E+06	I	1.19E+06	I	1.98
3HF	7.30E+05	I	2.85E+05	II	1.35
3H7MF	7.19E+05	I	3.02E+05	I	1.38
Apigenin	6.85E+05	I	1.05E+06	I	1.92
7,4'DM3HF	6.10E+05	I	3.02E+05	I	1.38
3,5DHF	6.10E+05	I	3.01E+05	I	1.38
3,6,4'THF	5.65E+05	I	3.02E+05	I	1.38
Naringenin	4.78E+05	I	1.42E+06	I	2.05
3H5MF	4.76E+05	I	2.85E+05	II	1.36
Glycetin	4.59E+05	I	3.02E+05	I	1.38
Resokaempferol	4.20E+05	I	1.48E+06	I	2.07
6,7DHF	3.80E+05	I	1.20E+06	I	1.98
6,4'DHF	3.13E+05	I	2.90E+05	II	1.36
3H6MF	3.13E+05	I	2.69E+05	II	1.33
Diadzein	2.93E+05	II	3.02E+05	I	1.38
3H4'MF	2.93E+05	II	2.85E+05	II	1.35
5,4'DHF	2.19E+05	II	1.38E+05	II	1.04
5,6DH7MF	1.96E+05	II	3.02E+05	I	1.38
Phloretin	1.68E+05	II	3.02E+05	I	1.38
7,4'DHF	1.29E+05	II	1.19E+06	I	1.97
6H7MF	1.28E+05	II	2.58E+05	II	1.31
5,7DM3HF	1.04E+05	II	3.02E+05	I	1.38

4'HF	9.43E+04	II	1.67E+05	II	1.12
Prunetin	8.33E+04	II	2.98E+05	II	1.37
7H4'MF	8.20E+04	II	1.32E+06	I	2.02
Biochanin A	5.95E+04	II	3.02E+05	I	1.38
Compound	**Experimental Cl_{int}**	**Designated Class**	**Estimated Cl_{int}**	**Predicted Class**	**FIT Value**
Training Set	4.95E+04	II	3.01E+05	I	1.38
5H7MF	2.29E+04	II	3.01E+05	I	1.38
6H4'MF	1.87E+04	II	2.52E+05	II	1.30
4'H6MF	6.62E+03	II	2.82E+05	II	1.35
Predictive ability				**64.86**	
Test Set					
5,6DHF	2.88E+05	II	5.67E+05	I	1.65
3,4'DHF	5.43E+05	I	4.66E+05	I	1.57
Genistein	3.13E+05	I	4.61E+05	I	1.56
4'H7MF	1.73E+04	II	4.28E+05	I	1.53
5HF	1.16E+05	II	1.47E+05	II	1.07
2'HF	1.74E+05	II	1.35E+05	II	1.03
6HF	3.86E+04	II	1.11E+05	II	0.95
3'HF	1.90E+05	II	3.10E+04	II	0.39
Predictive ability				**66.67**	

Table E6 Prediction of training and test set compounds by pharmacophore of Group IX

Compound	Experimental Cl_{int}	Designated Class	Estimated Cl_{int}	Predicted Class	FIT Value
Training Set					
3,7DHF	2.69E+07	I	1.07E+06	I	2.16
3,6DHF	2.21E+06	I	2.89E+05	II	1.59
Baicalein	1.99E+06	I	1.01E+06	I	2.13
5,7DHF	1.82E+06	I	1.06E+06	I	2.15
Galangin	1.47E+06	I	1.06E+06	I	2.16
Luteolin	1.30E+06	I	1.27E+06	I	2.23
3HF	7.30E+05	I	2.86E+05	II	1.59
3H7MF	7.19E+05	I	2.84E+05	II	1.58
7,4'DM3HF	6.10E+05	I	2.87E+05	II	1.59
3,5DHF	6.10E+05	I	2.85E+05	II	1.58
3,6,4'THF	5.65E+05	I	6.56E+05	I	1.95
3,4'DHF	5.43E+05	I	6.34E+05	I	1.93
Naringenin	4.78E+05	I	1.52E+06	I	2.31
3H5MF	4.76E+05	I	2.88E+05	II	1.59
Glycetin	4.59E+05	I	4.24E+05	I	1.76
Resokaempferol	4.20E+05	I	1.10E+06	I	2.17
6,7DHF	3.80E+05	I	1.01E+06	I	2.13
3H6MF	3.13E+05	I	2.91E+05	II	1.59
Genistein	3.13E+05	I	2.87E+05	II	1.59
Diadzein	2.93E+05	II	2.87E+05	II	1.59
5,6DHF	2.88E+05	II	2.21E+05	II	1.47
5,6DH7MF	1.96E+05	II	2.49E+05	II	1.53
3'HF	1.90E+05	II	2.78E+05	II	1.57
2'HF	1.74E+05	II	2.92E+05	II	1.59
Phloretin	1.68E+05	II	6.40E+05	I	1.94
7,4'DHF	1.29E+05	II	1.11E+06	I	2.18
6H7MF	1.28E+05	II	1.83E+05	II	1.39
5,7DM3HF	1.04E+05	II	2.91E+05	II	1.59
4'HF	9.43E+04	II	2.04E+05	II	1.44

Prunetin	8.33E+04	II	2.88E+05	II	1.59
7H4'MF	8.20E+04	II	1.19E+06	I	2.21
Biochanin A	5.95E+04	II	4.93E+05	II	1.82
5,4'DH7MF	4.95E+04	II	2.55E+05	II	1.54
Compound	**Experimental Cl_{int}**	**Designated Class**	**Estimated Cl_{int}**	**Predicted Class**	**FIT Value**
6HF	3.86E+04	II	2.07E+05	II	1.45
5H7MF	2.29E+04	II	2.51E+05	II	1.53
4'H7MF	1.73E+04	II	2.44E+05	II	1.52
4'H6MF	6.62E+03	II	2.46E+05	II	1.52
Predictive ability				**72.97**	
Test Set					
Quercetin	1.49E+06	I	1.58E+06	I	2.33
Apigenin	6.85E+05	I	1.55E+06	I	2.32
Kaempferol	2.95E+06	I	1.48E+06	I	2.30
7HF	5.21E+05	I	1.46E+06	I	2.30
6H4'MF	1.87E+04	II	6.64E+05	I	1.95
6,4'DHF	3.13E+05	I	5.28E+05	I	1.85
5,4'DHF	2.19E+05	II	4.58E+05	I	1.79
3H4'MF	2.93E+05	II	7.30E+04	II	0.99
5HF	1.16E+05	II	1.02E+04	II	0.14
Predictive ability				**77.78**	

Table E7 Prediction of training and test set compounds by pharmacophore of Group X

Compound	Experimental Cl_{int}	Designated Class	Estimated Cl_{int}	Predicted Class	FIT Value
Training Set					
3,7DHF	2.69E+07	I	1.99E+06	I	2.54
Kaempferol	2.95E+06	I	2.00E+06	I	2.54
3,6DHF	2.21E+06	I	2.85E+05	II	1.70
Baicalein	1.99E+06	I	1.40E+06	I	2.39
5,7DHF	1.82E+06	I	1.53E+06	I	2.42
Quercetin	1.49E+06	I	2.00E+06	I	2.54
Luteolin	1.30E+06	I	1.53E+06	I	2.42
3HF	7.30E+05	I	2.65E+05	II	1.66
3H7MF	7.19E+05	I	2.86E+05	II	1.70
Apigenin	6.85E+05	I	1.37E+06	I	2.38
7,4'DM3HF	6.10E+05	I	2.91E+05	II	1.70
3,5DHF	6.10E+05	I	2.86E+05	II	1.70
3,4'DHF	5.43E+05	I	2.86E+05	II	1.70
7HF	5.21E+05	I	4.83E+05	I	1.92
3H5MF	4.76E+05	I	2.69E+05	II	1.67
Resokaempferol	4.20E+05	I	1.99E+06	I	2.54
6,7DHF	3.80E+05	I	1.53E+06	I	2.42
3H6MF	3.13E+05	I	2.72E+05	II	1.67
Genistein	3.13E+05	I	1.84E+05	II	1.51
Diadzein	2.93E+05	II	2.63E+05	II	1.66
3H4'MF	2.93E+05	II	1.93E+05	II	1.53
5,6DHF	2.88E+05	II	2.41E+05	II	1.62
5,6DH7MF	1.96E+05	II	2.34E+05	II	1.61
3'HF	1.90E+05	II	1.21E+05	II	1.32
2'HF	1.74E+05	II	2.69E+05	II	1.67
6H7MF	1.28E+05	II	2.37E+05	II	1.61
5HF	1.16E+05	II	1.21E+05	II	1.32
5,7DM3HF	1.04E+05	II	2.85E+05	II	1.69
4'HF	9.43E+04	II	1.52E+05	II	1.42

Prunetin	8.33E+04	II	1.75E+05	II	1.48
Biochanin A	5.95E+04	II	3.06E+05	I	1.73
5,4'DH7MF	4.95E+04	II	2.94E+05	II	1.71
6HF	3.86E+04	II	1.27E+05	II	1.34
Compound	**Experimental Cl_{int}**	**Designated Class**	**Estimated Cl_{int}**	**Predicted Class**	**FIT Value**
5H7MF	2.29E+04	II	2.35E+05	II	1.61
6H4'MF	1.87E+04	II	2.34E+05	II	1.61
4'H7MF	1.73E+04	II	2.89E+05	II	1.70
4'H6MF	6.62E+03	II	2.38E+05	II	1.62
Predictive ability				**72.97**	
Test Set					
Naringenin	4.78E+05	I	2.06E+06	I	2.55
Galangin	1.47E+06	I	2.06E+06	I	2.55
7H4'MF	8.20E+04	II	2.04E+06	I	2.55
7,4'DHF	1.29E+05	II	2.04E+06	I	2.55
Phloretin	1.68E+05	II	1.75E+06	I	2.48
3,6,4'THF	5.65E+05	I	5.65E+05	I	1.99
Glycetin	4.59E+05	I	4.96E+05	I	1.94
6,4'DHF	3.13E+05	I	4.23E+05	I	1.87
5,4'DHF	2.19E+05	II	6.72E+04	II	1.07
Predictive ability				**66.67**	

Appendix F. Time course of apical and basolateral excretion of regiospecific glucuronides, total glucuronide and sulfates conjugates of flavonoids in the Caco-2 cell culture model.

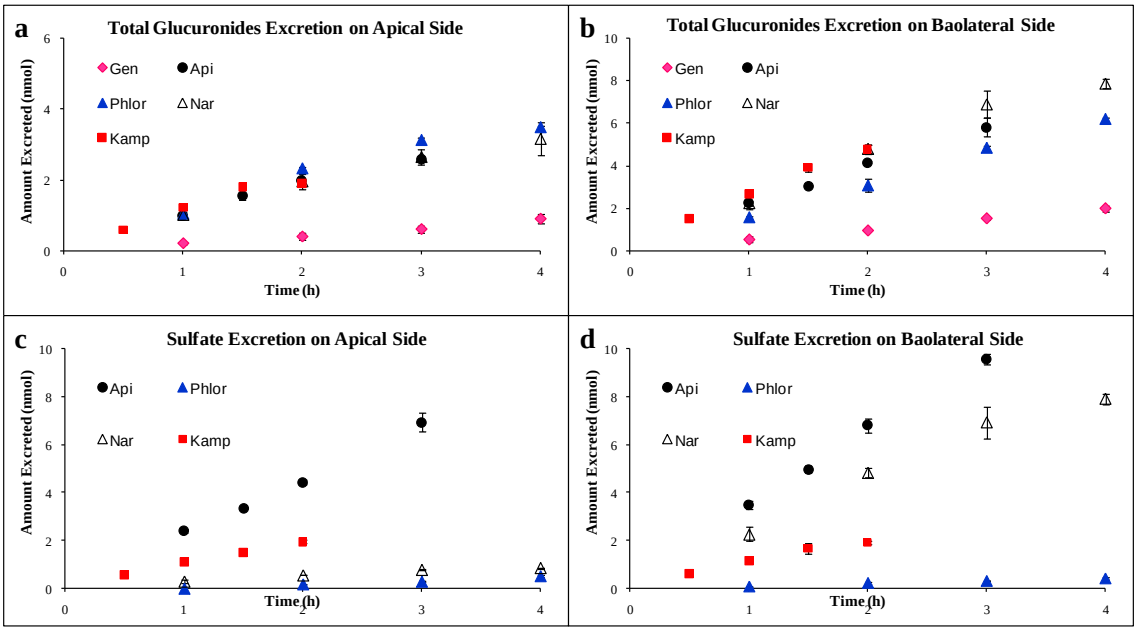

Figure F1. Time course of excretion of conjugates of five flavonoids in the Caco-2 cell culture model, apical glucuronides, basolateral glucuronides (b), apical sulfate (c), and basolateral sulfate (d). Amount of glucuronides and sulfate excreted on AP and BL side during AP (pH =7.4) to BL (pH =7.4) transport of flavonoids in the Caco-2 cell monolayer at 37ºC. The incubation time points for apigenin was 1, 1.5, 2 and 3 hrs; for kaempferol was 0.5, 1, 1.5 and 2 hrs; and 1, 2, 3 and 4 hrs for genistein, naringenin and phloretin. The flavones concentration in the donor solution was 10µM. Each data point represented the average of three determinations, and the error bars were the standard deviations of the means.

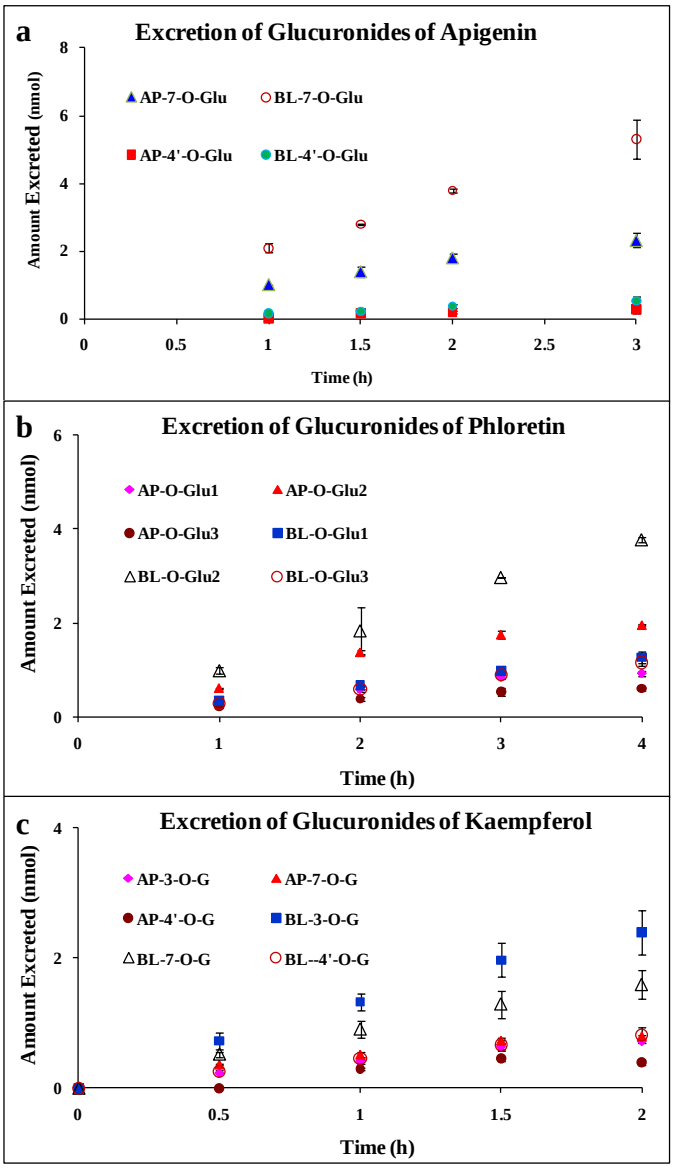

Figure F2. Time course of apigenin (a), phloretin (b), and kaempferol (c) multiple glucuronides excretion in the Caco-2 cell culture model. Amount of individual glucuronides excreted on apical (AP) and basolateral (BL) side during AP (pH =7.4) to BL (pH =7.4) transport of flavones in the Caco-2 cell monolayer at 37ºC. The incubation time points for apigenin was 1, 1.5, 2 and 3 hrs; for kaempferol was 0.5, 1, 1.5 and 2 hrs; and 1, 2, 3 and 4 hrs for genistein, naringenin and phloretin. The flavones concentration in the donor solution was 10µM. Each data point represented the average of three determinations, and the error bars were the standard deviations of the means.

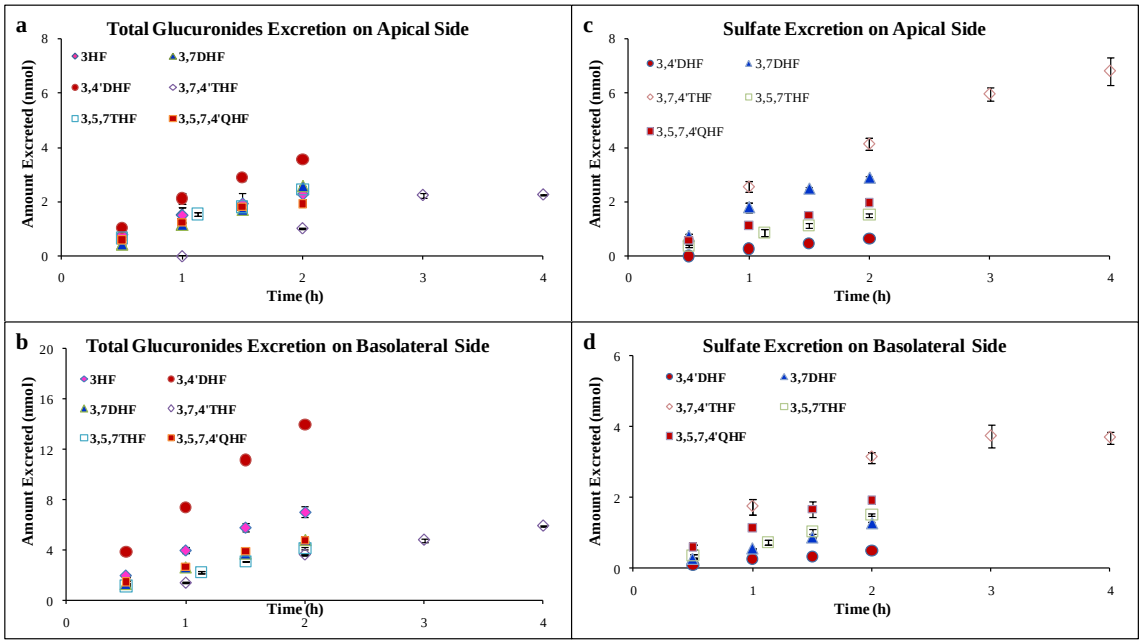

Figure F3. Time course of excretion of conjugates of six flavonols in the Caco-2 cell culture model, apical glucuronides, basolateral glucuronides (b), apical sulfate (c), and basolateral sulfate (d). Amount of glucuronides and sulfate excreted on AP and BL side during AP (pH =7.4) to BL (pH =7.4) transport of flavonols in the Caco-2 cell monolayer at 37ºC. The incubation time points for 3,7,4'THF were 1, 2, 3 and 4 hrs while for all other flavones were 0.5, 1, 1.5 and 2 hrs. The flavonols concentration in the donor solution was 10µM. Each data point represented the average of three determinations, and the error bars were the standard deviations of the means.

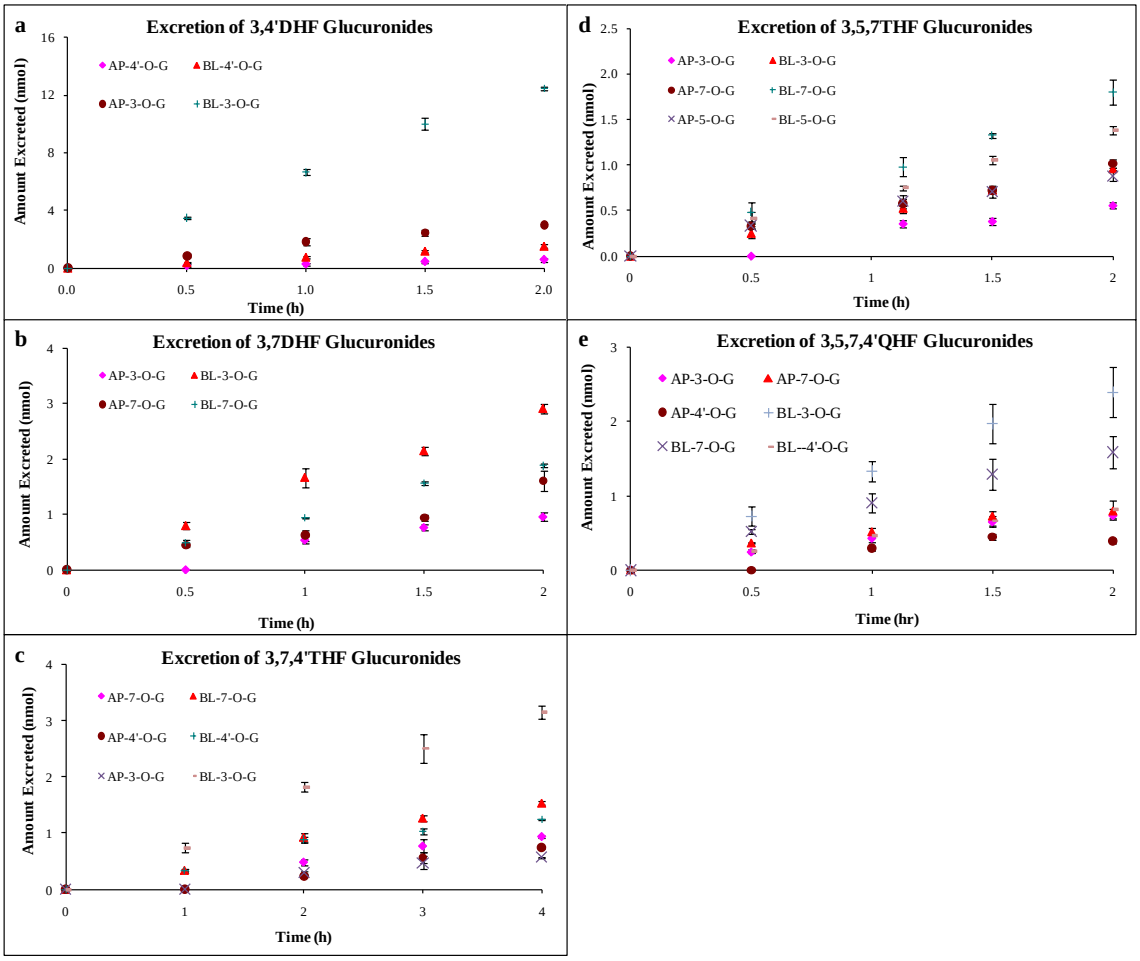

Figure F4. Time course of 3,4'DHF (a), 3,7DHF (b), 3,7,4'THF (c), 3,5,7THF (d) and 3,5,7,4'QHF (e) regiospecific glucuronides excretion in the Caco-2 cell culture model. Amount of individual glucuronides excreted on apical (AP) and basolateral (BL) side during AP (pH =7.4) to BL (pH =7.4) transport of flavones in the Caco-2 cell monolayer at 37ºC. The incubation time points for 3,7,4'THF were 1, 2, 3 and 4 hrs while for all other flavones were 0.5, 1, 1.5 and 2 hrs. The flavonols concentration in the donor solution was 10µM. Each data point represented the average of three determinations, and the error bars were the standard deviations of the means.

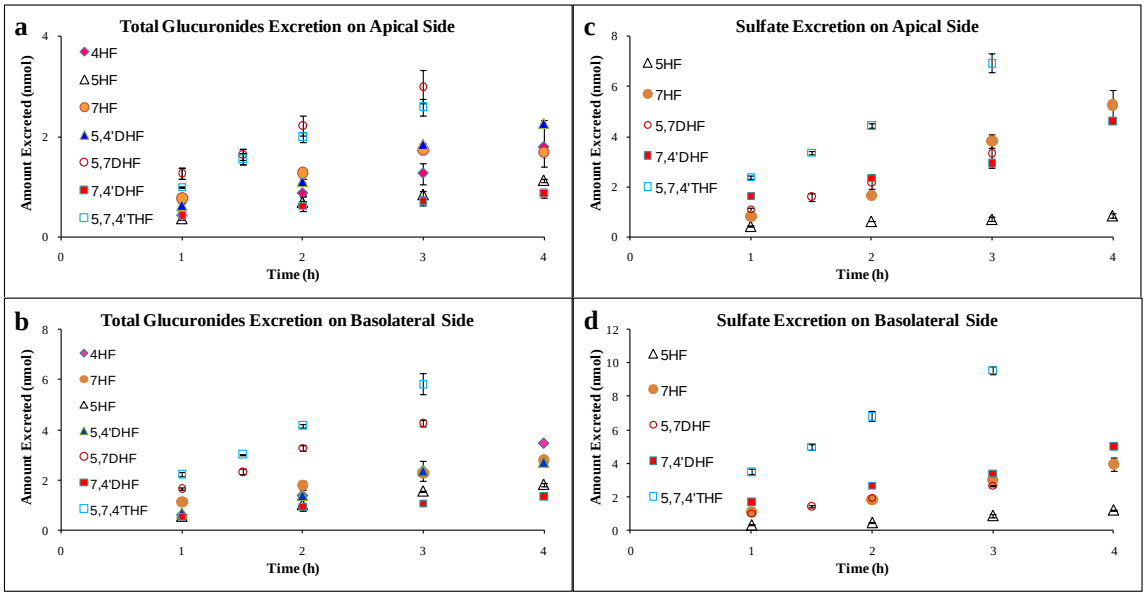

Figure F5. Time course of excretion of conjugates of seven flavones in the Caco-2 cell culture model, apical glucuronides, basolateral glucuronides (b), apical sulfate (c), and basolateral sulfate (d). Amount of glucuronides and sulfate excreted on AP and BL side during AP (pH =7.4) to BL (pH =7.4) transport of flavonols in the Caco-2 cell monolayer at 37ºC. The incubation time points for 5,7DHF and 5,7,4'THF were 1, 1.5, 2 and 3 hrs and 1, 2, 3 and 4 hrs for other compounds. The flavones concentration in the donor solution was 10µM (5µM for 5HF). Each data point represented the average of three determinations, and the error bars were the standard deviations of the means.

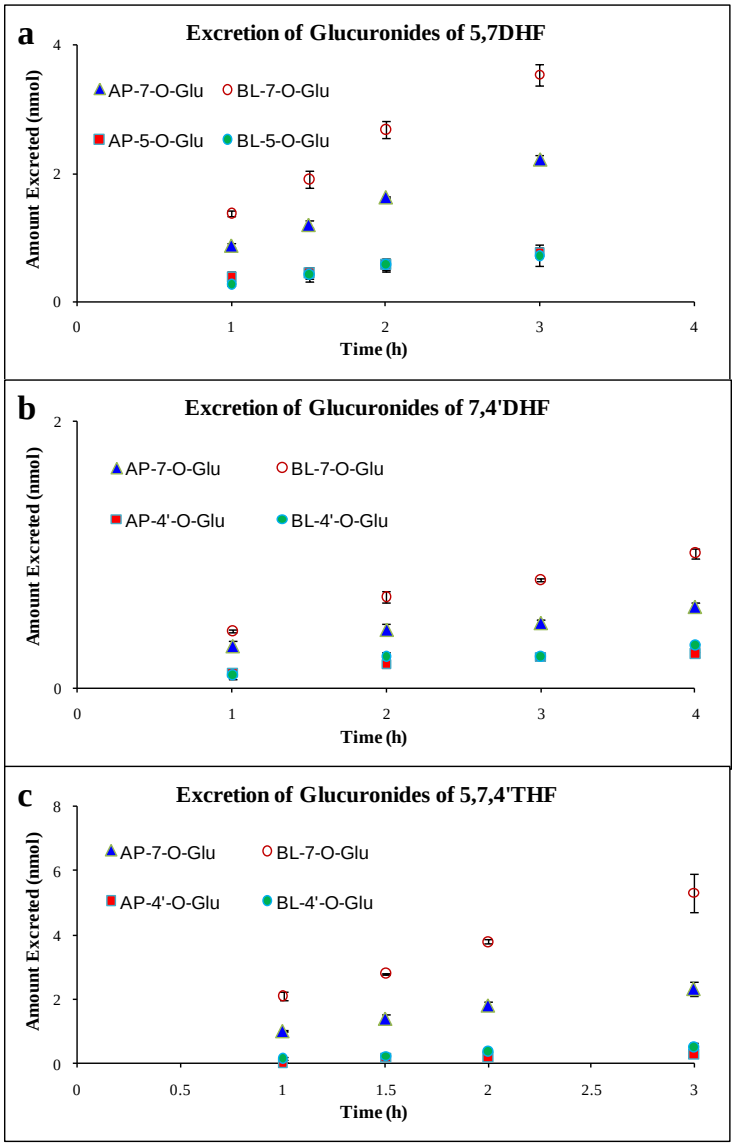

Figure F6. Time course of 5,7DHF (A), 7,4'DHF (B), and 5,7,4'THF (C) regiospecific glucuronides excretion in the Caco-2 cell culture model. Amount of individual glucuronides excreted on apical (AP) and basolateral (BL) side during AP (pH =7.4) to BL (pH =7.4) transport of flavones in the Caco-2 cell monolayer at 37ºC. The incubation time points for 7,4'DHF were 1, 2, 3 and 4 hrs, whereas for 5,7DHF and 5,7,4'THF were 1, 1.5, 2 and 3 hrs. The flavones concentration in the donor solution was 10µM. Each data point represented the average of three determinations, and the error bars were the standard deviations of the means.

Appendix G. Rates of formation of apigenin-7-*O*-sulfate with recombinant human SULT isoforms

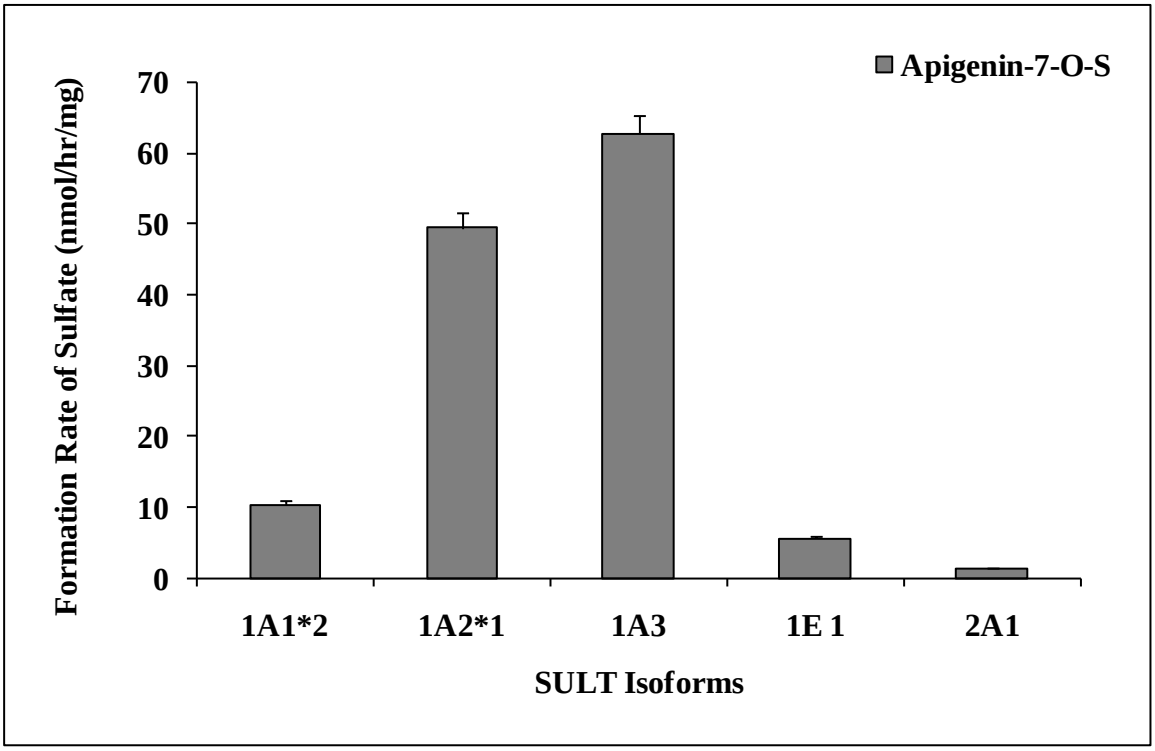

Figure G1. Rates of formation of apigenin-7-*O*-sulfate with recombinant human SULT isoforms. Apigenin at 10µM concentration was incubated at 37ºC for 8 hours with different SULT isoforms, 1A1*2, 1A2*1, 1A3, 1E1 or 2A1 (final protein concentration ~ 0.015 mg/ml) in presence of 0.3mM of magnesium chloride and 0.1 mM of 3'-phosphoadenosine-5'-phoshosulfate (PAPS) as co-factor. The rates of formation of apigenin sulfate was calculated as the amount of sulfate formed (nmol) per hr per mg of protein. Each bar represents the average of three determinations, and the error bars are the standard deviations of the means (n=3) (Curtsey of Dr. Wei Zhu).

Appendix H. Permission letter from ASPET for re-printing Figure 2